University at Buffalo
The State University of New York

# Further Results on the Assessment of Performance of Seismically Isolated Electrical Transformers

by
**Shoma Kitayama and Michael C. Constantinou**

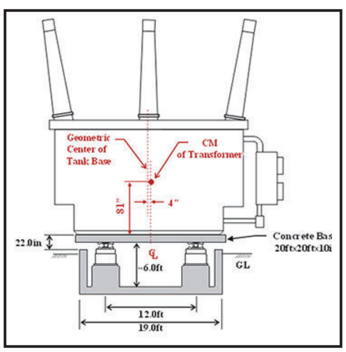


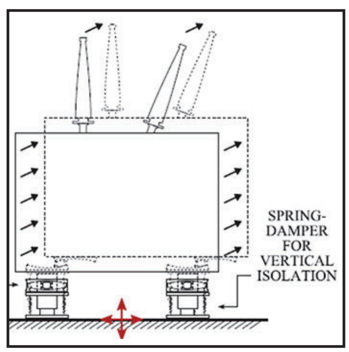

**Technical Report MCEER-20-0002**

**June 30, 2020**

MCEER: Earthquake Engineering to Extreme Events

# Further Results on the Assessment of Performance of Seismically Isolated Electrical Transformers

by

Shoma Kitayama[1] and Michael C. Constantinou[2]

Publication Date: June 30, 2020
Submittal Date: October 16, 2019

Technical Report MCEER-20-0002

1. Postdoctoral Associate, Department of Civil, Structural and Environmental Engineering, University at Buffalo, The State University of New York
2 Samuel P. Capen Professor, SUNY Distinguished Professor, Department of Civil, Structural and Environmental Engineering, University at Buffalo, The State University of New York

**MCEER: Earthquake Engineering to Extreme Events**
University at Buffalo, The State University of New York
212 Ketter Hall, Buffalo, NY 14260
*mceer@buffalo.edu*; *buffalo.edu/mceer*

# Preface

MCEER is a national center of excellence dedicated to the discovery and development of new knowledge, tools and technologies that equip communities to become more disaster resilient in the face of earthquakes and other extreme events. MCEER accomplishes this through a system of multidisciplinary, multi-hazard research, in tandem with complimentary education and outreach initiatives.

Headquartered at the University at Buffalo, The State University of New York, MCEER was originally established by the National Science Foundation in 1986, as the first National Center for Earthquake Engineering Research (NCEER). In 1998, it became known as the Multidisciplinary Center for Earthquake Engineering Research (MCEER), from which the current name, MCEER, evolved.

Comprising a consortium of researchers and industry partners from numerous disciplines and institutions throughout the United States, MCEER's mission has expanded from its original focus on earthquake engineering to one which addresses the technical and socio-economic impacts of a variety of hazards, both natural and man-made, on critical infrastructure, facilities, and society.

The Center derives support from several Federal agencies, including the National Science Foundation, Federal Highway Administration, Department of Energy, Nuclear Regulatory Commission, and the State of New York, foreign governments and private industry.

*This report presents results on the probability of failure in a lifetime of 50 years of non-isolated and seismically isolated transformers at ten locations in the Western US. This study considers: (a) scaling the ground motions for use in the incremental dynamic analysis by adjusting the spectral acceleration at the fundamental period (or effective period for isolated transformers) instead of the peak ground acceleration (PGA) in the earlier studies, (b) correcting for the spectral shape effects, which were ignored in the earlier studies, and (c) accounting for uncertainties, which were neglected in earlier studies. Moreover, the report presents sample results for near-field motions, which do not differ much from the results obtained for far-field motions. The results of this report, documented in numerous tables, may be used to decide on the benefits offered by a seismic isolation system depending on the location of the transformer and the form and properties of the seismic isolation system. The benefit is assessed on the basis of the probability of failure in a lifetime of 50 years. The information may also be used to assess the seismic performance of electric transmission networks under scenarios of component failures.*

## PREFACE

MCEER is a national center of excellence dedicated to the discovery and development of new knowledge, tools and technologies that equip communities to become more disaster resilient in the face of earthquakes and other extreme events. MCEER accomplishes this through a system of multidisciplinary, multi-hazard research, in tandem with complimentary education and outreach initiatives.

Headquartered at the University at Buffalo, The State University of New York, MCEER was originally established by the National Science Foundation in 1986, as the fi rst National Center for Earthquake Engineering Research (NCEER). In 1998, it became known as the Multidisciplinary Center for Earthquake Engineering Research (MCEER), from which the current name, MCEER, evolved.

Comprising a consortium of researchers and industry partners from numerous disciplines and institutions throughout the United States, MCEER's mission has expanded from its original focus on earthquake engineering to one which addresses the technical and socioeconomic impacts of a variety of hazards, both natural and man-made, on critical infrastructure, facilities, and society.

The Center derives support from several Federal agencies, including the National Science Foundation, Federal Highway Administration, National Institute of Standards and Technology, Department of Homeland Security/Federal Emergency Management Agency, and the State of New York, other state governments, academic institutions, foreign governments and private industry.

This report presents results on the probability of failure in a lifetime of 50 years of non-isolated and seismically isolated transformers at ten locations in the Western US. This study considers: (a) scaling the ground motions for use in the incremental dynamic analysis by adjusting the spectral acceleration at the fundamental period (or effective period for isolated transformers) instead of the peak ground acceleration (PGA) in the earlier studies, (b) correcting for the spectral shape effects, which were ignored in the earlier studies, and (c) accounting for uncertainties, which were neglected in earlier studies. Moreover, the report presents sample results for near-field motions, which do not much differ from the results obtained for far-field motions. The results of this report, documented in numerous tables, may be used to decide on the benefits offered by a seismic isolation system depending on the location of the transformer and the form and properties of the seismic isolation system. The benefit is assessed on the basis of the probability of failure in 50 years of lifetime. The information may also be used to assess

# ABSTRACT

This report presents results on the probability of failure in a lifetime of 50 years of non-isolated and seismically isolated transformers at ten locations in the Western US. This report presents an investigation of the limitations of past studies by considering: (a) scaling the ground motions for use in the incremental dynamic analysis by adjusting the spectral acceleration at the fundamental period (or effective period for isolated transformers) instead of the peak ground acceleration (PGA) in the earlier studies, (b) correcting for the spectral shape effects, which were ignored in the earlier studies, and (c) accounting for uncertainties, which were neglected in earlier studies. Moreover, the report presents sample results for near-field motions, which however, could not be corrected for spectral shape effects.

Results obtained for far-field motions show that, in general, scaling of the ground motions based on the spectral acceleration at the fundamental period or the effective period results in significant increases in the probability of failure for the isolated transformers, which are significantly moderated by corrections for the spectral shape effects. By comparison, the changes in the probability of failure of the studied non-isolated transformers were small due to the fact that the fundamental period was very small so that the spectral acceleration at the fundamental period was very close to the PGA which was used in the earlier studies for the scaling.

Based on the new results in this report, combined horizontal-vertical seismic isolation systems offer the lowest probabilities of failure for all cases of transformer and isolation system parameters, and for all considered sites. Horizontal only isolation offers no or offers insignificant advantages over non-isolation when the bushing transverse acceleration limit is 2g. However, horizontal only isolation offers important advantages over non-isolation when the bushing transverse acceleration limit is 1g.

The results of this report, documented in numerous tables, may be used to decide on the benefits offered by a seismic isolation system depending on the location of the transformer and the form and properties of the seismic isolation system. The benefit is assessed on the basis of the probability of failure in 50 years of lifetime. The information may also be used to assess the seismic performance of electric transmission networks under scenarios of component failures.

# ACKNOWLEDGEMENTS

This work was made possible with financial support by the Bonneville Power Administration (BPA) with Dr. Leon Kempner, Jr. as the responsible technical officer. This support is gratefully acknowledged.

# TABLE OF CONTENTS

# LIST OF FIGURES

## LIST OF FIGURES (CONT'D)

# LIST OF FIGURES (CONT'D)

# LIST OF FIGURES (CONT'D)

# LIST OF FIGURES (CONT'D)

# LIST OF FIGURES (CONT'D)

# LIST OF FIGURES (CONT'D)

## LIST OF FIGURES (CONT'D)

# LIST OF TABLES

## LIST OF TABLES (CONT'D)

# LIST OF TABLES (CONT'D)

## LIST OF TABLES (CONT'D)

# LIST OF TABLES (CONT'D)

## LIST OF TABLES (CONT'D)

# LIST OF TABLES (CONT'D)

# LIST OF TABLES (CONT'D)

## LIST OF TABLES (CONT'D)

# LIST OF TABLES (CONT'D)

# LIST OF TABLES (CONT'D)

# LIST OF TABLES (CONT'D)

# LIST OF TABLES (CONT'D)

# LIST OF TABLES (CONT'D)

# LIST OF TABLES (CONT'D)

# SECTION 1
# INTRODUCTION

Earlier studies on the assessment of seismic performance of seismically isolated electrical power transformers (Kitayama et al., 2016, 2017) utilized FEMA P695 procedures (FEMA, 2009) with the following limitations:

1) The peak ground acceleration (*PGA*) was selected as the measure of seismic intensity in the scaling of ground motions used in the incremental dynamic analysis for constructing fragility curves. While many studies of seismic assessment of electrical transformers used the *PGA* as a measure of seismic intensity (Shinozuka et al., 2007; Shumuta, 2007), the spectral acceleration at the fundamental period $S_a(T_1)$ of the analyzed structure is thought to be a more appropriate measure of intensity and has been used in building performance studies. FEMA (2009), Masroor and Mosqueda (2015) and Kitayama and Constantinou (2018a, 2018b, 2019a, 2019b) used the spectral acceleration at the fundamental period as the measure of ground motion intensity for seismically isolated structures. The selection of the measure of seismic intensity affects the scaling of the motions for analysis and accordingly affects the results. An example in Section 2 demonstrates the effect.

2) The fragility analysis did not account for spectral shape effects. The analysis used a large sample of actual ground motions and increased their intensity until failure was detected in an approach that only accounted for the ground-motion intensity in the assessment of failure. The approach did not account for the changing spectral shape of the motions as intensity is increased. Appendix A presents more details of the spectral shape effects and the procedure used to account for them in this study.

3) The fragility analysis results and the calculated probabilities of failure did not account for uncertainties other than the record-to-record variability (aleatory uncertainty) and only considered modeling uncertainties (epistemic uncertainty) through a limited bounding analysis by considering a range of model parameters. The analysis did not consider uncertainties related to the quality of the analysis model and the quality of construction of the transformer. Kitayama and Constantinou (2018a, 2018b, 2019a, 2019b) demonstrated the effects of uncertainties on the calculated probabilities of collapse of isolated buildings.

4) The study only considered far-field motions. Two of the ten considered sites in the transformer performance evaluation are in close proximity to active faults so that near-fault

motions (see Section 11.4.1 of ASCE/SEI 7-16 standard for identification; ASCE, 2017) should have been considered. Such motions often result in larger isolator displacement demands and thus may affect the failure performance.

This report presents an investigation of the limitations of past studies by considering other measures of seismic intensity, including spectral shape effects, incorporating uncertainties and performing representative analyses with near-field ground motions. The studies are performed with a representative transformer model out of those studied in Kitayama et al. (2016). The reader should first read the report of Kitayama et al. (2016) to be able to follow the work in this report. The selected transformer is the one with 420kip weight and an inclined (20 degrees) bushing of 4.3Hz or 7.7Hz or 11.3Hz frequency ($W$=420kip, $f_{AI}$=4.3 or 7.7 or 11.3Hz). Table 1-1 lists the properties of the three considered bushings. In its non-isolated version, the transformer model has an inherent damping of 3% of critical in all its modes. Inherent damping was realized in the analysis model by adding translational and rotational viscous damping elements at selected locations as described in Kitayama et al. (2016). When isolated, the transformer model was placed on top of the seismic isolation model and interconnected without any specification for global damping in order to avoid affecting the behavior of the isolation system.

Table 1-1 Properties of bushings used in study (after Kitayama et al., 2016)

| | Unit | Bushing 3 | Bushing 6 | Bushing 8 |
|---|---|---|---|---|
| Voltage capacity | kV | 550 | 196/230 | 550 |
| Total height | meter | 6.22 | 3.85 | 6.48 |
| Length over mounting flange: $H_{UB}$ | meter | 4.95 | 2.32 | 4.83 |
| Length below mounting flange: $H_{LB}$ | meter | 1.27 | 1.52 | 1.65 |
| Total weight | kN | 12.5 | 3.74 | 9.70 |
| Upper bushing weight: $m_{UB}\cdot g$ | kN | 9.59 | 1.99 | 6.98 |
| Location of upper bushing center of gravity: $H_{CM\_UB}$ | meter | 2.23 | 0.86 | 2.16 |
| Lower bushing weight: $m_{LB}\cdot g$ | kN | 2.46 | 1.30 | 2.27 |
| Location of lower bushing center of gravity: $H_{CM\_LB}$ | meter | 1.50 | 0.71 | 0.99 |
| Connection housing weight: $m_{CH}\cdot g$ | kN | 0.44 | 0.44 | 0.44 |
| Weight per unit length | kN/m | 1.94 | 0.86 | 1.43 |
| Distance to the flange (half of center pocket): $H_F$ | meter | 0.29 | 0.34 | 0.29 |
| Fixed frequency: $f_{Fix}$ | Hz | 9.36 | 21.00 | 9.35 |
| As-installed frequency: $f_{AI}$ | Hz | 4.25 | 11.25 | 7.70 |
| Material of insulator | - | Porcelain | Porcelain | Porcelain |

When seismically isolated, the horizontal isolators considered in the study were Triple FP isolators with ultimate displacement capacity of 17.7inch or 31.3inch without an inner restrainer. The fiction properties considered were for the lower bound conditions as those always resulted in the largest probabilities of failure ($W$=420kip, $f_{AI}$=4.3 or 7.7 or 11.3Hz, 20 degree inclined bushing, $D_{Capacity}$=17.7inch or 31.3inch, lower bound conditions with $\mu_1$=$\mu_4$=0.12 and $\mu_2$=$\mu_3$=0.08) (the values of the friction coefficient $\mu_1$ and $\mu_4$ apply for the outer sliding interfaces 1 and 4 and the values of the friction coefficient $\mu_2$ and $\mu_3$ apply for the inner sliding interfaces 2 and 3 as shown in Figure 1-1). The intermediate size isolator with $D_{Capacity}$=27.7inch considered in Kitayama et al. (2016) was not considered as its displacement capacity was close to the one with capacity of 31.3inch. When vertically isolated, the vertical isolation system consisted of four isolators, each with stiffness $K$=44kip/in, damping constant $C$=3.4kip-sec/in and a stroke capacity of 5inch. The system in the vertical direction had a frequency of 2.0Hz and a damping ratio of 0.50. Vertical isolation systems with either complete restraint against rocking (using a second very stiff base) (results identified as "without rocking") or free to rock (results identified as "with rocking") were analyzed.

Figures 1-1 and 1-2 present sections of the two isolators. Note that the two isolators differ in the displacement capacity and in the radius of curvature of the two main concave plates. This is important in understanding some of the results of this study.

The bushing failure acceleration limits considered were (a) 1$g$ or 2$g$ in the bushing transverse direction, and (b) 5$g$ in the bushing longitudinal direction. Other transformer failure criteria used in the fragility analysis were (a) exceedance of isolator horizontal displacement capacity $D_{Capacity}$, (b) isolator uplift exceeding 2inch, and (c) numerical instability in the analysis. The interested reader is referred to the report of Kitayama et al. (2016) for details on the selection of and justification for the acceleration limits of the bushings. In general, the failure criteria of the bushings are based on comparisons of predicted fragility curves of analyzed non-isolated transformers to empirical fragility curves based on observations of damage to electrical equipment in earthquakes.

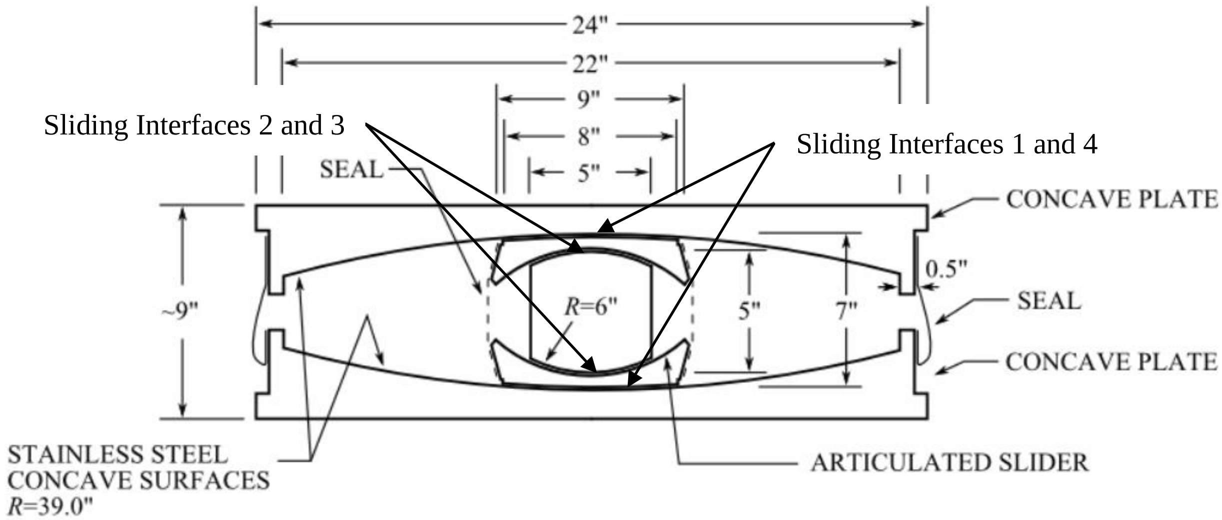


Figure 1-1 Section of smallest isolator with displacement capacity $D_{\text{Capacity}}$=17.7inch

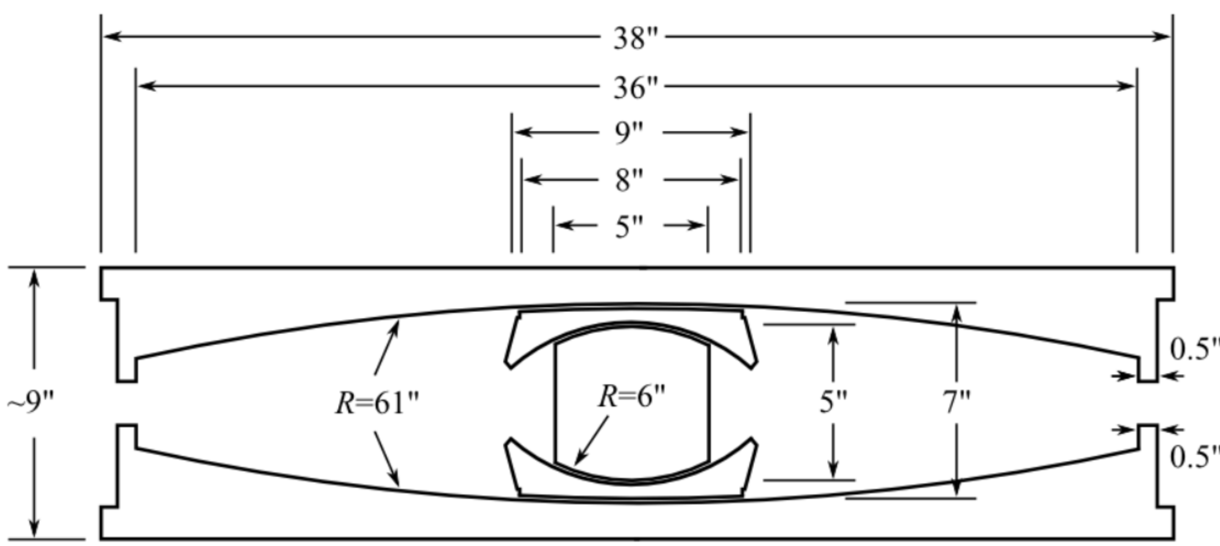


Figure 1-2 Section of largest isolator with displacement capacity $D_{\text{Capacity}}$=31.3inch

The locations considered for the transformer were the ten sites considered in the Kitayama et al. (2016) study (Vancouver, WA; Saranap, CA; Loma Linda, CA; Aberdeen, WA; Chehalis, WA; Hillsboro, OR; Eugene, OR; Wilsonville, OR; Curry County, OR; Troutdale, OR) (see Table 2-1 in Kitayama et al., 2016). Figure 1-3 shows these locations. These locations have different seismic hazard curves, which should result in different probabilities of failure in 50 years. For example, Chehalis, WA is a moderate seismicity site, Loma Linda, CA is a high seismicity site, and

Troutdale, OR is a low seismicity site. Figures 1-4 to 1-13 presents seismic hazard curves for the 10 locations at periods of zero, 0.1, 0.2, 2 and 3second. These periods are relevant to the analysis in this report. The seismic hazard curves were obtained from the United States Geological Survey (http://geohazards.usgs.gov/hazardtool/application.php) in the form of the annual frequency of exceedance as function of the spectral acceleration at selected values of period for the site locations and soil conditions.


Figure 1-3 Location of transformers considered in this study

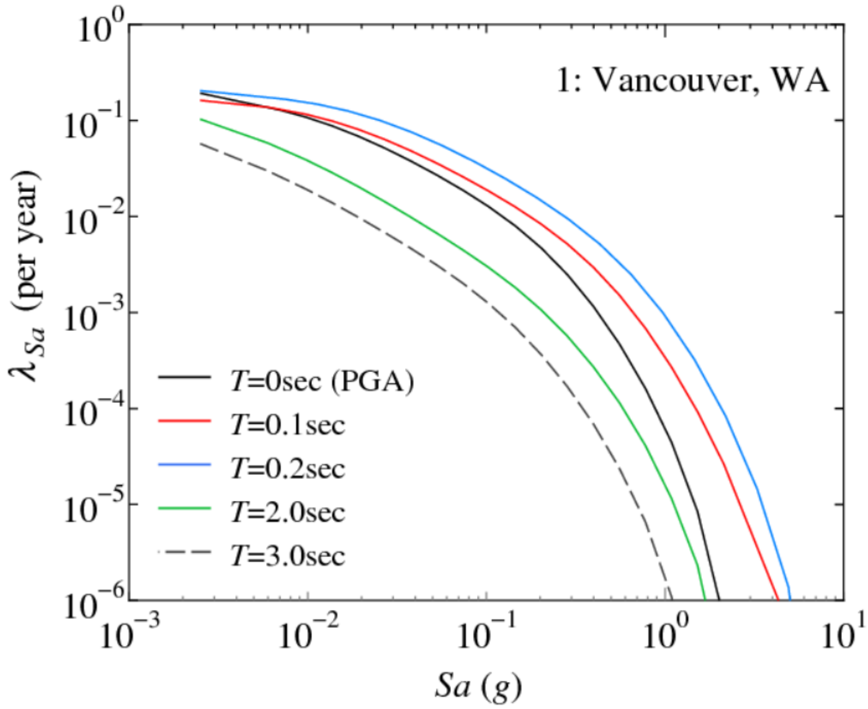


Figure 1-4 Seismic hazard curves for zero, 0.1, 0.2, 2 and 3sec period at Vancouver, WA

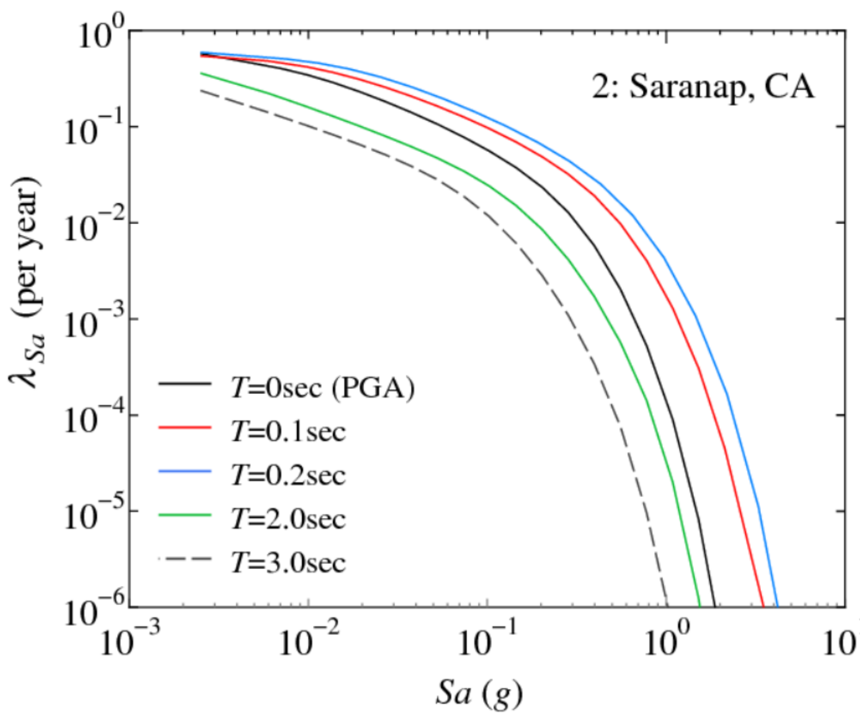


Figure 1-5 Seismic hazard curves for zero, 0.1, 0.2, 2 and 3sec period at Saranap, CA

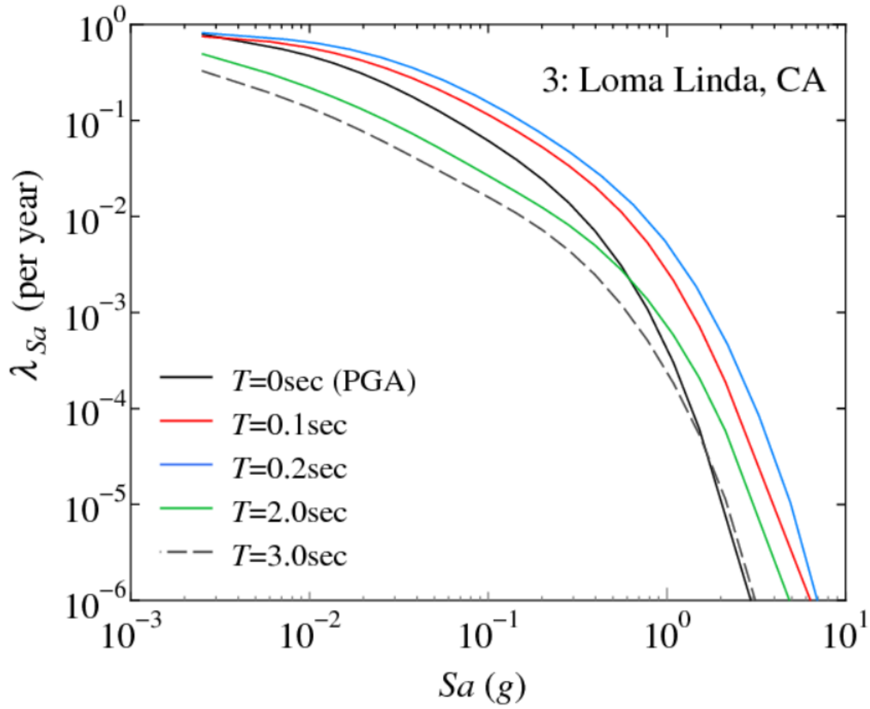


Figure 1-6 Seismic hazard curves for zero, 0.1, 0.2, 2 and 3sec period at Loma Linda, CA

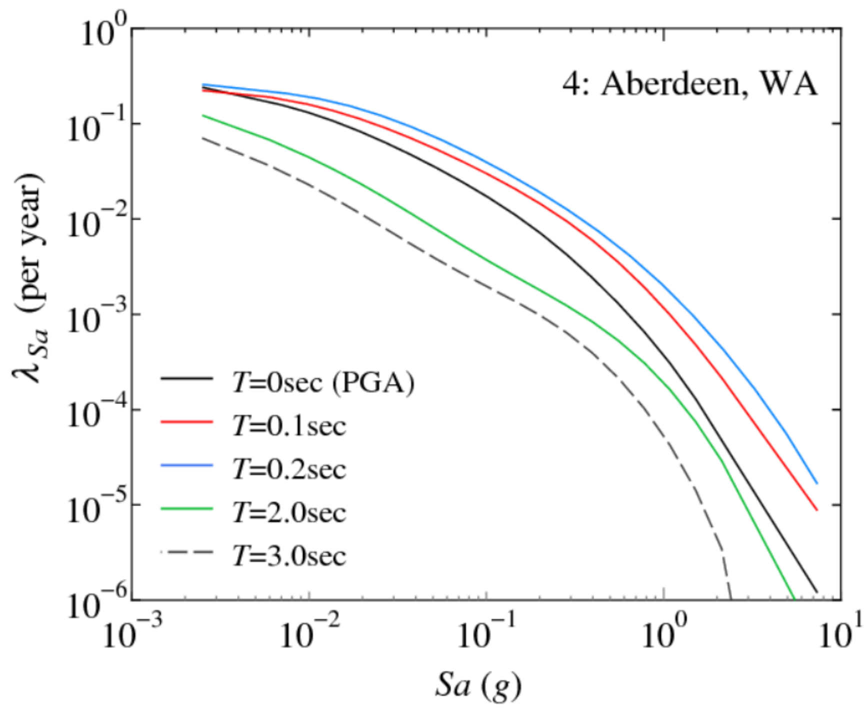


Figure 1-7 Seismic hazard curves for zero, 0.1, 0.2, 2 and 3sec period at Aberdeen, WA

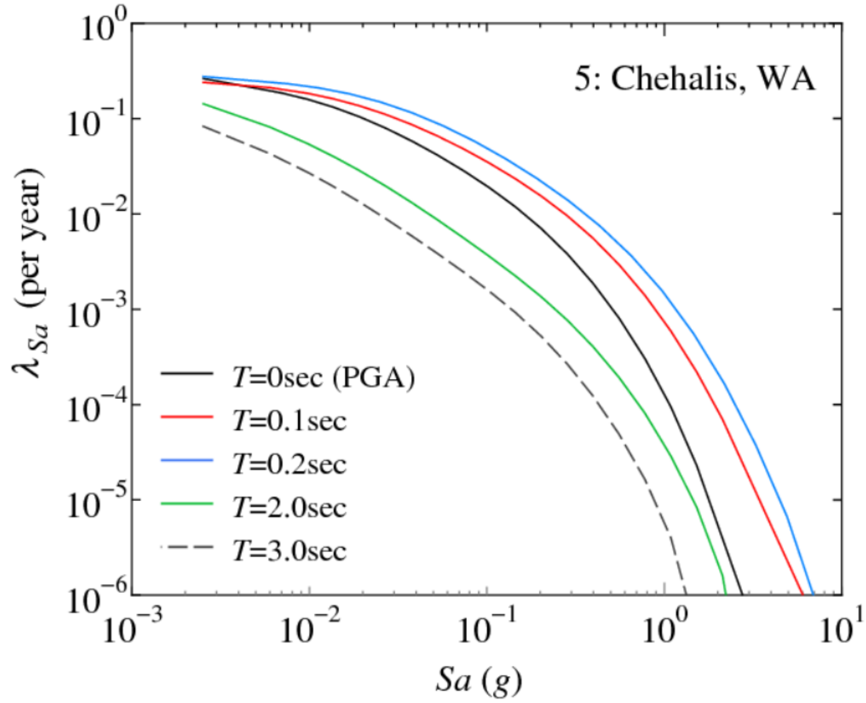


Figure 1-8 Seismic hazard curves for zero, 0.1, 0.2, 2 and 3sec period at Chehalis, WA

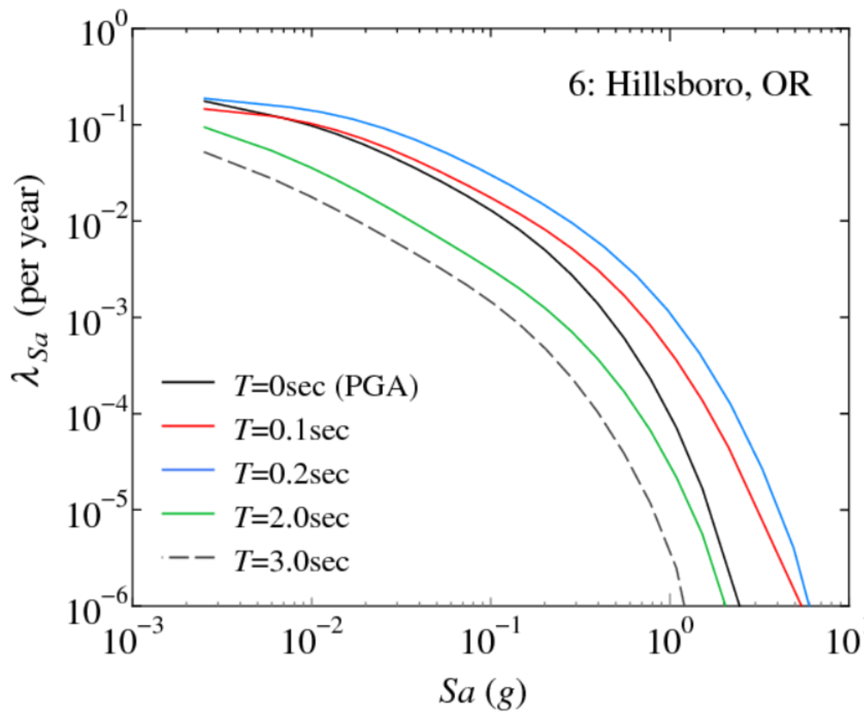


Figure 1-9 Seismic hazard curves for zero, 0.1, 0.2, 2 and 3sec period at Hillsboro, OR

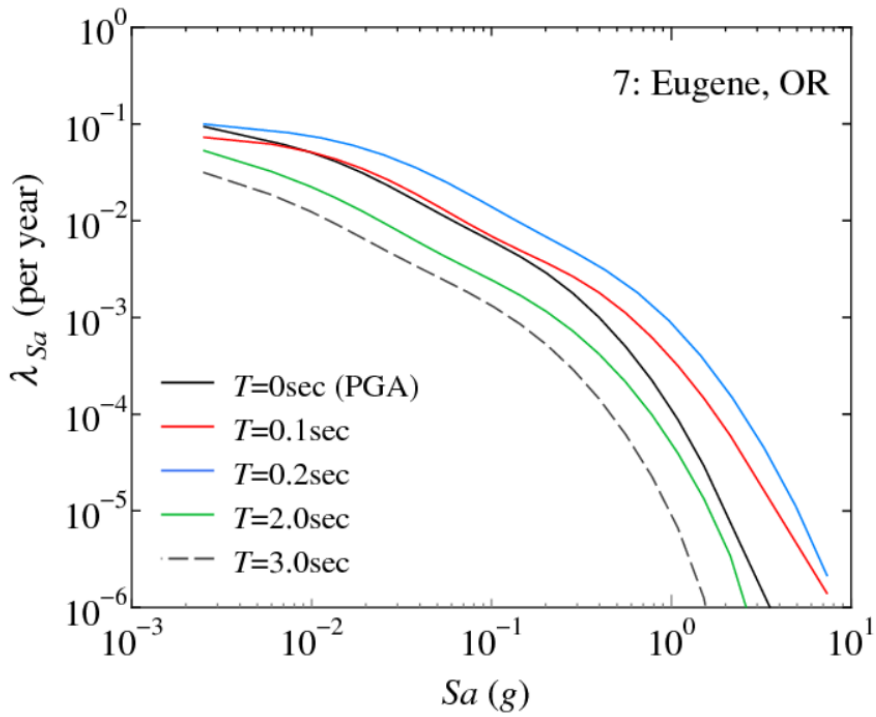


Figure 1-10 Seismic hazard curves for zero, 0.1, 0.2, 2 and 3sec period at Eugene, OR

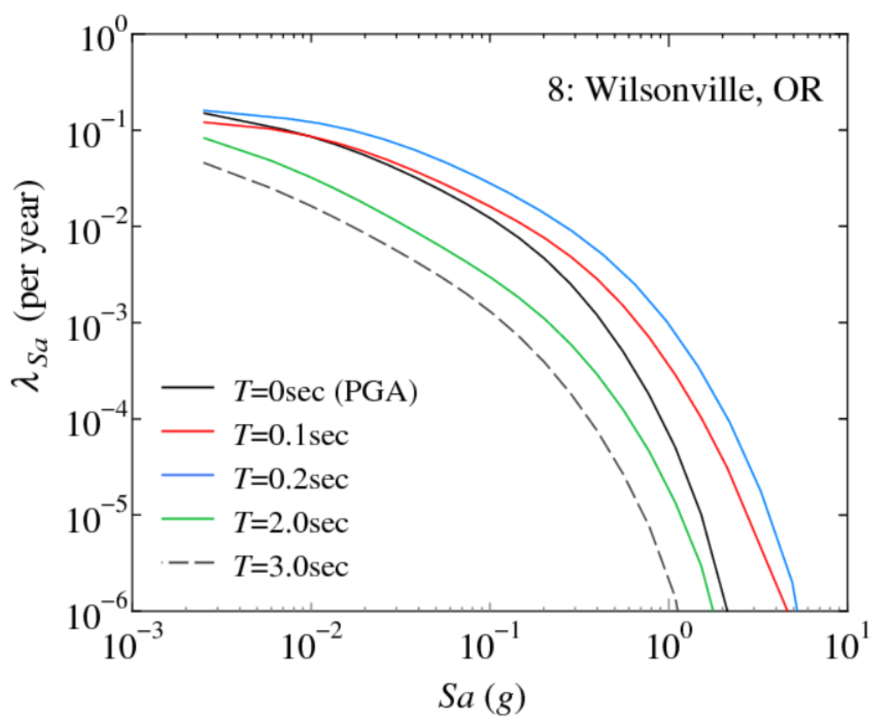


Figure 1-11 Seismic hazard curves for zero, 0.1, 0.2, 2 and 3sec period at Wilsonville, OR

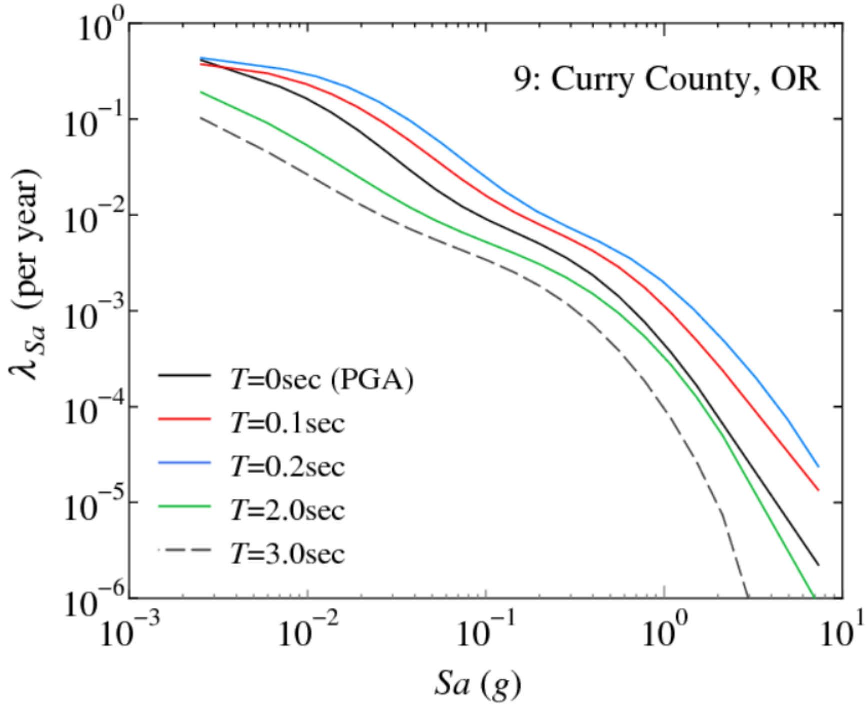


Figure 1-12 Seismic hazard curves for zero, 0.1, 0.2, 2 and 3sec period at Curry County, OR

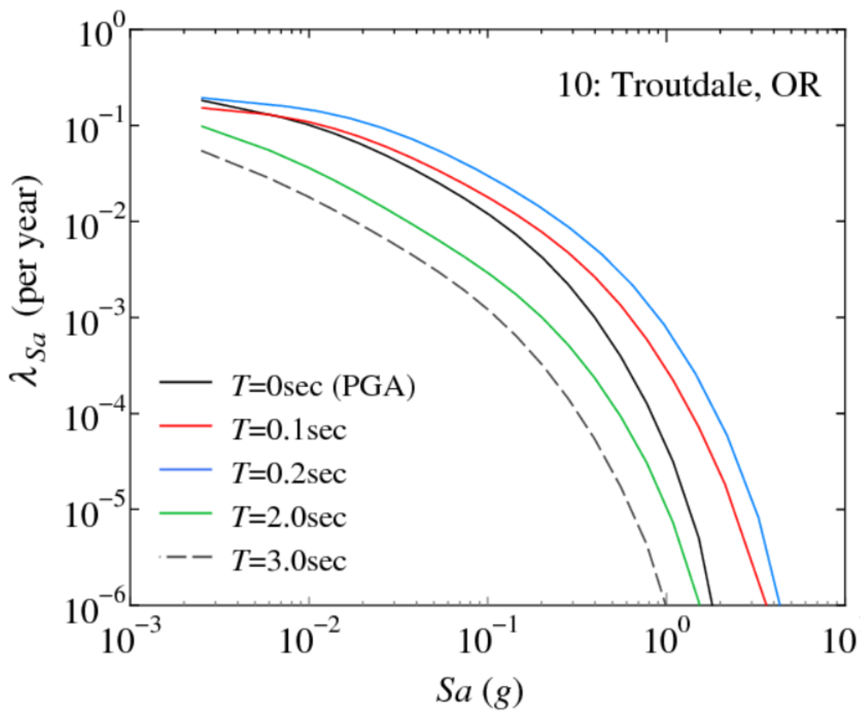


Figure 1-13 Seismic hazard curves for zero, 0.1, 0.2, 2 and 3sec period at Troutdale, OR

Results obtained for near-field and far-field motions, both without correction for spectral shape effects, reveal that for the studied isolated transformers there is a small difference between the results of the two sets of motions. We suggest that the considered isolators of low stiffness and large displacement capacity for near-field applications did not experience failure and did not cause any significant increase in the bushing acceleration as the isolator displacement demand increased due to the effects of the near-field motions. It was concluded that near-field motions do not appreciably change the results obtained for the far-field motions when isolators of appropriately larger displacement capacity and low stiffness are used.

Results obtained for far-field motions show that, in general, scaling of the ground motions based on the spectral acceleration at the fundamental period or the effective period results in significant increases in the probability of failure for the isolated transformers, which are then significantly moderated by corrections for the spectral shape effects. By comparison, the changes in the probability of failure of the studied non-isolated transformers were small due to the fact that the fundamental period was very small so that the spectral acceleration at the fundamental period was very close to the PGA which was used in the earlier studies for the scaling.

Based on the new results in this report, combined horizontal-vertical seismic isolation systems offer the lowest probabilities of failure for all cases of transformer and isolation system parameters, and for all considered sites. Horizontal only isolation offers no or offers insignificant advantages over non-isolation when the bushing transverse acceleration limit is 2g. However, horizontal only isolation offers important advantages over non-isolation when the bushing transverse acceleration limit is 1g.

The results of this report, documented in numerous tables, may be used to decide on the benefits offered by a seismic isolation system depending on the location of the transformer and the form and properties of the seismic isolation system. The benefit is assessed on the basis of the probability of failure in 50 years of lifetime. The information may also be used to assess the seismic performance of electric transmission networks under scenarios of component failures.

# SECTION 2
# EVALUATING THE EFFECT OF SEISMIC GROUND MOTION INTENSITY MEASURES ON FRAGILITY

Figure 2-1 illustrates how the selection of the measure of the ground motion intensity affects the calculation of the probability of failure (fragility curve) and by extension the mean annual frequency of failure $\lambda_F$ and the probability of failure over a specified time. The figure shows the 5%-damped response spectra of ground motions used in Incremental Dynamic Analysis (IDA) for constructing the fragility curves. The ground motions are first scaled so that their 5%-damped spectral acceleration values are the same at a selected period. Figure 2-1 shows the result of the scaling when the selected period is (near) zero (so that the intensity measure is the *PGA*) and another period $T_i$ (so that the intensity measure is $S_a$ ($T_i$)). Response history analysis is then performed by increasing the ground motion intensity in small steps while detecting failure in each step. Conceptually, the results should be relatively insensitive to the conditioning period provided that the records are representative of the site in consideration and the number of records is large enough. However, in this study the same set of records is used for several sites and, therefore, it is expected that the scaling procedure should have some effect.

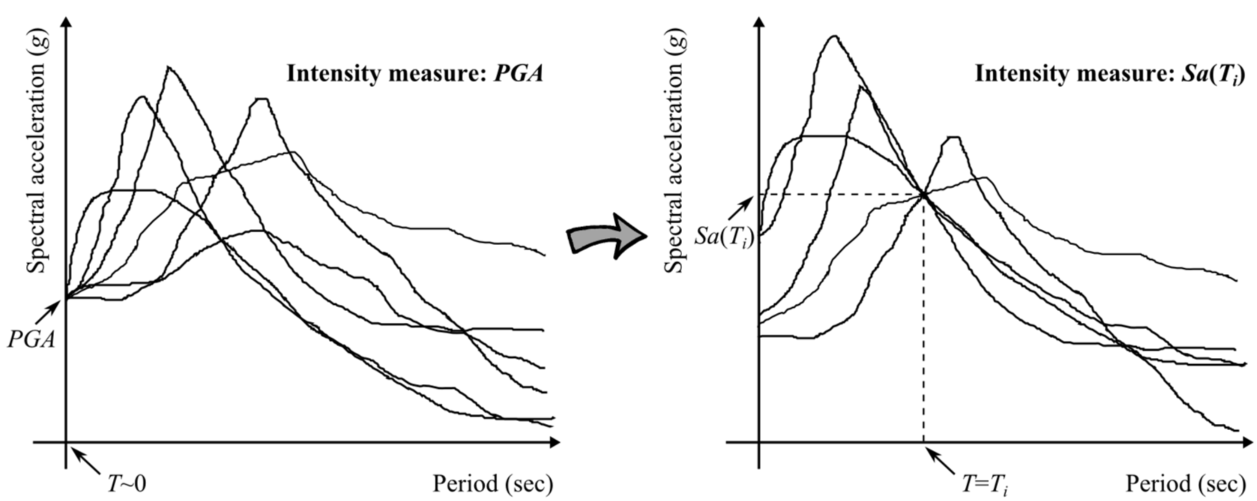


Figure 2-1 Scaling of ground motions so that the spectral acceleration values of the horizontal components are the same at zero period (left) and at period $T_i$ (right)

Studies reported in Kitayama et al. (2016, 2017) presented results on the mean annual frequency of failure $\lambda_F$ and the probability of failure in a lifetime of 50 years of several isolated and non-isolated electrical transformers at the ten locations shown in Figure 1-3. These results of $\lambda_F$ were obtained by using the *PGA* as the measure of ground motion intensity. A procedure is described below for converting the results acquired on the basis of *PGA* scaling to new results based on scaling of the ground motions using the spectral acceleration at an arbitrary period $T_i$, which is now considered a variable. The information used from the results of the earlier studies is the peak ground acceleration at failure of the transformer in each conducted IDA with the scaling of the ground motions based on the *PGA* as the measure of seismic intensity.

Consider the case of the far-field motions studied in Kitayama et al. (2016, 2017). There are 40 pairs of horizontal-vertical components of ground motions. The following analysis steps are followed to convert the results:

1. Start with a period $T_i$. We considered 300 different values of period, that is, $i$=1 to 300, with the minimum value of $T_i$ being 0.02second, the maximum value being 6.0second and the increment being 0.02second.

2. From the $j^{th}$ un-scaled acceleration response spectrum of each of 40 horizontal ground motions ($j$=1 to 40), obtain ratio of $PGA_j$ to $Sa_j(T_i)$:

$$Ratio_{Sa/PGA_j} = \frac{Sa_j(T_i)}{PGA_j} \tag{2-1}$$

   Note that the value of $Ratio_{Sa/PGA}$ remains constant as the motions are scaled for conducting the IDA.

3. The value of the peak ground acceleration at failure of a particular transformer $PGA_{F,j}$ for the $j^{th}$ ground motion is known from Kitayama et al. (2016, 2017). Obtain the spectral acceleration at period $T_i$ that causes failure of transformer or $S_{aF,j}(T_i)$ as follows:

$$Sa_{F,j}(T_i) = PGA_{F,j} \cdot Ratio_{Sa/PGA_j} \tag{2-2}$$

4. Calculate the median of the natural logarithm of $Sa_{F,j}(T_i)$:

$$\widehat{Sa}_F(T_i) = \text{Median}\langle Sa_{F,1}(T_i), Sa_{F,2}(T_i), Sa_{F,3}(T_i), \ldots, Sa_{F,40}(T_i)\rangle \tag{2-3}$$

Quantity $\widehat{Sa}_F(T_i)$ is the measure of intensity (spectral acceleration at period $T_i$) that results in a 50% probability of failure of the transformer (that is, 20 of 40 analyses result in failure).

5. Calculate the standard deviation of the natural logarithm of $Sa_{F,j}(T_i)$:

$$\beta_{RTRi} = \mathrm{std}\langle \ln\left[Sa_{F,1}(T_i)\right], \ln\left[Sa_{F,2}(T_i)\right], \ln\left[Sa_{F,3}(T_i)\right], \dots, \ln\left[Sa_{F,40}(T_i)\right]\rangle \quad (2\text{-}4)$$

   Quantity $\beta_{RTRi}$ is the dispersion coefficient that accounts for the record-to-record variability in the ground motions. Note that "std" is the operation for calculating the standard deviation.

   Parameters $\widehat{Sa}_F(T_i)$ and $\beta_{RTRi}$ describe the fragility curve as a lognormal distribution given by Equation (2-5) in the form of the cumulative distribution function:

$$P_F \mid Sa(T_i)(x) = \int_0^x \frac{1}{s\beta_{RTRi}\sqrt{2\pi}} \exp\left[-\frac{\left(\ln s - \ln \hat{S}a_{\mathrm{F}}(T_i)\right)^2}{2\beta_{RTRi}^{\ 2}}\right] ds \quad (2\text{-}5)$$

   In Equation (2-5), $P_F|S_a(T_i)$ is the fragility curve (probability of failure given the value of $S_a(T_i)$) (variable x representing the spectral acceleration at period $T_i$).

6. For the location of the transformer, construct the seismic hazard curve for period $T_i$ (see figure 2-3 in Kitayama et al., 2016).

7. Calculate the mean annual frequency of failure, $\lambda_{F,i}$, for $i^{th}$ period $T_i$, by using information on the fragility curve (from steps 3 and 4) and the seismic hazard curve (from step 5). Quantity $\lambda_{F,i}$ is given by Equation (2-6) (Krawinkler et al., 2006) in which $(P_F|Sa)$ is the fragility curve (probability of failure given the value of $S_a$) and $\frac{d\lambda_{Sa}}{d(Sa)}$ is the slope of the seismic hazard curve.

$$\lambda_{F,i} = \int_0^\infty (P_F|Sa) \left|\frac{d\lambda_{Sa}}{d(Sa)}\right| \cdot d(Sa) \quad (2\text{-}6)$$

Note that in the calculation of Equation (2-6) the seismic hazard curve is obtained from the curves shown in Figures 1-4 to 1-14 by interpolation at the value of the period used for the scaling of the records.

8. The probability of failure over the lifetime of the transformer, $n$ years, can be calculated by assuming that the earthquake occurrence follows a Poisson distribution:

$$P_{\mathrm{F},i}(n \cdot \text{years}) = 1 - \exp(-\lambda_{\mathrm{F}} \cdot n) \tag{2-7}$$

9. Repeat for different period ($T_i$ where $i$=1 to 300) and calculate $P_{\mathrm{F},i}$ for each value of period.

Note that in this process of converting the available results based on scaling using the *PGA* as the measure of intensity to one based on the spectral acceleration at another value of the period for the intensity measure, every pair of horizontal-vertical ground motion used in the analysis maintained its original as-recorded characteristics. That is, while all horizontal components used in the analysis have the same value of their spectral acceleration at the selected period, the vertical components have different spectral acceleration values at the same period. Guidelines for the scaling of the vertical ground motions for seismic performance evaluation do not exist in FEMA (2009). Some guidance provided for design practice in NIST (2011) implies that is appropriate to use horizontal and vertical ground motions scaled to represent conditional horizontal and vertical spectra where the conditioning periods in the horizontal and vertical directions are related to modal properties in those two directions. That is for the horizontally only isolated transformer the vertical conditioning period should be zero and for the horizontally-vertically isolated transformer should be 0.5sec. The procedure then to perform a failure performance evaluation would be to generate suites of such pairs of motions, each for several seismic intensities starting from very low to very high (say return periods of 50 to 10000 years) and perform dynamic analysis. Kitayama and Constantinou (2018a, 2019a) applied this approach to the seismic performance of isolated buildings but without the vertical ground motion.

Figures 2-2 to 2-37 present results for the case of isolators with $D_{\mathrm{Capacity}}$=17.7inch for three out of the ten studied sites: Chehalis, WA, Loma Linda, CA and Troutdale, OR. Each of these figures presents graphs of the calculated probability of failure in a lifetime of 50 years $P_{\mathrm{F}}$ (50 years) as function of the selected period $T_i$ used in the scaling of the motions. Vertical lines in these figures show the value of the fundamental period of the analyzed system. For the non-isolated transformer this period is $T_1$=0.24sec (=1/4.3Hz) or 0.13sec (=1/7.7Hz) or 0.088sec (=1/11.3Hz). For the isolated transformers, the period used is average effective isolation period in the horizontal direction at the displacement of 13.0inch (a displacement just prior to initiation of stiffening in the smallest isolator) and in the lower bound conditions. This period was calculated as 2.1sec for the smallest isolator and as 2.7sec for the largest isolator. The difference is due to differences in the radii of curvature of the two isolators. The average value $T_{eff}$=$T_1$=2.4sec was used for all isolated transformers. When isolated in the vertical direction, the system has linear elastic and linear viscous behavior with vertical frequency of 2.0Hz and a corresponding damping ratio of 0.50. The corresponding vertical period is 0.5sec.

The results demonstrate that the selection of the period for scaling the ground motions has an effect on the probability of failure, which is significant in the case of the isolated transformers. When the scaling of ground motions is based on the short periods of 0.088sec to 0.23sec, which is appropriate for the case of the non-isolated transformers, there is a small reduction of the probability of failure by comparison to when using the zero period for scaling. When the scaling is based on the effective period of 2.4sec, which is appropriate for the case of the horizontally isolated transformers, there is an increase of the probability of failure by comparison to when using the zero period for scaling. As an example, consider the Loma Linda, CA location in Figures 2-6 and 2-7 for the non-isolated and the horizontally isolated transformers, respectively. Consider the case of 1*g* limit for the bushing transverse acceleration. For the non-isolated transformer, the probability of failure in 50 years is 0.398 when scaling is based on the *PGA* (as reported in Kitayama et al., 2016) and is 0.343 when scaling is based on the spectral acceleration at the fundamental period of 0.13sec. For the isolated transformer, the probability of failure in 50 years is 0.102 when scaling is based on the *PGA* (as reported in Kitayama et al., 2016) and is 0.301 when scaling is based on the spectral acceleration at the fundamental period of 2.4sec. Based on these results, one would conclude that horizontal isolation does not offer any important advantage (probability of failure of 0.301 versus 0.343 when non-isolated). However, the data in Figures 2-2 to 2-37 have not been corrected for the effects of spectral shape. When the correction is made, as described in Section 3, the results change drastically. The probability of failure for the non-isolated transformer changes from 0.343 to 0.297 and for the isolated transformer from 0.301 to 0.100. The adjusted probabilities of failure now justify the use of horizontal isolation.

***As-installed bushing of 7.7Hz***

**Isolator $D_{Capacity}$=17.7inch, Lower Bound Conditions with $\mu_1=\mu_4=0.12$ and $\mu_2=\mu_3=0.08$**

**Location Chehalis, WA**

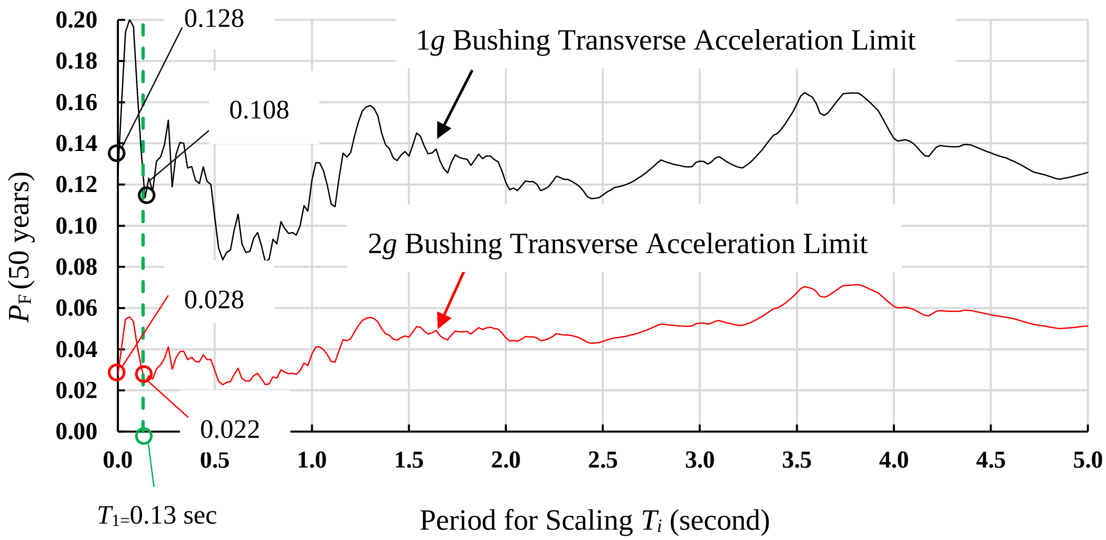


Figure 2-2 Probability of failure in lifetime of 50 years of non-isolated transformer ($W$=420kip, $f_{AI}$=7.7Hz, inclined bushing) located at Chehalis, WA as function of period used for scaling the ground motions

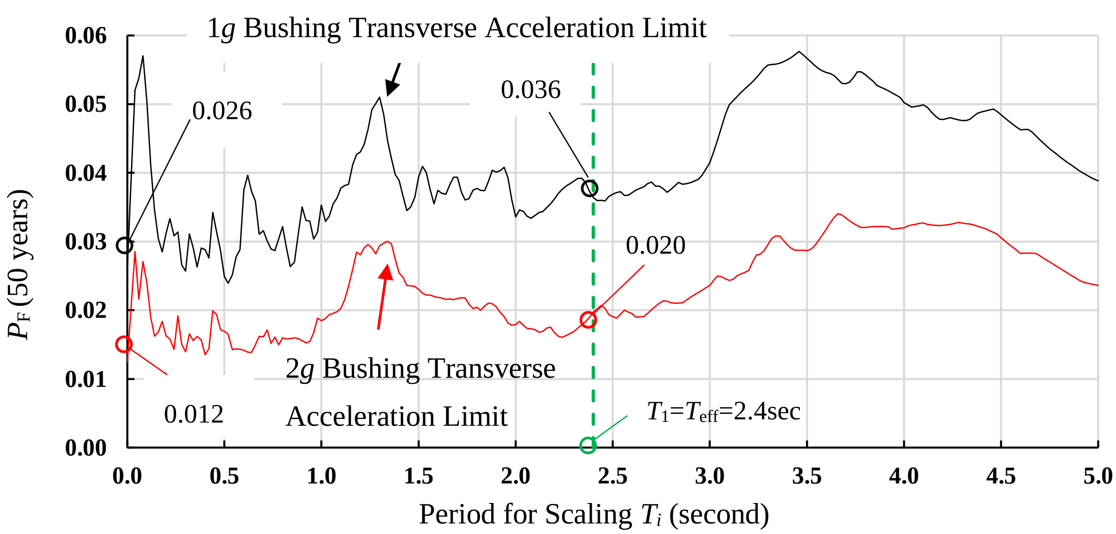


Figure 2-3 Probability of failure in lifetime of 50 years of horizontally isolated transformer ($W$=420kip, $f_{AI}$=7.7Hz, inclined bushing, $D_{Capacity}$=17.7inch, lower bound) located at Chehalis, WA as function of period used for scaling the ground motions

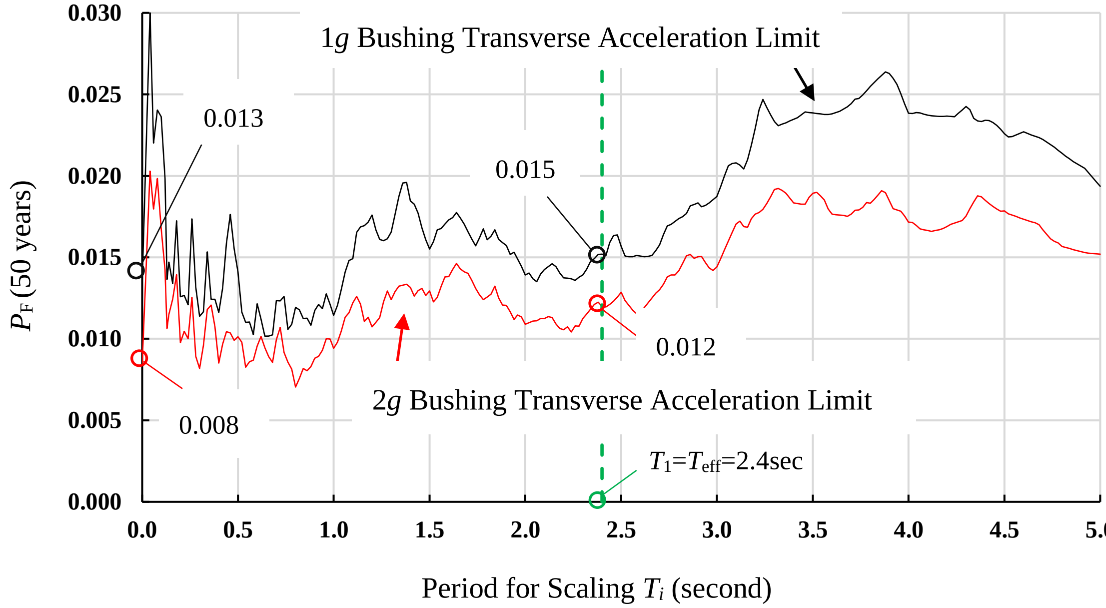


Figure 2-4 Probability of failure in lifetime of 50 years of horizontally-vertically isolated transformer without rocking ($W$=420kip, $f_{AI}$=7.7Hz, inclined bushing, $D_{Capacity}$=17.7inch, lower bound) located at Chehalis, WA as function of period used for scaling the ground motions

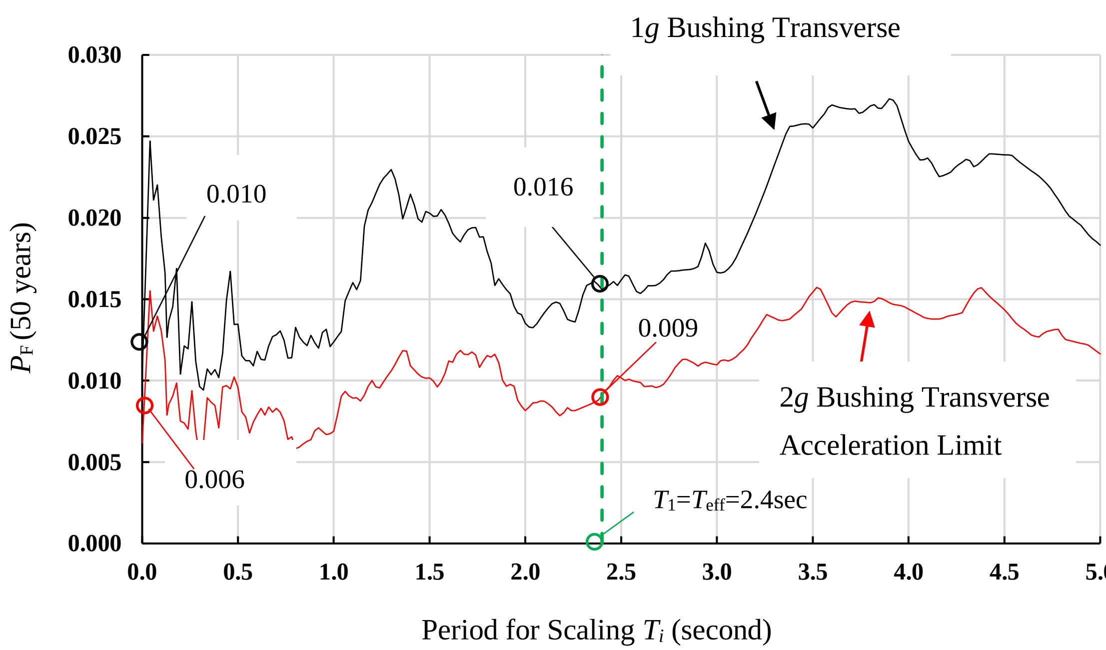


Figure 2-5 Probability of failure in lifetime of 50 years of horizontally-vertically isolated transformer with rocking ($W$=420kip, $f_{AI}$=7.7Hz, inclined bushing, $D_{Capacity}$=17.7inch, lower bound) located at Chehalis, WA as function of period used for scaling the ground motions

***As-installed bushing of 7.7Hz***

**Isolator $D_{Capacity}$=17.7inch, Lower Bound Conditions with $\mu_1=\mu_4=0.12$ and $\mu_2=\mu_3=0.08$**

**Location Loma Linda, CA**

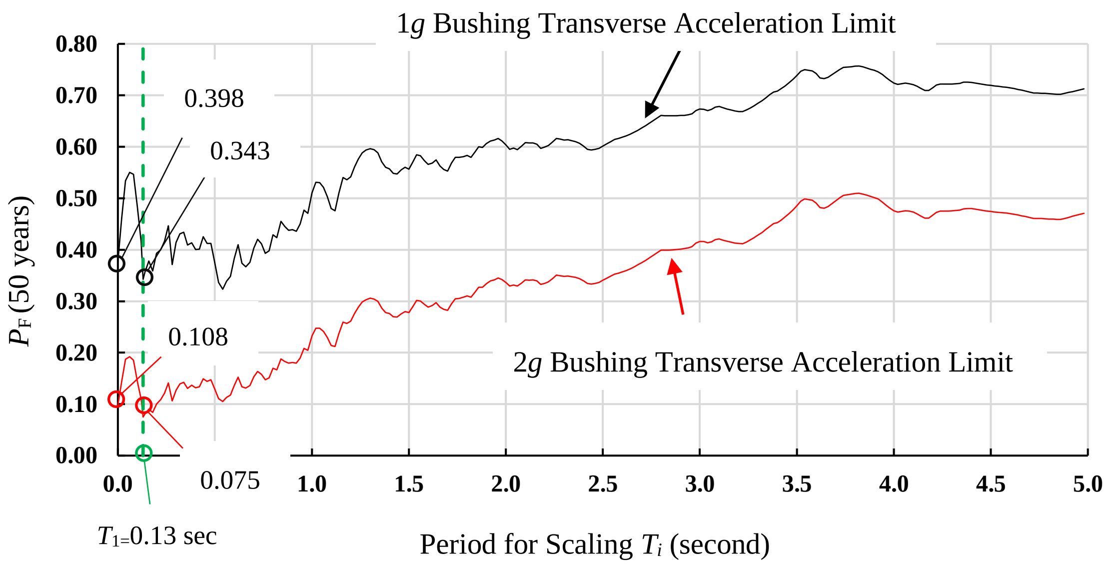


Figure 2-6 Probability of failure in lifetime of 50 years of non-isolated transformer ($W$=420kip, $f_{AI}$=7.7Hz, inclined bushing) located at Loma Linda, CA as function of period used for scaling the ground motions

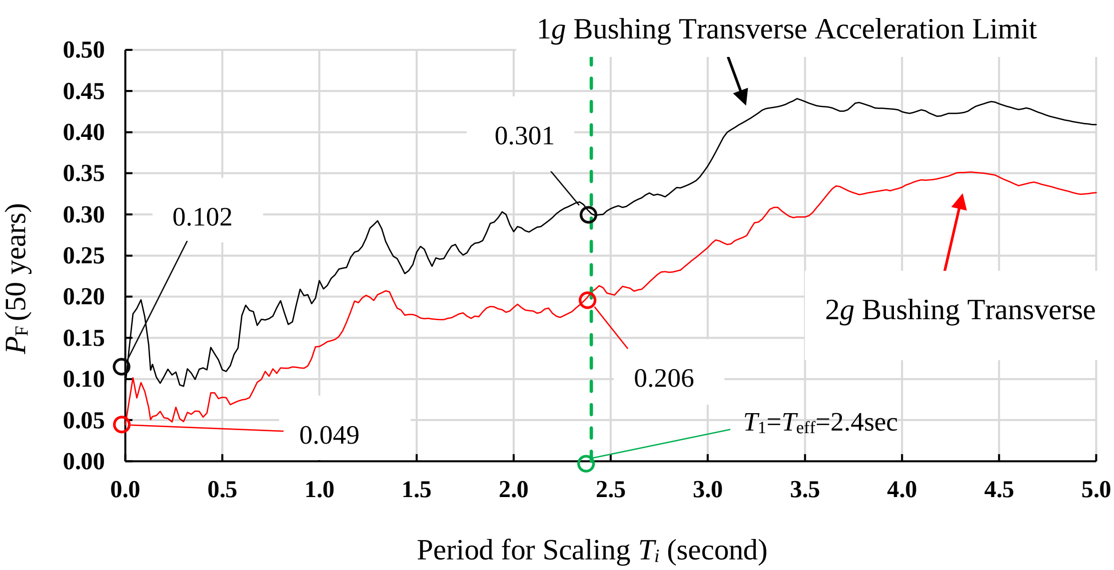


Figure 2-7 Probability of failure in lifetime of 50 years of horizontally isolated transformer ($W$=420kip, $f_{AI}$=7.7Hz, inclined bushing, $D_{Capacity}$=17.7inch, lower bound) located at Loma Linda, CA as function of period used for scaling the ground motion

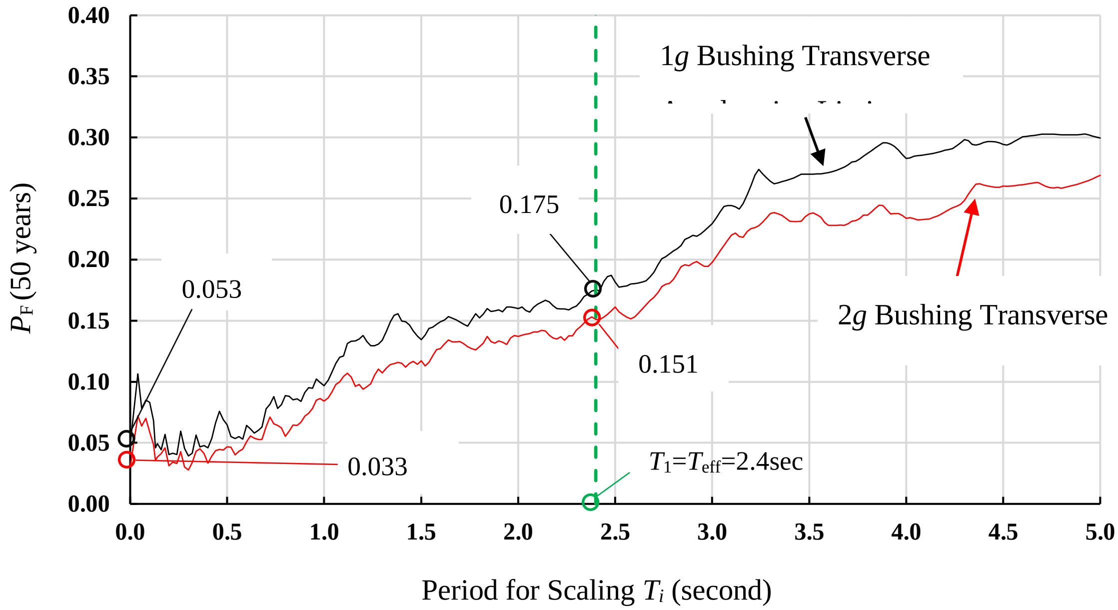


Figure 2-8 Probability of failure in lifetime of 50 years of horizontally-vertically isolated transformer without rocking ($W$=420kip, $f_{AI}$=7.7Hz, inclined bushing, $D_{Capacity}$=17.7inch, lower bound) located at Loma Linda, CA as function of period used for scaling the ground motions

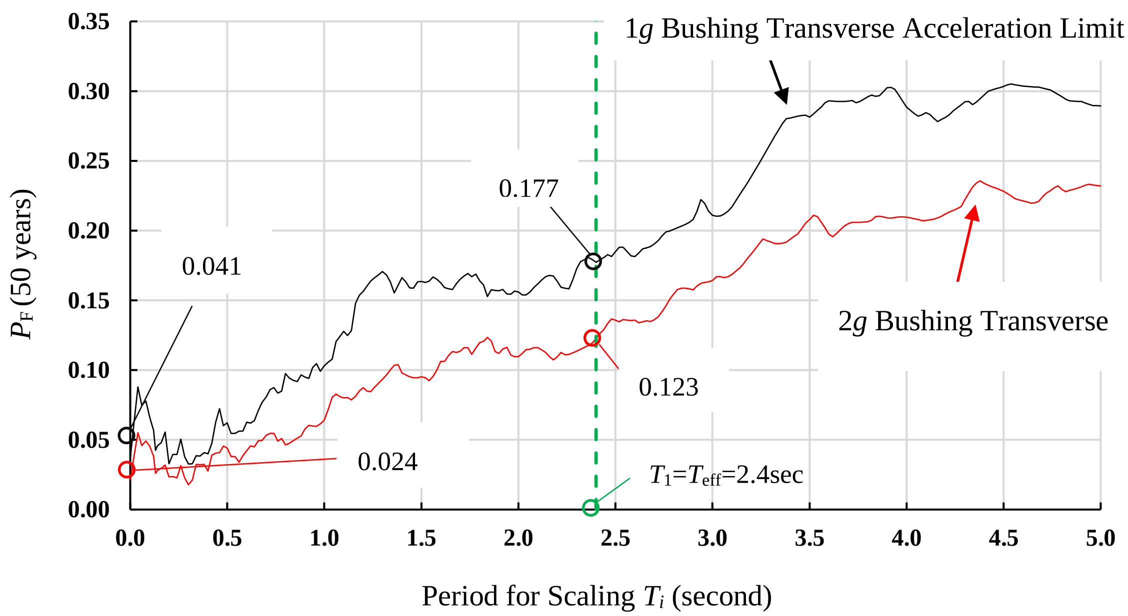


Figure 2-9 Probability of failure in lifetime of 50 years of horizontally-vertically isolated transformer with rocking ($W$=420kip, $f_{AI}$=7.7Hz, inclined bushing, $D_{Capacity}$=17.7inch, lower bound) located at Loma Linda, CA as function of period used for scaling the ground motions

***As-installed bushing of 7.7Hz***

**Isolator $D_{Capacity}$=17.7inch, Lower Bound Conditions with $\mu_1=\mu_4=0.12$ and $\mu_2=\mu_3=0.08$**

**Location Troutdale, OR**

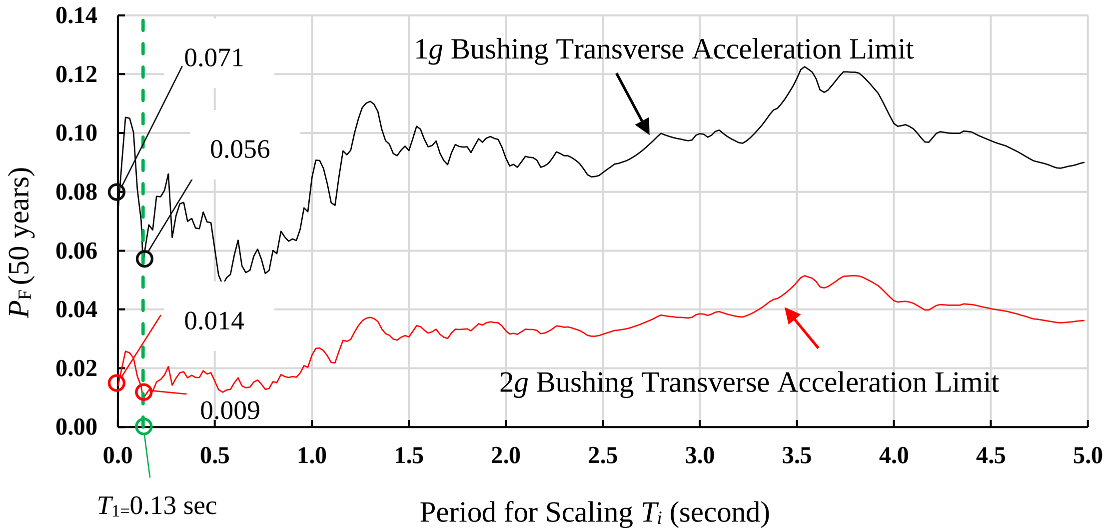


Figure 2-10 Probability of failure in lifetime of 50 years of non-isolated transformer ($W$=420kip, $f_{AI}$=7.7Hz, inclined bushing) located at Troutdale, OR as function of period used for scaling the ground motions

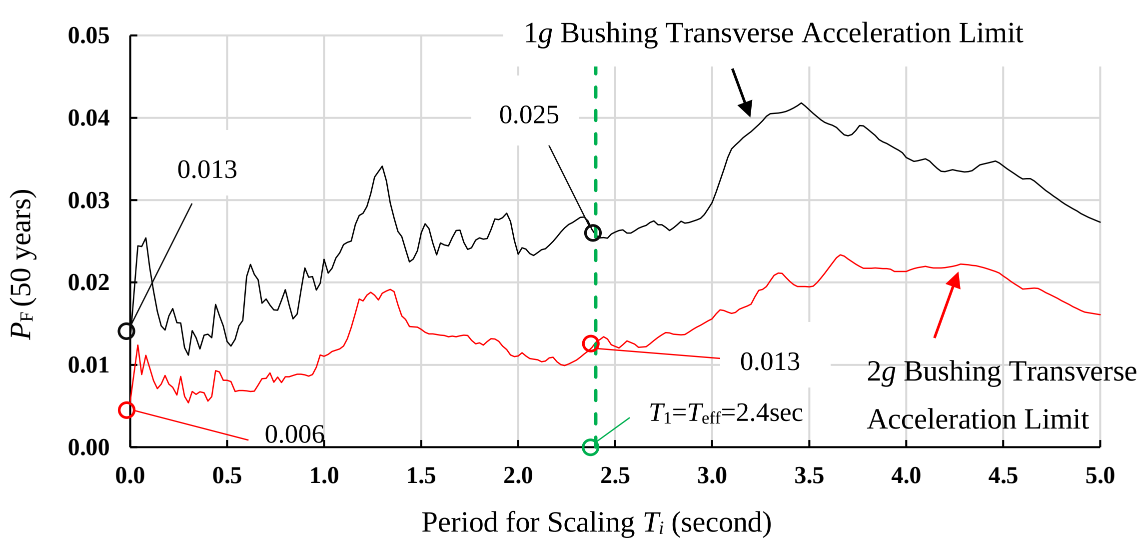


Figure 2-11 Probability of failure in lifetime of 50 years of horizontally isolated transformer ($W$=420kip, $f_{AI}$=7.7Hz, inclined bushing, $D_{Capacity}$=17.7inch, lower bound) located at Troutdale, OR as function of period used for scaling the ground motions

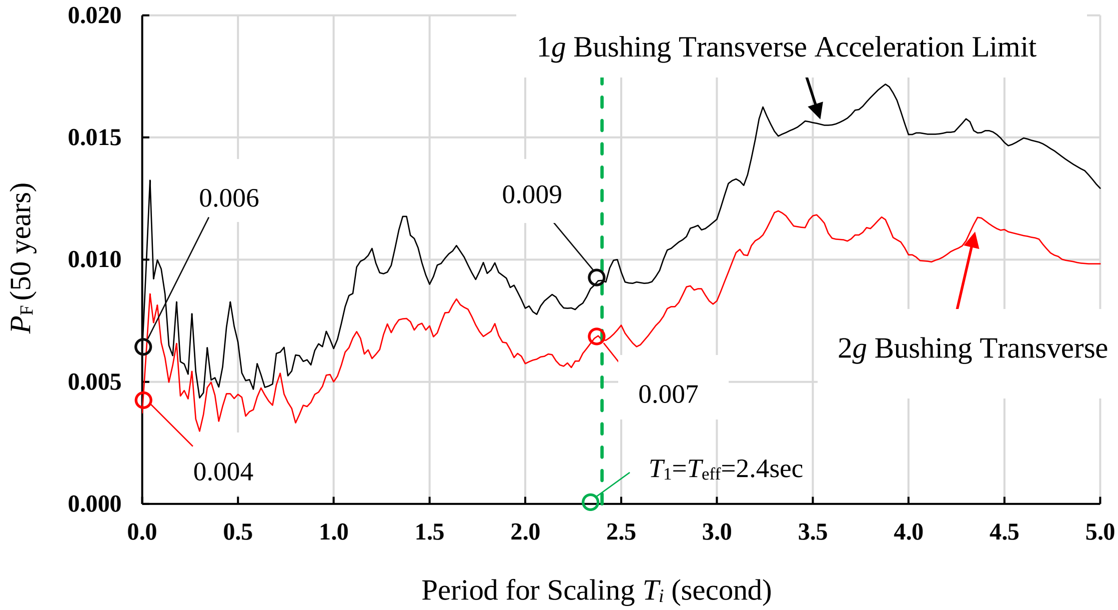


Figure 2-12 Probability of failure in lifetime of 50 years of horizontally-vertically isolated transformer without rocking ($W$=420kip, $f_{AI}$=7.7Hz, inclined bushing, $D_{Capacity}$=17.7inch, lower bound) located at Troutdale, OR as function of period used for scaling the ground motions

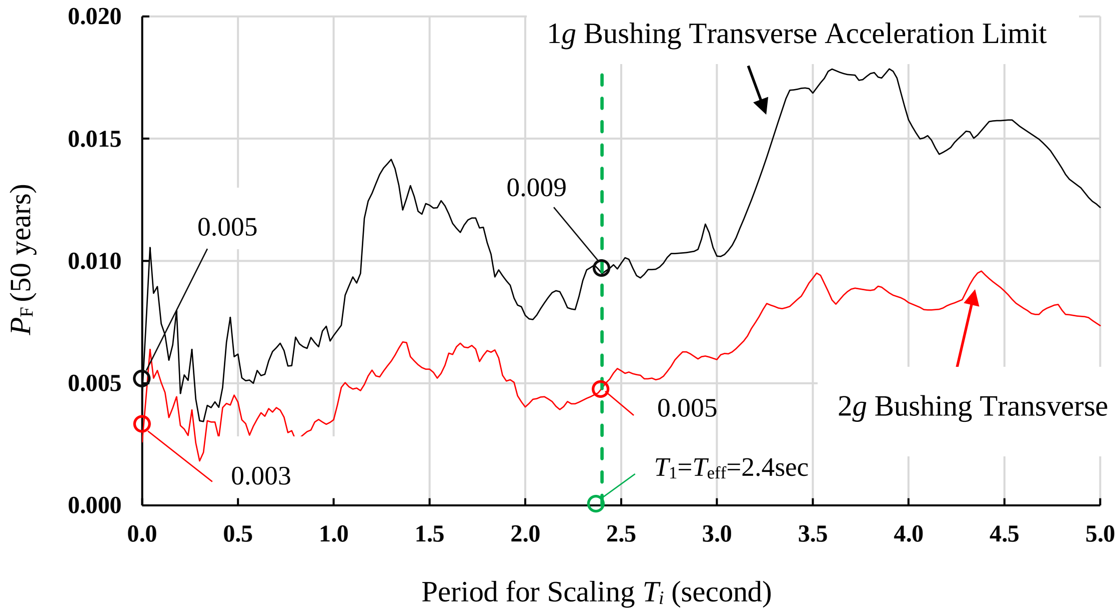


Figure 2-13 Probability of failure in lifetime of 50 years of horizontally-vertically isolated transformer with rocking ($W$=420kip, $f_{AI}$=7.7Hz, inclined bushing, $D_{Capacity}$=17.7inch, lower bound) located at Troutdale, OR as function of period used for scaling the ground motions

***As-installed bushing of 4.3Hz***

**Isolator $D_{Capacity}$=17.7inch, Lower Bound Conditions with $\mu_1=\mu_4$=0.12 and $\mu_2=\mu_3$=0.08**

**Location Chehalis, WA**

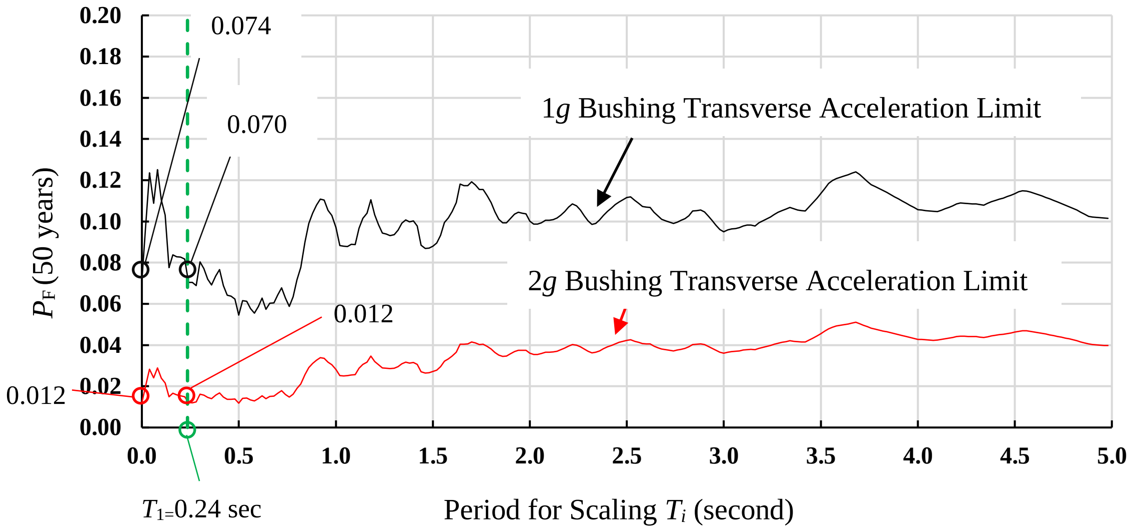


Figure 2-14 Probability of failure in lifetime of 50 years of non-isolated transformer ($W$=420kip, $f_{AI}$=4.3Hz, inclined bushing) located at Chehalis, WA as function of period used for scaling the ground motions

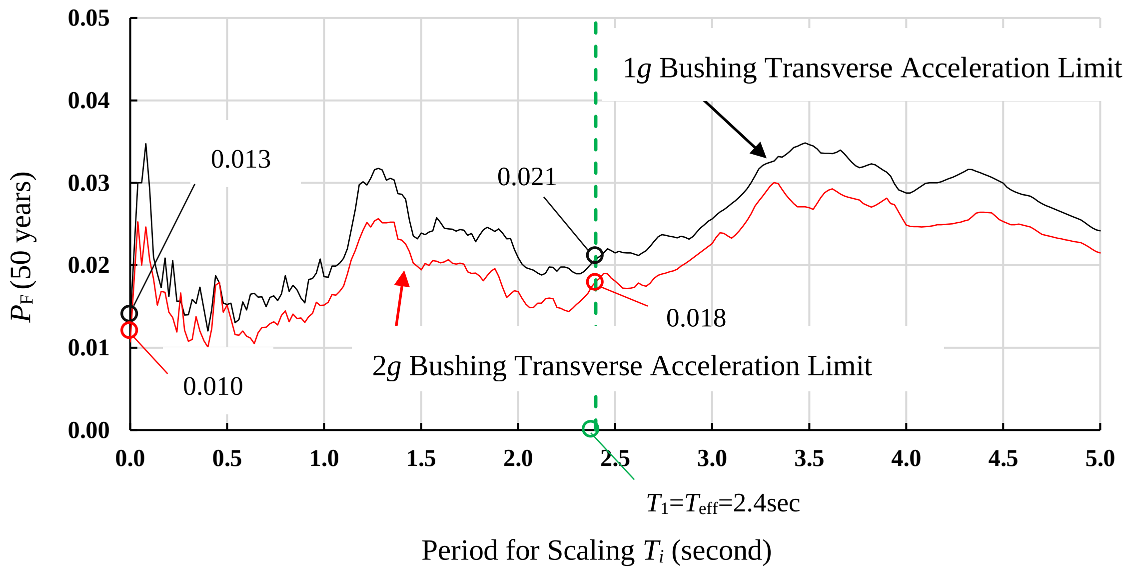


Figure 2-15 Probability of failure in lifetime of 50 years of horizontally isolated transformer ($W$=420kip, $f_{AI}$=4.3Hz, inclined bushing, $D_{Capacity}$=17.7inch, lower bound) located at Chehalis, WA as function of period used for scaling the ground motions

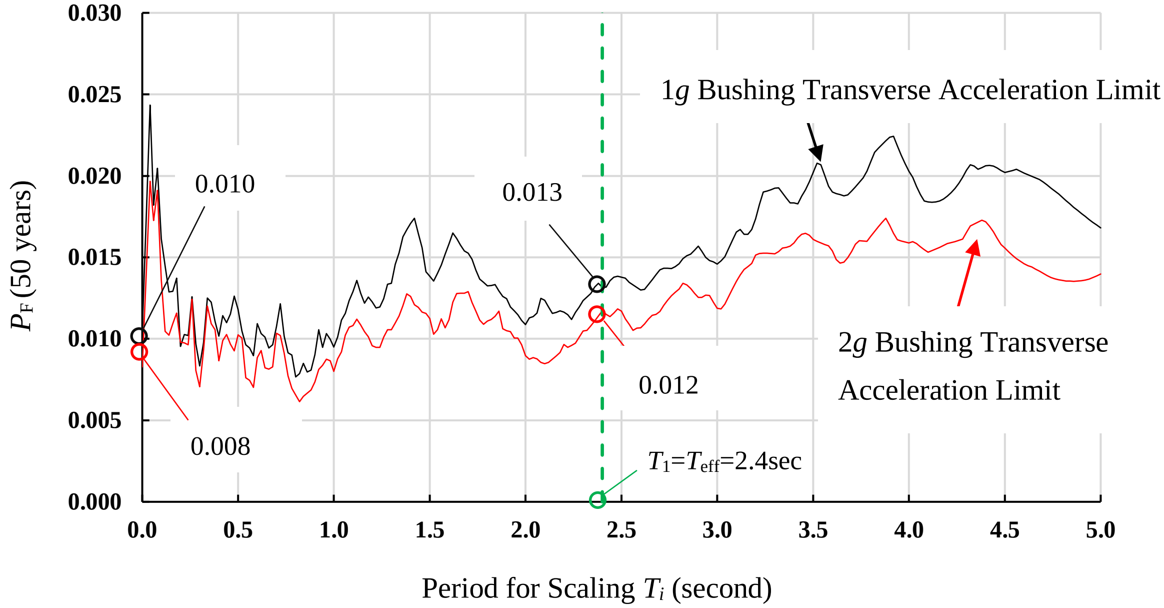


Figure 2-16 Probability of failure in lifetime of 50 years of horizontally-vertically isolated transformer without rocking ($W$=420kip, $f_{AI}$=4.3Hz, inclined bushing, $D_{Capacity}$=17.7inch, lower bound) located at Chehalis, WA as function of period used for scaling the ground motions

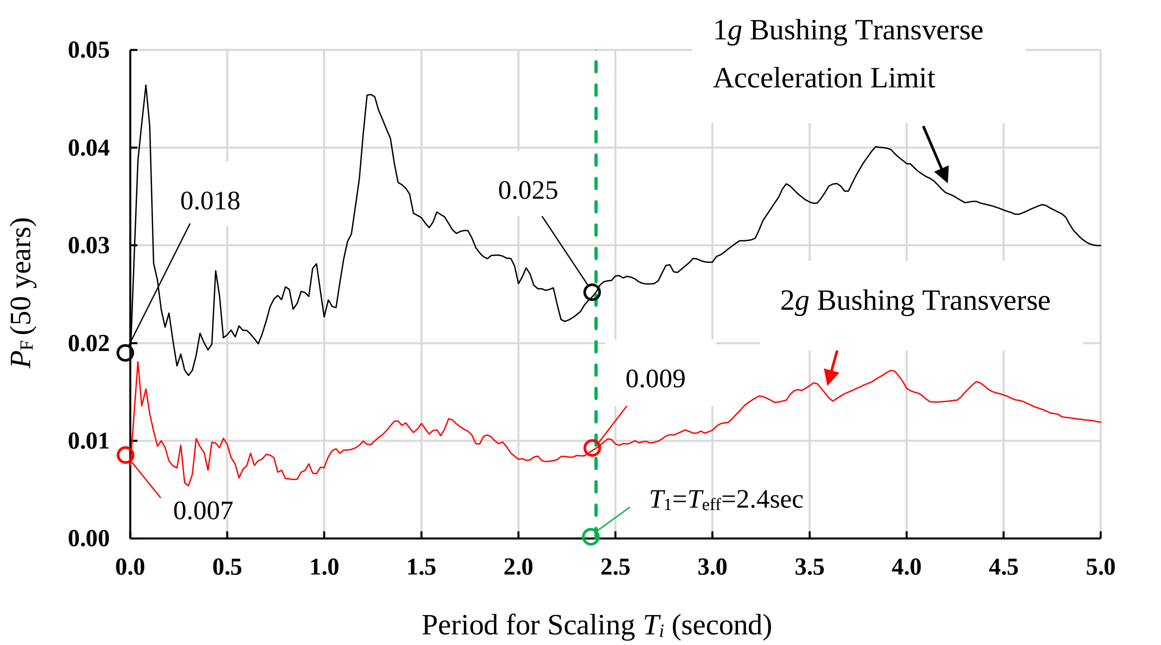


Figure 2-17 Probability of failure in lifetime of 50 years of horizontally-vertically isolated transformer with rocking ($W$=420kip, $f_{AI}$=4.3Hz, inclined bushing, $D_{Capacity}$=17.7inch, lower bound) located at Chehalis, WA as function of period used for scaling the ground motions

***As-installed bushing of 4.3Hz***

**Isolator $D_{Capacity}$=17.7inch, Lower Bound Conditions with $\mu_1=\mu_4=0.12$ and $\mu_2=\mu_3=0.08$**

**Location Loma Linda, CA**

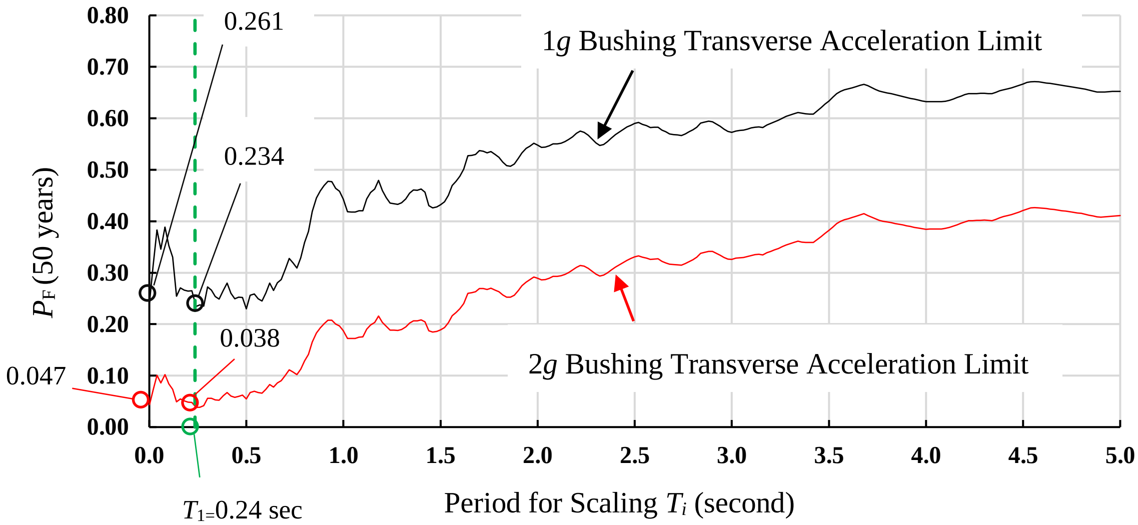


Figure 2-18 Probability of failure in lifetime of 50 years of non-isolated transformer ($W$=420kip, $f_{AI}$=4.3Hz, inclined bushing) located at Loma Linda, CA as function of period used for scaling the ground motions

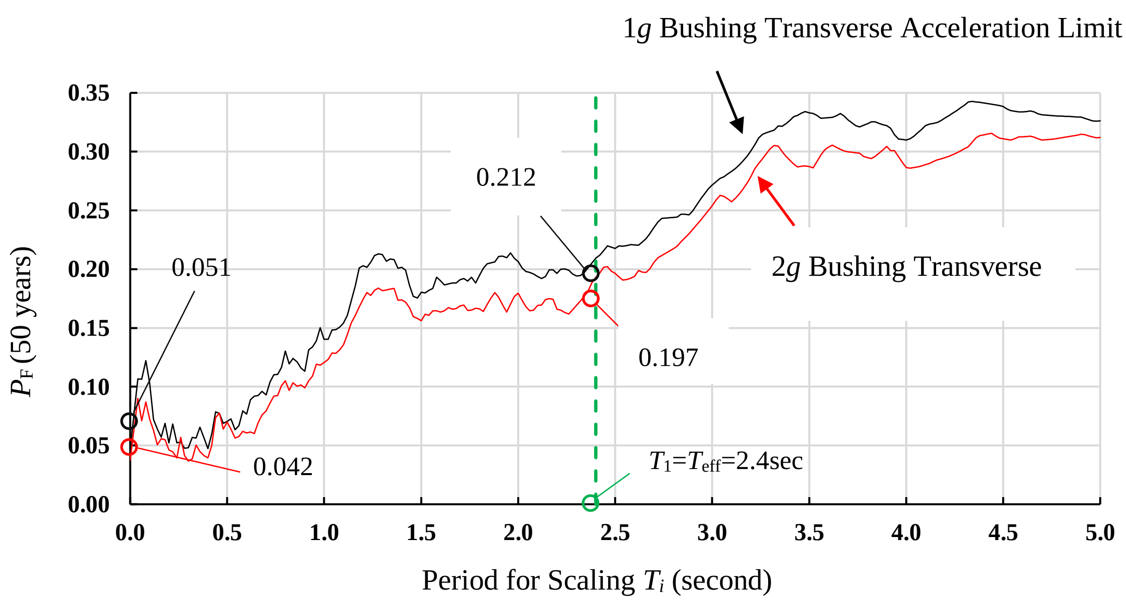


Figure 2-19 Probability of failure in lifetime of 50 years of horizontally isolated transformer ($W$=420kip, $f_{AI}$=4.3Hz, inclined bushing, $D_{Capacity}$=17.7inch, lower bound) located at Loma Linda, CA as function of period used for scaling the ground motions

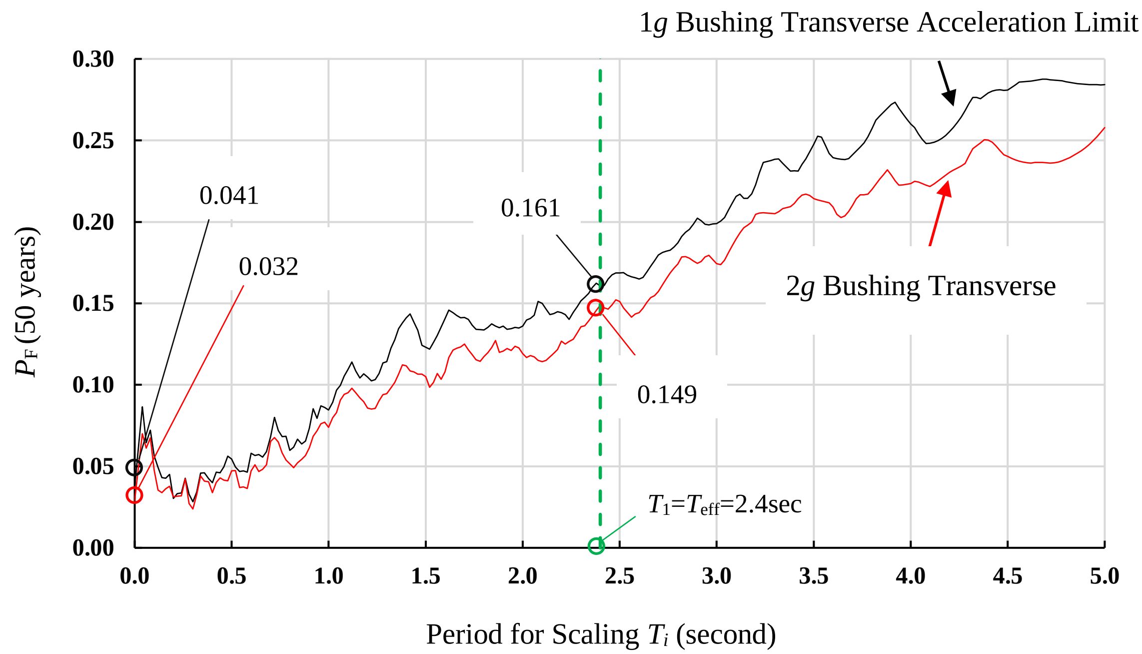


Figure 2-20 Probability of failure in lifetime of 50 years of horizontally-vertically isolated transformer without rocking ($W$=420kip, $f_{AI}$=4.3Hz, inclined bushing, $D_{Capacity}$=17.7inch, lower bound) located at Loma Linda, CA as function of period used for scaling the ground motions

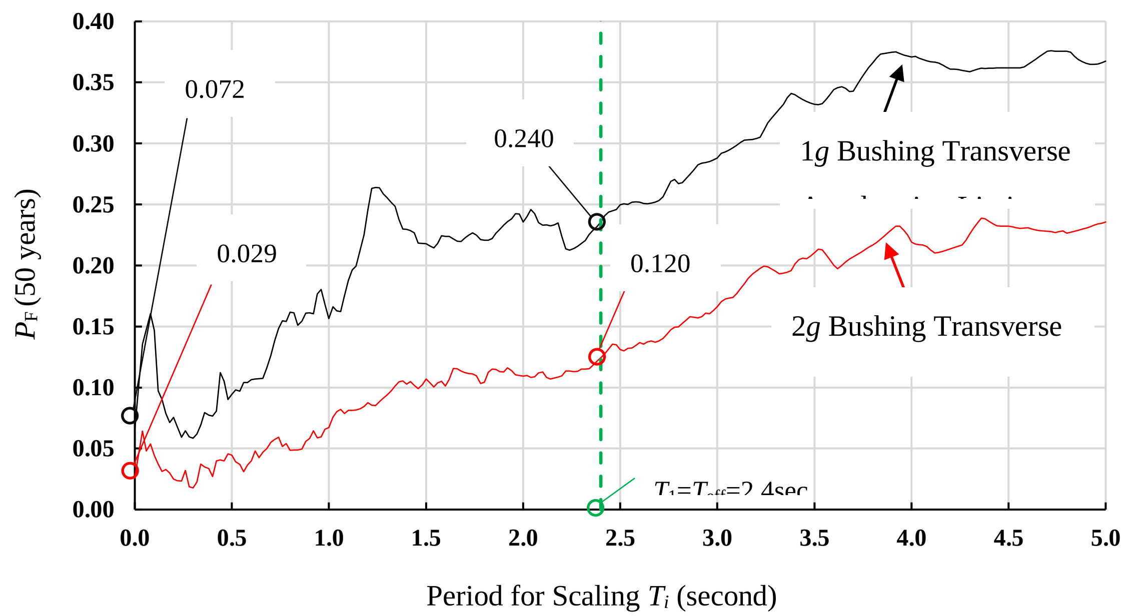


Figure 2-21 Probability of failure in lifetime of 50 years of horizontally-vertically isolated transformer with rocking ($W$=420kip, $f_{AI}$=4.3Hz, inclined bushing, $D_{Capacity}$=17.7inch, lower bound) located at Loma Linda, CA as function of period used for scaling the ground motions

***As-installed bushing of 4.3Hz***

**Isolator $D_{Capacity}$=17.7inch, Lower Bound Conditions with $\mu_1=\mu_4$=0.12 and $\mu_2=\mu_3$=0.08**

**Location Troutdale, OR**

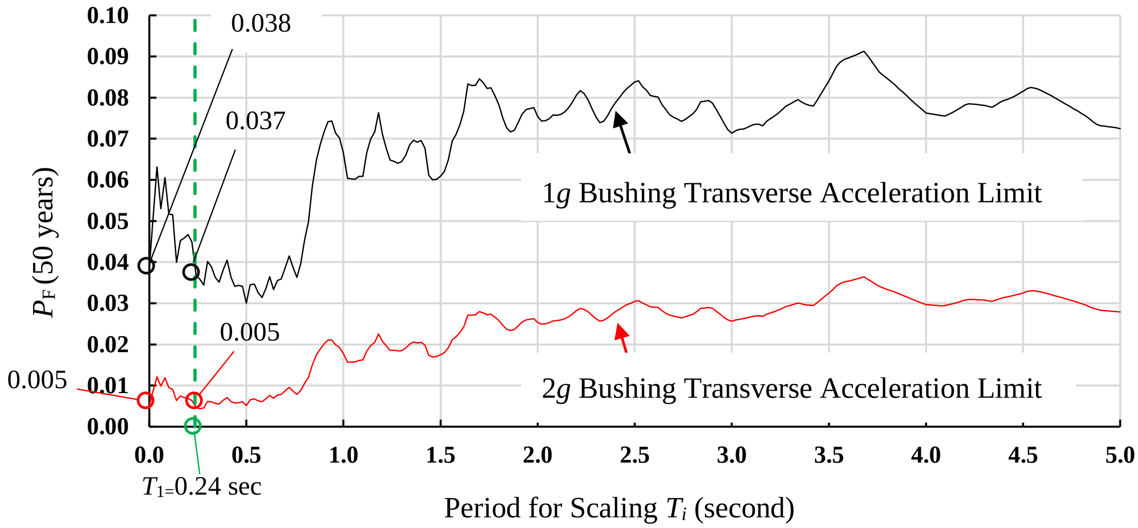


Figure 2-22 Probability of failure in lifetime of 50 years of non-isolated transformer ($W$=420kip, $f_{AI}$=4.3Hz, inclined bushing) located at Troutdale, OR as function of period used for scaling the ground motions

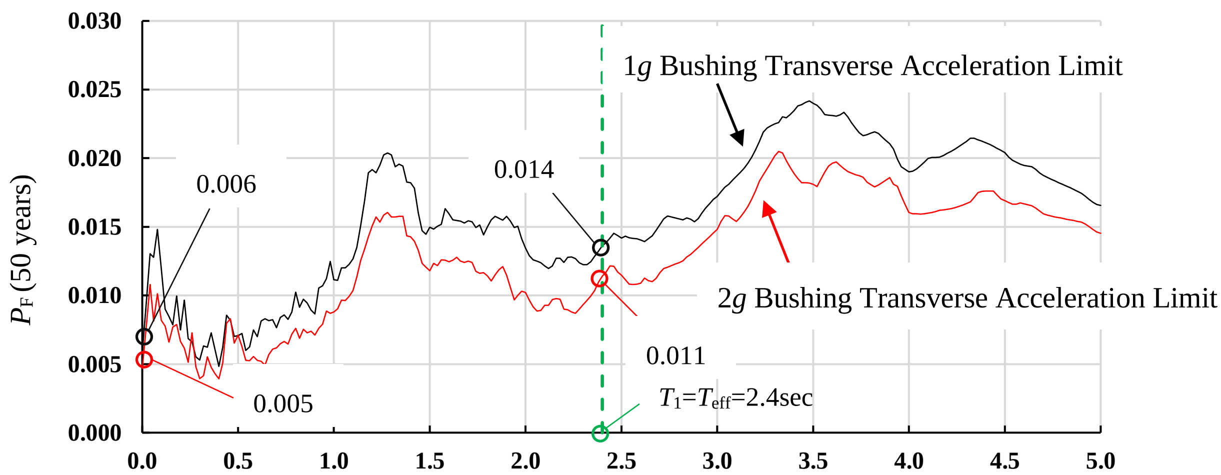


Period for Scaling $T_i$ (second)

Figure 2-23 Probability of failure in lifetime of 50 years of horizontally isolated transformer ($W$=420kip, $f_{AI}$=4.3Hz, inclined bushing, $D_{Capacity}$=17.7inch, lower bound) located at Troutdale, OR as function of period used for scaling the ground motions

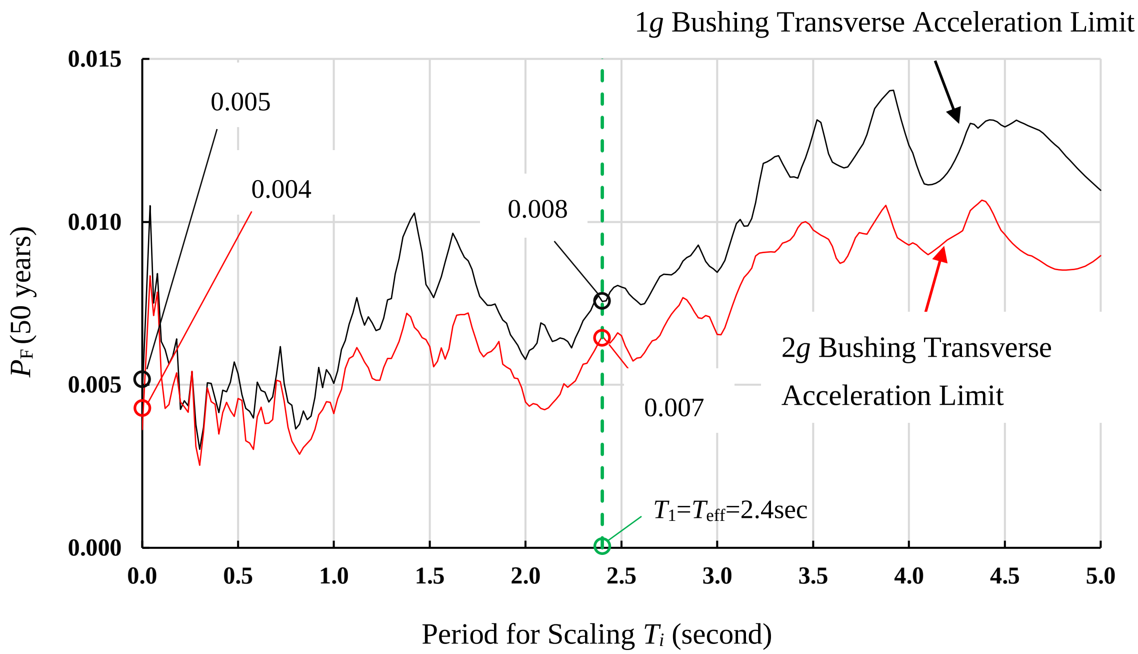


Figure 2-24 Probability of failure in lifetime of 50 years of horizontay-vertically isolated transformer without rocking ($W$=420kip, $f_{AI}$=4.3Hz, inclined bushing, $D_{Capacity}$=17.7inch, lower bound) located at Troutdale, OR as function of period used for scaling the ground motions

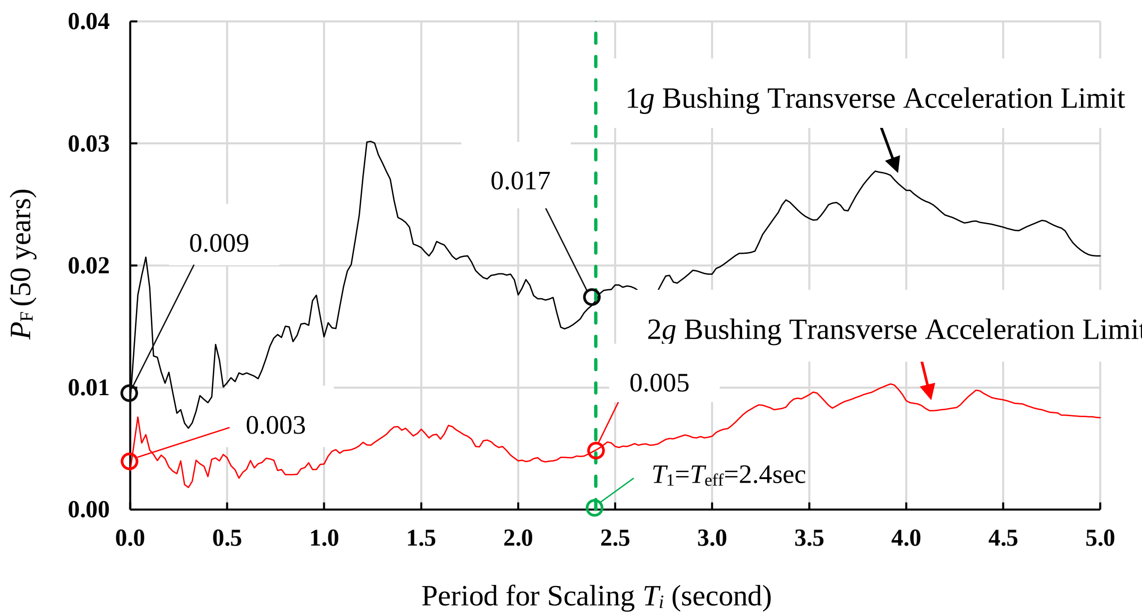


Figure 2-25 Probability of failure in lifetime of 50 years of horizontally-vertically isolated transformer with rocking ($W$=420kip, $f_{AI}$=4.3Hz, inclined bushing, $D_{Capacity}$=17.7inch, lower bound) located at Troutdale, OR as function of period used for scaling the ground motions

***As-installed bushing of 11.3Hz***

**Isolator $D_{Capacity}$=17.7inch, Lower Bound Conditions with $\mu_1=\mu_4$=0.12 and $\mu_2=\mu_3$=0.08**

**Location Chehalis, WA**

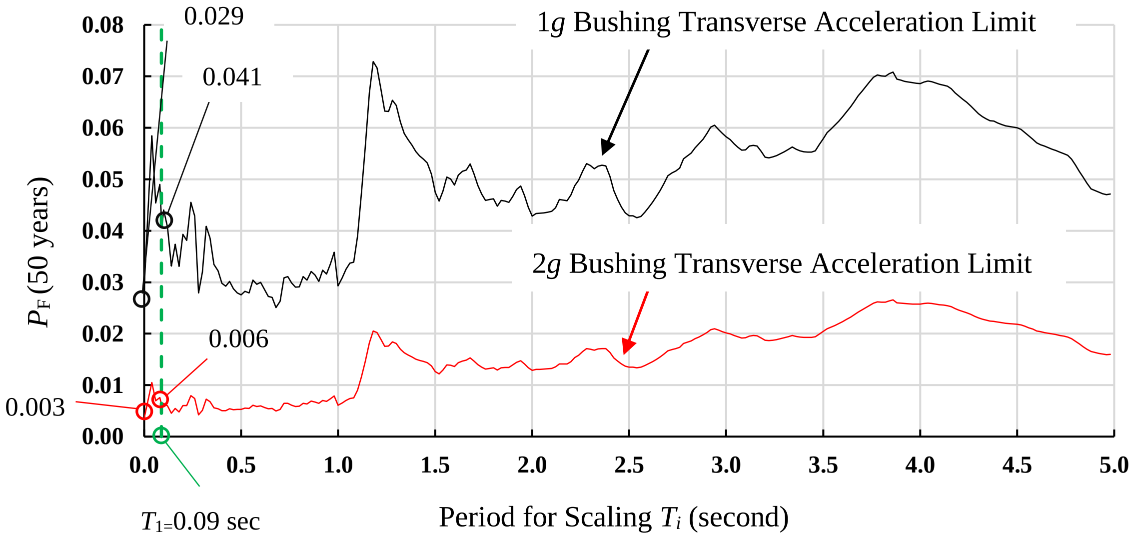


Figure 2-26 Probability of failure in lifetime of 50 years of non-isolated transformer ($W$=420kip, $f_{AI}$=11.3Hz, inclined bushing) located at Chehalis, WA as function of period used for scaling the ground motions

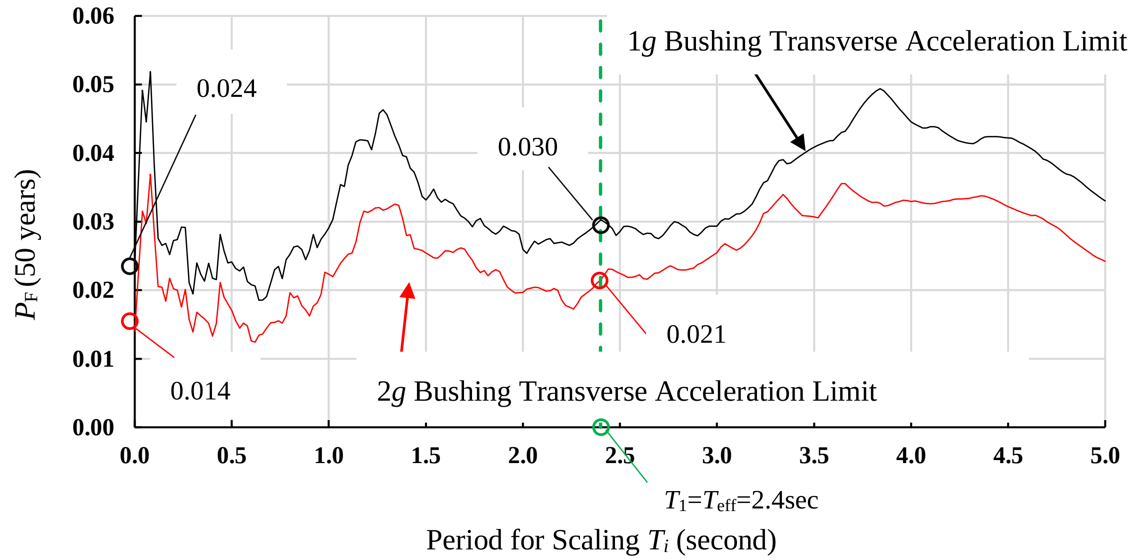


Figure 2-27 Probability of failure in lifetime of 50 years of horizontally isolated transformer ($W$=420kip, $f_{AI}$=11.3Hz, inclined bushing, $D_{Capacity}$=17.7inch, lower bound) located at Chehalis, WA as function of period used for scaling the ground motions

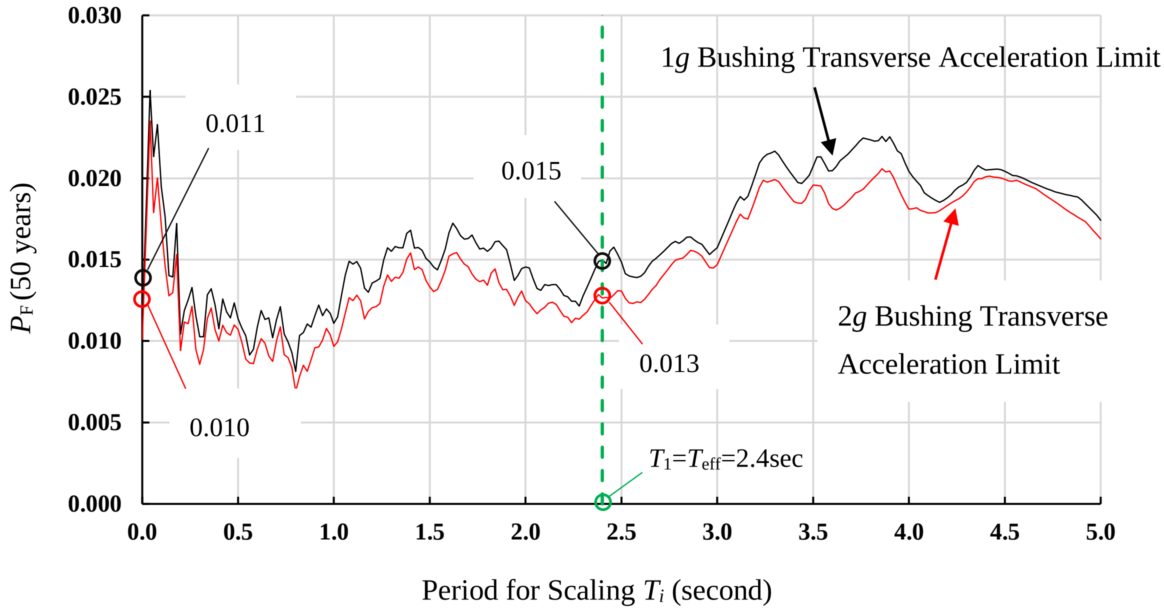


Figure 2-28 Probability of failure in lifetime of 50 years of horizontally-vertically isolated transformer without rocking ($W$=420kip, $f_{AI}$=11.3Hz, inclined bushing, $D_{Capacity}$=17.7inch, lower bound) located at Chehalis, WA as function of period used for scaling the ground motions

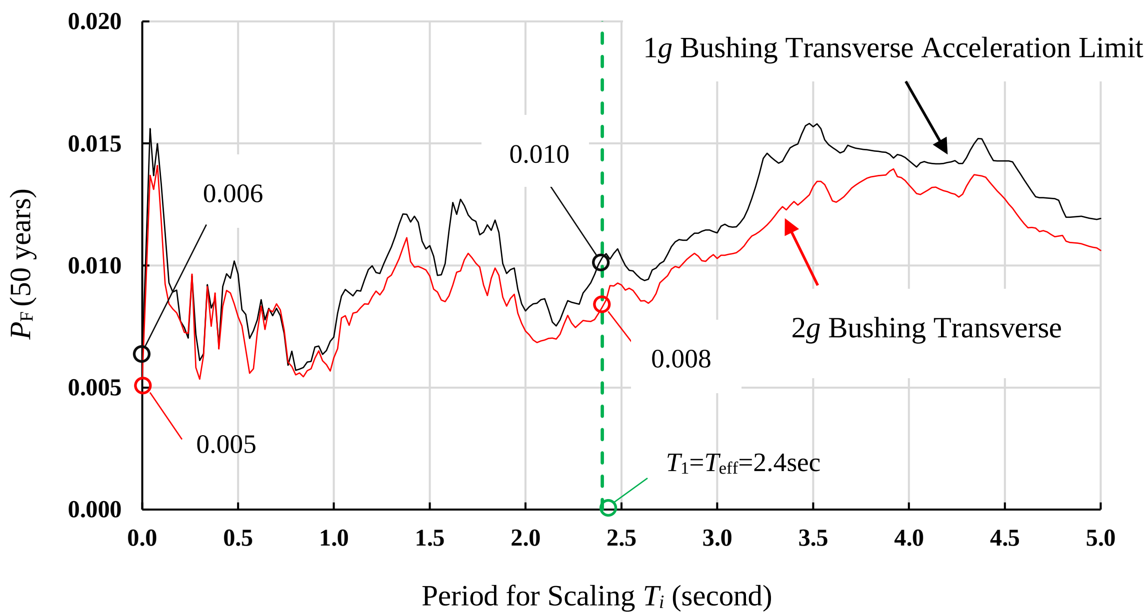


Figure 2-29 Probability of failure in lifetime of 50 years of horizontally-vertically isolated transformer with rocking ($W$=420kip, $f_{AI}$=11.3Hz, inclined bushing, $D_{Capacity}$=17.7inch, lower bound) located at Chehalis, WA as function of period used for scaling the ground motions

***As-installed bushing of 11.3Hz***

**Isolator $D_{Capacity}$=17.7inch, Lower Bound Conditions with $\mu_1=\mu_4$=0.12 and $\mu_2=\mu_3$=0.08**

**Location Loma Linda, CA**

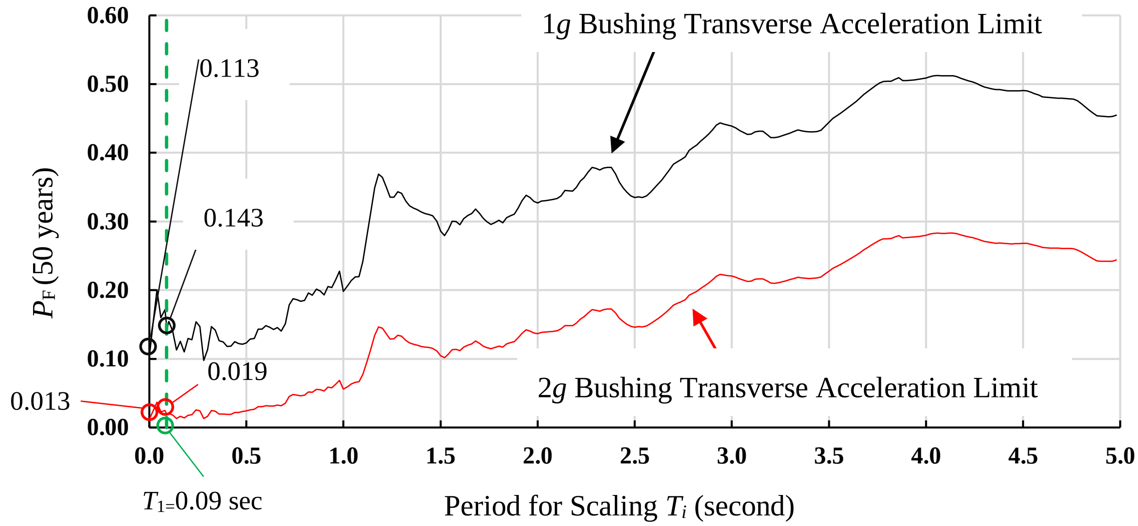


Figure 2-30 Probability of failure in lifetime of 50 years of non-isolated transformer ($W$=420kip, $f_{AI}$=11.3Hz, inclined bushing) located at Loma Linda, CA as function of period used for scaling the ground motions

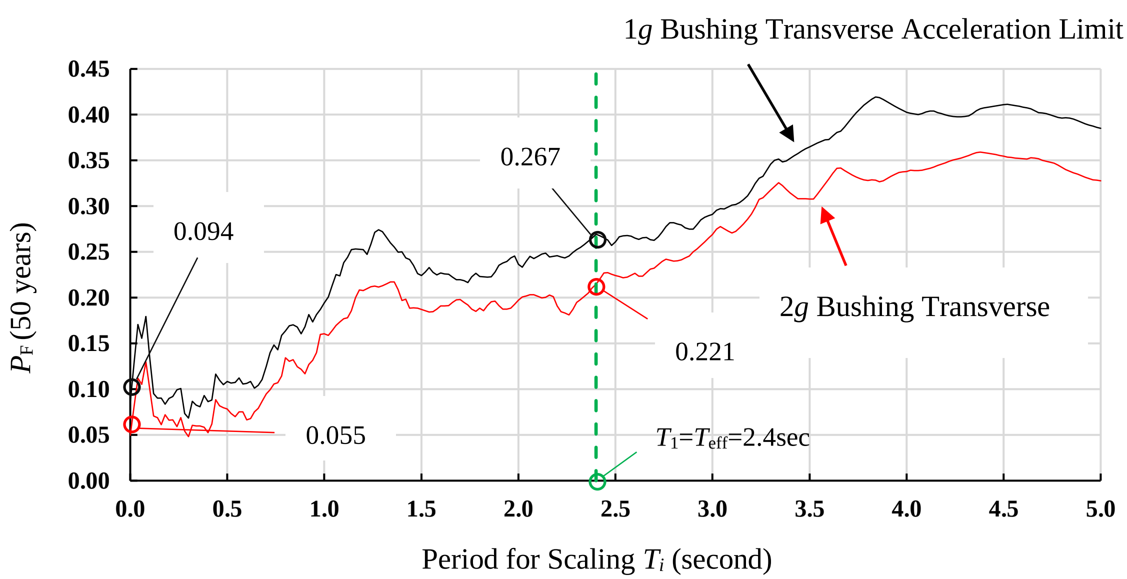


Figure 2-31 Probability of failure in lifetime of 50 years of horizontally isolated transformer ($W$=420kip, $f_{AI}$=11.3Hz, inclined bushing, $D_{Capacity}$=17.7inch, lower bound) located at Loma Linda, CA as function of period used for scaling the ground motions

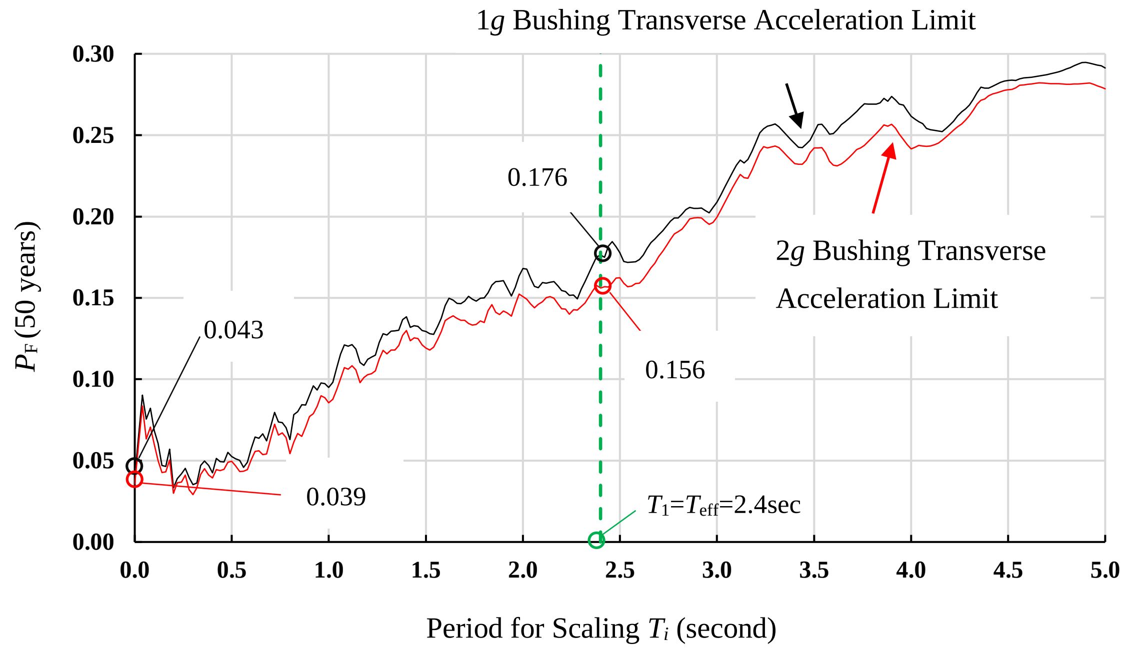


Figure 2-32 Probability of failure in lifetime of 50 years of horizontally-vertically isolated transformer without rocking ($W$=420kip, $f_{AI}$=11.3Hz, inclined bushing, $D_{Capacity}$=17.7inch, lower bound) located at Loma Linda, CA as function of period used for scaling the ground motions

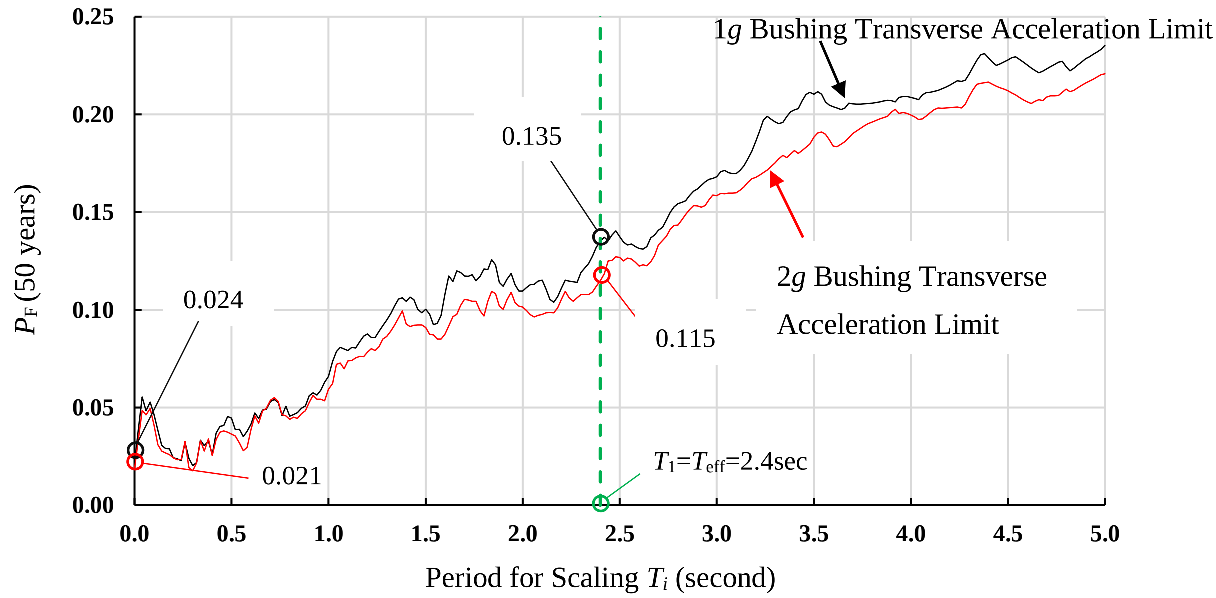


Figure 2-33 Probability of failure in lifetime of 50 years of horizontally-vertically isolated transformer with rocking ($W$=420kip, $f_{AI}$=11.3Hz, inclined bushing, $D_{Capacity}$=17.7inch, lower bound) located at Loma Linda, CA as function of period used for scaling the ground motions

***As-installed bushing of 11.3Hz***

**Isolator $D_{Capacity}$=17.7inch, Lower Bound Conditions with $\mu_1=\mu_4=0.12$ and $\mu_2=\mu_3=0.08$**

**Location Troutdale, OR**

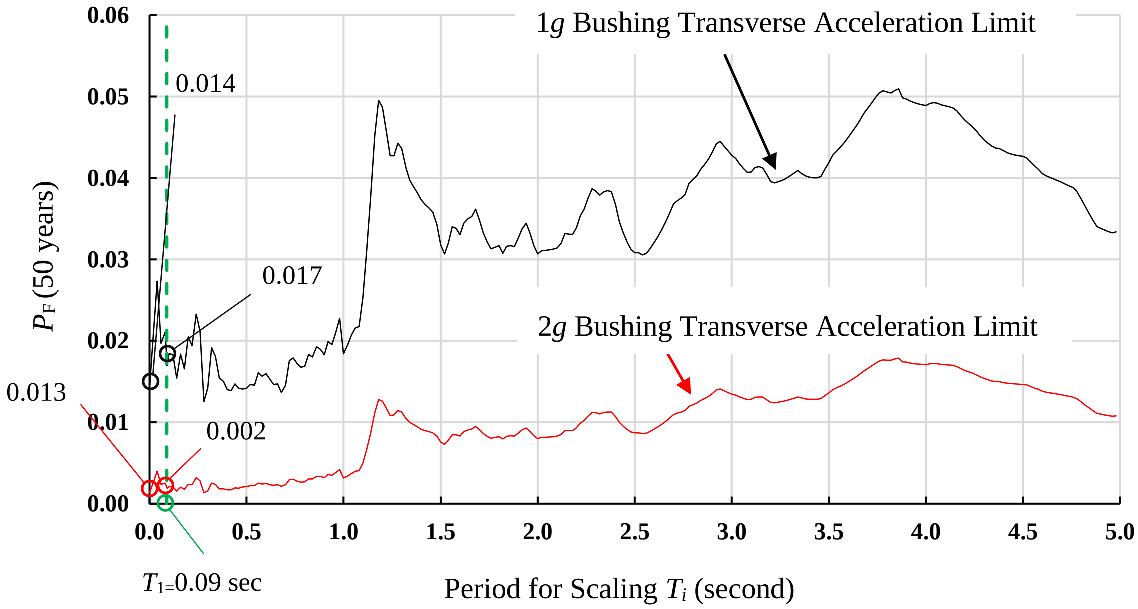


Figure 2-34 Probability of failure in lifetime of 50 years of non-isolated transformer ($W$=420kip, $f_{AI}$=11.3Hz, inclined bushing) located at Troutdale, OR as function of period used for scaling the ground motions

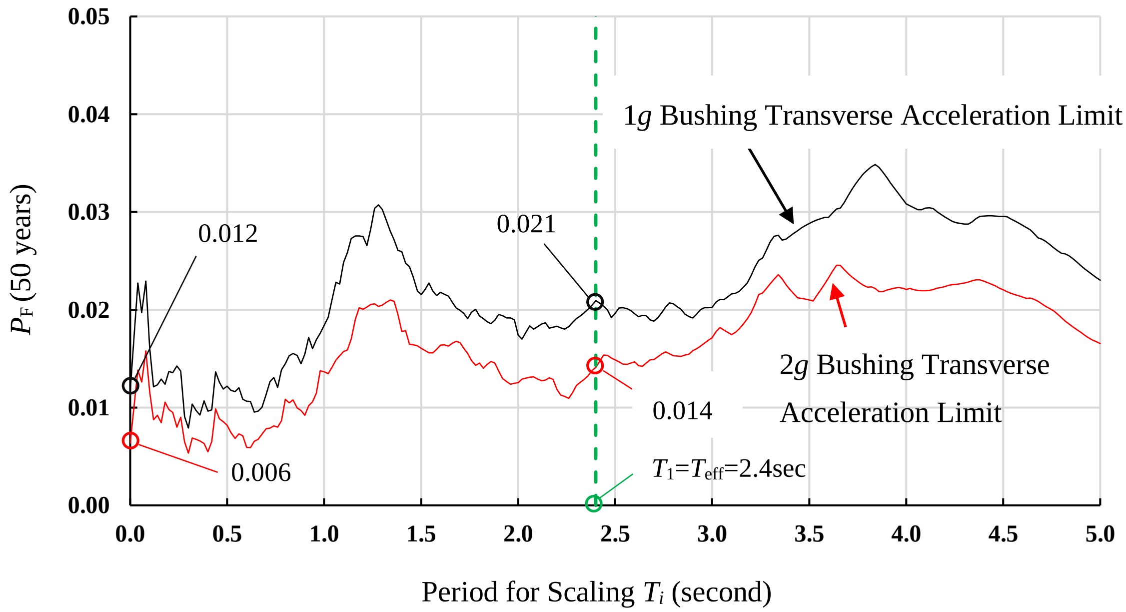


Figure 2-35 Probability of failure in lifetime of 50 years of horizontally isolated transformer ($W$=420kip, $f_{AI}$=11.3Hz, inclined bushing, $D_{Capacity}$=17.7inch, lower bound) located at Troutdale, OR as function of period used for scaling the ground motions

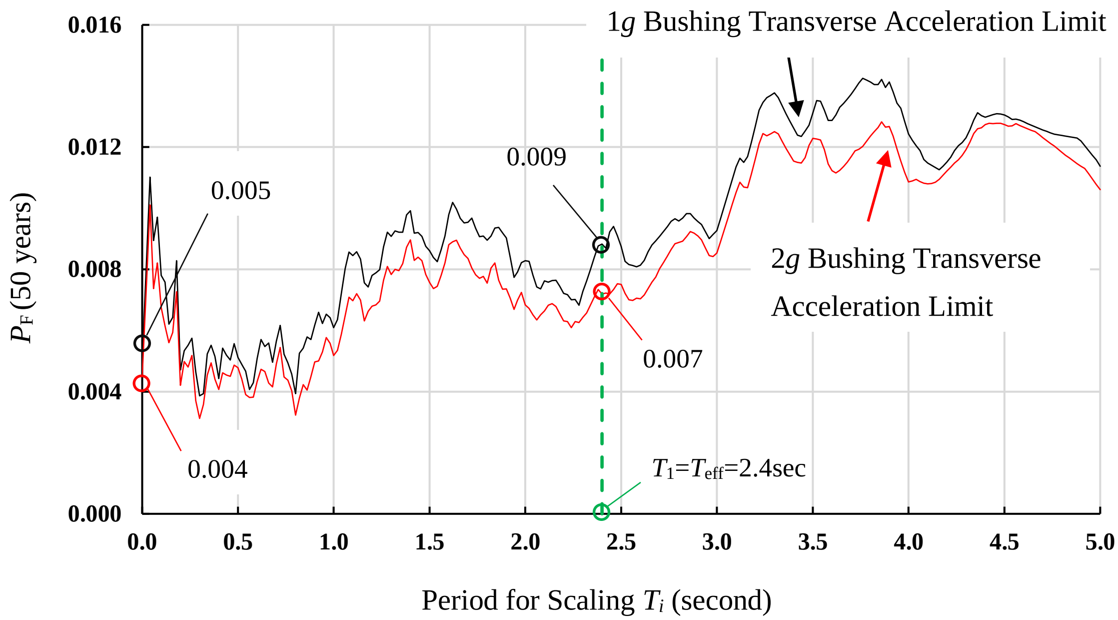


Figure 2-36 Probability of failure in lifetime of 50 years of horizontally-vertically isolated transformer without rocking ($W$=420kip, $f_{AI}$=11.3Hz, inclined bushing, $D_{Capacity}$=17.7inch, lower bound) located at Troutdale, OR as function of period used for scaling the ground motions

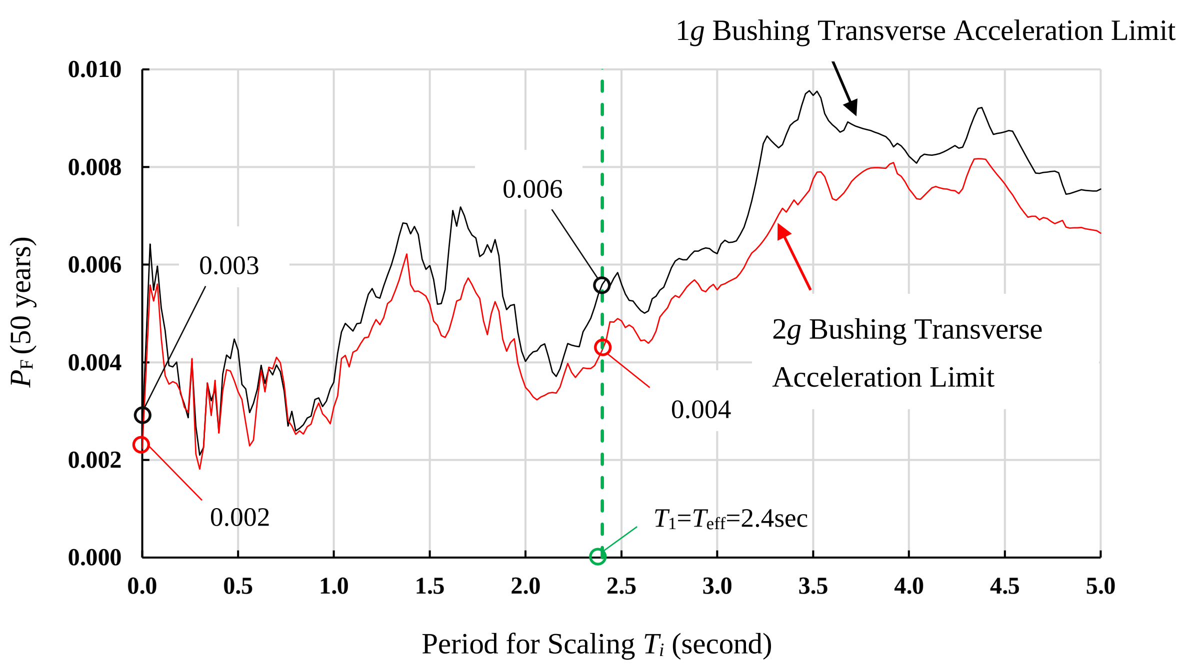


Figure 2-37 Probability of failure in lifetime of 50 years of horizontally-vertically isolated transformer with rocking ($W$=420kip, $f_{AI}$=11.3Hz, inclined bushing, $D_{Capacity}$=17.7inch, lower bound) located at Troutdale, OR as function of period used for scaling the ground motions

# SECTION 3
# EFFECT OF SPECTRAL SHAPE ON THE FRAGILITY OF ELECTRICAL TRANSFORMERS

The results in Figures 2-2 to 2-37 are based on analyses in which the original as-recorded motions have been scaled without any consideration of the spectral shape effects. These effects are the subject of this section. In general, these effects are dependent on the value of the target expected "epsilon" (see Appendix A) which differs between the ten considered sites and is also dependent on the period.

In general, consideration of the spectral shape effects results in a change in the median spectral acceleration at failure at the fundamental period $T_i$ (quantity $\widehat{Sa}_F(T_i)$ obtained by use of Equation 2-3). In addition, consideration of uncertainties results in increases of the dispersion coefficient (quantity $\beta_{RTR}$ calculated using Equation 2-4).

We corrected for the spectral shape effects for the non-isolated and the isolated transformers studied when the scaling is based on the spectral acceleration at the fundamental period $Sa(T_i)$ where $T_i$ is either 0.13sec or 2.3sec. Tables 3-1 to 3-60 present the results on the probability of failure in 50 years of lifetime for all considered cases (10 locations, 3 bushing frequencies and 2 isolator displacement capacities for the 420 kip transformer). Appendix A describes the method for adjusting the results for spectral shape effects, and presents details of the method for representative cases.

Tables 3-1 to 3-60 also include the value of the probability of failure reported in report MCEER-16-0010 (Kitayama et al, 2016) for which the scaling of ground motions was based on the *PGA* (spectral acceleration at zero period) and the spectral shape effects were not considered. We considered only the record-to-record uncertainty in the calculation of all values of the probability of failure in these tables, without any adjustment of the results for additional uncertainties. Section 4 addresses uncertainties.

The results in Tables 3-1 to 3-60 demonstrate that scaling of the ground motions at the fundamental period and consideration of spectral shape effects change the probabilities of failure which generally increase for the isolated transformers and slightly decrease for the non-isolated transformers. Note that there is a significant increase in the probability of failure for the isolated transformers due to the scaling using as measure of intensity the spectral acceleration at the fundamental period of 2.4sec instead of the *PGA*. This increase is then modified due to the effects of the spectral shape in some cases by a minor amount, whereas in others (e.g., Loma Linda site) the probabilities of failure are reduced by significant amounts. Nevertheless, the probabilities of failure for seismically isolated transformers are smaller than those of non-isolated transformers, particularly for the case of the bushing acceleration limit of $1g$. The benefits of seismic isolation further improve when the larger displacement capacity isolator is considered although, as it will be discussed later this is due, in some cases, to the increased displacement capacity, whereas in other cases is due to the lower stiffness of the isolator.

Note that the values of the median spectral acceleration at the fundamental period $\widehat{Sa}_F(T_1)$ and of the dispersion coefficient $\beta_{RTR}$ that describe the fragility curve without the correction for the spectral shape effects are independent of the location of the transformer. However, the median spectral acceleration value changes when the correction for the spectral shape effects is applied and then it depends on the location. The dependence on the location results from the dependence of the correction for the spectral shape effects on the expected value of epsilon at the location of the transformer (see details in Appendix A).

Moreover, note that the values of the dispersion coefficient are generally in the range of about 0.2 to about 0.4 except for the case of the horizontally only isolated transformers where the values are larger and about 0.5 to 0.7. (In addition, one case of the horizontally-vertically isolated transformer with rocking, 4.3Hz frequency bushing of 1g acceleration limit resulted in a large value of the dispersion coefficient). Values of the dispersion coefficient beyond 0.4 have not been computed in any of the FEMA (2009) studies or any of those of Kitayama and Constantinou (2018a, 2018b; 2019a, 2019b) for seismically isolated buildings, all of which utilized the same set of ground motions. We believe this difference results in from the use of vertical ground motion. The vertical ground motion has important effects on the horizontally isolated transformer (as a result of uplift and impact-see Kitayama et al., 2016 for modeling details) but has lesser effects on the horizontally-vertically isolated transformer (uplift and impact are essentially eliminated), and has practically no effect on the non-isolated transformer. The origin of the problem is related to the methodology used to carry out the incremental dynamic analysis in which the scaling of the horizontal components of the ground motions was based on the horizontal spectral acceleration value at the fundamental period, whereas the vertical component maintained its original as-recorded characteristics as discussed in more detail in Section 2.

FEMA (2009) recommends the use of an upper bound value of 0.4 for the record-to-record dispersion coefficient. This has not been done in the results presented in Tables 30-1 to 3-60 that follow. Accordingly, the computed probabilities of failure for the horizontally only isolated transformers may have been overestimated. Section 4 further addresses this issue and presents summary results on the probability of failure including adjusted results for the effects of additional uncertainties.

Table 3-1 Summary of results for probability of failure for isolated and non-isolated transformer with $W$=420kip, $f_{AI}$=7.7Hz and inclined bushing. When isolated, $D_{Capacity}$=17.7inch and lower bound friction properties. Location: **Vancouver, WA**

| System | Transverse Bushing Acceleration Limit (g) | Without Spectral Shape Effects | | | With Spectral Shape Effects | | | Reported in MCEER-16-0010 |
|---|---|---|---|---|---|---|---|---|
| | | Median $\widehat{Sa}_F(T_1)$ (g) | $\beta_{RTR}$ | $P_F$ (50 years) | Median $\widehat{Sa}_F(T_1)$ (g) | $\beta_{RTR}$ | $P_F$ (50 years) | $P_F$ (50 years) |
| Non-isolated $T_1$=0.13sec | 1g | 0.735 | 0.276 | 0.063 | 0.704 | 0.276 | 0.069 | 0.089 |
| | 2g | 1.470 | 0.276 | 0.012 | 1.408 | 0.276 | 0.013 | 0.016 |
| Horizontally isolated $T_1$=2.4sec | 1g | 0.331 | 0.656 | 0.028 | 0.284 | 0.656 | 0.036 | 0.015 |
| | 2g | 0.410 | 0.492 | 0.014 | 0.369 | 0.492 | 0.018 | 0.007 |
| Horizontally-vertically isolated without rocking $T_1$=2.4sec | 1g | 0.442 | 0.393 | 0.010 | 0.415 | 0.393 | 0.012 | 0.008 |
| | 2g | 0.466 | 0.296 | 0.008 | 0.462 | 0.296 | 0.008 | 0.005 |
| Horizontally-vertically isolated with rocking $T_1$=2.4sec | 1g | 0.439 | 0.411 | 0.011 | 0.411 | 0.411 | 0.013 | 0.006 |
| | 2g | 0.525 | 0.293 | 0.006 | 0.512 | 0.293 | 0.006 | 0.003 |

Table 3-2 Summary of results for probability of failure for isolated and non-isolated transformer with W=420kip, $f_{AI}$=7.7Hz and inclined bushing. When isolated, $D_{Capacity}$=17.7inch and lower bound friction properties. Location: **Saranap, CA**

| System | Transverse Bushing Acceleration Limit (g) | Without Spectral Shape Effects | | | With Spectral Shape Effects | | | Reported in MCEER-16-0010 |
|---|---|---|---|---|---|---|---|---|
| | | Median $\widehat{Sa}_F(T_1)$ (g) | $\beta_{RTR}$ | $P_F$ (50 years) | Median $\widehat{Sa}_F(T_1)$ (g) | $\beta_{RTR}$ | $P_F$ (50 years) | $P_F$ (50 years) |
| Non-isolated $T_1$=0.13sec | 1g | 0.735 | 0.276 | 0.300 | 0.782 | 0.276 | 0.266 | 0.359 |
| | 2g | 1.470 | 0.276 | 0.047 | 1.564 | 0.276 | 0.038 | 0.077 |
| Horizontally isolated $T_1$=2.4sec | 1g | 0.331 | 0.656 | 0.197 | 0.588 | 0.656 | 0.067 | 0.072 |
| | 2g | 0.410 | 0.492 | 0.100 | 0.644 | 0.492 | 0.033 | 0.029 |
| Horizontally-vertically isolated without rocking $T_1$=2.4sec | 1g | 0.442 | 0.393 | 0.068 | 0.620 | 0.393 | 0.027 | 0.033 |
| | 2g | 0.466 | 0.296 | 0.048 | 0.639 | 0.296 | 0.018 | 0.019 |
| Horizontally-vertically isolated with rocking $T_1$=2.4sec | 1g | 0.439 | 0.411 | 0.072 | 0.646 | 0.411 | 0.025 | 0.024 |
| | 2g | 0.525 | 0.293 | 0.034 | 0.704 | 0.293 | 0.013 | 0.013 |

Table 3-3 Summary of results for probability of failure for isolated and non-isolated transformer with $W$=420kip, $f_{AI}$=7.7Hz and inclined bushing. When isolated, $D_{Capacity}$=17.7inch and lower bound friction properties. Location: **Loma Linda, CA**

| System | Transverse Bushing Acceleration Limit (g) | Without Spectral Shape Effects | | | With Spectral Shape Effects | | | Reported in MCEER-16-0010 |
|---|---|---|---|---|---|---|---|---|
| | | Median $\widehat{Sa}_F(T_1)$ (g) | $\beta_{RTR}$ | $P_F$ (50 years) | Median $\widehat{Sa}_F(T_1)$ (g) | $\beta_{RTR}$ | $P_F$ (50 years) | $P_F$ (50 years) |
| Non-isolated $T_1$=0.13sec | 1g | 0.735 | 0.276 | 0.108 | 0.782 | 0.276 | 0.309 | 0.398 |
| | 2g | 1.470 | 0.276 | 0.075 | 1.565 | 0.276 | 0.063 | 0.108 |
| Horizontally isolated $T_1$=2.4sec | 1g | 0.331 | 0.656 | 0.301 | 0.744 | 0.656 | 0.103 | 0.102 |
| | 2g | 0.410 | 0.492 | 0.206 | 0.770 | 0.492 | 0.078 | 0.049 |
| Horizontally-vertically isolated without rocking $T_1$=2.4sec | 1g | 0.442 | 0.393 | 0.175 | 0.706 | 0.393 | 0.081 | 0.053 |
| | 2g | 0.466 | 0.296 | 0.151 | 0.709 | 0.296 | 0.073 | 0.033 |
| Horizontally-vertically isolated with rocking $T_1$=2.4sec | 1g | 0.439 | 0.411 | 0.177 | 0.748 | 0.411 | 0.074 | 0.041 |
| | 2g | 0.525 | 0.293 | 0.123 | 0.780 | 0.293 | 0.059 | 0.024 |

Table 3-4 Summary of results for probability of failure for isolated and non-isolated transformer with W=420kip, $f_{AI}$=7.7Hz and inclined bushing. When isolated, $D_{Capacity}$=17.7inch and lower bound friction properties. Location: **Aberdeen, WA**

| System | Transverse Bushing Acceleration Limit (g) | Without Spectral Shape Effects | | | With Spectral Shape Effects | | | Reported in MCEER-16-0010 |
|---|---|---|---|---|---|---|---|---|
| | | Median $\widehat{Sa}_F(T_1)$ (g) | $\beta_{RTR}$ | $P_F$ (50 years) | Median $\widehat{Sa}_F(T_1)$ (g) | $\beta_{RTR}$ | $P_F$ (50 years) | $P_F$ (50 years) |
| Non-isolated $T_1$=0.13sec | 1g | 0.735 | 0.276 | 0.129 | 0.737 | 0.276 | 0.128 | 0.145 |
| | 2g | 1.470 | 0.276 | 0.038 | 1.473 | 0.276 | 0.038 | 0.044 |
| Horizontally isolated $T_1$=2.4sec | 1g | 0.331 | 0.656 | 0.051 | 0.359 | 0.656 | 0.047 | 0.042 |
| | 2g | 0.410 | 0.492 | 0.036 | 0.441 | 0.492 | 0.033 | 0.025 |
| Horizontally-vertically isolated without rocking $T_1$=2.4sec | 1g | 0.442 | 0.393 | 0.031 | 0.472 | 0.393 | 0.028 | 0.025 |
| | 2g | 0.466 | 0.296 | 0.027 | 0.513 | 0.296 | 0.024 | 0.018 |
| Horizontally-vertically isolated with rocking $T_1$=2.4sec | 1g | 0.439 | 0.411 | 0.031 | 0.475 | 0.411 | 0.028 | 0.022 |
| | 2g | 0.525 | 0.293 | 0.023 | 0.567 | 0.293 | 0.021 | 0.014 |

Table 3-5 Summary of results for probability of failure for isolated and non-isolated transformer with $W$=420kip, $f_{AI}$=7.7Hz and inclined bushing. When isolated, $D_{Capacity}$=17.7inch and lower bound friction properties. Location: **Chehalis, WA**

| System | Transverse Bushing Acceleration Limit (g) | Without Spectral Shape Effects | | | With Spectral Shape Effects | | | Reported in MCEER-16-0010 |
|---|---|---|---|---|---|---|---|---|
| | | Median $\widehat{Sa}_F(T_1)$ (g) | $\beta_{RTR}$ | $P_F$ (50 years) | Median $\widehat{Sa}_F(T_1)$ (g) | $\beta_{RTR}$ | $P_F$ (50 years) | $P_F$ (50 years) |
| Non-isolated $T_1$=0.13sec | 1g | 0.735 | 0.276 | 0.108 | 0.717 | 0.276 | 0.113 | 0.128 |
| | 2g | 1.470 | 0.276 | 0.022 | 1.434 | 0.276 | 0.024 | 0.028 |
| Horizontally isolated $T_1$=2.4sec | 1g | 0.331 | 0.656 | 0.036 | 0.286 | 0.656 | 0.045 | 0.026 |
| | 2g | 0.410 | 0.492 | 0.020 | 0.372 | 0.492 | 0.024 | 0.012 |
| Horizontally-vertically isolated without rocking $T_1$=2.4sec | 1g | 0.442 | 0.393 | 0.015 | 0.415 | 0.393 | 0.017 | 0.013 |
| | 2g | 0.466 | 0.296 | 0.012 | 0.462 | 0.296 | 0.012 | 0.008 |
| Horizontally-vertically isolated with rocking $T_1$=2.4sec | 1g | 0.439 | 0.411 | 0.016 | 0.411 | 0.411 | 0.018 | 0.010 |
| | 2g | 0.525 | 0.293 | 0.009 | 0.513 | 0.293 | 0.010 | 0.006 |

Table 3-6 Summary of results for probability of failure for isolated and non-isolated transformer with $W$=420kip, $f_{AI}$=7.7Hz and inclined bushing. When isolated, $D_{Capacity}$=17.7inch and lower bound friction properties. Location: **Hillsboro, OR**

| System | Transverse Bushing Acceleration Limit (g) | Without Spectral Shape Effects | | | With Spectral Shape Effects | | | Reported in MCEER-16-0010 |
|---|---|---|---|---|---|---|---|---|
| | | Median $\widehat{Sa}_F(T_1)$ (g) | $\beta_{RTR}$ | $P_F$ (50 years) | Median $\widehat{Sa}_F(T_1)$ (g) | $\beta_{RTR}$ | $P_F$ (50 years) | $P_F$ (50 years) |
| Non-isolated $T_1$=0.13sec | 1g | 0.735 | 0.276 | 0.071 | 0.711 | 0.276 | 0.076 | 0.094 |
| | 2g | 1.470 | 0.276 | 0.015 | 1.422 | 0.276 | 0.017 | 0.021 |
| Horizontally isolated $T_1$=2.4sec | 1g | 0.331 | 0.656 | 0.032 | 0.284 | 0.656 | 0.040 | 0.020 |
| | 2g | 0.410 | 0.492 | 0.018 | 0.369 | 0.492 | 0.022 | 0.009 |
| Horizontally-vertically isolated without rocking $T_1$=2.4sec | 1g | 0.442 | 0.393 | 0.014 | 0.415 | 0.393 | 0.016 | 0.010 |
| | 2g | 0.466 | 0.296 | 0.011 | 0.462 | 0.296 | 0.011 | 0.006 |
| Horizontally-vertically isolated with rocking $T_1$=2.4sec | 1g | 0.439 | 0.411 | 0.014 | 0.411 | 0.411 | 0.016 | 0.008 |
| | 2g | 0.525 | 0.293 | 0.008 | 0.512 | 0.293 | 0.009 | 0.005 |

Table 3-7 Summary of results for probability of failure for isolated and non-isolated transformer with $W$=420kip, $f_{AI}$=7.7Hz and inclined bushing. When isolated, $D_{Capacity}$=17.7inch and lower bound friction properties. Location: **Eugene, OR**

| System | Transverse Bushing Acceleration Limit (g) | Without Spectral Shape Effects | | | With Spectral Shape Effects | | | Reported in MCEER-16-0010 |
|---|---|---|---|---|---|---|---|---|
| | | Median $\widehat{Sa}_F(T_1)$ (g) | $\beta_{RTR}$ | $P_F$ (50 years) | Median $\widehat{Sa}_F(T_1)$ (g) | $\beta_{RTR}$ | $P_F$ (50 years) | $P_F$ (50 years) |
| Non-isolated $T_1$=0.13sec | 1g | 0.735 | 0.276 | 0.049 | 0.704 | 0.276 | 0.052 | 0.038 |
| | 2g | 1.470 | 0.276 | 0.014 | 1.407 | 0.276 | 0.015 | 0.007 |
| Horizontally isolated $T_1$=2.4sec | 1g | 0.331 | 0.656 | 0.030 | 0.279 | 0.656 | 0.038 | 0.007 |
| | 2g | 0.410 | 0.492 | 0.019 | 0.364 | 0.492 | 0.023 | 0.004 |
| Horizontally-vertically isolated without rocking $T_1$=2.4sec | 1g | 0.442 | 0.393 | 0.015 | 0.411 | 0.393 | 0.017 | 0.004 |
| | 2g | 0.466 | 0.296 | 0.013 | 0.458 | 0.296 | 0.013 | 0.003 |
| Horizontally-vertically isolated with rocking $T_1$=2.4sec | 1g | 0.439 | 0.411 | 0.016 | 0.406 | 0.411 | 0.018 | 0.003 |
| | 2g | 0.525 | 0.293 | 0.010 | 0.508 | 0.293 | 0.011 | 0.002 |

Table 3-8 Summary of results for probability of failure for isolated and non-isolated transformer with $W$=420kip, $f_{AI}$=7.7Hz and inclined bushing. When isolated, $D_{Capacity}$=17.7inch and lower bound friction properties. Location: **Wilsonville, OR**

| System | Transverse Bushing Acceleration Limit (g) | Without Spectral Shape Effects | | | With Spectral Shape Effects | | | Reported in MCEER-16-0010 |
|---|---|---|---|---|---|---|---|---|
| | | Median $\widehat{Sa}_F(T_1)$ (g) | $\beta_{RTR}$ | $P_F$ (50 years) | Median $\widehat{Sa}_F(T_1)$ (g) | $\beta_{RTR}$ | $P_F$ (50 years) | $P_F$ (50 years) |
| Non-isolated $T_1$=0.13sec | 1g | 0.735 | 0.276 | 0.064 | 0.705 | 0.276 | 0.069 | 0.087 |
| | 2g | 1.470 | 0.276 | 0.012 | 1.410 | 0.276 | 0.014 | 0.018 |
| Horizontally isolated $T_1$=2.4sec | 1g | 0.331 | 0.656 | 0.028 | 0.285 | 0.656 | 0.036 | 0.017 |
| | 2g | 0.410 | 0.492 | 0.015 | 0.370 | 0.492 | 0.018 | 0.008 |
| Horizontally-vertically isolated without rocking $T_1$=2.4sec | 1g | 0.442 | 0.393 | 0.011 | 0.416 | 0.393 | 0.013 | 0.008 |
| | 2g | 0.466 | 0.296 | 0.009 | 0.463 | 0.296 | 0.009 | 0.005 |
| Horizontally-vertically isolated with rocking $T_1$=2.4sec | 1g | 0.439 | 0.411 | 0.012 | 0.412 | 0.411 | 0.013 | 0.006 |
| | 2g | 0.525 | 0.293 | 0.006 | 0.513 | 0.293 | 0.007 | 0.004 |

Table 3-9 Summary of results for probability of failure for isolated and non-isolated transformer with $W$=420kip, $f_{AI}$=7.7Hz and inclined bushing. When isolated, $D_{Capacity}$=17.7inch and lower bound friction properties. Location: **Curry County, OR**

| System | Transverse Bushing Acceleration Limit (g) | Without Spectral Shape Effects | | | With Spectral Shape Effects | | | Reported in MCEER-16-0010 |
|---|---|---|---|---|---|---|---|---|
| | | Median $\widehat{Sa}_F(T_1)$ (g) | $\beta_{RTR}$ | $P_F$ (50 years) | Median $\widehat{Sa}_F(T_1)$ (g) | $\beta_{RTR}$ | $P_F$ (50 years) | $P_F$ (50 years) |
| Non-isolated $T_1$=0.24sec | 1g | 0.735 | 0.276 | 0.111 | 0.778 | 0.276 | 0.103 | 0.123 |
| | 2g | 1.470 | 0.276 | 0.038 | 1.556 | 0.276 | 0.034 | 0.047 |
| Horizontally isolated $T_1$=2.4sec | 1g | 0.331 | 0.656 | 0.085 | 0.571 | 0.656 | 0.046 | 0.046 |
| | 2g | 0.410 | 0.492 | 0.062 | 0.629 | 0.492 | 0.036 | 0.029 |
| Horizontally-vertically isolated without rocking $T_1$=2.4sec | 1g | 0.441 | 0.393 | 0.055 | 0.610 | 0.393 | 0.035 | 0.030 |
| | 2g | 0.466 | 0.296 | 0.049 | 0.630 | 0.296 | 0.031 | 0.022 |
| Horizontally-vertically isolated with rocking $T_1$=2.4sec | 1g | 0.439 | 0.411 | 0.055 | 0.634 | 0.411 | 0.033 | 0.026 |
| | 2g | 0.525 | 0.293 | 0.041 | 0.695 | 0.293 | 0.027 | 0.017 |

Table 3-10 Summary of results for probability of failure for isolated and non-isolated transformer with $W$=420kip, $f_{AI}$=7.7Hz and inclined bushing. When isolated, $D_{Capacity}$=17.7inch and lower bound friction properties. Location: **Troutdale, OR**

| System | Transverse Bushing Acceleration Limit (g) | Without Spectral Shape Effects | | | With Spectral Shape Effects | | | Reported in MCEER-16-0010 |
|---|---|---|---|---|---|---|---|---|
| | | Median $\widehat{Sa}_F(T_1)$ (g) | $\beta_{RTR}$ | $P_F$ (50 years) | Median $\widehat{Sa}_F(T_1)$ (g) | $\beta_{RTR}$ | $P_F$ (50 years) | $P_F$ (50 years) |
| Non-isolated $T_1$=0.13sec | 1g | 0.735 | 0.276 | 0.056 | 0.702 | 0.276 | 0.061 | 0.071 |
| | 2g | 1.470 | 0.276 | 0.009 | 1.403 | 0.276 | 0.011 | 0.014 |
| Horizontally isolated $T_1$=2.4sec | 1g | 0.331 | 0.656 | 0.025 | 0.277 | 0.656 | 0.035 | 0.013 |
| | 2g | 0.410 | 0.492 | 0.013 | 0.362 | 0.492 | 0.017 | 0.006 |
| Horizontally-vertically isolated without rocking $T_1$=2.4sec | 1g | 0.442 | 0.393 | 0.009 | 0.410 | 0.393 | 0.011 | 0.006 |
| | 2g | 0.466 | 0.296 | 0.007 | 0.457 | 0.296 | 0.007 | 0.004 |
| Horizontally-vertically isolated with rocking $T_1$=2.4sec | 1g | 0.439 | 0.411 | 0.009 | 0.405 | 0.411 | 0.012 | 0.005 |
| | 2g | 0.525 | 0.293 | 0.005 | 0.507 | 0.293 | 0.005 | 0.003 |

Table 3-11 Summary of results for probability of failure for isolated and non-isolated transformer with $W$=420kip, $f_{AI}$=4.3Hz and inclined bushing. When isolated, $D_{Capacity}$=17.7inch and lower bound friction properties. Location: **Vancouver, WA**

| System | Transverse Bushing Acceleration Limit (g) | Without Spectral Shape Effects | | | With Spectral Shape Effects | | | Reported in MCEER-16-0010 |
|---|---|---|---|---|---|---|---|---|
| | | Median $\widehat{Sa}_F(T_1)$ (g) | $\beta_{RTR}$ | $P_F$ (50 years) | Median $\widehat{Sa}_F(T_1)$ (g) | $\beta_{RTR}$ | $P_F$ (50 years) | $P_F$ (50 years) |
| Non-isolated $T_1$=0.24sec | 1g | 1.033 | 0.173 | 0.043 | 1.019 | 0.173 | 0.045 | 0.045 |
| | 2g | 2.066 | 0.173 | 0.006 | 2.038 | 0.173 | 0.006 | 0.007 |
| Horizontally isolated $T_1$=2.4sec | 1g | 0.418 | 0.551 | 0.015 | 0.378 | 0.551 | 0.019 | 0.007 |
| | 2g | 0.425 | 0.477 | 0.013 | 0.414 | 0.477 | 0.014 | 0.006 |
| Horizontally-vertically isolated without rocking $T_1$=2.4sec | 1g | 0.457 | 0.322 | 0.009 | 0.464 | 0.322 | 0.008 | 0.006 |
| | 2g | 0.471 | 0.278 | 0.008 | 0.502 | 0.278 | 0.006 | 0.005 |
| Horizontally-vertically isolated with rocking $T_1$=2.4sec | 1g | 0.395 | 0.620 | 0.019 | 0.355 | 0.620 | 0.023 | 0.011 |
| | 2g | 0.520 | 0.289 | 0.006 | 0.529 | 0.289 | 0.006 | 0.004 |

Table 3-12 Summary of results for probability of failure for isolated and non-isolated transformer with $W$=420kip, $f_{AI}$=4.3Hz and inclined bushing. When isolated, $D_{Capacity}$=17.7inch and lower bound friction properties. Location: **Saranap, CA**

| System | Transverse Bushing Acceleration Limit (g) | Without Spectral Shape Effects | | | With Spectral Shape Effects | | | Reported in MCEER-16-0010 |
|---|---|---|---|---|---|---|---|---|
| | | Median $\widehat{Sa}_F(T_1)$ (g) | $\beta_{RTR}$ | $P_F$ (50 years) | Median $\widehat{Sa}_F(T_1)$ (g) | $\beta_{RTR}$ | $P_F$ (50 years) | $P_F$ (50 years) |
| Non-isolated $T_1$=0.24sec | 1g | 1.033 | 0.173 | 0.182 | 1.105 | 0.173 | 0.153 | 0.211 |
| | 2g | 2.066 | 0.173 | 0.016 | 2.211 | 0.173 | 0.012 | 0.027 |
| Horizontally isolated $T_1$=2.4sec | 1g | 0.418 | 0.551 | 0.108 | 0.696 | 0.551 | 0.032 | 0.031 |
| | 2g | 0.425 | 0.477 | 0.089 | 0.702 | 0.477 | 0.024 | 0.024 |
| Horizontally-vertically isolated without rocking $T_1$=2.4sec | 1g | 0.457 | 0.322 | 0.054 | 0.644 | 0.322 | 0.019 | 0.025 |
| | 2g | 0.471 | 0.278 | 0.045 | 0.662 | 0.278 | 0.015 | 0.019 |
| Horizontally-vertically isolated with rocking $T_1$=2.4sec | 1g | 0.395 | 0.620 | 0.137 | 0.724 | 0.620 | 0.037 | 0.048 |
| | 2g | 0.520 | 0.289 | 0.034 | 0.706 | 0.289 | 0.012 | 0.016 |

Table 3-13 Summary of results for probability of failure for isolated and non-isolated transformer with $W$=420kip, $f_{AI}$=4.3Hz and inclined bushing. When isolated, $D_{Capacity}$=17.7inch and lower bound friction properties. Location: **Chehalis, WA**

| System | Transverse Bushing Acceleration Limit (g) | Without Spectral Shape Effects | | | With Spectral Shape Effects | | | Reported in MCEER-16-0010 |
|---|---|---|---|---|---|---|---|---|
| | | Median $\widehat{Sa}_F(T_1)$ (g) | $\beta_{RTR}$ | $P_F$ (50 years) | Median $\widehat{Sa}_F(T_1)$ (g) | $\beta_{RTR}$ | $P_F$ (50 years) | $P_F$ (50 years) |
| Non-isolated $T_1$=0.24sec | 1g | 1.033 | 0.173 | 0.070 | 1.042 | 0.173 | 0.069 | 0.074 |
| | 2g | 2.066 | 0.173 | 0.012 | 2.085 | 0.173 | 0.011 | 0.012 |
| Horizontally isolated $T_1$=2.4sec | 1g | 0.418 | 0.551 | 0.021 | 0.354 | 0.551 | 0.028 | 0.013 |
| | 2g | 0.425 | 0.477 | 0.018 | 0.391 | 0.477 | 0.021 | 0.010 |
| Horizontally-vertically isolated without rocking $T_1$=2.4sec | 1g | 0.457 | 0.322 | 0.013 | 0.448 | 0.322 | 0.014 | 0.010 |
| | 2g | 0.471 | 0.278 | 0.012 | 0.487 | 0.278 | 0.011 | 0.008 |
| Horizontally-vertically isolated with rocking $T_1$=2.4sec | 1g | 0.395 | 0.620 | 0.025 | 0.328 | 0.620 | 0.035 | 0.018 |
| | 2g | 0.520 | 0.289 | 0.009 | 0.512 | 0.289 | 0.010 | 0.007 |

Table 3-14 Summary of results for probability of failure for isolated and non-isolated transformer with $W$=420kip, $f_{AI}$=4.3Hz and inclined bushing. When isolated, $D_{Capacity}$=17.7inch and lower bound friction properties. Location: **Aberdeen, WA**

| System | Transverse Bushing Acceleration Limit (g) | Without Spectral Shape Effects | | | With Spectral Shape Effects | | | Reported in MCEER-16-0010 |
|---|---|---|---|---|---|---|---|---|
| | | Median $\widehat{Sa}_F(T_1)$ (g) | $\beta_{RTR}$ | $P_F$ (50 years) | Median $\widehat{Sa}_F(T_1)$ (g) | $\beta_{RTR}$ | $P_F$ (50 years) | $P_F$ (50 years) |
| Non-isolated $T_1$=0.24sec | 1g | 1.033 | 0.173 | 0.095 | 1.064 | 0.173 | 0.091 | 0.095 |
| | 2g | 2.066 | 0.173 | 0.027 | 2.130 | 0.173 | 0.026 | 0.025 |
| Horizontally isolated $T_1$=2.4sec | 1g | 0.418 | 0.551 | 0.036 | 0.439 | 0.551 | 0.034 | 0.026 |
| | 2g | 0.425 | 0.477 | 0.034 | 0.471 | 0.477 | 0.030 | 0.022 |
| Horizontally-vertically isolated without rocking $T_1$=2.4sec | 1g | 0.457 | 0.322 | 0.029 | 0.503 | 0.322 | 0.025 | 0.021 |
| | 2g | 0.471 | 0.278 | 0.027 | 0.537 | 0.278 | 0.022 | 0.018 |
| Horizontally-vertically isolated with rocking $T_1$=2.4sec | 1g | 0.395 | 0.620 | 0.041 | 0.423 | 0.620 | 0.038 | 0.032 |
| | 2g | 0.520 | 0.289 | 0.024 | 0.568 | 0.289 | 0.021 | 0.016 |

Table 3-15 Summary of results for probability of failure for isolated and non-isolated transformer with $W$=420kip, $f_{AI}$=4.3Hz and inclined bushing. When isolated, $D_{Capacity}$=17.7inch and lower bound friction properties. Location: **Loma Linda, CA**

| System | Transverse Bushing Acceleration Limit (g) | Without Spectral Shape Effects | | | With Spectral Shape Effects | | | Reported in MCEER-16-0010 |
|---|---|---|---|---|---|---|---|---|
| | | Median $\widehat{Sa}_F(T_1)$ (g) | $\beta_{RTR}$ | $P_F$ (50 years) | Median $\widehat{Sa}_F(T_1)$ (g) | $\beta_{RTR}$ | $P_F$ (50 years) | $P_F$ (50 years) |
| Non-isolated $T_1$=0.24sec | 1g | 1.033 | 0.173 | 0.234 | 1.109 | 0.173 | 0.203 | 0.261 |
| | 2g | 2.066 | 0.173 | 0.038 | 2.220 | 0.173 | 0.029 | 0.047 |
| Horizontally isolated $T_1$=2.4sec | 1g | 0.418 | 0.551 | 0.212 | 0.865 | 0.551 | 0.068 | 0.051 |
| | 2g | 0.425 | 0.477 | 0.197 | 0.847 | 0.477 | 0.064 | 0.042 |
| Horizontally-vertically isolated without rocking $T_1$=2.4sec | 1g | 0.457 | 0.322 | 0.161 | 0.724 | 0.322 | 0.071 | 0.041 |
| | 2g | 0.471 | 0.278 | 0.149 | 0.730 | 0.278 | 0.067 | 0.032 |
| Horizontally-vertically isolated with rocking $T_1$=2.4sec | 1g | 0.395 | 0.620 | 0.024 | 0.935 | 0.620 | 0.066 | 0.072 |
| | 2g | 0.520 | 0.289 | 0.012 | 0.782 | 0.289 | 0.059 | 0.029 |

Table 3-16 Summary of results for probability of failure for isolated and non-isolated transformer with $W$=420kip, $f_{AI}$=4.3Hz and inclined bushing. When isolated, $D_{Capacity}$=17.7inch and lower bound friction properties. Location: **Hillsboro, OR**

| System | Transverse Bushing Acceleration Limit (g) | Without Spectral Shape Effects | | | With Spectral Shape Effects | | | Reported in MCEER-16-0010 |
|---|---|---|---|---|---|---|---|---|
| | | Median $\widehat{Sa}_F(T_1)$ (g) | $\beta_{RTR}$ | $P_F$ (50 years) | Median $\widehat{Sa}_F(T_1)$ (g) | $\beta_{RTR}$ | $P_F$ (50 years) | $P_F$ (50 years) |
| Non-isolated $T_1$=0.24sec | 1g | 1.033 | 0.173 | 0.052 | 1.037 | 0.173 | 0.051 | 0.055 |
| | 2g | 2.066 | 0.173 | 0.009 | 2.074 | 0.173 | 0.009 | 0.009 |
| Horizontally isolated $T_1$=2.4sec | 1g | 0.418 | 0.551 | 0.019 | 0.352 | 0.551 | 0.025 | 0.010 |
| | 2g | 0.425 | 0.477 | 0.016 | 0.390 | 0.477 | 0.019 | 0.008 |
| Horizontally-vertically isolated without rocking $T_1$=2.4sec | 1g | 0.457 | 0.322 | 0.012 | 0.447 | 0.322 | 0.012 | 0.008 |
| | 2g | 0.471 | 0.278 | 0.010 | 0.487 | 0.278 | 0.010 | 0.006 |
| Horizontally-vertically isolated with rocking $T_1$=2.4sec | 1g | 0.395 | 0.620 | 0.023 | 0.328 | 0.620 | 0.031 | 0.014 |
| | 2g | 0.520 | 0.289 | 0.008 | 0.512 | 0.289 | 0.009 | 0.006 |

Table 3-17 Summary of results for probability of failure for isolated and non-isolated transformer with $W$=420kip, $f_{AI}$=4.3Hz and inclined bushing. When isolated, $D_{Capacity}$=17.7inch and lower bound friction properties. Location: **Eugene, OR**

| System | Transverse Bushing Acceleration Limit (g) | Without Spectral Shape Effects | | | With Spectral Shape Effects | | | Reported in MCEER-16-0010 |
|---|---|---|---|---|---|---|---|---|
| | | Median $\widehat{Sa}_F(T_1)$ (g) | $\beta_{RTR}$ | $P_F$ (50 years) | Median $\widehat{Sa}_F(T_1)$ (g) | $\beta_{RTR}$ | $P_F$ (50 years) | $P_F$ (50 years) |
| Non-isolated $T_1$=0.24sec | 1g | 1.033 | 0.173 | 0.042 | 1.030 | 0.173 | 0.043 | 0.019 |
| | 2g | 2.066 | 0.173 | 0.010 | 2.062 | 0.173 | 0.010 | 0.004 |
| Horizontally isolated $T_1$=2.4sec | 1g | 0.418 | 0.551 | 0.019 | 0.347 | 0.551 | 0.026 | 0.004 |
| | 2g | 0.425 | 0.477 | 0.018 | 0.385 | 0.477 | 0.021 | 0.003 |
| Horizontally-vertically isolated without rocking $T_1$=2.4sec | 1g | 0.457 | 0.322 | 0.013 | 0.443 | 0.322 | 0.012 | 0.003 |
| | 2g | 0.471 | 0.278 | 0.012 | 0.483 | 0.278 | 0.010 | 0.003 |
| Horizontally-vertically isolated with rocking $T_1$=2.4sec | 1g | 0.395 | 0.620 | 0.023 | 0.321 | 0.620 | 0.030 | 0.005 |
| | 2g | 0.520 | 0.289 | 0.010 | 0.508 | 0.289 | 0.011 | 0.003 |

Table 3-18 Summary of results for probability of failure for isolated and non-isolated transformer with $W$=420kip, $f_{AI}$=4.3Hz and inclined bushing. When isolated, $D_{Capacity}$=17.7inch and lower bound friction properties. Location: **Wilsonville, OR**

| System | Transverse Bushing Acceleration Limit (g) | Without Spectral Shape Effects | | | With Spectral Shape Effects | | | Reported in MCEER-16-0010 |
|---|---|---|---|---|---|---|---|---|
| | | Median $\widehat{Sa}_F(T_1)$ (g) | $\beta_{RTR}$ | $P_F$ (50 years) | Median $\widehat{Sa}_F(T_1)$ (g) | $\beta_{RTR}$ | $P_F$ (50 years) | $P_F$ (50 years) |
| Non-isolated $T_1$=0.24sec | 1g | 1.033 | 0.173 | 0.045 | 1.030 | 0.173 | 0.045 | 0.050 |
| | 2g | 2.066 | 0.173 | 0.007 | 2.061 | 0.173 | 0.007 | 0.007 |
| Horizontally isolated $T_1$=2.4sec | 1g | 0.418 | 0.551 | 0.016 | 0.354 | 0.551 | 0.022 | 0.008 |
| | 2g | 0.425 | 0.477 | 0.014 | 0.392 | 0.477 | 0.016 | 0.006 |
| Horizontally-vertically isolated without rocking $T_1$=2.4sec | 1g | 0.457 | 0.322 | 0.009 | 0.448 | 0.322 | 0.010 | 0.006 |
| | 2g | 0.471 | 0.278 | 0.008 | 0.488 | 0.278 | 0.008 | 0.005 |
| Horizontally-vertically isolated with rocking $T_1$=2.4sec | 1g | 0.395 | 0.620 | 0.020 | 0.329 | 0.620 | 0.029 | 0.012 |
| | 2g | 0.520 | 0.289 | 0.006 | 0.513 | 0.289 | 0.011 | 0.004 |

Table 3-19 Summary of results for probability of failure for isolated and non-isolated transformer with $W$=420kip, $f_{AI}$=4.3Hz and inclined bushing. When isolated, $D_{Capacity}$=17.7inch and lower bound friction properties. Location: **Curry County, OR**

| System | Transverse Bushing Acceleration Limit (g) | Without Spectral Shape Effects | | | With Spectral Shape Effects | | | Reported in MCEER-16-0010 |
|---|---|---|---|---|---|---|---|---|
| | | Median $\widehat{Sa}_F(T_1)$ (g) | $\beta_{RTR}$ | $P_F$ (50 years) | Median $\widehat{Sa}_F(T_1)$ (g) | $\beta_{RTR}$ | $P_F$ (50 years) | $P_F$ (50 years) |
| Non-isolated $T_1$=0.24sec | 1g | 1.033 | 0.173 | 0.095 | 1.107 | 0.173 | 0.087 | 0.092 |
| | 2g | 2.066 | 0.173 | 0.031 | 2.215 | 0.173 | 0.027 | 0.029 |
| Horizontally isolated $T_1$=2.4sec | 1g | 0.418 | 0.551 | 0.063 | 0.676 | 0.551 | 0.034 | 0.031 |
| | 2g | 0.425 | 0.477 | 0.059 | 0.685 | 0.477 | 0.031 | 0.026 |
| Horizontally-vertically isolated without rocking $T_1$=2.4sec | 1g | 0.457 | 0.322 | 0.051 | 0.634 | 0.322 | 0.032 | 0.025 |
| | 2g | 0.471 | 0.278 | 0.048 | 0.653 | 0.278 | 0.029 | 0.021 |
| Horizontally-vertically isolated with rocking $T_1$=2.4sec | 1g | 0.395 | 0.620 | 0.069 | 0.701 | 0.620 | 0.034 | 0.036 |
| | 2g | 0.520 | 0.289 | 0.042 | 0.696 | 0.289 | 0.027 | 0.020 |

Table 3-20 Summary of results for probability of failure for isolated and non-isolated transformer with $W$=420kip, $f_{AI}$=4.3Hz and inclined bushing. When isolated, $D_{Capacity}$=17.7inch and lower bound friction properties. Location: **Troutdale, OR**

| System | Transverse Bushing Acceleration Limit (g) | Without Spectral Shape Effects | | | With Spectral Shape Effects | | | Reported in MCEER-16-0010 |
|---|---|---|---|---|---|---|---|---|
| | | Median $\widehat{Sa}_F(T_1)$ (g) | $\beta_{RTR}$ | $P_F$ (50 years) | Median $\widehat{Sa}_F(T_1)$ (g) | $\beta_{RTR}$ | $P_F$ (50 years) | $P_F$ (50 years) |
| Non-isolated $T_1$=0.24sec | 1g | 1.033 | 0.173 | 0.037 | 1.023 | 0.173 | 0.038 | 0.038 |
| | 2g | 2.066 | 0.173 | 0.005 | 2.047 | 0.173 | 0.005 | 0.005 |
| Horizontally isolated $T_1$=2.4sec | 1g | 0.418 | 0.551 | 0.014 | 0.345 | 0.551 | 0.020 | 0.006 |
| | 2g | 0.425 | 0.477 | 0.011 | 0.383 | 0.477 | 0.015 | 0.005 |
| Horizontally-vertically isolated without rocking $T_1$=2.4sec | 1g | 0.457 | 0.322 | 0.008 | 0.442 | 0.322 | 0.008 | 0.005 |
| | 2g | 0.471 | 0.278 | 0.007 | 0.482 | 0.278 | 0.006 | 0.004 |
| Horizontally-vertically isolated with rocking $T_1$=2.4sec | 1g | 0.395 | 0.620 | 0.017 | 0.320 | 0.620 | 0.026 | 0.009 |
| | 2g | 0.520 | 0.289 | 0.005 | 0.507 | 0.289 | 0.005 | 0.003 |

Table 3-21 Summary of results for probability of failure for isolated and non-isolated transformer with $W$=420kip, $f_{AI}$=11.3Hz and inclined bushing. When isolated, $D_{Capacity}$=17.7inch and lower bound friction properties. Location: **Vancouver, WA**

| System | Transverse Bushing Acceleration Limit (g) | Without Spectral Shape Effects | | | With Spectral Shape Effects | | | Reported in MCEER-16-0010 |
|---|---|---|---|---|---|---|---|---|
| | | Median $\widehat{Sa}_F(T_1)$ (g) | $\beta_{RTR}$ | $P_F$ (50 years) | Median $\widehat{Sa}_F(T_1)$ (g) | $\beta_{RTR}$ | $P_F$ (50 years) | $P_F$ (50 years) |
| Non-isolated $T_1$=0.09sec | 1g | 1.031 | 0.303 | 0.020 | 0.955 | 0.303 | 0.024 | 0.017 |
| | 2g | 2.063 | 0.303 | 0.002 | 1.909 | 0.303 | 0.003 | 0.002 |
| Horizontally isolated $T_1$=2.4sec | 1g | 0.352 | 0.600 | 0.023 | 0.302 | 0.600 | 0.030 | 0.014 |
| | 2g | 0.406 | 0.548 | 0.016 | 0.344 | 0.548 | 0.022 | 0.008 |
| Horizontally-vertically isolated without rocking $T_1$=2.4sec | 1g | 0.430 | 0.323 | 0.010 | 0.420 | 0.323 | 0.011 | 0.006 |
| | 2g | 0.462 | 0.316 | 0.008 | 0.442 | 0.316 | 0.009 | 0.006 |
| Horizontally-vertically isolated with rocking $T_1$=2.4sec | 1g | 0.497 | 0.291 | 0.007 | 0.500 | 0.291 | 0.007 | 0.003 |
| | 2g | 0.541 | 0.271 | 0.005 | 0.526 | 0.271 | 0.006 | 0.003 |

Table 3-22 Summary of results for probability of failure for isolated and non-isolated transformer with $W$=420kip, $f_{AI}$=11.3Hz and inclined bushing. When isolated, $D_{Capacity}$=17.7inch and lower bound friction properties. Location: **Saranap, CA**

| System | Transverse Bushing Acceleration Limit (g) | Without Spectral Shape Effects | | | With Spectral Shape Effects | | | Reported in MCEER-16-0010 |
|---|---|---|---|---|---|---|---|---|
| | | Median $\widehat{Sa}_F(T_1)$ (g) | $\beta_{RTR}$ | $P_F$ (50 years) | Median $\widehat{Sa}_F(T_1)$ (g) | $\beta_{RTR}$ | $P_F$ (50 years) | $P_F$ (50 years) |
| Non-isolated $T_1$=0.09sec | 1g | 1.031 | 0.303 | 0.105 | 1.140 | 0.303 | 0.078 | 0.079 |
| | 2g | 2.063 | 0.303 | 0.008 | 2.281 | 0.303 | 0.005 | 0.006 |
| Horizontally isolated $T_1$=2.4sec | 1g | 0.352 | 0.600 | 0.163 | 0.677 | 0.600 | 0.041 | 0.064 |
| | 2g | 0.406 | 0.548 | 0.114 | 0.717 | 0.548 | 0.029 | 0.034 |
| Horizontally-vertically isolated without rocking $T_1$=2.4sec | 1g | 0.430 | 0.323 | 0.064 | 0.616 | 0.323 | 0.022 | 0.026 |
| | 2g | 0.462 | 0.316 | 0.051 | 0.637 | 0.316 | 0.019 | 0.024 |
| Horizontally-vertically isolated with rocking $T_1$=2.4sec | 1g | 0.497 | 0.291 | 0.040 | 0.702 | 0.291 | 0.013 | 0.013 |
| | 2g | 0.541 | 0.271 | 0.029 | 0.715 | 0.271 | 0.011 | 0.011 |

Table 3-23 Summary of results for probability of failure for isolated and non-isolated transformer with $W$=420kip, $f_{AI}$=11.3Hz and inclined bushing. When isolated, $D_{Capacity}$=17.7inch and lower bound friction properties. Location: **Chehalis, WA**

| System | Transverse Bushing Acceleration Limit (g) | Without Spectral Shape Effects | | | With Spectral Shape Effects | | | Reported in MCEER-16-0010 |
|---|---|---|---|---|---|---|---|---|
| | | Median $\widehat{Sa}_F(T_1)$ (g) | $\beta_{RTR}$ | $P_F$ (50 years) | Median $\widehat{Sa}_F(T_1)$ (g) | $\beta_{RTR}$ | $P_F$ (50 years) | $P_F$ (50 years) |
| Non-isolated $T_1$=0.09sec | 1g | 1.031 | 0.303 | 0.041 | 0.959 | 0.303 | 0.048 | 0.029 |
| | 2g | 2.063 | 0.303 | 0.006 | 1.918 | 0.303 | 0.007 | 0.003 |
| Horizontally isolated $T_1$=2.4sec | 1g | 0.352 | 0.600 | 0.030 | 0.315 | 0.600 | 0.036 | 0.024 |
| | 2g | 0.406 | 0.548 | 0.021 | 0.358 | 0.548 | 0.028 | 0.014 |
| Horizontally-vertically isolated without rocking $T_1$=2.4sec | 1g | 0.430 | 0.323 | 0.015 | 0.428 | 0.323 | 0.015 | 0.011 |
| | 2g | 0.462 | 0.316 | 0.013 | 0.451 | 0.316 | 0.013 | 0.010 |
| Horizontally-vertically isolated with rocking $T_1$=2.4sec | 1g | 0.497 | 0.291 | 0.010 | 0.509 | 0.291 | 0.010 | 0.006 |
| | 2g | 0.541 | 0.271 | 0.008 | 0.534 | 0.271 | 0.009 | 0.005 |

Table 3-24 Summary of results for probability of failure for isolated and non-isolated transformer with $W$=420kip, $f_{AI}$=11.3Hz and inclined bushing. When isolated, $D_{Capacity}$=17.7inch and lower bound friction properties. Location: **Aberdeen, WA**

| System | Transverse Bushing Acceleration Limit (g) | Without Spectral Shape Effects | | | With Spectral Shape Effects | | | Reported in MCEER-16-0010 |
|---|---|---|---|---|---|---|---|---|
| | | Median $\widehat{Sa}_F(T_1)$ (g) | $\beta_{RTR}$ | $P_F$ (50 years) | Median $\widehat{Sa}_F(T_1)$ (g) | $\beta_{RTR}$ | $P_F$ (50 years) | $P_F$ (50 years) |
| Non-isolated $T_1$=0.09sec | 1g | 1.031 | 0.303 | 0.059 | 1.025 | 0.303 | 0.060 | 0.047 |
| | 2g | 2.063 | 0.303 | 0.014 | 2.049 | 0.303 | 0.014 | 0.010 |
| Horizontally isolated $T_1$=2.4sec | 1g | 0.352 | 0.600 | 0.046 | 0.402 | 0.600 | 0.039 | 0.040 |
| | 2g | 0.406 | 0.548 | 0.038 | 0.447 | 0.548 | 0.033 | 0.027 |
| Horizontally-vertically isolated without rocking $T_1$=2.4sec | 1g | 0.430 | 0.323 | 0.031 | 0.481 | 0.323 | 0.027 | 0.022 |
| | 2g | 0.462 | 0.316 | 0.028 | 0.503 | 0.316 | 0.025 | 0.021 |
| Horizontally-vertically isolated with rocking $T_1$=2.4sec | 1g | 0.497 | 0.291 | 0.025 | 0.564 | 0.291 | 0.021 | 0.014 |
| | 2g | 0.541 | 0.271 | 0.022 | 0.587 | 0.271 | 0.020 | 0.013 |

Table 3-25 Summary of results for probability of failure for isolated and non-isolated transformer with $W$=420kip, $f_{AI}$=11.3Hz and inclined bushing. When isolated, $D_{Capacity}$=17.7inch and lower bound friction properties. Location: **Loma Linda, CA**

| System | Transverse Bushing Acceleration Limit (g) | Without Spectral Shape Effects | | | With Spectral Shape Effects | | | Reported in MCEER-16-0010 |
|---|---|---|---|---|---|---|---|---|
| | | Median $\widehat{Sa}_F(T_1)$ (g) | $\beta_{RTR}$ | $P_F$ (50 years) | Median $\widehat{Sa}_F(T_1)$ (g) | $\beta_{RTR}$ | $P_F$ (50 years) | $P_F$ (50 years) |
| Non-isolated $T_1$=0.09sec | 1g | 1.031 | 0.303 | 0.143 | 1.135 | 0.303 | 0.114 | 0.113 |
| | 2g | 2.063 | 0.303 | 0.019 | 2.271 | 0.303 | 0.013 | 0.013 |
| Horizontally isolated $T_1$=2.4sec | 1g | 0.352 | 0.600 | 0.267 | 0.866 | 0.600 | 0.074 | 0.094 |
| | 2g | 0.406 | 0.548 | 0.221 | 0.897 | 0.548 | 0.064 | 0.055 |
| Horizontally-vertically isolated without rocking $T_1$=2.4sec | 1g | 0.430 | 0.323 | 0.176 | 0.693 | 0.323 | 0.078 | 0.043 |
| | 2g | 0.462 | 0.316 | 0.156 | 0.712 | 0.316 | 0.073 | 0.039 |
| Horizontally-vertically isolated with rocking $T_1$=2.4sec | 1g | 0.497 | 0.291 | 0.135 | 0.779 | 0.291 | 0.060 | 0.024 |
| | 2g | 0.541 | 0.271 | 0.115 | 0.786 | 0.271 | 0.057 | 0.021 |

Table 3-26 Summary of results for probability of failure for isolated and non-isolated transformer with $W$=420kip, $f_{AI}$=11.3Hz and inclined bushing. When isolated, $D_{Capacity}$=17.7inch and lower bound friction properties. Location: **Hillsboro, OR**

| System | Transverse Bushing Acceleration Limit (g) | Without Spectral Shape Effects | | | With Spectral Shape Effects | | | Reported in MCEER-16-0010 |
|---|---|---|---|---|---|---|---|---|
| | | Median $\widehat{Sa}_F(T_1)$ (g) | $\beta_{RTR}$ | $P_F$ (50 years) | Median $\widehat{Sa}_F(T_1)$ (g) | $\beta_{RTR}$ | $P_F$ (50 years) | $P_F$ (50 years) |
| Non-isolated $T_1$=0.09sec | 1g | 1.031 | 0.303 | 0.024 | 0.967 | 0.303 | 0.028 | 0.022 |
| | 2g | 2.063 | 0.303 | 0.004 | 1.934 | 0.303 | 0.005 | 0.003 |
| Horizontally isolated $T_1$=2.4sec | 1g | 0.352 | 0.600 | 0.027 | 0.314 | 0.600 | 0.032 | 0.018 |
| | 2g | 0.406 | 0.548 | 0.020 | 0.357 | 0.548 | 0.025 | 0.010 |
| Horizontally-vertically isolated without rocking $T_1$=2.4sec | 1g | 0.430 | 0.323 | 0.013 | 0.428 | 0.323 | 0.013 | 0.008 |
| | 2g | 0.462 | 0.316 | 0.011 | 0.450 | 0.316 | 0.012 | 0.008 |
| Horizontally-vertically isolated with rocking $T_1$=2.4sec | 1g | 0.497 | 0.291 | 0.009 | 0.508 | 0.291 | 0.009 | 0.005 |
| | 2g | 0.541 | 0.271 | 0.007 | 0.534 | 0.271 | 0.008 | 0.004 |

Table 3-27 Summary of results for probability of failure for isolated and non-isolated transformer with $W$=420kip, $f_{AI}$=11.3Hz and inclined bushing. When isolated, $D_{Capacity}$=17.7inch and lower bound friction properties. Location: **Eugene, OR**

| System | Transverse Bushing Acceleration Limit (g) | Without Spectral Shape Effects | | | With Spectral Shape Effects | | | Reported in MCEER-16-0010 |
|---|---|---|---|---|---|---|---|---|
| | | Median $\widehat{Sa}_F(T_1)$ (g) | $\beta_{RTR}$ | $P_F$ (50 years) | Median $\widehat{Sa}_F(T_1)$ (g) | $\beta_{RTR}$ | $P_F$ (50 years) | $P_F$ (50 years) |
| Non-isolated $T_1$=0.09sec | 1g | 1.031 | 0.303 | 0.019 | 0.949 | 0.303 | 0.023 | 0.007 |
| | 2g | 2.063 | 0.303 | 0.004 | 1.898 | 0.303 | 0.005 | 0.002 |
| Horizontally isolated $T_1$=2.4sec | 1g | 0.352 | 0.600 | 0.026 | 0.308 | 0.600 | 0.032 | 0.006 |
| | 2g | 0.406 | 0.548 | 0.020 | 0.351 | 0.548 | 0.025 | 0.004 |
| Horizontally-vertically isolated without rocking $T_1$=2.4sec | 1g | 0.430 | 0.323 | 0.015 | 0.424 | 0.323 | 0.015 | 0.003 |
| | 2g | 0.462 | 0.316 | 0.013 | 0.446 | 0.316 | 0.014 | 0.003 |
| Horizontally-vertically isolated with rocking $T_1$=2.4sec | 1g | 0.497 | 0.291 | 0.011 | 0.504 | 0.291 | 0.011 | 0.002 |
| | 2g | 0.541 | 0.271 | 0.009 | 0.530 | 0.271 | 0.010 | 0.002 |

Table 3-28 Summary of results for probability of failure for isolated and non-isolated transformer with $W$=420kip, $f_{AI}$=11.3Hz and inclined bushing. When isolated, $D_{Capacity}$=17.7inch and lower bound friction properties. Location: **Wilsonville, OR**

| System | Transverse Bushing Acceleration Limit (g) | Without Spectral Shape Effects | | | With Spectral Shape Effects | | | Reported in MCEER-16-0010 |
|---|---|---|---|---|---|---|---|---|
| | | Median $\widehat{Sa}_F(T_1)$ (g) | $\beta_{RTR}$ | $P_F$ (50 years) | Median $\widehat{Sa}_F(T_1)$ (g) | $\beta_{RTR}$ | $P_F$ (50 years) | $P_F$ (50 years) |
| Non-isolated $T_1$=0.09sec | 1g | 1.031 | 0.303 | 0.021 | 0.953 | 0.303 | 0.025 | 0.019 |
| | 2g | 2.063 | 0.303 | 0.003 | 1.907 | 0.303 | 0.004 | 0.002 |
| Horizontally isolated $T_1$=2.4sec | 1g | 0.352 | 0.600 | 0.023 | 0.316 | 0.600 | 0.028 | 0.015 |
| | 2g | 0.406 | 0.548 | 0.017 | 0.359 | 0.548 | 0.021 | 0.009 |
| Horizontally-vertically isolated without rocking $T_1$=2.4sec | 1g | 0.430 | 0.323 | 0.011 | 0.429 | 0.323 | 0.011 | 0.007 |
| | 2g | 0.462 | 0.316 | 0.009 | 0.451 | 0.316 | 0.010 | 0.006 |
| Horizontally-vertically isolated with rocking $T_1$=2.4sec | 1g | 0.497 | 0.291 | 0.007 | 0.509 | 0.291 | 0.007 | 0.004 |
| | 2g | 0.541 | 0.271 | 0.006 | 0.535 | 0.271 | 0.006 | 0.003 |

Table 3-29 Summary of results for probability of failure for isolated and non-isolated transformer with $W$=420kip, $f_{AI}$=11.3Hz and inclined bushing. When isolated, $D_{Capacity}$=17.7inch and lower bound friction properties. Location: **Curry County, OR**

| System | Transverse Bushing Acceleration Limit (g) | Without Spectral Shape Effects | | | With Spectral Shape Effects | | | Reported in MCEER-16-0010 |
|---|---|---|---|---|---|---|---|---|
| | | Median $\widehat{Sa}_F(T_1)$ (g) | $\beta_{RTR}$ | $P_F$ (50 years) | Median $\widehat{Sa}_F(T_1)$ (g) | $\beta_{RTR}$ | $P_F$ (50 years) | $P_F$ (50 years) |
| Non-isolated $T_1$=0.09sec | 1g | 1.031 | 0.303 | 0.055 | 1.123 | 0.303 | 0.048 | 0.052 |
| | 2g | 2.063 | 0.303 | 0.015 | 2.247 | 0.303 | 0.012 | 0.013 |
| Horizontally isolated $T_1$=2.4sec | 1g | 0.352 | 0.600 | 0.077 | 0.656 | 0.600 | 0.037 | 0.045 |
| | 2g | 0.406 | 0.548 | 0.065 | 0.697 | 0.548 | 0.032 | 0.032 |
| Horizontally-vertically isolated without rocking $T_1$=2.4sec | 1g | 0.430 | 0.323 | 0.055 | 0.607 | 0.323 | 0.034 | 0.026 |
| | 2g | 0.462 | 0.316 | 0.050 | 0.628 | 0.316 | 0.032 | 0.024 |
| Horizontally-vertically isolated with rocking $T_1$=2.4sec | 1g | 0.497 | 0.291 | 0.045 | 0.693 | 0.291 | 0.027 | 0.017 |
| | 2g | 0.541 | 0.271 | 0.039 | 0.707 | 0.271 | 0.026 | 0.016 |

Table 3-30 Summary of results for probability of failure for isolated and non-isolated transformer with $W$=420kip, $f_{AI}$=11.3Hz and inclined bushing. When isolated, $D_{Capacity}$=17.7inch and lower bound friction properties. Location: **Troutdale, OR**

| System | Transverse Bushing Acceleration Limit (g) | Without Spectral Shape Effects | | | With Spectral Shape Effects | | | Reported in MCEER-16-0010 |
|---|---|---|---|---|---|---|---|---|
| | | Median $\widehat{Sa}_F(T_1)$ (g) | $\beta_{RTR}$ | $P_F$ (50 years) | Median $\widehat{Sa}_F(T_1)$ (g) | $\beta_{RTR}$ | $P_F$ (50 years) | $P_F$ (50 years) |
| Non-isolated $T_1$=0.09sec | 1g | 1.031 | 0.303 | 0.014 | 0.948 | 0.303 | 0.021 | 0.014 |
| | 2g | 2.063 | 0.303 | 0.002 | 1.895 | 0.303 | 0.003 | 0.013 |
| Horizontally isolated $T_1$=2.4sec | 1g | 0.352 | 0.600 | 0.021 | 0.307 | 0.600 | 0.027 | 0.012 |
| | 2g | 0.406 | 0.548 | 0.014 | 0.349 | 0.548 | 0.020 | 0.006 |
| Horizontally-vertically isolated without rocking $T_1$=2.4sec | 1g | 0.430 | 0.323 | 0.009 | 0.423 | 0.323 | 0.009 | 0.005 |
| | 2g | 0.462 | 0.316 | 0.007 | 0.445 | 0.316 | 0.008 | 0.004 |
| Horizontally-vertically isolated with rocking $T_1$=2.4sec | 1g | 0.497 | 0.291 | 0.006 | 0.503 | 0.291 | 0.006 | 0.003 |
| | 2g | 0.541 | 0.271 | 0.004 | 0.529 | 0.271 | 0.005 | 0.002 |

Table 3-31 Summary of results for probability of failure for isolated and non-isolated transformer with $W$=420kip, $f_{AI}$=7.7Hz and inclined bushing. When isolated, $D_{Capacity}$=31.3inch and lower bound friction properties. Location: **Vancouver, WA**

| System | Transverse Bushing Acceleration Limit (g) | Without Spectral Shape Effects | | | With Spectral Shape Effects | | | Reported in MCEER-16-0010 |
|---|---|---|---|---|---|---|---|---|
| | | Median $\widehat{Sa}_F(T_1)$ (g) | $\beta_{RTR}$ | $P_F$ (50 years) | Median $\widehat{Sa}_F(T_1)$ (g) | $\beta_{RTR}$ | $P_F$ (50 years) | $P_F$ (50 years) |
| Non-isolated $T_1$=0.13sec | 1g | 0.735 | 0.276 | 0.063 | 0.706 | 0.276 | 0.069 | 0.089 |
| | 2g | 1.470 | 0.276 | 0.012 | 1.411 | 0.276 | 0.013 | 0.016 |
| Horizontally isolated $T_1$=2.4sec | 1g | 0.345 | 0.744 | 0.030 | 0.304 | 0.744 | 0.037 | 0.014 |
| | 2g | 0.512 | 0.611 | 0.012 | 0.430 | 0.611 | 0.016 | 0.004 |
| Horizontally-vertically isolated without rocking $T_1$=2.4sec | 1g | 0.459 | 0.405 | 0.010 | 0.414 | 0.405 | 0.012 | 0.003 |
| | 2g | 0.483 | 0.319 | 0.008 | 0.451 | 0.319 | 0.009 | 0.002 |
| Horizontally-vertically isolated with rocking $T_1$=2.4sec | 1g | 0.458 | 0.404 | 0.010 | 0.423 | 0.404 | 0.012 | 0.002 |
| | 2g | 0.523 | 0.302 | 0.006 | 0.481 | 0.302 | 0.008 | 0.001 |

Table 3-32 Summary of results for probability of failure for isolated and non-isolated transformer with $W$=420kip, $f_{AI}$=7.7Hz and inclined bushing. When isolated, $D_{Capacity}$=31.3inch and lower bound friction properties. Location: **Saranap, CA**

| System | Transverse Bushing Acceleration Limit (g) | Without Spectral Shape Effects | | | With Spectral Shape Effects | | | Reported in MCEER-16-0010 |
|---|---|---|---|---|---|---|---|---|
| | | Median $\widehat{Sa}_F(T_1)$ (g) | $\beta_{RTR}$ | $P_F$ (50 years) | Median $\widehat{Sa}_F(T_1)$ (g) | $\beta_{RTR}$ | $P_F$ (50 years) | $P_F$ (50 years) |
| Non-isolated $T_1$=0.13sec | 1g | 0.735 | 0.276 | 0.300 | 0.782 | 0.276 | 0.266 | 0.359 |
| | 2g | 1.470 | 0.276 | 0.047 | 1.564 | 0.276 | 0.038 | 0.077 |
| Horizontally isolated $T_1$=2.4sec | 1g | 0.345 | 0.744 | 0.210 | 0.700 | 0.744 | 0.058 | 0.067 |
| | 2g | 0.512 | 0.611 | 0.080 | 0.911 | 0.611 | 0.019 | 0.015 |
| Horizontally-vertically isolated without rocking $T_1$=2.4sec | 1g | 0.459 | 0.405 | 0.064 | 0.653 | 0.405 | 0.024 | 0.010 |
| | 2g | 0.483 | 0.319 | 0.046 | 0.665 | 0.319 | 0.017 | 0.006 |
| Horizontally-vertically isolated with rocking $T_1$=2.4sec | 1g | 0.458 | 0.404 | 0.064 | 0.676 | 0.404 | 0.021 | 0.006 |
| | 2g | 0.523 | 0.302 | 0.035 | 0.699 | 0.302 | 0.013 | 0.003 |

Table 3-33 Summary of results for probability of failure for isolated and non-isolated transformer with $W$=420kip, $f_{AI}$=7.7Hz and inclined bushing. When isolated, $D_{Capacity}$=31.3inch and lower bound friction properties. Location: **Loma Linda, CA**

| System | Transverse Bushing Acceleration Limit (g) | Without Spectral Shape Effects | | | With Spectral Shape Effects | | | Reported in MCEER-16-0010 |
|---|---|---|---|---|---|---|---|---|
| | | Median $\widehat{Sa}_F(T_1)$ (g) | $\beta_{RTR}$ | $P_F$ (50 years) | Median $\widehat{Sa}_F(T_1)$ (g) | $\beta_{RTR}$ | $P_F$ (50 years) | $P_F$ (50 years) |
| Non-isolated $T_1$=0.13sec | 1g | 0.735 | 0.276 | 0.108 | 0.782 | 0.276 | 0.297 | 0.398 |
| | 2g | 1.470 | 0.276 | 0.075 | 1.565 | 0.276 | 0.059 | 0.108 |
| Horizontally isolated $T_1$=2.4sec | 1g | 0.345 | 0.744 | 0.307 | 0.902 | 0.744 | 0.087 | 0.093 |
| | 2g | 0.512 | 0.611 | 0.170 | 1.146 | 0.611 | 0.044 | 0.026 |
| Horizontally-vertically isolated without rocking $T_1$=2.4sec | 1g | 0.459 | 0.405 | 0.167 | 0.751 | 0.405 | 0.073 | 0.019 |
| | 2g | 0.483 | 0.319 | 0.146 | 0.749 | 0.319 | 0.066 | 0.012 |
| Horizontally-vertically isolated with rocking $T_1$=2.4sec | 1g | 0.458 | 0.404 | 0.168 | 0.780 | 0.404 | 0.068 | 0.012 |
| | 2g | 0.523 | 0.302 | 0.127 | 0.783 | 0.302 | 0.060 | 0.006 |

Table 3-34 Summary of results for probability of failure for isolated and non-isolated transformer with $W$=420kip, $f_{AI}$=7.7Hz and inclined bushing. When isolated, $D_{Capacity}$=31.3inch and lower bound friction properties. Location: **Aberdeen, WA**

| System | Transverse Bushing Acceleration Limit (g) | Without Spectral Shape Effects | | | With Spectral Shape Effects | | | Reported in MCEER-16-0010 |
|---|---|---|---|---|---|---|---|---|
| | | Median $\widehat{Sa}_F(T_1)$ (g) | $\beta_{RTR}$ | $P_F$ (50 years) | Median $\widehat{Sa}_F(T_1)$ (g) | $\beta_{RTR}$ | $P_F$ (50 years) | $P_F$ (50 years) |
| Non-isolated $T_1$=0.13sec | 1g | 0.735 | 0.276 | 0.129 | 0.737 | 0.276 | 0.135 | 0.145 |
| | 2g | 1.470 | 0.276 | 0.038 | 1.473 | 0.276 | 0.040 | 0.044 |
| Horizontally isolated $T_1$=2.4sec | 1g | 0.345 | 0.744 | 0.053 | 0.409 | 0.744 | 0.043 | 0.038 |
| | 2g | 0.512 | 0.611 | 0.029 | 0.562 | 0.611 | 0.026 | 0.015 |
| Horizontally-vertically isolated without rocking $T_1$=2.4sec | 1g | 0.459 | 0.405 | 0.030 | 0.487 | 0.405 | 0.027 | 0.012 |
| | 2g | 0.483 | 0.319 | 0.026 | 0.518 | 0.319 | 0.024 | 0.009 |
| Horizontally-vertically isolated with rocking $T_1$=2.4sec | 1g | 0.458 | 0.404 | 0.030 | 0.500 | 0.404 | 0.026 | 0.009 |
| | 2g | 0.523 | 0.302 | 0.024 | 0.550 | 0.302 | 0.022 | 0.006 |

Table 3-35 Summary of results for probability of failure for isolated and non-isolated transformer with $W$=420kip, $f_{AI}$=7.7Hz and inclined bushing. When isolated, $D_{Capacity}$=31.3inch and lower bound friction properties. Location: **Chehalis, WA**

| System | Transverse Bushing Acceleration Limit (g) | Without Spectral Shape Effects | | | With Spectral Shape Effects | | | Reported in MCEER-16-0010 |
|---|---|---|---|---|---|---|---|---|
| | | Median $\widehat{Sa}_F(T_1)$ (g) | $\beta_{RTR}$ | $P_F$ (50 years) | Median $\widehat{Sa}_F(T_1)$ (g) | $\beta_{RTR}$ | $P_F$ (50 years) | $P_F$ (50 years) |
| Non-isolated $T_1$=0.13sec | 1g | 0.735 | 0.276 | 0.108 | 0.717 | 0.276 | 0.113 | 0.128 |
| | 2g | 1.470 | 0.276 | 0.022 | 1.434 | 0.276 | 0.024 | 0.028 |
| Horizontally isolated $T_1$=2.4sec | 1g | 0.345 | 0.744 | 0.039 | 0.318 | 0.744 | 0.044 | 0.024 |
| | 2g | 0.512 | 0.611 | 0.016 | 0.448 | 0.611 | 0.021 | 0.007 |
| Horizontally-vertically isolated without rocking $T_1$=2.4sec | 1g | 0.459 | 0.405 | 0.014 | 0.424 | 0.405 | 0.017 | 0.005 |
| | 2g | 0.483 | 0.319 | 0.012 | 0.460 | 0.319 | 0.013 | 0.003 |
| Horizontally-vertically isolated with rocking $T_1$=2.4sec | 1g | 0.458 | 0.404 | 0.014 | 0.433 | 0.404 | 0.016 | 0.003 |
| | 2g | 0.523 | 0.302 | 0.010 | 0.491 | 0.302 | 0.011 | 0.002 |

Table 3-36 Summary of results for probability of failure for isolated and non-isolated transformer with $W$=420kip, $f_{AI}$=7.7Hz and inclined bushing. When isolated, $D_{Capacity}$=31.3inch and lower bound friction properties. Location: **Hillsboro, OR**

| System | Transverse Bushing Acceleration Limit (g) | Without Spectral Shape Effects | | | With Spectral Shape Effects | | | Reported in MCEER-16-0010 |
|---|---|---|---|---|---|---|---|---|
| | | Median $\widehat{Sa}_F(T_1)$ (g) | $\beta_{RTR}$ | $P_F$ (50 years) | Median $\widehat{Sa}_F(T_1)$ (g) | $\beta_{RTR}$ | $P_F$ (50 years) | $P_F$ (50 years) |
| Non-isolated $T_1$=0.13sec | 1g | 0.735 | 0.276 | 0.071 | 0.711 | 0.276 | 0.076 | 0.094 |
| | 2g | 1.470 | 0.276 | 0.015 | 1.422 | 0.276 | 0.017 | 0.021 |
| Horizontally isolated $T_1$=2.4sec | 1g | 0.345 | 0.744 | 0.034 | 0.317 | 0.744 | 0.038 | 0.018 |
| | 2g | 0.512 | 0.611 | 0.014 | 0.447 | 0.611 | 0.018 | 0.005 |
| Horizontally-vertically isolated without rocking $T_1$=2.4sec | 1g | 0.459 | 0.405 | 0.013 | 0.423 | 0.405 | 0.015 | 0.004 |
| | 2g | 0.483 | 0.319 | 0.010 | 0.460 | 0.319 | 0.011 | 0.002 |
| Horizontally-vertically isolated with rocking $T_1$=2.4sec | 1g | 0.458 | 0.404 | 0.013 | 0.433 | 0.404 | 0.014 | 0.002 |
| | 2g | 0.523 | 0.302 | 0.008 | 0.490 | 0.302 | 0.010 | 0.001 |

Table 3-37 Summary of results for probability of failure for isolated and non-isolated transformer with $W$=420kip, $f_{AI}$=7.7Hz and inclined bushing. When isolated, $D_{Capacity}$=31.3inch and lower bound friction properties. Location: **Eugene, OR**

| System | Transverse Bushing Acceleration Limit (g) | Without Spectral Shape Effects | | | With Spectral Shape Effects | | | Reported in MCEER-16-0010 |
|---|---|---|---|---|---|---|---|---|
| | | Median $\widehat{Sa}_F(T_1)$ (g) | $\beta_{RTR}$ | $P_F$ (50 years) | Median $\widehat{Sa}_F(T_1)$ (g) | $\beta_{RTR}$ | $P_F$ (50 years) | $P_F$ (50 years) |
| Non-isolated $T_1$=0.13sec | 1g | 0.735 | 0.276 | 0.049 | 0.704 | 0.276 | 0.052 | 0.038 |
| | 2g | 1.470 | 0.276 | 0.014 | 1.407 | 0.276 | 0.015 | 0.007 |
| Horizontally isolated $T_1$=2.4sec | 1g | 0.345 | 0.744 | 0.031 | 0.311 | 0.744 | 0.035 | 0.007 |
| | 2g | 0.512 | 0.611 | 0.015 | 0.439 | 0.611 | 0.019 | 0.002 |
| Horizontally-vertically isolated without rocking $T_1$=2.4sec | 1g | 0.459 | 0.405 | 0.014 | 0.419 | 0.405 | 0.017 | 0.002 |
| | 2g | 0.483 | 0.319 | 0.012 | 0.456 | 0.319 | 0.014 | 0.001 |
| Horizontally-vertically isolated with rocking $T_1$=2.4sec | 1g | 0.458 | 0.404 | 0.014 | 0.428 | 0.404 | 0.016 | 0.001 |
| | 2g | 0.523 | 0.302 | 0.010 | 0.486 | 0.302 | 0.012 | 0.001 |

Table 3-38 Summary of results for probability of failure for isolated and non-isolated transformer with $W$=420kip, $f_{AI}$=7.7Hz and inclined bushing. When isolated, $D_{Capacity}$=31.3inch and lower bound friction properties. Location: **Wilsonville, OR**

| System | Transverse Bushing Acceleration Limit (g) | Without Spectral Shape Effects | | | With Spectral Shape Effects | | | Reported in MCEER-16-0010 |
|---|---|---|---|---|---|---|---|---|
| | | Median $\widehat{Sa}_F(T_1)$ (g) | $\beta_{RTR}$ | $P_F$ (50 years) | Median $\widehat{Sa}_F(T_1)$ (g) | $\beta_{RTR}$ | $P_F$ (50 years) | $P_F$ (50 years) |
| Non-isolated $T_1$=0.13sec | 1g | 0.735 | 0.276 | 0.064 | 0.705 | 0.276 | 0.069 | 0.087 |
| | 2g | 1.470 | 0.276 | 0.012 | 1.410 | 0.276 | 0.014 | 0.018 |
| Horizontally isolated $T_1$=2.4sec | 1g | 0.345 | 0.744 | 0.030 | 0.319 | 0.744 | 0.034 | 0.002 |
| | 2g | 0.512 | 0.611 | 0.012 | 0.449 | 0.611 | 0.015 | 0.004 |
| Horizontally-vertically isolated without rocking $T_1$=2.4sec | 1g | 0.459 | 0.405 | 0.010 | 0.425 | 0.405 | 0.012 | 0.003 |
| | 2g | 0.483 | 0.319 | 0.008 | 0.461 | 0.319 | 0.009 | 0.002 |
| Horizontally-vertically isolated with rocking $T_1$=2.4sec | 1g | 0.458 | 0.404 | 0.010 | 0.434 | 0.404 | 0.012 | 0.002 |
| | 2g | 0.523 | 0.302 | 0.007 | 0.492 | 0.302 | 0.008 | 0.001 |

Table 3-39 Summary of results for probability of failure for isolated and non-isolated transformer with $W$=420kip, $f_{AI}$=7.7Hz and inclined bushing. When isolated, $D_{Capacity}$=31.3inch and lower bound friction properties. Location: **Curry County, OR**

| System | Transverse Bushing Acceleration Limit (g) | Without Spectral Shape Effects | | | With Spectral Shape Effects | | | Reported in MCEER-16-0010 |
|---|---|---|---|---|---|---|---|---|
| | | Median $\widehat{Sa}_F(T_1)$ (g) | $\beta_{RTR}$ | $P_F$ (50 years) | Median $\widehat{Sa}_F(T_1)$ (g) | $\beta_{RTR}$ | $P_F$ (50 years) | $P_F$ (50 years) |
| Non-isolated $T_1$=0.24sec | 1g | 0.735 | 0.276 | 0.111 | 0.778 | 0.276 | 0.107 | 0.123 |
| | 2g | 1.470 | 0.276 | 0.038 | 1.556 | 0.276 | 0.036 | 0.047 |
| Horizontally isolated $T_1$=2.4sec | 1g | 0.345 | 0.744 | 0.085 | 0.677 | 0.744 | 0.040 | 0.042 |
| | 2g | 0.512 | 0.611 | 0.051 | 0.885 | 0.611 | 0.024 | 0.019 |
| Horizontally-vertically isolated without rocking $T_1$=2.4sec | 1g | 0.459 | 0.405 | 0.052 | 0.642 | 0.405 | 0.033 | 0.015 |
| | 2g | 0.483 | 0.319 | 0.047 | 0.655 | 0.319 | 0.030 | 0.011 |
| Horizontally-vertically isolated with rocking $T_1$=2.4sec | 1g | 0.458 | 0.404 | 0.052 | 0.664 | 0.404 | 0.030 | 0.011 |
| | 2g | 0.523 | 0.302 | 0.042 | 0.689 | 0.302 | 0.027 | 0.007 |

Table 3-40 Summary of results for probability of failure for isolated and non-isolated transformer with $W$=420kip, $f_{AI}$=7.7Hz and inclined bushing. When isolated, $D_{Capacity}$=31.3inch and lower bound friction properties. Location: **Troutdale, OR**

| System | Transverse Bushing Acceleration Limit (g) | Without Spectral Shape Effects | | | With Spectral Shape Effects | | | Reported in MCEER-16-0010 |
|---|---|---|---|---|---|---|---|---|
| | | Median $\widehat{Sa}_F(T_1)$ (g) | $\beta_{RTR}$ | $P_F$ (50 years) | Median $\widehat{Sa}_F(T_1)$ (g) | $\beta_{RTR}$ | $P_F$ (50 years) | $P_F$ (50 years) |
| Non-isolated $T_1$=0.13sec | 1g | 0.735 | 0.276 | 0.056 | 0.702 | 0.276 | 0.061 | 0.071 |
| | 2g | 1.470 | 0.276 | 0.009 | 1.403 | 0.276 | 0.011 | 0.014 |
| Horizontally isolated $T_1$=2.4sec | 1g | 0.345 | 0.744 | 0.028 | 0.310 | 0.744 | 0.033 | 0.012 |
| | 2g | 0.512 | 0.611 | 0.010 | 0.437 | 0.611 | 0.014 | 0.003 |
| Horizontally-vertically isolated without rocking $T_1$=2.4sec | 1g | 0.459 | 0.405 | 0.009 | 0.418 | 0.405 | 0.011 | 0.002 |
| | 2g | 0.483 | 0.319 | 0.007 | 0.454 | 0.319 | 0.008 | 0.001 |
| Horizontally-vertically isolated with rocking $T_1$=2.4sec | 1g | 0.458 | 0.404 | 0.009 | 0.427 | 0.404 | 0.010 | 0.001 |
| | 2g | 0.523 | 0.302 | 0.005 | 0.485 | 0.302 | 0.006 | 0.001 |

Table 3-41 Summary of results for probability of failure for isolated and non-isolated transformer with $W$=420kip, $f_{AI}$=4.3Hz and inclined bushing. When isolated, $D_{Capacity}$=31.3inch and lower bound friction properties. Location: **Vancouver, WA**

| System | Transverse Bushing Acceleration Limit (g) | Without Spectral Shape Effects | | | With Spectral Shape Effects | | | Reported in MCEER-16-0010 |
|---|---|---|---|---|---|---|---|---|
| | | Median $\widehat{Sa}_F(T_1)$ (g) | $\beta_{RTR}$ | $P_F$ (50 years) | Median $\widehat{Sa}_F(T_1)$ (g) | $\beta_{RTR}$ | $P_F$ (50 years) | $P_F$ (50 years) |
| Non-isolated $T_1$=0.24sec | 1g | 1.033 | 0.173 | 0.043 | 1.030 | 0.173 | 0.045 | 0.045 |
| | 2g | 2.066 | 0.173 | 0.006 | 2.061 | 0.173 | 0.006 | 0.007 |
| Horizontally isolated $T_1$=2.4sec | 1g | 0.472 | 0.672 | 0.015 | 0.408 | 0.672 | 0.020 | NA |
| | 2g | 0.592 | 0.607 | 0.009 | 0.470 | 0.607 | 0.014 | NA |
| Horizontally-vertically isolated without rocking $T_1$=2.4sec | 1g | 0.676 | 0.423 | 0.004 | 0.563 | 0.423 | 0.006 | NA |
| | 2g | 0.718 | 0.341 | 0.003 | 0.647 | 0.341 | 0.004 | NA |
| Horizontally-vertically isolated with rocking $T_1$=2.4sec | 1g | 0.454 | 0.746 | 0.019 | 0.370 | 0.746 | 0.027 | NA |
| | 2g | 0.738 | 0.388 | 0.003 | 0.664 | 0.388 | 0.004 | NA |

Table 3-42 Summary of results for probability of failure for isolated and non-isolated transformer with $W$=420kip, $f_{AI}$=4.3Hz and inclined bushing. When isolated, $D_{Capacity}$=31.3inch and lower bound friction properties. Location: **Saranap, CA**

| System | Transverse Bushing Acceleration Limit (g) | Without Spectral Shape Effects | | | With Spectral Shape Effects | | | Reported in MCEER-16-0010 |
|---|---|---|---|---|---|---|---|---|
| | | Median $\widehat{Sa}_F(T_1)$ (g) | $\beta_{RTR}$ | $P_F$ (50 years) | Median $\widehat{Sa}_F(T_1)$ (g) | $\beta_{RTR}$ | $P_F$ (50 years) | $P_F$ (50 years) |
| Non-isolated $T_1$=0.24sec | 1g | 1.033 | 0.173 | 0.182 | 1.105 | 0.173 | 0.153 | 0.211 |
| | 2g | 2.066 | 0.173 | 0.016 | 2.211 | 0.173 | 0.012 | 0.027 |
| Horizontally isolated $T_1$=2.4sec | 1g | 0.472 | 0.672 | 0.109 | 0.920 | 0.672 | 0.024 | NA |
| | 2g | 0.592 | 0.607 | 0.057 | 1.014 | 0.607 | 0.014 | NA |
| Horizontally-vertically isolated without rocking $T_1$=2.4sec | 1g | 0.676 | 0.423 | 0.023 | 0.928 | 0.423 | 0.008 | NA |
| | 2g | 0.718 | 0.341 | 0.014 | 0.973 | 0.341 | 0.004 | NA |
| Horizontally-vertically isolated with rocking $T_1$=2.4sec | 1g | 0.454 | 0.746 | 0.135 | 0.959 | 0.746 | 0.029 | NA |
| | 2g | 0.738 | 0.388 | 0.015 | 1.037 | 0.388 | 0.004 | NA |

Table 3-43 Summary of results for probability of failure for isolated and non-isolated transformer with $W$=420kip, $f_{AI}$=4.3Hz and inclined bushing. When isolated, $D_{Capacity}$=31.3inch and lower bound friction properties. Location: **Chehalis, WA**

| System | Transverse Bushing Acceleration Limit (g) | Without Spectral Shape Effects | | | With Spectral Shape Effects | | | Reported in MCEER-16-0010 |
|---|---|---|---|---|---|---|---|---|
| | | Median $\widehat{Sa}_F(T_1)$ (g) | $\beta_{RTR}$ | $P_F$ (50 years) | Median $\widehat{Sa}_F(T_1)$ (g) | $\beta_{RTR}$ | $P_F$ (50 years) | $P_F$ (50 years) |
| Non-isolated $T_1$=0.24sec | 1g | 1.033 | 0.173 | 0.070 | 1.043 | 0.173 | 0.069 | 0.074 |
| | 2g | 2.066 | 0.173 | 0.012 | 2.087 | 0.173 | 0.011 | 0.012 |
| Horizontally isolated $T_1$=2.4sec | 1g | 0.472 | 0.672 | 0.021 | 0.426 | 0.672 | 0.025 | NA |
| | 2g | 0.592 | 0.607 | 0.012 | 0.489 | 0.607 | 0.017 | NA |
| Horizontally-vertically isolated without rocking $T_1$=2.4sec | 1g | 0.676 | 0.423 | 0.007 | 0.579 | 0.423 | 0.009 | NA |
| | 2g | 0.718 | 0.341 | 0.005 | 0.661 | 0.341 | 0.006 | NA |
| Horizontally-vertically isolated with rocking $T_1$=2.4sec | 1g | 0.454 | 0.746 | 0.025 | 0.389 | 0.746 | 0.032 | NA |
| | 2g | 0.738 | 0.388 | 0.005 | 0.680 | 0.388 | 0.006 | NA |

Table 3-44 Summary of results for probability of failure for isolated and non-isolated transformer with $W$=420kip, $f_{AI}$=4.3Hz and inclined bushing. When isolated, $D_{Capacity}$=31.3inch and lower bound friction properties. Location: **Aberdeen, WA**

| System | Transverse Bushing Acceleration Limit (g) | Without Spectral Shape Effects | | | With Spectral Shape Effects | | | Reported in MCEER-16-0010 |
|---|---|---|---|---|---|---|---|---|
| | | Median $\widehat{Sa}_F(T_1)$ (g) | $\beta_{RTR}$ | $P_F$ (50 years) | Median $\widehat{Sa}_F(T_1)$ (g) | $\beta_{RTR}$ | $P_F$ (50 years) | $P_F$ (50 years) |
| Non-isolated $T_1$=0.24sec | 1g | 1.033 | 0.173 | 0.095 | 1.064 | 0.173 | 0.091 | 0.095 |
| | 2g | 2.066 | 0.173 | 0.027 | 2.130 | 0.173 | 0.026 | 0.025 |
| Horizontally isolated $T_1$=2.4sec | 1g | 0.472 | 0.672 | 0.034 | 0.545 | 0.672 | 0.029 | NA |
| | 2g | 0.592 | 0.607 | 0.024 | 0.618 | 0.607 | 0.023 | NA |
| Horizontally-vertically isolated without rocking $T_1$=2.4sec | 1g | 0.676 | 0.423 | 0.017 | 0.673 | 0.423 | 0.017 | NA |
| | 2g | 0.718 | 0.341 | 0.015 | 0.748 | 0.341 | 0.014 | NA |
| Horizontally-vertically isolated with rocking $T_1$=2.4sec | 1g | 0.454 | 0.746 | 0.038 | 0.519 | 0.746 | 0.033 | NA |
| | 2g | 0.738 | 0.388 | 0.015 | 0.778 | 0.388 | 0.013 | NA |

Table 3-45 Summary of results for probability of failure for isolated and non-isolated transformer with $W$=420kip, $f_{AI}$=4.3Hz and inclined bushing. When isolated, $D_{Capacity}$=31.3inch and lower bound friction properties. Location: **Loma Linda, CA**

| System | Transverse Bushing Acceleration Limit (g) | Without Spectral Shape Effects | | | With Spectral Shape Effects | | | Reported in MCEER-16-0010 |
|---|---|---|---|---|---|---|---|---|
| | | Median $\widehat{Sa}_F(T_1)$ (g) | $\beta_{RTR}$ | $P_F$ (50 years) | Median $\widehat{Sa}_F(T_1)$ (g) | $\beta_{RTR}$ | $P_F$ (50 years) | $P_F$ (50 years) |
| Non-isolated $T_1$=0.24sec | 1g | 1.033 | 0.173 | 0.234 | 1.119 | 0.173 | 0.203 | 0.261 |
| | 2g | 2.066 | 0.173 | 0.038 | 2.241 | 0.173 | 0.029 | 0.047 |
| Horizontally isolated $T_1$=2.4sec | 1g | 0.472 | 0.672 | 0.201 | 0.925 | 0.672 | 0.074 | NA |
| | 2g | 0.592 | 0.607 | 0.138 | 1.019 | 0.607 | 0.055 | NA |
| Horizontally-vertically isolated without rocking $T_1$=2.4sec | 1g | 0.676 | 0.423 | 0.090 | 0.931 | 0.423 | 0.048 | NA |
| | 2g | 0.718 | 0.341 | 0.074 | 0.976 | 0.341 | 0.039 | NA |
| Horizontally-vertically isolated with rocking $T_1$=2.4sec | 1g | 0.454 | 0.746 | 0.226 | 0.965 | 0.746 | 0.078 | NA |
| | 2g | 0.738 | 0.388 | 0.074 | 1.040 | 0.388 | 0.036 | NA |

Table 3-46 Summary of results for probability of failure for isolated and non-isolated transformer with $W$=420kip, $f_{AI}$=4.3Hz and inclined bushing. When isolated, $D_{Capacity}$=31.3inch and lower bound friction properties. Location: **Hillsboro, OR**

| System | Transverse Bushing Acceleration Limit (g) | Without Spectral Shape Effects | | | With Spectral Shape Effects | | | Reported in MCEER-16-0010 |
|---|---|---|---|---|---|---|---|---|
| | | Median $\widehat{Sa}_F(T_1)$ (g) | $\beta_{RTR}$ | $P_F$ (50 years) | Median $\widehat{Sa}_F(T_1)$ (g) | $\beta_{RTR}$ | $P_F$ (50 years) | $P_F$ (50 years) |
| Non-isolated $T_1$=0.24sec | 1g | 1.033 | 0.173 | 0.052 | 1.037 | 0.173 | 0.051 | 0.055 |
| | 2g | 2.066 | 0.173 | 0.009 | 2.074 | 0.173 | 0.009 | 0.009 |
| Horizontally isolated $T_1$=2.4sec | 1g | 0.472 | 0.672 | 0.018 | 0.425 | 0.672 | 0.022 | NA |
| | 2g | 0.592 | 0.607 | 0.011 | 0.488 | 0.607 | 0.016 | NA |
| Horizontally-vertically isolated without rocking $T_1$=2.4sec | 1g | 0.676 | 0.423 | 0.006 | 0.578 | 0.423 | 0.008 | NA |
| | 2g | 0.718 | 0.341 | 0.004 | 0.660 | 0.341 | 0.005 | NA |
| Horizontally-vertically isolated with rocking $T_1$=2.4sec | 1g | 0.454 | 0.746 | 0.022 | 0.388 | 0.746 | 0.028 | NA |
| | 2g | 0.738 | 0.388 | 0.004 | 0.679 | 0.388 | 0.005 | NA |

Table 3-47 Summary of results for probability of failure for isolated and non-isolated transformer with $W$=420kip, $f_{AI}$=4.3Hz and inclined bushing. When isolated, $D_{Capacity}$=31.3inch and lower bound friction properties. Location: **Eugene, OR**

| System | Transverse Bushing Acceleration Limit (g) | Without Spectral Shape Effects | | | With Spectral Shape Effects | | | Reported in MCEER-16-0010 |
|---|---|---|---|---|---|---|---|---|
| | | Median $\widehat{Sa}_F(T_1)$ (g) | $\beta_{RTR}$ | $P_F$ (50 years) | Median $\widehat{Sa}_F(T_1)$ (g) | $\beta_{RTR}$ | $P_F$ (50 years) | $P_F$ (50 years) |
| Non-isolated $T_1$=0.24sec | 1g | 1.033 | 0.173 | 0.042 | 1.030 | 0.173 | 0.043 | 0.019 |
| | 2g | 2.066 | 0.173 | 0.010 | 2.062 | 0.173 | 0.010 | 0.004 |
| Horizontally isolated $T_1$=2.4sec | 1g | 0.472 | 0.672 | 0.018 | 0.417 | 0.672 | 0.022 | NA |
| | 2g | 0.592 | 0.607 | 0.012 | 0.479 | 0.607 | 0.017 | NA |
| Horizontally-vertically isolated without rocking $T_1$=2.4sec | 1g | 0.676 | 0.423 | 0.007 | 0.571 | 0.423 | 0.010 | NA |
| | 2g | 0.718 | 0.341 | 0.006 | 0.654 | 0.341 | 0.007 | NA |
| Horizontally-vertically isolated with rocking $T_1$=2.4sec | 1g | 0.454 | 0.746 | 0.021 | 0.380 | 0.746 | 0.027 | NA |
| | 2g | 0.738 | 0.388 | 0.006 | 0.672 | 0.388 | 0.007 | NA |

Table 3-48 Summary of results for probability of failure for isolated and non-isolated transformer with $W$=420kip, $f_{AI}$=4.3Hz and inclined bushing. When isolated, $D_{Capacity}$=31.3inch and lower bound friction properties. Location: **Wilsonville, OR**

| System | Transverse Bushing Acceleration Limit (g) | Without Spectral Shape Effects | | | With Spectral Shape Effects | | | Reported in MCEER-16-0010 |
|---|---|---|---|---|---|---|---|---|
| | | Median $\widehat{Sa}_F(T_1)$ (g) | $\beta_{RTR}$ | $P_F$ (50 years) | Median $\widehat{Sa}_F(T_1)$ (g) | $\beta_{RTR}$ | $P_F$ (50 years) | $P_F$ (50 years) |
| Non-isolated $T_1$=0.24sec | 1g | 1.033 | 0.173 | 0.045 | 1.030 | 0.173 | 0.045 | 0.050 |
| | 2g | 2.066 | 0.173 | 0.007 | 2.061 | 0.173 | 0.007 | 0.007 |
| Horizontally isolated $T_1$=2.4sec | 1g | 0.472 | 0.672 | 0.016 | 0.427 | 0.672 | 0.019 | NA |
| | 2g | 0.592 | 0.607 | 0.009 | 0.491 | 0.607 | 0.013 | NA |
| Horizontally-vertically isolated without rocking $T_1$=2.4sec | 1g | 0.676 | 0.423 | 0.004 | 0.580 | 0.423 | 0.006 | NA |
| | 2g | 0.718 | 0.341 | 0.003 | 0.662 | 0.341 | 0.004 | NA |
| Horizontally-vertically isolated with rocking $T_1$=2.4sec | 1g | 0.454 | 0.746 | 0.019 | 0.391 | 0.746 | 0.025 | NA |
| | 2g | 0.738 | 0.388 | 0.003 | 0.681 | 0.388 | 0.004 | NA |

Table 3-49 Summary of results for probability of failure for isolated and non-isolated transformer with $W$=420kip, $f_{AI}$=4.3Hz and inclined bushing. When isolated, $D_{Capacity}$=31.3inch and lower bound friction properties. Location: **Curry County, OR**

| System | Transverse Bushing Acceleration Limit (g) | Without Spectral Shape Effects | | | With Spectral Shape Effects | | | Reported in MCEER-16-0010 |
|---|---|---|---|---|---|---|---|---|
| | | Median $\widehat{Sa}_F(T_1)$ (g) | $\beta_{RTR}$ | $P_F$ (50 years) | Median $\widehat{Sa}_F(T_1)$ (g) | $\beta_{RTR}$ | $P_F$ (50 years) | $P_F$ (50 years) |
| Non-isolated $T_1$=0.24sec | 1g | 1.033 | 0.173 | 0.095 | 1.107 | 0.173 | 0.087 | 0.092 |
| | 2g | 2.066 | 0.173 | 0.031 | 2.215 | 0.173 | 0.027 | 0.029 |
| Horizontally isolated $T_1$=2.4sec | 1g | 0.472 | 0.672 | 0.058 | 0.891 | 0.672 | 0.025 | NA |
| | 2g | 0.592 | 0.607 | 0.042 | 0.984 | 0.607 | 0.020 | NA |
| Horizontally-vertically isolated without rocking $T_1$=2.4sec | 1g | 0.676 | 0.423 | 0.031 | 0.910 | 0.423 | 0.019 | NA |
| | 2g | 0.718 | 0.341 | 0.026 | 0.958 | 0.341 | 0.016 | NA |
| Horizontally-vertically isolated with rocking $T_1$=2.4sec | 1g | 0.454 | 0.746 | 0.064 | 0.924 | 0.746 | 0.026 | NA |
| | 2g | 0.738 | 0.388 | 0.026 | 1.019 | 0.388 | 0.015 | NA |

Table 3-50 Summary of results for probability of failure for isolated and non-isolated transformer with $W$=420kip, $f_{AI}$=4.3Hz and inclined bushing. When isolated, $D_{Capacity}$=31.3inch and lower bound friction properties. Location: **Troutdale, OR**

| System | Transverse Bushing Acceleration Limit (g) | Without Spectral Shape Effects | | | With Spectral Shape Effects | | | Reported in MCEER-16-0010 |
|---|---|---|---|---|---|---|---|---|
| | | Median $\widehat{Sa}_F(T_1)$ (g) | $\beta_{RTR}$ | $P_F$ (50 years) | Median $\widehat{Sa}_F(T_1)$ (g) | $\beta_{RTR}$ | $P_F$ (50 years) | $P_F$ (50 years) |
| Non-isolated $T_1$=0.24sec | 1g | 1.033 | 0.173 | 0.037 | 1.023 | 0.173 | 0.038 | 0.038 |
| | 2g | 2.066 | 0.173 | 0.005 | 2.047 | 0.173 | 0.005 | 0.005 |
| Horizontally isolated $T_1$=2.4sec | 1g | 0.472 | 0.672 | 0.014 | 0.415 | 0.672 | 0.018 | NA |
| | 2g | 0.592 | 0.607 | 0.008 | 0.477 | 0.607 | 0.012 | NA |
| Horizontally-vertically isolated without rocking $T_1$=2.4sec | 1g | 0.676 | 0.423 | 0.003 | 0.569 | 0.423 | 0.005 | NA |
| | 2g | 0.718 | 0.341 | 0.002 | 0.653 | 0.341 | 0.003 | NA |
| Horizontally-vertically isolated with rocking $T_1$=2.4sec | 1g | 0.454 | 0.746 | 0.017 | 0.377 | 0.746 | 0.024 | NA |
| | 2g | 0.738 | 0.388 | 0.002 | 0.670 | 0.388 | 0.003 | NA |

Table 3-51 Summary of results for probability of failure for isolated and non-isolated transformer with $W$=420kip, $f_{AI}$=11.3Hz and inclined bushing. When isolated, $D_{Capacity}$=31.3inch and lower bound friction properties. Location: **Vancouver, WA**

| System | Transverse Bushing Acceleration Limit (g) | Without Spectral Shape Effects | | | With Spectral Shape Effects | | | Reported in MCEER-16-0010 |
|---|---|---|---|---|---|---|---|---|
| | | Median $\widehat{Sa}_F(T_1)$ (g) | $\beta_{RTR}$ | $P_F$ (50 years) | Median $\widehat{Sa}_F(T_1)$ (g) | $\beta_{RTR}$ | $P_F$ (50 years) | $P_F$ (50 years) |
| Non-isolated $T_1$=0.09sec | 1g | 1.031 | 0.303 | 0.020 | 0.955 | 0.303 | 0.024 | 0.017 |
| | 2g | 2.063 | 0.303 | 0.002 | 1.909 | 0.303 | 0.003 | 0.002 |
| Horizontally isolated $T_1$=2.4sec | 1g | 0.439 | 0.714 | 0.019 | 0.350 | 0.714 | 0.028 | NA |
| | 2g | 0.583 | 0.672 | 0.010 | 0.425 | 0.672 | 0.019 | NA |
| Horizontally-vertically isolated without rocking $T_1$=2.4sec | 1g | 0.636 | 0.437 | 0.005 | 0.546 | 0.437 | 0.007 | NA |
| | 2g | 0.657 | 0.415 | 0.004 | 0.572 | 0.415 | 0.006 | NA |
| Horizontally-vertically isolated with rocking $T_1$=2.4sec | 1g | 0.729 | 0.381 | 0.003 | 0.648 | 0.381 | 0.004 | NA |
| | 2g | 0.763 | 0.346 | 0.002 | 0.692 | 0.346 | 0.003 | NA |

Table 3-52 Summary of results for probability of failure for isolated and non-isolated transformer with $W$=420kip, $f_{AI}$=11.3Hz and inclined bushing. When isolated, $D_{Capacity}$=31.3inch and lower bound friction properties. Location: **Saranap, CA**

| System | Transverse Bushing Acceleration Limit (g) | Without Spectral Shape Effects | | | With Spectral Shape Effects | | | Reported in MCEER-16-0010 |
|---|---|---|---|---|---|---|---|---|
| | | Median $\widehat{Sa}_F(T_1)$ (g) | $\beta_{RTR}$ | $P_F$ (50 years) | Median $\widehat{Sa}_F(T_1)$ (g) | $\beta_{RTR}$ | $P_F$ (50 years) | $P_F$ (50 years) |
| Non-isolated $T_1$=0.09sec | 1g | 1.031 | 0.303 | 0.105 | 1.139 | 0.303 | 0.079 | 0.079 |
| | 2g | 2.063 | 0.303 | 0.008 | 2.277 | 0.303 | 0.005 | 0.006 |
| Horizontally isolated $T_1$=2.4sec | 1g | 0.439 | 0.714 | 0.135 | 0.656 | 0.714 | 0.062 | NA |
| | 2g | 0.583 | 0.672 | 0.071 | 0.767 | 0.672 | 0.038 | NA |
| Horizontally-vertically isolated without rocking $T_1$=2.4sec | 1g | 0.636 | 0.437 | 0.028 | 0.771 | 0.437 | 0.016 | NA |
| | 2g | 0.657 | 0.415 | 0.024 | 0.795 | 0.415 | 0.013 | NA |
| Horizontally-vertically isolated with rocking $T_1$=2.4sec | 1g | 0.729 | 0.381 | 0.015 | 0.875 | 0.381 | 0.008 | NA |
| | 2g | 0.763 | 0.346 | 0.011 | 0.914 | 0.346 | 0.006 | NA |

Table 3-53 Summary of results for probability of failure for isolated and non-isolated transformer with $W$=420kip, $f_{AI}$=11.3Hz and inclined bushing. When isolated, $D_{Capacity}$=31.3inch and lower bound friction properties. Location: **Chehalis, WA**

| System | Transverse Bushing Acceleration Limit (g) | Without Spectral Shape Effects | | | With Spectral Shape Effects | | | Reported in MCEER-16-0010 |
|---|---|---|---|---|---|---|---|---|
| | | Median $\widehat{Sa}_F(T_1)$ (g) | $\beta_{RTR}$ | $P_F$ (50 years) | Median $\widehat{Sa}_F(T_1)$ (g) | $\beta_{RTR}$ | $P_F$ (50 years) | $P_F$ (50 years) |
| Non-isolated $T_1$=0.09sec | 1g | 1.031 | 0.303 | 0.041 | 0.959 | 0.303 | 0.048 | 0.029 |
| | 2g | 2.063 | 0.303 | 0.006 | 1.918 | 0.303 | 0.007 | 0.003 |
| Horizontally isolated $T_1$=2.4sec | 1g | 0.439 | 0.714 | 0.025 | 0.367 | 0.714 | 0.034 | NA |
| | 2g | 0.583 | 0.672 | 0.014 | 0.445 | 0.672 | 0.023 | NA |
| Horizontally-vertically isolated without rocking $T_1$=2.4sec | 1g | 0.636 | 0.437 | 0.008 | 0.561 | 0.437 | 0.010 | NA |
| | 2g | 0.657 | 0.415 | 0.007 | 0.587 | 0.415 | 0.009 | NA |
| Horizontally-vertically isolated with rocking $T_1$=2.4sec | 1g | 0.729 | 0.381 | 0.005 | 0.663 | 0.381 | 0.006 | NA |
| | 2g | 0.763 | 0.346 | 0.004 | 0.707 | 0.346 | 0.005 | NA |

Table 3-54 Summary of results for probability of failure for isolated and non-isolated transformer with $W$=420kip, $f_{AI}$=11.3Hz and inclined bushing. When isolated, $D_{Capacity}$=31.3inch and lower bound friction properties. Location: **Aberdeen, WA**

| System | Transverse Bushing Acceleration Limit (g) | Without Spectral Shape Effects | | | With Spectral Shape Effects | | | Reported in MCEER-16-0010 |
|---|---|---|---|---|---|---|---|---|
| | | Median $\widehat{Sa}_F(T_1)$ (g) | $\beta_{RTR}$ | $P_F$ (50 years) | Median $\widehat{Sa}_F(T_1)$ (g) | $\beta_{RTR}$ | $P_F$ (50 years) | $P_F$ (50 years) |
| Non-isolated $T_1$=0.09sec | \ | 1.031 | 0.303 | 0.059 | 1.025 | 0.303 | 0.060 | 0.047 |
| | 2g | 2.063 | 0.303 | 0.014 | 2.049 | 0.303 | 0.014 | 0.010 |
| Horizontally isolated $T_1$=2.4sec | 1g | 0.439 | 0.714 | 0.039 | 0.487 | 0.714 | 0.034 | NA |
| | 2g | 0.583 | 0.672 | 0.026 | 0.580 | 0.672 | 0.026 | NA |
| Horizontally-vertically isolated without rocking $T_1$=2.4sec | 1g | 0.636 | 0.437 | 0.019 | 0.655 | 0.437 | 0.018 | NA |
| | 2g | 0.657 | 0.415 | 0.018 | 0.681 | 0.415 | 0.017 | NA |
| Horizontally-vertically isolated with rocking $T_1$=2.4sec | 1g | 0.729 | 0.381 | 0.015 | 0.759 | 0.381 | 0.014 | NA |
| | 2g | 0.763 | 0.346 | 0.014 | 0.801 | 0.346 | 0.013 | NA |

Table 3-55 Summary of results for probability of failure for isolated and non-isolated transformer with $W$=420kip, $f_{AI}$=11.3Hz and inclined bushing. When isolated, $D_{Capacity}$=31.3inch and lower bound friction properties. Location: **Loma Linda, CA**

| System | Transverse Bushing Acceleration Limit (g) | Without Spectral Shape Effects | | | With Spectral Shape Effects | | | Reported in MCEER-16-0010 |
|---|---|---|---|---|---|---|---|---|
| | | Median $\widehat{Sa}_F(T_1)$ (g) | $\beta_{RTR}$ | $P_F$ (50 years) | Median $\widehat{Sa}_F(T_1)$ (g) | $\beta_{RTR}$ | $P_F$ (50 years) | $P_F$ (50 years) |
| Non-isolated $T_1$=0.09sec | 1g | 1.031 | 0.303 | 0.143 | 1.135 | 0.303 | 0.114 | 0.113 |
| | 2g | 2.063 | 0.303 | 0.019 | 2.271 | 0.303 | 0.013 | 0.013 |
| Horizontally isolated $T_1$=2.4sec | 1g | 0.439 | 0.714 | 0.229 | 1.183 | 0.714 | 0.051 | NA |
| | 2g | 0.583 | 0.672 | 0.152 | 1.333 | 0.672 | 0.037 | NA |
| Horizontally-vertically isolated without rocking $T_1$=2.4sec | 1g | 0.636 | 0.437 | 0.102 | 1.065 | 0.437 | 0.037 | NA |
| | 2g | 0.657 | 0.415 | 0.094 | 1.083 | 0.415 | 0.034 | NA |
| Horizontally-vertically isolated with rocking $T_1$=2.4sec | 1g | 0.729 | 0.381 | 0.075 | 1.160 | 0.381 | 0.027 | NA |
| | 2g | 0.763 | 0.346 | 0.066 | 1.186 | 0.346 | 0.024 | NA |

Table 3-56 Summary of results for probability of failure for isolated and non-isolated transformer with $W$=420kip, $f_{AI}$=11.3Hz and inclined bushing. When isolated, $D_{Capacity}$=31.3inch and lower bound friction properties. Location: **Hillsboro, OR**

| System | Transverse Bushing Acceleration Limit (g) | Without Spectral Shape Effects | | | With Spectral Shape Effects | | | Reported in MCEER-16-0010 |
|---|---|---|---|---|---|---|---|---|
| | | Median $\widehat{Sa}_F(T_1)$ (g) | $\beta_{RTR}$ | $P_F$ (50 years) | Median $\widehat{Sa}_F(T_1)$ (g) | $\beta_{RTR}$ | $P_F$ (50 years) | $P_F$ (50 years) |
| Non-isolated $T_1$=0.09sec | 1g | 1.031 | 0.303 | 0.024 | 0.967 | 0.303 | 0.028 | 0.022 |
| | 2g | 2.063 | 0.303 | 0.004 | 1.934 | 0.303 | 0.005 | 0.003 |
| Horizontally isolated $T_1$=2.4sec | 1g | 0.439 | 0.714 | 0.022 | 0.365 | 0.714 | 0.030 | NA |
| | 2g | 0.583 | 0.672 | 0.013 | 0.443 | 0.672 | 0.020 | NA |
| Horizontally-vertically isolated without rocking $T_1$=2.4sec | 1g | 0.636 | 0.437 | 0.007 | 0.560 | 0.437 | 0.009 | NA |
| | 2g | 0.657 | 0.415 | 0.006 | 0.586 | 0.415 | 0.008 | NA |
| Horizontally-vertically isolated with rocking $T_1$=2.4sec | 1g | 0.729 | 0.381 | 0.004 | 0.662 | 0.381 | 0.006 | NA |
| | 2g | 0.763 | 0.346 | 0.004 | 0.706 | 0.346 | 0.004 | NA |

Table 3-57 Summary of results for probability of failure for isolated and non-isolated transformer with $W$=420kip, $f_{AI}$=11.3Hz and inclined bushing. When isolated, $D_{Capacity}$=31.3inch and lower bound friction properties. Location: **Eugene, OR**

| System | Transverse Bushing Acceleration Limit (g) | Without Spectral Shape Effects | | | With Spectral Shape Effects | | | Reported in MCEER-16-0010 |
|---|---|---|---|---|---|---|---|---|
| | | Median $\widehat{Sa}_F(T_1)$ (g) | $\beta_{RTR}$ | $P_F$ (50 years) | Median $\widehat{Sa}_F(T_1)$ (g) | $\beta_{RTR}$ | $P_F$ (50 years) | $P_F$ (50 years) |
| Non-isolated $T_1$=0.09sec | 1g | 1.031 | 0.303 | 0.019 | 0.949 | 0.303 | 0.023 | 0.007 |
| | 2g | 2.063 | 0.303 | 0.004 | 1.898 | 0.303 | 0.005 | 0.002 |
| Horizontally isolated $T_1$=2.4sec | 1g | 0.439 | 0.714 | 0.022 | 0.358 | 0.714 | 0.029 | NA |
| | 2g | 0.583 | 0.672 | 0.013 | 0.434 | 0.672 | 0.021 | NA |
| Horizontally-vertically isolated without rocking $T_1$=2.4sec | 1g | 0.636 | 0.437 | 0.008 | 0.553 | 0.437 | 0.011 | NA |
| | 2g | 0.657 | 0.415 | 0.007 | 0.579 | 0.415 | 0.010 | NA |
| Horizontally-vertically isolated with rocking $T_1$=2.4sec | 1g | 0.729 | 0.381 | 0.006 | 0.655 | 0.381 | 0.007 | NA |
| | 2g | 0.763 | 0.346 | 0.005 | 0.699 | 0.346 | 0.006 | NA |

Table 3-58 Summary of results for probability of failure for isolated and non-isolated transformer with $W$=420kip, $f_{AI}$=11.3Hz and inclined bushing. When isolated, $D_{Capacity}$=31.3inch and lower bound friction properties. Location: **Wilsonville, OR**

| System | Transverse Bushing Acceleration Limit (g) | Without Spectral Shape Effects | | | With Spectral Shape Effects | | | Reported in MCEER-16-0010 |
|---|---|---|---|---|---|---|---|---|
| | | Median $\widehat{Sa}_F(T_1)$ (g) | $\beta_{RTR}$ | $P_F$ (50 years) | Median $\widehat{Sa}_F(T_1)$ (g) | $\beta_{RTR}$ | $P_F$ (50 years) | $P_F$ (50 years) |
| Non-isolated $T_1$=0.09sec | 1g | 1.031 | 0.303 | 0.021 | 0.953 | 0.303 | 0.025 | 0.019 |
| | 2g | 2.063 | 0.303 | 0.003 | 1.906 | 0.303 | 0.004 | 0.002 |
| Horizontally isolated $T_1$=2.4sec | 1g | 0.439 | 0.714 | 0.019 | 0.369 | 0.714 | 0.026 | NA |
| | 2g | 0.583 | 0.672 | 0.011 | 0.447 | 0.672 | 0.017 | NA |
| Horizontally-vertically isolated without rocking $T_1$=2.4sec | 1g | 0.636 | 0.437 | 0.005 | 0.562 | 0.437 | 0.007 | NA |
| | 2g | 0.657 | 0.415 | 0.005 | 0.588 | 0.415 | 0.006 | NA |
| Horizontally-vertically isolated with rocking $T_1$=2.4sec | 1g | 0.729 | 0.381 | 0.003 | 0.665 | 0.381 | 0.004 | NA |
| | 2g | 0.763 | 0.346 | 0.003 | 0.708 | 0.346 | 0.003 | NA |

Table 3-59 Summary of results for probability of failure for isolated and non-isolated transformer with $W$=420kip, $f_{AI}$=11.3Hz and inclined bushing. When isolated, $D_{Capacity}$=31.3inch and lower bound friction properties. Location: **Curry County, OR**

| System | Transverse Bushing Acceleration Limit (g) | Without Spectral Shape Effects | | | With Spectral Shape Effects | | | Reported in MCEER-16-0010 |
|---|---|---|---|---|---|---|---|---|
| | | Median $\widehat{Sa}_F(T_1)$ (g) | $\beta_{RTR}$ | $P_F$ (50 years) | Median $\widehat{Sa}_F(T_1)$ (g) | $\beta_{RTR}$ | $P_F$ (50 years) | $P_F$ (50 years) |
| Non-isolated $T_1$=0.09sec | 1g | 1.031 | 0.303 | 0.055 | 1.123 | 0.303 | 0.048 | 0.052 |
| | 2g | 2.063 | 0.303 | 0.015 | 2.247 | 0.303 | 0.012 | 0.013 |
| Horizontally isolated $T_1$=2.4sec | 1g | 0.439 | 0.714 | 0.065 | 0.857 | 0.714 | 0.028 | NA |
| | 2g | 0.583 | 0.672 | 0.045 | 0.986 | 0.672 | 0.022 | NA |
| Horizontally-vertically isolated without rocking $T_1$=2.4sec | 1g | 0.636 | 0.437 | 0.034 | 0.893 | 0.437 | 0.020 | NA |
| | 2g | 0.657 | 0.415 | 0.032 | 0.915 | 0.415 | 0.018 | NA |
| Horizontally-vertically isolated with rocking $T_1$=2.4sec | 1g | 0.729 | 0.381 | 0.026 | 0.995 | 0.381 | 0.015 | NA |
| | 2g | 0.763 | 0.346 | 0.024 | 1.029 | 0.346 | 0.014 | NA |

Table 3-60 Summary of results for probability of failure for isolated and non-isolated transformer with $W$=420kip, $f_{AI}$=11.3Hz and inclined bushing. When isolated, $D_{Capacity}$=31.3inch and lower bound friction properties. Location: **Troutdale, OR**

| System | Transverse Bushing Acceleration Limit (g) | Without Spectral Shape Effects | | | With Spectral Shape Effects | | | Reported in MCEER-16-0010 |
|---|---|---|---|---|---|---|---|---|
| | | Median $\widehat{Sa}_F(T_1)$ (g) | $\beta_{RTR}$ | $P_F$ (50 years) | Median $\widehat{Sa}_F(T_1)$ (g) | $\beta_{RTR}$ | $P_F$ (50 years) | $P_F$ (50 years) |
| Non-isolated $T_1$=0.09sec | 1g | 1.031 | 0.303 | 0.014 | 0.948 | 0.303 | 0.021 | 0.014 |
| | 2g | 2.063 | 0.303 | 0.002 | 1.895 | 0.303 | 0.003 | 0.013 |
| Horizontally isolated $T_1$=2.4sec | 1g | 0.439 | 0.714 | 0.017 | 0.356 | 0.714 | 0.025 | NA |
| | 2g | 0.583 | 0.672 | 0.009 | 0.432 | 0.672 | 0.016 | NA |
| Horizontally-vertically isolated without rocking $T_1$=2.4sec | 1g | 0.636 | 0.437 | 0.004 | 0.551 | 0.437 | 0.006 | NA |
| | 2g | 0.657 | 0.415 | 0.004 | 0.577 | 0.415 | 0.005 | NA |
| Horizontally-vertically isolated with rocking $T_1$=2.4sec | 1g | 0.729 | 0.381 | 0.002 | 0.653 | 0.381 | 0.003 | NA |
| | 2g | 0.763 | 0.346 | 0.002 | 0.697 | 0.346 | 0.003 | NA |

# SECTION 4
# CONSIDERATIONS FOR UNCERTAINTIES

Many sources of uncertainties contribute to variability in the calculated probability of failure. These uncertainties include the record-to-record variability, which is accounted for by the use of a large number of actual ground motions in the incremental dynamic analysis, and by correcting the results for the spectral shape effects as discussed in Section 3. It may be seen in the results of Tables 3-1 to 3-60 that the record-to-record variability is reflected in the value of the dispersion coefficient $\beta_{RTR}$ whereas the correction for the spectral shape effects is reflected in an adjusted value of the median of the spectral acceleration at the fundamental period $\widehat{Sa}_F(T_1)$. These two parameters describe the fragility curve in the form of the lognormal distribution in Equation (2-5) which is presented again below in the form of a cumulative distribution function with a slightly different interpretation of parameters:

$$P_F \mid Sa(T_1)(x) = \int_0^x \frac{1}{s\beta\sqrt{2\pi}} \exp\left[-\frac{\left(\ln s - \ln \hat{S}a_{\mathrm{F}}(T_1)\right)^2}{2\beta^2}\right] ds \tag{4-1}$$

In Equation (4-1), $P_F|S_a(T_1)$ is the fragility curve (probability of failure given the value of $Sa(T_1)$) (variable x representing the spectral acceleration at the fundamental period). Parameter $\beta$ is the total value of the dispersion coefficient that includes all uncertainties. Note that the values of probabilities reported in Tables 3-1 to 3-60 are based on the use of Equations (2-6) and (2-7) for computing the probability of failure in the lifetime of the equipment with due consideration for only the record-to-record variability.

In general, uncertainties should affect the fragility curve, thus both the median value $\widehat{Sa}_F(T_1)$ and the dispersion coefficient. Uncertainties exist in the transformer model for analysis, the isolation system mechanical properties, the isolation system force and displacement capacities, the bushing failure limits and the ground motions used in the analysis. In addition, uncertainties should affect the seismic hazard curve used in Equation (2-6) to compute the mean annual frequency of failure, from which the probability of failure over a specific time period is calculated (Equation 2-7). The approach followed in this study is to adjust the dispersion coefficient to account for uncertainties in the transformer model whereas all other uncertainties are accounted for by limited deterministic analyses using bounding values of properties of the isolation system and bushings. Specifically:

1) A simple model of a representative generic transformer is used with the understanding that uncertainties in the model can be accounted for by adjustments of the dispersion coefficient obtained in the IDA and reported in Tables 3-1 to 3-60. Moreover, the results presented in this report are meant to be representative results for ten locations in the Western United States for use by responsible officials to aid in their decision to implement seismic isolation. This decision needs to be made on the basis of the potential benefit to be provided by seismic isolation by comparing probabilities of failure of non-isolated and isolated models of transformers of identical parameters, which are parametrically varied.

2) The transformer model utilizes a typical weight of 420kip. Studies in Kitayama et al. (2016) (see Figure 8-7 of the Kitayama reference) have demonstrated insignificant difference in the fragilities curves as the weight varied from 320 to 520kip while the same isolators were used (however, the isolator properties were adjusted to reflect the effect of changes of weight on the friction coefficient). Accordingly, weight does not have any important effect to warrant additional studies.

3) The damping ratio of the transformer model was set at 3% of critical for all modes. It is an appropriate value based on field studies (Villaverde et al., 2001). Higher values certainly result in reduction of the probabilities of failure. Accordingly, the results based on the 3% value are representative of real conditions.

4) The plan dimension of the planar transformer model had a single value of 110inch between supports. While this dimension does not affect the results of the non-isolated model, it does for the isolated model through uplift of the isolators. The 110-inch value represents the smaller plan dimension of some actual transformers (see examples in Oikonomou et al., 2016 and Lee and Constantinou, 2017). Placing isolators at a distance equal to the smaller dimension is neither necessary, nor recommended (in Lee and Constantinou, 2017 the isolators were placed further away under a concrete base). Accordingly, the results for the horizontally isolated transformers may be slightly conservative, particularly for the cases of the smallest displacement capacity isolator and the largest bushing acceleration limit where impact on the displacement restraint and uplift were more likely to occur.

5) A single inclined bushing having an as-installed frequency of either 4.3 or 7.7 or 11.3Hz (three cases) was used to represent the transformer. This represents a realistic range of frequencies for most bushings (Kitayama et al., 2016). The as-installed frequency has an important effect on the probability of failure as seen in the results of Tables 3-1 to 3-60.

Given that there is uncertainty on the as-installed frequency of a bushing, and that transformers have many bushings of different as-installed frequencies, it is appropriate to consider the results of all three cases in this report in assessing the benefits of isolation for a transformer.

6) The bushing failure acceleration limits considered were 1g and 2g in the transverse direction at its upper part center of mass (see Kitayama et al., 2016 for details). These two limits were established by comparing analytically constructed fragility curves of non-isolated transformers to empirical fragility curves of seven different types of transformers with two different bushing voltages (230 or 500kV) (Kitayama et al., 2016). It was observed that the 2g limit was representative of failures not attributed to bushing failure but rather of some other component, whereas the 1g limit appeared as an appropriate lower bound limit. We believe that an assessment of performance based on the data presented in this report should be based on the 1g bushing acceleration limit as it results in conservative estimates of the probability of failure. Any consideration of uncertainties on the value of the acceleration would have caused a further increase of a conservatively estimated probability of failure.

7) The isolation system frictional properties considered are the lower bound values as studies in Kitayama et al. (2016) demonstrated generally small differences between the two cases of upper and lower bound friction, with the lower bound resulting in slightly larger probabilities of failure. For the case of 1g bushing acceleration limit in the study of Kitayama et al. (2016), the two cases of bounds for friction produced very close fragility curves.

8) Two FP isolator sizes in terms of their displacement capacity were considered, one small ($D_{Capacity}$=17.7inch) and one large ($D_{Capacity}$=31.3inch). These two isolators can be readily produced, with the small one having been used in some applications in the Western United States. The larger isolator has a different radius of curvature ($R$=61inch) than the small isolator ($R$=39inch) and is intended for use in areas of higher seismic hazard. These two cases should provide sufficient information for deciding on the use of seismic isolation. We note that larger displacement capacity isolators can be produced, but their use will likely be very special due primarily to the requirement to detail the electrical connections of the isolated transformer for accommodating large displacements.

9) A single set of vertical isolator properties has been considered with parameters identical to those of a tested system in Lee and Constantinou (2017, 2018). The results show some benefits with the use of the vertical isolation system for some locations but the decision to use it should consider the complexities in its construction (for example the system "without rocking" requires a massive base-see example in Lee and Constantinou, 2017). Realistically only the system "with rocking" is practical but should be reserved for very special cases where the vertical ground acceleration of a horizontally-only isolated transformer causes global uplift and bouncing. Recognizing that there are additional uncertainties in the model of analysis for the horizontally-vertically isolated transformer by comparison to the horizontally only transformer, we will propose different parameters when computing the probabilities of collapse in the two cases.

Based on the considerations discussed above, it is assumed that the results on the probability of failure presented in this report in Section 3 encompass a range of possible properties of transformers and are useful in assessing performance and in deciding on the utility of seismic isolation. The only remaining consideration is to adjust the results for additional uncertainties related to the transformer model, which are perceived different for the various considered configurations. Following the paradigm of FEMA P695 (FEMA, 2009), we define the value of the dispersion coefficient in Equation (4-1) as

$$\beta = \sqrt{\beta_{\mathrm{RTR}}^2 + \beta_{\mathrm{MDL}}^2} \tag{4-2}$$

In this equation, $\beta_{RTR}$ is the dispersion coefficient due to the record-to-record variability (or record-to-record failure uncertainty) as reported in Tables 3-1 to 3-60, and $\beta_{\mathrm{MDL}}$ is the modeling uncertainty to account for how well the model of analysis represents the actual transformer, isolated or non-isolated. We use of the following values based on FEMA (2009) and the following considerations:

1) For non-isolated transformers $\beta_{MDL}$=0.3 as the model captures a wide range of the transformer properties space but the model accuracy and robustness is fair.

2) For horizontally-vertically isolated transformers $\beta_{MDL}$=0.2 as the model captures a wide range of the transformer properties space and the model accuracy and robustness is medium.

3) For horizontally isolated transformers $\beta_{MDL}$=0.1 as the model captures a wide range of the transformer properties space and the model accuracy and robustness is superior.

Moreover, we recognize that the selection and scaling of the pairs of horizontal-vertical ground motions may have not been appropriate for incremental dynamic analysis and this affected the calculated record-to-record dispersion for the horizontally only transformer models. Accordingly, calculations will be performed for the values of $\beta_{RTR}$ and then again using an upper bound of 0.4 for $\beta_{RTR}$. This will better inform the user of the results in deciding which probabilities of failure are relevant in the decision process.

## SECTION 5
## SUMMARY OF RESULTS FOR FAR-FIELD MOTIONS

Tables 5-1 to 5-60 present a summary of the fragility analysis results and the probabilities of failure in a lifetime of 50 years for all analyzed cases using the far-field motions. The presented fragility analysis results (values of $\widehat{Sa}_F(T_1)$ and $\beta_{RTR}$) include the spectral shape effects. The probabilities of failure are presented for two cases, one using the computed value of $\beta_{RTR}$ and one based on an upper bound of 0.4 for $\beta_{RTR}$. All probabilities of collapse have been computed using the total value of the dispersion coefficient per Equation (4-2) and using the values of $\beta_{MDL}$ in Section 4.

Table 5-1 Summary of results for probability of failure when considering uncertainties for isolated and non-isolated transformer with W=420kip, $f_{AI}$=7.7Hz and inclined bushing. When isolated, $D_{Capacity}$=17.7inch and lower bound friction properties. Location: **Vancouver, WA**. Far-field motions

| System | Transverse Bushing Acceleration Limit (g) | Fragility Parameters with Spectral Shape Effects | | | $\beta_{RTR}$ as computed. $\beta_{MDL}$ as defined in Section 4 | | $\beta_{RTR}$ bound by 0.4. $\beta_{MDL}$ as defined in Section 4 | |
|---|---|---|---|---|---|---|---|---|
| | | Median $\widehat{Sa}_F(T_1)$ (g) | $\beta_{RTR}$ | $P_F$ (50 years) | $\beta$ | $P_F$ (50 years) | $\beta$ | $P_F$ (50 years) |
| Non-isolated $T_1$=0.13sec | 1g | 0.704 | 0.276 | 0.069 | 0.408 | 0.080 | 0.408 | 0.080 |
| | 2g | 1.408 | 0.276 | 0.013 | 0.408 | 0.017 | 0.408 | 0.017 |
| Horizontally isolated $T_1$=2.4sec | 1g | 0.284 | 0.656 | 0.036 | 0.664 | 0.036 | 0.412 | 0.026 |
| | 2g | 0.369 | 0.492 | 0.018 | 0.502 | 0.018 | 0.412 | 0.016 |
| Horizontally-vertically isolated without rocking $T_1$=2.4sec | 1g | 0.415 | 0.393 | 0.012 | 0.441 | 0.013 | 0.441 | 0.013 |
| | 2g | 0.462 | 0.296 | 0.008 | 0.357 | 0.009 | 0.357 | 0.009 |
| Horizontally-vertically isolated with rocking $T_1$=2.4sec | 1g | 0.411 | 0.411 | 0.013 | 0.457 | 0.014 | 0.447 | 0.013 |
| | 2g | 0.512 | 0.293 | 0.006 | 0.355 | 0.007 | 0.355 | 0.007 |

Table 5-2 Summary of results for probability of failure when considering uncertainties for isolated and non-isolated transformer with W=420kip, $f_{AI}$=7.7Hz and inclined bushing. When isolated, $D_{Capacity}$=17.7inch and lower bound friction properties. Location: **Saranap, CA**. Far-field motions

| System | Transverse Bushing Acceleration Limit (g) | Fragility Parameters with Spectral Shape Effects | | | $\beta_{RTR}$ as computed. $\beta_{MDL}$ as defined in Section 4 | | $\beta_{RTR}$ bound by 0.4. $\beta_{MDL}$ as defined in Section 4 | |
|---|---|---|---|---|---|---|---|---|
| | | Median $\widehat{Sa}_F(T_1)$ (g) | $\beta_{RTR}$ | $P_F$ (50 years) | $\beta$ | $P_F$ (50 years) | $\beta$ | $P_F$ (50 years) |
| Non-isolated $T_1$=0.13sec | 1g | 0.782 | 0.276 | 0.266 | 0.408 | 0.307 | 0.408 | 0.307 |
| | 2g | 1.564 | 0.276 | 0.038 | 0.408 | 0.058 | 0.408 | 0.058 |
| Horizontally isolated $T_1$=2.4sec | 1g | 0.588 | 0.656 | 0.067 | 0.664 | 0.068 | 0.412 | 0.033 |
| | 2g | 0.644 | 0.492 | 0.033 | 0.502 | 0.034 | 0.412 | 0.025 |
| Horizontally-vertically isolated without rocking $T_1$=2.4sec | 1g | 0.620 | 0.393 | 0.027 | 0.441 | 0.031 | 0.441 | 0.031 |
| | 2g | 0.639 | 0.296 | 0.018 | 0.357 | 0.022 | 0.357 | 0.022 |
| Horizontally-vertically isolated with rocking $T_1$=2.4sec | 1g | 0.646 | 0.411 | 0.025 | 0.457 | 0.029 | 0.447 | 0.028 |
| | 2g | 0.704 | 0.293 | 0.013 | 0.355 | 0.016 | 0.355 | 0.016 |

Table 5-3 Summary of results for probability of failure when considering uncertainties for isolated and non-isolated transformer with W=420kip, $f_{AI}$=7.7Hz and inclined bushing. When isolated, $D_{Capacity}$=17.7inch and lower bound friction properties. Location: **Loma Linda, CA**. Far-field motions

| System | Transverse Bushing Acceleration Limit (g) | Fragility Parameters with Spectral Shape Effects | | | $\beta_{RTR}$ as computed. $\beta_{MDL}$ as defined in Section 4 | | $\beta_{RTR}$ bound by 0.4. $\beta_{MDL}$ as defined in Section 4 | |
|---|---|---|---|---|---|---|---|---|
| | | Median $\widehat{Sa}_F(T_1)$ (g) | $\beta_{RTR}$ | $P_F$ (50 years) | $\beta$ | $P_F$ (50 years) | $\beta$ | $P_F$ (50 years) |
| Non-isolated $T_1$=0.13sec | 1g | 0.782 | 0.276 | 0.309 | 0.408 | 0.346 | 0.408 | 0.346 |
| | 2g | 1.565 | 0.276 | 0.063 | 0.408 | 0.084 | 0.408 | 0.084 |
| Horizontally isolated $T_1$=2.4sec | 1g | 0.744 | 0.656 | 0.103 | 0.664 | 0.104 | 0.412 | 0.075 |
| | 2g | 0.770 | 0.492 | 0.078 | 0.502 | 0.079 | 0.412 | 0.070 |
| Horizontally-vertically isolated without rocking $T_1$=2.4sec | 1g | 0.706 | 0.393 | 0.081 | 0.441 | 0.085 | 0.441 | 0.085 |
| | 2g | 0.709 | 0.296 | 0.073 | 0.357 | 0.077 | 0.357 | 0.077 |
| Horizontally-vertically isolated with rocking $T_1$=2.4sec | 1g | 0.748 | 0.411 | 0.074 | 0.457 | 0.078 | 0.447 | 0.077 |
| | 2g | 0.780 | 0.293 | 0.059 | 0.355 | 0.064 | 0.355 | 0.064 |

Table 5-4 Summary of results for probability of failure when considering uncertainties for isolated and non-isolated transformer with $W$=420kip, $f_{AI}$=7.7Hz and inclined bushing. When isolated, $D_{Capacity}$=17.7inch and lower bound friction properties. Location: **Aberdeen, WA**. Far-field motions

| System | Transverse Bushing Acceleration Limit (g) | Fragility Parameters with Spectral Shape Effects | | | $\beta_{RTR}$ as computed. $\beta_{MDL}$ as defined in Section 4 | | $\beta_{RTR}$ bound by 0.4. $\beta_{MDL}$ as defined in Section 4 | |
|---|---|---|---|---|---|---|---|---|
| | | Median $\widehat{Sa}_F(T_1)$ (g) | $\beta_{RTR}$ | $P_F$ (50 years) | $\beta$ | $P_F$ (50 years) | $\beta$ | $P_F$ (50 years) |
| Non-isolated $T_1$=0.13sec | 1$g$ | 0.737 | 0.276 | 0.128 | 0.408 | 0.141 | 0.408 | 0.141 |
| | 2$g$ | 1.473 | 0.276 | 0.038 | 0.408 | 0.044 | 0.408 | 0.044 |
| Horizontally isolated $T_1$=2.4sec | 1$g$ | 0.359 | 0.656 | 0.047 | 0.664 | 0.047 | 0.412 | 0.040 |
| | 2$g$ | 0.441 | 0.492 | 0.033 | 0.502 | 0.033 | 0.412 | 0.031 |
| Horizontally-vertically isolated without rocking $T_1$=2.4sec | 1$g$ | 0.472 | 0.393 | 0.028 | 0.441 | 0.029 | 0.441 | 0.029 |
| | 2$g$ | 0.513 | 0.296 | 0.024 | 0.357 | 0.025 | 0.357 | 0.025 |
| Horizontally-vertically isolated with rocking $T_1$=2.4sec | 1$g$ | 0.475 | 0.411 | 0.028 | 0.457 | 0.029 | 0.447 | 0.029 |
| | 2$g$ | 0.567 | 0.293 | 0.021 | 0.355 | 0.021 | 0.355 | 0.021 |

Table 5-5 Summary of results for probability of failure when considering uncertainties for isolated and non-isolated transformer with $W$=420kip, $f_{AI}$=7.7Hz and inclined bushing. When isolated, $D_{Capacity}$=17.7inch and lower bound friction properties. Location: **Chehalis, WA**. Far-field motions

| System | Transverse Bushing Acceleration Limit (g) | Fragility Parameters with Spectral Shape Effects | | | $\beta_{RTR}$ as computed. $\beta_{MDL}$ as defined in Section 4 | | $\beta_{RTR}$ bound by 0.4. $\beta_{MDL}$ as defined in Section 4 | |
|---|---|---|---|---|---|---|---|---|
| | | Median $\widehat{Sa}_F(T_1)$ (g) | $\beta_{RTR}$ | $P_F$ (50 years) | $\beta$ | $P_F$ (50 years) | $\beta$ | $P_F$ (50 years) |
| Non-isolated $T_1$=0.13sec | 1$g$ | 0.717 | 0.276 | 0.113 | 0.408 | 0.129 | 0.408 | 0.129 |
| | 2$g$ | 1.434 | 0.276 | 0.024 | 0.408 | 0.030 | 0.408 | 0.030 |
| Horizontally isolated $T_1$=2.4sec | 1$g$ | 0.286 | 0.656 | 0.045 | 0.664 | 0.046 | 0.412 | 0.034 |
| | 2$g$ | 0.372 | 0.492 | 0.024 | 0.502 | 0.024 | 0.412 | 0.022 |
| Horizontally-vertically isolated without rocking $T_1$=2.4sec | 1$g$ | 0.415 | 0.393 | 0.017 | 0.441 | 0.018 | 0.441 | 0.018 |
| | 2$g$ | 0.462 | 0.296 | 0.012 | 0.357 | 0.013 | 0.357 | 0.013 |
| Horizontally-vertically isolated with rocking $T_1$=2.4sec | 1$g$ | 0.411 | 0.411 | 0.018 | 0.457 | 0.019 | 0.447 | 0.019 |
| | 2$g$ | 0.513 | 0.293 | 0.010 | 0.355 | 0.011 | 0.355 | 0.011 |

Table 5-6 Summary of results for probability of failure when considering uncertainties for isolated and non-isolated transformer with $W$=420kip, $f_{AI}$=7.7Hz and inclined bushing. When isolated, $D_{Capacity}$=17.7inch and lower bound friction properties. Location: **Hillsboro, OR**. Far-field motions

| System | Transverse Bushing Acceleration Limit (g) | Fragility Parameters with Spectral Shape Effects | | | $\beta_{RTR}$ as computed. $\beta_{MDL}$ as defined in Section 4 | | $\beta_{RTR}$ bound by 0.4. $\beta_{MDL}$ as defined in Section 4 | |
|---|---|---|---|---|---|---|---|---|
| | | Median $\widehat{Sa}_F(T_1)$ (g) | $\beta_{RTR}$ | $P_F$ (50 years) | $\beta$ | $P_F$ (50 years) | $\beta$ | $P_F$ (50 years) |
| Non-isolated $T_1$=0.13sec | 1g | 0.711 | 0.276 | 0.076 | 0.408 | 0.085 | 0.408 | 0.085 |
| | 2g | 1.422 | 0.276 | 0.017 | 0.408 | 0.021 | 0.408 | 0.021 |
| Horizontally isolated $T_1$=2.4sec | 1g | 0.284 | 0.656 | 0.040 | 0.664 | 0.041 | 0.412 | 0.031 |
| | 2g | 0.369 | 0.492 | 0.022 | 0.502 | 0.022 | 0.412 | 0.020 |
| Horizontally-vertically isolated without rocking $T_1$=2.4sec | 1g | 0.415 | 0.393 | 0.016 | 0.441 | 0.016 | 0.441 | 0.016 |
| | 2g | 0.462 | 0.296 | 0.011 | 0.357 | 0.012 | 0.357 | 0.012 |
| Horizontally-vertically isolated with rocking $T_1$=2.4sec | 1g | 0.411 | 0.411 | 0.016 | 0.457 | 0.017 | 0.447 | 0.017 |
| | 2g | 0.512 | 0.293 | 0.009 | 0.355 | 0.010 | 0.355 | 0.010 |

Table 5-7 Summary of results for probability of failure when considering uncertainties for isolated and non-isolated transformer with $W$=420kip, $f_{AI}$=7.7Hz and inclined bushing. When isolated, $D_{Capacity}$=17.7inch and lower bound friction properties. Location: **Eugene, OR**. Far-field motions.

| System | Transverse Bushing Acceleration Limit (g) | Fragility Parameters with Spectral Shape Effects | | | $\beta_{RTR}$ as computed. $\beta_{MDL}$ as defined in Section 4 | | $\beta_{RTR}$ bound by 0.4. $\beta_{MDL}$ as defined in Section 4 | |
|---|---|---|---|---|---|---|---|---|
| | | Median $\widehat{Sa}_F(T_1)$ (g) | $\beta_{RTR}$ | $P_F$ (50 years) | $\beta$ | $P_F$ (50 years) | $\beta$ | $P_F$ (50 years) |
| Non-isolated $T_1$=0.13sec | 1g | 0.704 | 0.276 | 0.052 | 0.408 | 0.056 | 0.408 | 0.056 |
| | 2g | 1.407 | 0.276 | 0.015 | 0.408 | 0.017 | 0.408 | 0.017 |
| Horizontally isolated $T_1$=2.4sec | 1g | 0.279 | 0.656 | 0.038 | 0.664 | 0.038 | 0.412 | 0.032 |
| | 2g | 0.364 | 0.492 | 0.023 | 0.502 | 0.023 | 0.412 | 0.021 |
| Horizontally-vertically isolated without rocking $T_1$=2.4sec | 1g | 0.411 | 0.393 | 0.017 | 0.441 | 0.018 | 0.441 | 0.018 |
| | 2g | 0.458 | 0.296 | 0.013 | 0.357 | 0.014 | 0.357 | 0.014 |
| Horizontally-vertically isolated with rocking $T_1$=2.4sec | 1g | 0.406 | 0.411 | 0.018 | 0.457 | 0.019 | 0.447 | 0.018 |
| | 2g | 0.508 | 0.293 | 0.011 | 0.355 | 0.011 | 0.355 | 0.011 |

Table 5-8 Summary of results for probability of failure when considering uncertainties for isolated and non-isolated transformer with $W$=420kip, $f_{AI}$=7.7Hz and inclined bushing. When isolated, $D_{Capacity}$=17.7inch and lower bound friction properties. Location: **Wilsonville, OR**. Far-field motions

| System | Transverse Bushing Acceleration Limit (g) | Fragility Parameters with Spectral Shape Effects | | | $\beta_{RTR}$ as computed. $\beta_{MDL}$ as defined in Section 4 | | $\beta_{RTR}$ bound by 0.4. $\beta_{MDL}$ as defined in Section 4 | |
|---|---|---|---|---|---|---|---|---|
| | | Median $\widehat{Sa}_F(T_1)$ (g) | $\beta_{RTR}$ | $P_F$ (50 years) | $\beta$ | $P_F$ (50 years) | $\beta$ | $P_F$ (50 years) |
| Non-isolated $T_1$=0.13sec | 1g | 0.705 | 0.276 | 0.069 | 0.408 | 0.079 | 0.408 | 0.079 |
| | 2g | 1.410 | 0.276 | 0.014 | 0.408 | 0.018 | 0.408 | 0.018 |
| Horizontally isolated $T_1$=2.4sec | 1g | 0.285 | 0.656 | 0.036 | 0.664 | 0.036 | 0.412 | 0.027 |
| | 2g | 0.370 | 0.492 | 0.018 | 0.502 | 0.019 | 0.412 | 0.017 |
| Horizontally-vertically isolated without rocking $T_1$=2.4sec | 1g | 0.416 | 0.393 | 0.013 | 0.441 | 0.014 | 0.441 | 0.014 |
| | 2g | 0.463 | 0.296 | 0.009 | 0.357 | 0.010 | 0.357 | 0.010 |
| Horizontally-vertically isolated with rocking $T_1$=2.4sec | 1g | 0.412 | 0.411 | 0.013 | 0.457 | 0.014 | 0.447 | 0.014 |
| | 2g | 0.513 | 0.293 | 0.007 | 0.355 | 0.007 | 0.355 | 0.007 |

Table 5-9 Summary of results for probability of failure when considering uncertainties for isolated and non-isolated transformer with $W$=420kip, $f_{AI}$=7.7Hz and inclined bushing. When isolated, $D_{Capacity}$=17.7inch and lower bound friction properties. Location: **Curry County, OR**. Far-field motions

| System | Transverse Bushing Acceleration Limit (g) | Fragility Parameters with Spectral Shape Effects | | | $\beta_{RTR}$ as computed. $\beta_{MDL}$ as defined in Section 4 | | $\beta_{RTR}$ bound by 0.4. $\beta_{MDL}$ as defined in Section 4 | |
|---|---|---|---|---|---|---|---|---|
| | | Median $\widehat{Sa}_F(T_1)$ (g) | $\beta_{RTR}$ | $P_F$ (50 years) | $\beta$ | $P_F$ (50 years) | $\beta$ | $P_F$ (50 years) |
| Non-isolated $T_1$=0.13sec | 1g | 0.778 | 0.276 | 0.103 | 0.408 | 0.108 | 0.408 | 0.108 |
| | 2g | 1.556 | 0.276 | 0.034 | 0.408 | 0.039 | 0.408 | 0.039 |
| Horizontally isolated $T_1$=2.4sec | 1g | 0.571 | 0.656 | 0.046 | 0.664 | 0.046 | 0.412 | 0.039 |
| | 2g | 0.629 | 0.492 | 0.036 | 0.502 | 0.036 | 0.412 | 0.034 |
| Horizontally-vertically isolated without rocking $T_1$=2.4sec | 1g | 0.610 | 0.393 | 0.035 | 0.441 | 0.036 | 0.441 | 0.036 |
| | 2g | 0.630 | 0.296 | 0.031 | 0.357 | 0.033 | 0.357 | 0.033 |
| Horizontally-vertically isolated with rocking $T_1$=2.4sec | 1g | 0.634 | 0.411 | 0.033 | 0.457 | 0.035 | 0.447 | 0.034 |
| | 2g | 0.695 | 0.293 | 0.027 | 0.355 | 0.028 | 0.355 | 0.028 |

Table 5-10 Summary of results for probability of failure when considering uncertainties for isolated and non-isolated transformer with $W$=420kip, $f_{AI}$=7.7Hz and inclined bushing. When isolated, $D_{Capacity}$=17.7inch and lower bound friction properties. Location: **Troutdale, OR**. Far-field motions

| System | Transverse Bushing Acceleration Limit (g) | Fragility Parameters with Spectral Shape Effects | | | $\beta_{RTR}$ as computed. $\beta_{MDL}$ as defined in Section 4 | | $\beta_{RTR}$ bound by 0.4. $\beta_{MDL}$ as defined in Section 4 | |
|---|---|---|---|---|---|---|---|---|
| | | Median $\widehat{Sa}_F(T_1)$ (g) | $\beta_{RTR}$ | $P_F$ (50 years) | $\beta$ | $P_F$ (50 years) | $\beta$ | $P_F$ (50 years) |
| Non-isolated $T_1$=0.13sec | 1g | 0.702 | 0.276 | 0.061 | 0.408 | 0.071 | 0.408 | 0.071 |
| | 2g | 1.403 | 0.276 | 0.011 | 0.408 | 0.015 | 0.408 | 0.015 |
| Horizontally isolated $T_1$=2.4sec | 1g | 0.277 | 0.656 | 0.035 | 0.664 | 0.035 | 0.412 | 0.025 |
| | 2g | 0.362 | 0.492 | 0.017 | 0.502 | 0.017 | 0.412 | 0.015 |
| Horizontally-vertically isolated without rocking $T_1$=2.4sec | 1g | 0.410 | 0.393 | 0.011 | 0.441 | 0.012 | 0.441 | 0.012 |
| | 2g | 0.457 | 0.296 | 0.007 | 0.357 | 0.008 | 0.357 | 0.008 |
| Horizontally-vertically isolated with rocking $T_1$=2.4sec | 1g | 0.405 | 0.411 | 0.012 | 0.457 | 0.013 | 0.447 | 0.012 |
| | 2g | 0.507 | 0.293 | 0.005 | 0.355 | 0.006 | 0.355 | 0.006 |

Table 5-11 Summary of results for probability of failure when considering uncertainties for isolated and non-isolated transformer with $W$=420kip, $f_{AI}$=4.3Hz and inclined bushing. When isolated, $D_{Capacity}$=17.7inch and lower bound friction properties. Location: **Vancouver, WA**. Far-field motions

| System | Transverse Bushing Acceleration Limit (g) | Fragility Parameters with Spectral Shape Effects | | | $\beta_{RTR}$ as computed. $\beta_{MDL}$ as defined in Section 4 | | $\beta_{RTR}$ bound by 0.4. $\beta_{MDL}$ as defined in Section 4 | |
|---|---|---|---|---|---|---|---|---|
| | | Median $\widehat{Sa}_F(T_1)$ (g) | $\beta_{RTR}$ | $P_F$ (50 years) | $\beta$ | $P_F$ (50 years) | $\beta$ | $P_F$ (50 years) |
| Non-isolated $T_1$=0.24sec | 1g | 1.019 | 0.173 | 0.045 | 0.346 | 0.053 | 0.346 | 0.053 |
| | 2g | 2.038 | 0.173 | 0.006 | 0.346 | 0.009 | 0.346 | 0.009 |
| Horizontally isolated $T_1$=2.4sec | 1g | 0.378 | 0.551 | 0.019 | 0.560 | 0.019 | 0.412 | 0.015 |
| | 2g | 0.414 | 0.477 | 0.014 | 0.487 | 0.014 | 0.412 | 0.013 |
| Horizontally-vertically isolated without rocking $T_1$=2.4sec | 1g | 0.464 | 0.322 | 0.008 | 0.379 | 0.009 | 0.379 | 0.009 |
| | 2g | 0.502 | 0.278 | 0.006 | 0.342 | 0.007 | 0.342 | 0.007 |
| Horizontally-vertically isolated with rocking $T_1$=2.4sec | 1g | 0.355 | 0.620 | 0.023 | 0.651 | 0.025 | 0.447 | 0.018 |
| | 2g | 0.529 | 0.289 | 0.006 | 0.351 | 0.006 | 0.351 | 0.006 |

Table 5-12 Summary of results for probability of failure when considering uncertainties for isolated and non-isolated transformer with $W$=420kip, $f_{AI}$=4.3Hz and inclined bushing. When isolated, $D_{Capacity}$=17.7inch and lower bound friction properties. Location: **Saranap, CA**. Far-field motions

| System | Transverse Bushing Acceleration Limit (g) | Fragility Parameters with Spectral Shape Effects | | | $\beta_{RTR}$ as computed. $\beta_{MDL}$ as defined in Section 4 | | $\beta_{RTR}$ bound by 0.4. $\beta_{MDL}$ as defined in Section 4 | |
|---|---|---|---|---|---|---|---|---|
| | | Median $\widehat{Sa}_F(T_1)$ (g) | $\beta_{RTR}$ | $P_F$ (50 years) | $\beta$ | $P_F$ (50 years) | $\beta$ | $P_F$ (50 years) |
| Non-isolated $T_1$=0.24sec | 1g | 1.105 | 0.173 | 0.153 | 0.346 | 0.192 | 0.346 | 0.192 |
| | 2g | 2.211 | 0.173 | 0.012 | 0.346 | 0.023 | 0.346 | 0.023 |
| Horizontally isolated $T_1$=2.4sec | 1g | 0.696 | 0.551 | 0.032 | 0.560 | 0.033 | 0.412 | 0.020 |
| | 2g | 0.702 | 0.477 | 0.024 | 0.487 | 0.025 | 0.412 | 0.019 |
| Horizontally-vertically isolated without rocking $T_1$=2.4sec | 1g | 0.644 | 0.322 | 0.019 | 0.379 | 0.023 | 0.379 | 0.023 |
| | 2g | 0.662 | 0.278 | 0.015 | 0.342 | 0.018 | 0.342 | 0.018 |
| Horizontally-vertically isolated with rocking $T_1$=2.4sec | 1g | 0.724 | 0.620 | 0.037 | 0.651 | 0.041 | 0.447 | 0.020 |
| | 2g | 0.706 | 0.289 | 0.012 | 0.351 | 0.015 | 0.351 | 0.015 |

Table 5-13 Summary of results for probability of failure when considering uncertainties for isolated and non-isolated transformer with $W$=420kip, $f_{AI}$=4.3Hz and inclined bushing. When isolated, $D_{Capacity}$=17.7inch and lower bound friction properties. Location: **Chehalis, WA**. Far-field motions

| System | Transverse Bushing Acceleration Limit (g) | Fragility Parameters with Spectral Shape Effects | | | $\beta_{RTR}$ as computed. $\beta_{MDL}$ as defined in Section 4 | | $\beta_{RTR}$ bound by 0.4. $\beta_{MDL}$ as defined in Section 4 | |
|---|---|---|---|---|---|---|---|---|
| | | Median $\widehat{Sa}_F(T_1)$ (g) | $\beta_{RTR}$ | $P_F$ (50 years) | $\beta$ | $P_F$ (50 years) | $\beta$ | $P_F$ (50 years) |
| Non-isolated $T_1$=0.24sec | 1g | 1.042 | 0.173 | 0.069 | 0.346 | 0.081 | 0.346 | 0.081 |
| | 2g | 2.085 | 0.173 | 0.011 | 0.346 | 0.016 | 0.346 | 0.016 |
| Horizontally isolated $T_1$=2.4sec | 1g | 0.354 | 0.551 | 0.028 | 0.560 | 0.029 | 0.412 | 0.024 |
| | 2g | 0.391 | 0.477 | 0.021 | 0.487 | 0.022 | 0.412 | 0.020 |
| Horizontally-vertically isolated without rocking $T_1$=2.4sec | 1g | 0.448 | 0.322 | 0.014 | 0.379 | 0.015 | 0.379 | 0.015 |
| | 2g | 0.487 | 0.278 | 0.011 | 0.342 | 0.012 | 0.342 | 0.012 |
| Horizontally-vertically isolated with rocking $T_1$=2.4sec | 1g | 0.328 | 0.620 | 0.035 | 0.651 | 0.037 | 0.447 | 0.028 |
| | 2g | 0.512 | 0.289 | 0.010 | 0.351 | 0.011 | 0.351 | 0.011 |

Table 5-14 Summary of results for probability of failure when considering uncertainties for isolated and non-isolated transformer with $W$=420kip, $f_{AI}$=4.3Hz and inclined bushing. When isolated, $D_{Capacity}$=17.7inch and lower bound friction properties. Location: **Aberdeen, WA**. Far-field motions

| System | Transverse Bushing Acceleration Limit (g) | Fragility Parameters with Spectral Shape Effects | | | $\beta_{RTR}$ as computed. $\beta_{MDL}$ as defined in Section 4 | | $\beta_{RTR}$ bound by 0.4. $\beta_{MDL}$ as defined in Section 4 | |
|---|---|---|---|---|---|---|---|---|
| | | Median $\widehat{Sa}_F(T_1)$ (g) | $\beta_{RTR}$ | $P_F$ (50 years) | $\beta$ | $P_F$ (50 years) | $\beta$ | $P_F$ (50 years) |
| Non-isolated $T_1$=0.24sec | 1g | 1.064 | 0.173 | 0.091 | 0.346 | 0.100 | 0.346 | 0.100 |
| | 2g | 2.130 | 0.173 | 0.026 | 0.346 | 0.030 | 0.346 | 0.030 |
| Horizontally isolated $T_1$=2.4sec | 1g | 0.439 | 0.551 | 0.034 | 0.560 | 0.034 | 0.412 | 0.031 |
| | 2g | 0.471 | 0.477 | 0.030 | 0.487 | 0.030 | 0.412 | 0.029 |
| Horizontally-vertically isolated without rocking $T_1$=2.4sec | 1g | 0.503 | 0.322 | 0.025 | 0.379 | 0.026 | 0.379 | 0.026 |
| | 2g | 0.537 | 0.278 | 0.022 | 0.342 | 0.023 | 0.342 | 0.023 |
| Horizontally-vertically isolated with rocking $T_1$=2.4sec | 1g | 0.423 | 0.620 | 0.038 | 0.651 | 0.038 | 0.447 | 0.034 |
| | 2g | 0.568 | 0.289 | 0.021 | 0.351 | 0.021 | 0.351 | 0.021 |

Table 5-15 Summary of results for probability of failure when considering uncertainties for isolated and non-isolated transformer with $W$=420kip, $f_{AI}$=4.3Hz and inclined bushing. When isolated, $D_{Capacity}$=17.7inch and lower bound friction properties. Location: **Loma Linda, CA**. Far-field motions

| System | Transverse Bushing Acceleration Limit (g) | Fragility Parameters with Spectral Shape Effects | | | $\beta_{RTR}$ as computed. $\beta_{MDL}$ as defined in Section 4 | | $\beta_{RTR}$ bound by 0.4. $\beta_{MDL}$ as defined in Section 4 | |
|---|---|---|---|---|---|---|---|---|
| | | Median $\widehat{Sa}_F(T_1)$ (g) | $\beta_{RTR}$ | $P_F$ (50 years) | $\beta$ | $P_F$ (50 years) | $\beta$ | $P_F$ (50 years) |
| Non-isolated $T_1$=0.24sec | 1g | 1.109 | 0.173 | 0.203 | 0.346 | 0.236 | 0.346 | 0.236 |
| | 2g | 2.220 | 0.173 | 0.029 | 0.346 | 0.043 | 0.346 | 0.043 |
| Horizontally isolated $T_1$=2.4sec | 1g | 0.865 | 0.551 | 0.068 | 0.560 | 0.069 | 0.412 | 0.056 |
| | 2g | 0.847 | 0.477 | 0.064 | 0.487 | 0.065 | 0.412 | 0.058 |
| Horizontally-vertically isolated without rocking $T_1$=2.4sec | 1g | 0.724 | 0.322 | 0.071 | 0.379 | 0.076 | 0.379 | 0.076 |
| | 2g | 0.730 | 0.278 | 0.067 | 0.342 | 0.072 | 0.342 | 0.072 |
| Horizontally-vertically isolated with rocking $T_1$=2.4sec | 1g | 0.935 | 0.620 | 0.066 | 0.651 | 0.070 | 0.447 | 0.050 |
| | 2g | 0.782 | 0.289 | 0.059 | 0.351 | 0.063 | 0.351 | 0.063 |

Table 5-16 Summary of results for probability of failure when considering uncertainties for isolated and non-isolated transformer with $W$=420kip, $f_{AI}$=4.3Hz and inclined bushing. When isolated, $D_{Capacity}$=17.7inch and lower bound friction properties. Location: **Hillsboro, OR**. Far-field motions

| System | Transverse Bushing Acceleration Limit (g) | Fragility Parameters with Spectral Shape Effects | | | $\beta_{RTR}$ as computed. $\beta_{MDL}$ as defined in Section 4 | | $\beta_{RTR}$ bound by 0.4. $\beta_{MDL}$ as defined in Section 4 | |
|---|---|---|---|---|---|---|---|---|
| | | Median $\widehat{Sa}_F(T_1)$ (g) | $\beta_{RTR}$ | $P_F$ (50 years) | $\beta$ | $P_F$ (50 years) | $\beta$ | $P_F$ (50 years) |
| Non-isolated $T_1$=0.24sec | 1g | 1.037 | 0.173 | 0.051 | 0.346 | 0.059 | 0.346 | 0.059 |
| | 2g | 2.074 | 0.173 | 0.009 | 0.346 | 0.012 | 0.346 | 0.012 |
| Horizontally isolated $T_1$=2.4sec | 1g | 0.352 | 0.551 | 0.025 | 0.560 | 0.026 | 0.412 | 0.022 |
| | 2g | 0.390 | 0.477 | 0.019 | 0.487 | 0.020 | 0.412 | 0.018 |
| Horizontally-vertically isolated without rocking $T_1$=2.4sec | 1g | 0.447 | 0.322 | 0.012 | 0.379 | 0.013 | 0.379 | 0.013 |
| | 2g | 0.487 | 0.278 | 0.010 | 0.342 | 0.010 | 0.342 | 0.010 |
| Horizontally-vertically isolated with rocking $T_1$=2.4sec | 1g | 0.328 | 0.620 | 0.031 | 0.651 | 0.032 | 0.447 | 0.025 |
| | 2g | 0.512 | 0.289 | 0.009 | 0.351 | 0.009 | 0.351 | 0.009 |

Table 5-17 Summary of results for probability of failure when considering uncertainties for isolated and non-isolated transformer with $W$=420kip, $f_{AI}$=4.3Hz and inclined bushing. When isolated, $D_{Capacity}$=17.7inch and lower bound friction properties. Location: **Eugene, OR**. Far-field motions

| System | Transverse Bushing Acceleration Limit (g) | Fragility Parameters with Spectral Shape Effects | | | $\beta_{RTR}$ as computed. $\beta_{MDL}$ as defined in Section 4 | | $\beta_{RTR}$ bound by 0.4. $\beta_{MDL}$ as defined in Section 4 | |
|---|---|---|---|---|---|---|---|---|
| | | Median $\widehat{Sa}_F(T_1)$ (g) | $\beta_{RTR}$ | $P_F$ (50 years) | $\beta$ | $P_F$ (50 years) | $\beta$ | $P_F$ (50 years) |
| Non-isolated $T_1$=0.24sec | 1g | 1.030 | 0.173 | 0.043 | 0.346 | 0.046 | 0.346 | 0.046 |
| | 2g | 2.062 | 0.173 | 0.010 | 0.346 | 0.012 | 0.346 | 0.012 |
| Horizontally isolated $T_1$=2.4sec | 1g | 0.347 | 0.551 | 0.026 | 0.560 | 0.026 | 0.412 | 0.023 |
| | 2g | 0.385 | 0.477 | 0.021 | 0.487 | 0.021 | 0.412 | 0.020 |
| Horizontally-vertically isolated without rocking $T_1$=2.4sec | 1g | 0.443 | 0.322 | 0.012 | 0.379 | 0.015 | 0.379 | 0.015 |
| | 2g | 0.483 | 0.278 | 0.010 | 0.342 | 0.012 | 0.342 | 0.012 |
| Horizontally-vertically isolated with rocking $T_1$=2.4sec | 1g | 0.321 | 0.620 | 0.030 | 0.651 | 0.031 | 0.447 | 0.027 |
| | 2g | 0.508 | 0.289 | 0.011 | 0.351 | 0.011 | 0.351 | 0.011 |

Table 5-18 Summary of results for probability of failure when considering uncertainties for isolated and non-isolated transformer with $W$=420kip, $f_{AI}$=4.3Hz and inclined bushing. When isolated, $D_{Capacity}$=17.7inch and lower bound friction properties. Location: **Wilsonville, OR**. Far-field motions

| System | Transverse Bushing Acceleration Limit (g) | Fragility Parameters with Spectral Shape Effects | | | $\beta_{RTR}$ as computed. $\beta_{MDL}$ as defined in Section 4 | | $\beta_{RTR}$ bound by 0.4. $\beta_{MDL}$ as defined in Section 4 | |
|---|---|---|---|---|---|---|---|---|
| | | Median $\widehat{Sa}_F(T_1)$ (g) | $\beta_{RTR}$ | $P_F$ (50 years) | $\beta$ | $P_F$ (50 years) | $\beta$ | $P_F$ (50 years) |
| Non-isolated $T_1$=0.24sec | 1g | 1.030 | 0.173 | 0.045 | 0.346 | 0.053 | 0.346 | 0.053 |
| | 2g | 2.061 | 0.173 | 0.007 | 0.346 | 0.010 | 0.346 | 0.010 |
| Horizontally isolated $T_1$=2.4sec | 1g | 0.354 | 0.551 | 0.022 | 0.560 | 0.022 | 0.412 | 0.018 |
| | 2g | 0.392 | 0.477 | 0.016 | 0.487 | 0.016 | 0.412 | 0.015 |
| Horizontally-vertically isolated without rocking $T_1$=2.4sec | 1g | 0.448 | 0.322 | 0.010 | 0.379 | 0.011 | 0.379 | 0.011 |
| | 2g | 0.488 | 0.278 | 0.008 | 0.342 | 0.008 | 0.342 | 0.008 |
| Horizontally-vertically isolated with rocking $T_1$=2.4sec | 1g | 0.329 | 0.620 | 0.029 | 0.651 | 0.029 | 0.447 | 0.022 |
| | 2g | 0.513 | 0.289 | 0.007 | 0.351 | 0.007 | 0.351 | 0.007 |

Table 5-19 Summary of results for probability of failure when considering uncertainties for isolated and non-isolated transformer with $W$=420kip, $f_{AI}$=4.3Hz and inclined bushing. When isolated, $D_{Capacity}$=17.7inch and lower bound friction properties. Location: **Curry County, OR**. Far-field motions

| System | Transverse Bushing Acceleration Limit (g) | Fragility Parameters with Spectral Shape Effects | | | $\beta_{RTR}$ as computed. $\beta_{MDL}$ as defined in Section 4 | | $\beta_{RTR}$ bound by 0.4. $\beta_{MDL}$ as defined in Section 4 | |
|---|---|---|---|---|---|---|---|---|
| | | Median $\widehat{Sa}_F(T_1)$ (g) | $\beta_{RTR}$ | $P_F$ (50 years) | $\beta$ | $P_F$ (50 years) | $\beta$ | $P_F$ (50 years) |
| Non-isolated $T_1$=0.24sec | 1g | 1.107 | 0.173 | 0.087 | 0.346 | 0.092 | 0.346 | 0.092 |
| | 2g | 2.215 | 0.173 | 0.027 | 0.346 | 0.031 | 0.346 | 0.031 |
| Horizontally isolated $T_1$=2.4sec | 1g | 0.676 | 0.551 | 0.034 | 0.560 | 0.034 | 0.412 | 0.030 |
| | 2g | 0.685 | 0.477 | 0.031 | 0.487 | 0.031 | 0.412 | 0.030 |
| Horizontally-vertically isolated without rocking $T_1$=2.4sec | 1g | 0.634 | 0.322 | 0.032 | 0.379 | 0.033 | 0.379 | 0.033 |
| | 2g | 0.653 | 0.278 | 0.029 | 0.342 | 0.031 | 0.342 | 0.031 |
| Horizontally-vertically isolated with rocking $T_1$=2.4sec | 1g | 0.701 | 0.620 | 0.034 | 0.651 | 0.035 | 0.447 | 0.029 |
| | 2g | 0.696 | 0.289 | 0.027 | 0.351 | 0.028 | 0.351 | 0.028 |

Table 5-20 Summary of results for probability of failure when considering uncertainties for isolated and non-isolated transformer with $W$=420kip, $f_{AI}$=4.3Hz and inclined bushing. When isolated, $D_{Capacity}$=17.7inch and lower bound friction properties. Location: **Troutdale, OR**. Far-field motions

| System | Transverse Bushing Acceleration Limit (g) | Fragility Parameters with Spectral Shape Effects | | | $\beta_{RTR}$ as computed. $\beta_{MDL}$ as defined in Section 4 | | $\beta_{RTR}$ bound by 0.4. $\beta_{MDL}$ as defined in Section 4 | |
|---|---|---|---|---|---|---|---|---|
| | | Median $\widehat{Sa}_F(T_1)$ (g) | $\beta_{RTR}$ | $P_F$ (50 years) | $\beta$ | $P_F$ (50 years) | $\beta$ | $P_F$ (50 years) |
| Non-isolated $T_1$=0.24sec | 1g | 1.023 | 0.173 | 0.038 | 0.346 | 0.046 | 0.346 | 0.046 |
| | 2g | 2.047 | 0.173 | 0.005 | 0.346 | 0.007 | 0.346 | 0.007 |
| Horizontally isolated $T_1$=2.4sec | 1g | 0.345 | 0.551 | 0.020 | 0.560 | 0.021 | 0.412 | 0.016 |
| | 2g | 0.383 | 0.477 | 0.015 | 0.487 | 0.015 | 0.412 | 0.013 |
| Horizontally-vertically isolated without rocking $T_1$=2.4sec | 1g | 0.442 | 0.322 | 0.008 | 0.379 | 0.009 | 0.379 | 0.009 |
| | 2g | 0.482 | 0.278 | 0.006 | 0.342 | 0.007 | 0.342 | 0.007 |
| Horizontally-vertically isolated with rocking $T_1$=2.4sec | 1g | 0.320 | 0.620 | 0.026 | 0.651 | 0.027 | 0.447 | 0.020 |
| | 2g | 0.507 | 0.289 | 0.005 | 0.351 | 0.006 | 0.351 | 0.006 |

Table 5-21 Summary of results for probability of failure when considering uncertainties for isolated and non-isolated transformer with $W$=420kip, $f_{AI}$=11.3Hz and inclined bushing. When isolated, $D_{Capacity}$=17.7inch and lower bound friction properties. Location: **Vancouver, WA**. Far-field motions

| System | Transverse Bushing Acceleration Limit (g) | Fragility Parameters with Spectral Shape Effects | | | $\beta_{RTR}$ as computed. $\beta_{MDL}$ as defined in Section 4 | | $\beta_{RTR}$ bound by 0.4. $\beta_{MDL}$ as defined in Section 4 | |
|---|---|---|---|---|---|---|---|---|
| | | Median $\widehat{Sa}_F(T_1)$ (g) | $\beta_{RTR}$ | $P_F$ (50 years) | $\beta$ | $P_F$ (50 years) | $\beta$ | $P_F$ (50 years) |
| Non-isolated $T_1$=0.09sec | 1g | 0.955 | 0.303 | 0.024 | 0.426 | 0.030 | 0.426 | 0.030 |
| | 2g | 1.909 | 0.303 | 0.003 | 0.426 | 0.005 | 0.426 | 0.005 |
| Horizontally isolated $T_1$=2.4sec | 1g | 0.302 | 0.600 | 0.030 | 0.608 | 0.030 | 0.412 | 0.024 |
| | 2g | 0.344 | 0.548 | 0.022 | 0.557 | 0.022 | 0.412 | 0.018 |
| Horizontally-vertically isolated without rocking $T_1$=2.4sec | 1g | 0.420 | 0.323 | 0.011 | 0.380 | 0.012 | 0.380 | 0.012 |
| | 2g | 0.442 | 0.316 | 0.009 | 0.374 | 0.010 | 0.374 | 0.010 |
| Horizontally-vertically isolated with rocking $T_1$=2.4sec | 1g | 0.500 | 0.291 | 0.007 | 0.353 | 0.007 | 0.353 | 0.007 |
| | 2g | 0.526 | 0.271 | 0.006 | 0.337 | 0.006 | 0.337 | 0.006 |

Table 5-22 Summary of results for probability of failure when considering uncertainties for isolated and non-isolated transformer with $W$=420kip, $f_{AI}$=11.3Hz and inclined bushing. When isolated, $D_{Capacity}$=17.7inch and lower bound friction properties. Location: **Saranap, CA**. Far-field motions

| System | Transverse Bushing Acceleration Limit (g) | Fragility Parameters with Spectral Shape Effects | | | $\beta_{RTR}$ as computed. $\beta_{MDL}$ as defined in Section 4 | | $\beta_{RTR}$ bound by 0.4. $\beta_{MDL}$ as defined in Section 4 | |
|---|---|---|---|---|---|---|---|---|
| | | Median $\widehat{Sa}_F(T_1)$ (g) | $\beta_{RTR}$ | $P_F$ (50 years) | $\beta$ | $P_F$ (50 years) | $\beta$ | $P_F$ (50 years) |
| Non-isolated $T_1$=0.13sec | 1g | 1.140 | 0.303 | 0.078 | 0.426 | 0.106 | 0.426 | 0.106 |
| | 2g | 2.281 | 0.303 | 0.005 | 0.426 | 0.011 | 0.426 | 0.011 |
| Horizontally isolated $T_1$=2.4sec | 1g | 0.677 | 0.600 | 0.041 | 0.608 | 0.042 | 0.412 | 0.022 |
| | 2g | 0.717 | 0.548 | 0.029 | 0.557 | 0.030 | 0.412 | 0.018 |
| Horizontally-vertically isolated without rocking $T_1$=2.4sec | 1g | 0.616 | 0.323 | 0.022 | 0.380 | 0.026 | 0.380 | 0.026 |
| | 2g | 0.637 | 0.316 | 0.019 | 0.374 | 0.023 | 0.374 | 0.023 |
| Horizontally-vertically isolated with rocking $T_1$=2.4sec | 1g | 0.702 | 0.291 | 0.013 | 0.353 | 0.016 | 0.353 | 0.016 |
| | 2g | 0.715 | 0.271 | 0.011 | 0.337 | 0.014 | 0.337 | 0.014 |

Table 5-23 Summary of results for probability of failure when considering uncertainties for isolated and non-isolated transformer with $W$=420kip, $f_{AI}$=11.3Hz and inclined bushing. When isolated, $D_{Capacity}$=17.7inch and lower bound friction properties. Location: **Chehalis, WA**. Far-field motions

| System | Transverse Bushing Acceleration Limit (g) | Fragility Parameters with Spectral Shape Effects | | | $\beta_{RTR}$ as computed. $\beta_{MDL}$ as defined in Section 4 | | $\beta_{RTR}$ bound by 0.4. $\beta_{MDL}$ as defined in Section 4 | |
|---|---|---|---|---|---|---|---|---|
| | | Median $\widehat{Sa}_F(T_1)$ (g) | $\beta_{RTR}$ | $P_F$ (50 years) | $\beta$ | $P_F$ (50 years) | $\beta$ | $P_F$ (50 years) |
| Non-isolated $T_1$=0.13sec | 1g | 0.959 | 0.303 | 0.048 | 0.426 | 0.058 | 0.426 | 0.058 |
| | 2g | 1.918 | 0.303 | 0.007 | 0.426 | 0.011 | 0.426 | 0.011 |
| Horizontally isolated $T_1$=2.4sec | 1g | 0.315 | 0.600 | 0.036 | 0.608 | 0.037 | 0.412 | 0.029 |
| | 2g | 0.358 | 0.548 | 0.028 | 0.557 | 0.028 | 0.412 | 0.023 |
| Horizontally-vertically isolated without rocking $T_1$=2.4sec | 1g | 0.428 | 0.323 | 0.015 | 0.380 | 0.016 | 0.380 | 0.016 |
| | 2g | 0.451 | 0.316 | 0.013 | 0.374 | 0.014 | 0.374 | 0.014 |
| Horizontally-vertically isolated with rocking $T_1$=2.4sec | 1g | 0.509 | 0.291 | 0.010 | 0.353 | 0.011 | 0.353 | 0.011 |
| | 2g | 0.534 | 0.271 | 0.009 | 0.337 | 0.010 | 0.337 | 0.010 |

Table 5-24 Summary of results for probability of failure when considering uncertainties for isolated and non-isolated transformer with $W$=420kip, $f_{AI}$=11.3Hz and inclined bushing. When isolated, $D_{Capacity}$=17.7inch and lower bound friction properties. Location: **Aberdeen, WA**. Far-field motions

| System | Transverse Bushing Acceleration Limit (g) | Fragility Parameters with Spectral Shape Effects | | | $\beta_{RTR}$ as computed. $\beta_{MDL}$ as defined in Section 4 | | $\beta_{RTR}$ bound by 0.4. $\beta_{MDL}$ as defined in Section 4 | |
|---|---|---|---|---|---|---|---|---|
| | | Median $\widehat{Sa}_F(T_1)$ (g) | $\beta_{RTR}$ | $P_F$ (50 years) | $\beta$ | $P_F$ (50 years) | $\beta$ | $P_F$ (50 years) |
| Non-isolated $T_1$=0.13sec | 1g | 1.025 | 0.303 | 0.060 | 0.426 | 0.068 | 0.426 | 0.068 |
| | 2g | 2.049 | 0.303 | 0.014 | 0.426 | 0.017 | 0.426 | 0.017 |
| Horizontally isolated $T_1$=2.4sec | 1g | 0.402 | 0.600 | 0.039 | 0.608 | 0.040 | 0.412 | 0.035 |
| | 2g | 0.447 | 0.548 | 0.033 | 0.557 | 0.034 | 0.412 | 0.031 |
| Horizontally-vertically isolated without rocking $T_1$=2.4sec | 1g | 0.481 | 0.323 | 0.027 | 0.380 | 0.027 | 0.380 | 0.027 |
| | 2g | 0.503 | 0.316 | 0.025 | 0.374 | 0.026 | 0.374 | 0.026 |
| Horizontally-vertically isolated with rocking $T_1$=2.4sec | 1g | 0.564 | 0.291 | 0.021 | 0.353 | 0.022 | 0.353 | 0.022 |
| | 2g | 0.587 | 0.271 | 0.020 | 0.337 | 0.020 | 0.337 | 0.020 |

Table 5-25 Summary of results for probability of failure when considering uncertainties for isolated and non-isolated transformer with $W$=420kip, $f_{AI}$=11.3Hz and inclined bushing. When isolated, $D_{Capacity}$=17.7inch and lower bound friction properties. Location: **Loma Linda, CA**. Far-field motions

| System | Transverse Bushing Acceleration Limit (g) | Fragility Parameters with Spectral Shape Effects | | | $\beta_{RTR}$ as computed. $\beta_{MDL}$ as defined in Section 4 | | $\beta_{RTR}$ bound by 0.4. $\beta_{MDL}$ as defined in Section 4 | |
|---|---|---|---|---|---|---|---|---|
| | | Median $\widehat{Sa}_F(T_1)$ (g) | $\beta_{RTR}$ | $P_F$ (50 years) | $\beta$ | $P_F$ (50 years) | $\beta$ | $P_F$ (50 years) |
| Non-isolated $T_1$=0.09sec | 1g | 1.135 | 0.303 | 0.114 | 0.426 | 0.140 | 0.426 | 0.140 |
| | 2g | 2.271 | 0.303 | 0.013 | 0.426 | 0.021 | 0.426 | 0.021 |
| Horizontally isolated $T_1$=2.4sec | 1g | 0.866 | 0.600 | 0.074 | 0.608 | 0.075 | 0.412 | 0.055 |
| | 2g | 0.897 | 0.548 | 0.064 | 0.557 | 0.064 | 0.412 | 0.052 |
| Horizontally-vertically isolated without rocking $T_1$=2.4sec | 1g | 0.693 | 0.323 | 0.078 | 0.380 | 0.082 | 0.380 | 0.082 |
| | 2g | 0.712 | 0.316 | 0.073 | 0.374 | 0.078 | 0.374 | 0.078 |
| Horizontally-vertically isolated with rocking $T_1$=2.4sec | 1g | 0.779 | 0.291 | 0.060 | 0.353 | 0.064 | 0.353 | 0.064 |
| | 2g | 0.786 | 0.271 | 0.057 | 0.337 | 0.061 | 0.337 | 0.061 |

Table 5-26 Summary of results for probability of failure when considering uncertainties for isolated and non-isolated transformer with $W$=420kip, $f_{AI}$=11.3Hz and inclined bushing. When isolated, $D_{Capacity}$=17.7inch and lower bound friction properties. Location: **Hillsboro, OR**. Far-field motions

| System | Transverse Bushing Acceleration Limit (g) | Fragility Parameters with Spectral Shape Effects | | | $\beta_{RTR}$ as computed. $\beta_{MDL}$ as defined in Section 4 | | $\beta_{RTR}$ bound by 0.4. $\beta_{MDL}$ as defined in Section 4 | |
|---|---|---|---|---|---|---|---|---|
| | | Median $\widehat{Sa}_F(T_1)$ (g) | $\beta_{RTR}$ | $P_F$ (50 years) | $\beta$ | $P_F$ (50 years) | $\beta$ | $P_F$ (50 years) |
| Non-isolated $T_1$=0.09sec | 1g | 0.967 | 0.303 | 0.028 | 0.426 | 0.034 | 0.426 | 0.034 |
| | 2g | 1.934 | 0.303 | 0.005 | 0.426 | 0.006 | 0.426 | 0.006 |
| Horizontally isolated $T_1$=2.4sec | 1g | 0.314 | 0.600 | 0.032 | 0.608 | 0.033 | 0.412 | 0.026 |
| | 2g | 0.357 | 0.548 | 0.025 | 0.557 | 0.258 | 0.412 | 0.236 |
| Horizontally-vertically isolated without rocking $T_1$=2.4sec | 1g | 0.428 | 0.323 | 0.013 | 0.380 | 0.014 | 0.380 | 0.014 |
| | 2g | 0.450 | 0.316 | 0.012 | 0.374 | 0.013 | 0.374 | 0.013 |
| Horizontally-vertically isolated with rocking $T_1$=2.4sec | 1g | 0.508 | 0.291 | 0.009 | 0.353 | 0.010 | 0.353 | 0.010 |
| | 2g | 0.534 | 0.271 | 0.008 | 0.337 | 0.008 | 0.337 | 0.008 |

Table 5-27 Summary of results for probability of failure when considering uncertainties for isolated and non-isolated transformer with $W$=420kip, $f_{AI}$=11.3Hz and inclined bushing. When isolated, $D_{Capacity}$=17.7inch and lower bound friction properties. Location: **Eugene, OR**. Far-field motions

| System | Transverse Bushing Acceleration Limit (g) | Fragility Parameters with Spectral Shape Effects | | | $\beta_{RTR}$ as computed. $\beta_{MDL}$ as defined in Section 4 | | $\beta_{RTR}$ bound by 0.4. $\beta_{MDL}$ as defined in Section 4 | |
|---|---|---|---|---|---|---|---|---|
| | | Median $\widehat{Sa}_F(T_1)$ (g) | $\beta_{RTR}$ | $P_F$ (50 years) | $\beta$ | $P_F$ (50 years) | $\beta$ | $P_F$ (50 years) |
| Non-isolated $T_1$=0.09sec | 1g | 0.949 | 0.303 | 0.023 | 0.426 | 0.026 | 0.426 | 0.026 |
| | 2g | 1.898 | 0.303 | 0.005 | 0.426 | 0.006 | 0.426 | 0.006 |
| Horizontally isolated $T_1$=2.4sec | 1g | 0.308 | 0.600 | 0.032 | 0.608 | 0.032 | 0.412 | 0.028 |
| | 2g | 0.351 | 0.548 | 0.025 | 0.557 | 0.025 | 0.412 | 0.023 |
| Horizontally-vertically isolated without rocking $T_1$=2.4sec | 1g | 0.424 | 0.323 | 0.015 | 0.380 | 0.016 | 0.380 | 0.016 |
| | 2g | 0.446 | 0.316 | 0.014 | 0.374 | 0.015 | 0.374 | 0.015 |
| Horizontally-vertically isolated with rocking $T_1$=2.4sec | 1g | 0.504 | 0.291 | 0.011 | 0.353 | 0.012 | 0.353 | 0.012 |
| | 2g | 0.530 | 0.271 | 0.010 | 0.337 | 0.010 | 0.337 | 0.010 |

Table 5-28 Summary of results for probability of failure when considering uncertainties for isolated and non-isolated transformer with $W$=420kip, $f_{AI}$=11.3Hz and inclined bushing. When isolated, $D_{Capacity}$=17.7inch and lower bound friction properties. Location: **Wilsonville, OR**. Far-field motions

| System | Transverse Bushing Acceleration Limit (g) | Fragility Parameters with Spectral Shape Effects | | | $\beta_{RTR}$ as computed. $\beta_{MDL}$ as defined in Section 4 | | $\beta_{RTR}$ bound by 0.4. $\beta_{MDL}$ as defined in Section 4 | |
|---|---|---|---|---|---|---|---|---|
| | | Median $\widehat{Sa}_F(T_1)$ (g) | $\beta_{RTR}$ | $P_F$ (50 years) | $\beta$ | $P_F$ (50 years) | $\beta$ | $P_F$ (50 years) |
| Non-isolated $T_1$=0.09sec | 1g | 0.953 | 0.303 | 0.025 | 0.426 | 0.030 | 0.426 | 0.030 |
| | 2g | 1.907 | 0.303 | 0.004 | 0.426 | 0.005 | 0.426 | 0.005 |
| Horizontally isolated $T_1$=2.4sec | 1g | 0.316 | 0.600 | 0.028 | 0.608 | 0.029 | 0.412 | 0.022 |
| | 2g | 0.359 | 0.548 | 0.021 | 0.557 | 0.021 | 0.412 | 0.018 |
| Horizontally-vertically isolated without rocking $T_1$=2.4sec | 1g | 0.429 | 0.323 | 0.011 | 0.380 | 0.012 | 0.380 | 0.012 |
| | 2g | 0.451 | 0.316 | 0.010 | 0.374 | 0.010 | 0.374 | 0.010 |
| Horizontally-vertically isolated with rocking $T_1$=2.4sec | 1g | 0.509 | 0.291 | 0.007 | 0.353 | 0.008 | 0.353 | 0.008 |
| | 2g | 0.535 | 0.271 | 0.006 | 0.337 | 0.007 | 0.337 | 0.007 |

Table 5-29 Summary of results for probability of failure when considering uncertainties for isolated and non-isolated transformer with $W$=420kip, $f_{AI}$=11.3Hz and inclined bushing. When isolated, $D_{Capacity}$=17.7inch and lower bound friction properties. Location: **Curry County, OR**. Far-field motions

| System | Transverse Bushing Acceleration Limit (g) | Fragility Parameters with Spectral Shape Effects | | | $\beta_{RTR}$ as computed. $\beta_{MDL}$ as defined in Section 4 | | $\beta_{RTR}$ bound by 0.4. $\beta_{MDL}$ as defined in Section 4 | |
|---|---|---|---|---|---|---|---|---|
| | | Median $\widehat{Sa}_F(T_1)$ (g) | $\beta_{RTR}$ | $P_F$ (50 years) | $\beta$ | $P_F$ (50 years) | $\beta$ | $P_F$ (50 years) |
| Non-isolated $T_1$=0.13sec | 1g | 1.123 | 0.303 | 0.048 | 0.426 | 0.053 | 0.426 | 0.053 |
| | 2g | 2.247 | 0.303 | 0.012 | 0.426 | 0.015 | 0.426 | 0.015 |
| Horizontally isolated $T_1$=2.4sec | 1g | 0.656 | 0.600 | 0.037 | 0.608 | 0.037 | 0.412 | 0.032 |
| | 2g | 0.697 | 0.548 | 0.032 | 0.557 | 0.033 | 0.412 | 0.029 |
| Horizontally-vertically isolated without rocking $T_1$=2.4sec | 1g | 0.607 | 0.323 | 0.034 | 0.380 | 0.035 | 0.380 | 0.035 |
| | 2g | 0.628 | 0.316 | 0.032 | 0.374 | 0.033 | 0.374 | 0.033 |
| Horizontally-vertically isolated with rocking $T_1$=2.4sec | 1g | 0.693 | 0.291 | 0.027 | 0.353 | 0.028 | 0.353 | 0.028 |
| | 2g | 0.707 | 0.271 | 0.026 | 0.337 | 0.027 | 0.337 | 0.027 |

Table 5-30 Summary of results for probability of failure when considering uncertainties for isolated and non-isolated transformer with $W$=420kip, $f_{AI}$=11.3Hz and inclined bushing. When isolated, $D_{Capacity}$=17.7inch and lower bound friction properties. Location: **Troutdale, OR**. Far-field motions

| System | Transverse Bushing Acceleration Limit (g) | Fragility Parameters with Spectral Shape Effects | | | $\beta_{RTR}$ as computed. $\beta_{MDL}$ as defined in Section 4 | | $\beta_{RTR}$ bound by 0.4. $\beta_{MDL}$ as defined in Section 4 | |
|---|---|---|---|---|---|---|---|---|
| | | Median $\widehat{Sa}_F(T_1)$ (g) | $\beta_{RTR}$ | $P_F$ (50 years) | $\beta$ | $P_F$ (50 years) | $\beta$ | $P_F$ (50 years) |
| Non-isolated $T_1$=0.13sec | 1g | 0.948 | 0.303 | 0.021 | 0.426 | 0.027 | 0.426 | 0.027 |
| | 2g | 1.895 | 0.303 | 0.003 | 0.426 | 0.004 | 0.426 | 0.004 |
| Horizontally isolated $T_1$=2.4sec | 1g | 0.307 | 0.600 | 0.027 | 0.608 | 0.027 | 0.412 | 0.021 |
| | 2g | 0.349 | 0.548 | 0.020 | 0.557 | 0.020 | 0.412 | 0.016 |
| Horizontally-vertically isolated without rocking $T_1$=2.4sec | 1g | 0.423 | 0.323 | 0.009 | 0.380 | 0.010 | 0.380 | 0.010 |
| | 2g | 0.445 | 0.316 | 0.008 | 0.374 | 0.009 | 0.374 | 0.009 |
| Horizontally-vertically isolated with rocking $T_1$=2.4sec | 1g | 0.503 | 0.291 | 0.006 | 0.353 | 0.006 | 0.353 | 0.006 |
| | 2g | 0.529 | 0.271 | 0.005 | 0.337 | 0.005 | 0.337 | 0.005 |

Table 5-31 Summary of results for probability of failure when considering uncertainties for isolated and non-isolated transformer with $W$=420kip, $f_{AI}$=7.7Hz and inclined bushing. When isolated, $D_{Capacity}$=31.3inch and lower bound friction properties. Location: **Vancouver, WA**. Far-field motions

| System | Transverse Bushing Acceleration Limit (g) | Fragility Parameters with Spectral Shape Effects | | | $\beta_{RTR}$ as computed. $\beta_{MDL}$ as defined in Section 4 | | $\beta_{RTR}$ bound by 0.4. $\beta_{MDL}$ as defined in Section 4 | |
|---|---|---|---|---|---|---|---|---|
| | | Median $\widehat{Sa}_F(T_1)$ (g) | $\beta_{RTR}$ | $P_F$ (50 years) | $\beta$ | $P_F$ (50 years) | $\beta$ | $P_F$ (50 years) |
| Non-isolated $T_1$=0.13sec | 1g | 0.706 | 0.276 | 0.069 | 0.408 | 0.080 | 0.408 | 0.080 |
| | 2g | 1.411 | 0.276 | 0.013 | 0.408 | 0.017 | 0.408 | 0.017 |
| Horizontally isolated $T_1$=2.4sec | 1g | 0.304 | 0.744 | 0.037 | 0.751 | 0.037 | 0.412 | 0.023 |
| | 2g | 0.430 | 0.611 | 0.016 | 0.619 | 0.017 | 0.412 | 0.012 |
| Horizontally-vertically isolated without rocking $T_1$=2.4sec | 1g | 0.414 | 0.405 | 0.012 | 0.452 | 0.013 | 0.447 | 0.013 |
| | 2g | 0.451 | 0.319 | 0.009 | 0.377 | 0.010 | 0.377 | 0.010 |
| Horizontally-vertically isolated with rocking $T_1$=2.4sec | 1g | 0.423 | 0.404 | 0.012 | 0.451 | 0.013 | 0.447 | 0.013 |
| | 2g | 0.481 | 0.302 | 0.008 | 0.362 | 0.008 | 0.362 | 0.008 |

Table 5-32 Summary of results for probability of failure when considering uncertainties for isolated and non-isolated transformer with $W$=420kip, $f_{AI}$=7.7Hz and inclined bushing. When isolated, $D_{Capacity}$=31.3inch and lower bound friction properties. Location: **Saranap, CA**. Far-field motions

| System | Transverse Bushing Acceleration Limit (g) | Fragility Parameters with Spectral Shape Effects | | | $\beta_{RTR}$ as computed. $\beta_{MDL}$ as defined in Section 4 | | $\beta_{RTR}$ bound by 0.4. $\beta_{MDL}$ as defined in Section 4 | |
|---|---|---|---|---|---|---|---|---|
| | | Median $\widehat{Sa}_F(T_1)$ (g) | $\beta_{RTR}$ | $P_F$ (50 years) | $\beta$ | $P_F$ (50 years) | $\beta$ | $P_F$ (50 years) |
| Non-isolated $T_1$=0.13sec | 1g | 0.782 | 0.276 | 0.266 | 0.408 | 0.307 | 0.408 | 0.307 |
| | 2g | 1.564 | 0.276 | 0.038 | 0.408 | 0.058 | 0.408 | 0.058 |
| Horizontally isolated $T_1$=2.4sec | 1g | 0.700 | 0.744 | 0.058 | 0.751 | 0.060 | 0.412 | 0.019 |
| | 2g | 0.911 | 0.611 | 0.019 | 0.619 | 0.020 | 0.412 | 0.008 |
| Horizontally-vertically isolated without rocking $T_1$=2.4sec | 1g | 0.653 | 0.405 | 0.024 | 0.452 | 0.028 | 0.447 | 0.027 |
| | 2g | 0.665 | 0.319 | 0.017 | 0.377 | 0.020 | 0.377 | 0.020 |
| Horizontally-vertically isolated with rocking $T_1$=2.4sec | 1g | 0.676 | 0.404 | 0.021 | 0.451 | 0.025 | 0.447 | 0.025 |
| | 2g | 0.699 | 0.302 | 0.013 | 0.362 | 0.016 | 0.362 | 0.016 |

Table 5-33 Summary of results for probability of failure when considering uncertainties for isolated and non-isolated transformer with $W$=420kip, $f_{AI}$=7.7Hz and inclined bushing. When isolated, $D_{Capacity}$=31.3inch and lower bound friction properties. Location: **Loma Linda, CA**. Far-field motions

| System | Transverse Bushing Acceleration Limit (g) | Fragility Parameters with Spectral Shape Effects | | | $\beta_{RTR}$ as computed. $\beta_{MDL}$ as defined in Section 4 | | $\beta_{RTR}$ bound by 0.4. $\beta_{MDL}$ as defined in Section 4 | |
|---|---|---|---|---|---|---|---|---|
| | | Median $\widehat{Sa}_F(T_1)$ (g) | $\beta_{RTR}$ | $P_F$ (50 years) | $\beta$ | $P_F$ (50 years) | $\beta$ | $P_F$ (50 years) |
| Non-isolated $T_1$=0.13sec | 1g | 0.782 | 0.276 | 0.297 | 0.408 | 0.346 | 0.408 | 0.346 |
| | 2g | 1.565 | 0.276 | 0.059 | 0.408 | 0.084 | 0.408 | 0.084 |
| Horizontally isolated $T_1$=2.4sec | 1g | 0.902 | 0.744 | 0.087 | 0.751 | 0.088 | 0.412 | 0.051 |
| | 2g | 1.146 | 0.611 | 0.044 | 0.619 | 0.045 | 0.412 | 0.030 |
| Horizontally-vertically isolated without rocking $T_1$=2.4sec | 1g | 0.751 | 0.405 | 0.073 | 0.452 | 0.077 | 0.447 | 0.077 |
| | 2g | 0.749 | 0.319 | 0.066 | 0.377 | 0.071 | 0.377 | 0.071 |
| Horizontally-vertically isolated with rocking $T_1$=2.4sec | 1g | 0.780 | 0.404 | 0.068 | 0.451 | 0.072 | 0.447 | 0.071 |
| | 2g | 0.783 | 0.302 | 0.060 | 0.362 | 0.064 | 0.362 | 0.064 |

Table 5-34 Summary of results for probability of failure when considering uncertainties for isolated and non-isolated transformer with $W$=420kip, $f_{AI}$=7.7Hz and inclined bushing. When isolated, $D_{Capacity}$=31.3inch and lower bound friction properties. Location: **Aberdeen, WA**. .Far-field motions

| System | Transverse Bushing Acceleration Limit (g) | Fragility Parameters with Spectral Shape Effects | | | $\beta_{RTR}$ as computed. $\beta_{MDL}$ as defined in Section 4 | | $\beta_{RTR}$ bound by 0.4. $\beta_{MDL}$ as defined in Section 4 | |
|---|---|---|---|---|---|---|---|---|
| | | Median $\widehat{Sa}_F(T_1)$ (g) | $\beta_{RTR}$ | $P_F$ (50 years) | $\beta$ | $P_F$ (50 years) | $\beta$ | $P_F$ (50 years) |
| Non-isolated $T_1$=0.13sec | 1g | 0.737 | 0.276 | 0.135 | 0.408 | 0.141 | 0.408 | 0.141 |
| | 2g | 1.473 | 0.276 | 0.040 | 0.408 | 0.044 | 0.408 | 0.044 |
| Horizontally isolated $T_1$=2.4sec | 1g | 0.409 | 0.744 | 0.043 | 0.751 | 0.044 | 0.412 | 0.034 |
| | 2g | 0.562 | 0.611 | 0.026 | 0.619 | 0.026 | 0.412 | 0.022 |
| Horizontally-vertically isolated without rocking $T_1$=2.4sec | 1g | 0.487 | 0.405 | 0.027 | 0.452 | 0.028 | 0.447 | 0.028 |
| | 2g | 0.518 | 0.319 | 0.024 | 0.377 | 0.025 | 0.377 | 0.025 |
| Horizontally-vertically isolated with rocking $T_1$=2.4sec | 1g | 0.500 | 0.404 | 0.026 | 0.451 | 0.027 | 0.447 | 0.027 |
| | 2g | 0.550 | 0.302 | 0.022 | 0.362 | 0.023 | 0.362 | 0.023 |

Table 5-35 Summary of results for probability of failure when considering uncertainties for isolated and non-isolated transformer with $W$=420kip, $f_{AI}$=7.7Hz and inclined bushing. When isolated, $D_{Capacity}$=31.3inch and lower bound friction properties. Location: **Chehalis, WA**. Far-field motions

| System | Transverse Bushing Acceleration Limit (g) | Fragility Parameters with Spectral Shape Effects | | | $\beta_{RTR}$ as computed. $\beta_{MDL}$ as defined in Section 4 | | $\beta_{RTR}$ bound by 0.4. $\beta_{MDL}$ as defined in Section 4 | |
|---|---|---|---|---|---|---|---|---|
| | | Median $\widehat{Sa}_F(T_1)$ (g) | $\beta_{RTR}$ | $P_F$ (50 years) | $\beta$ | $P_F$ (50 years) | $\beta$ | $P_F$ (50 years) |
| Non-isolated $T_1$=0.13sec | 1g | 0.717 | 0.276 | 0.113 | 0.408 | 0.129 | 0.408 | 0.129 |
| | 2g | 1.434 | 0.276 | 0.024 | 0.408 | 0.030 | 0.408 | 0.030 |
| Horizontally isolated $T_1$=2.4sec | 1g | 0.318 | 0.744 | 0.044 | 0.751 | 0.044 | 0.412 | 0.029 |
| | 2g | 0.448 | 0.611 | 0.021 | 0.619 | 0.021 | 0.412 | 0.015 |
| Horizontally-vertically isolated without rocking $T_1$=2.4sec | 1g | 0.424 | 0.405 | 0.017 | 0.452 | 0.018 | 0.447 | 0.018 |
| | 2g | 0.460 | 0.319 | 0.013 | 0.377 | 0.014 | 0.377 | 0.014 |
| Horizontally-vertically isolated with rocking $T_1$=2.4sec | 1g | 0.433 | 0.404 | 0.016 | 0.451 | 0.017 | 0.447 | 0.017 |
| | 2g | 0.491 | 0.302 | 0.011 | 0.362 | 0.012 | 0.362 | 0.012 |

Table 5-36 Summary of results for probability of failure when considering uncertainties for isolated and non-isolated transformer with $W$=420kip, $f_{AI}$=7.7Hz and inclined bushing. When isolated, $D_{Capacity}$=31.3inch and lower bound friction properties. Location: **Hillsboro, OR**. Far-field motions

| System | Transverse Bushing Acceleration Limit (g) | Fragility Parameters with Spectral Shape Effects | | | $\beta_{RTR}$ as computed. $\beta_{MDL}$ as defined in Section 4 | | $\beta_{RTR}$ bound by 0.4. $\beta_{MDL}$ as defined in Section 4 | |
|---|---|---|---|---|---|---|---|---|
| | | Median $\widehat{Sa}_F(T_1)$ (g) | $\beta_{RTR}$ | $P_F$ (50 years) | $\beta$ | $P_F$ (50 years) | $\beta$ | $P_F$ (50 years) |
| Non-isolated $T_1$=0.13sec | 1g | 0.711 | 0.276 | 0.076 | 0.408 | 0.085 | 0.408 | 0.085 |
| | 2g | 1.422 | 0.276 | 0.017 | 0.408 | 0.021 | 0.408 | 0.021 |
| Horizontally isolated $T_1$=2.4sec | 1g | 0.317 | 0.744 | 0.038 | 0.751 | 0.039 | 0.412 | 0.026 |
| | 2g | 0.447 | 0.611 | 0.018 | 0.619 | 0.019 | 0.412 | 0.014 |
| Horizontally-vertically isolated without rocking $T_1$=2.4sec | 1g | 0.423 | 0.405 | 0.015 | 0.452 | 0.016 | 0.447 | 0.016 |
| | 2g | 0.460 | 0.319 | 0.011 | 0.377 | 0.012 | 0.377 | 0.012 |
| Horizontally-vertically isolated with rocking $T_1$=2.4sec | 1g | 0.433 | 0.404 | 0.014 | 0.451 | 0.015 | 0.447 | 0.015 |
| | 2g | 0.490 | 0.302 | 0.010 | 0.362 | 0.011 | 0.362 | 0.011 |

Table 5-37 Summary of results for probability of failure when considering uncertainties for isolated and non-isolated transformer with $W$=420kip, $f_{AI}$=7.7Hz and inclined bushing. When isolated, $D_{Capacity}$=31.3inch and lower bound friction properties. Location: **Eugene, OR**. Far-field motions

| System | Transverse Bushing Acceleration Limit (g) | Fragility Parameters with Spectral Shape Effects | | | $\beta_{RTR}$ as computed. $\beta_{MDL}$ as defined in Section 4 | | $\beta_{RTR}$ bound by 0.4. $\beta_{MDL}$ as defined in Section 4 | |
|---|---|---|---|---|---|---|---|---|
| | | Median $\widehat{Sa}_F(T_1)$ (g) | $\beta_{RTR}$ | $P_F$ (50 years) | $\beta$ | $P_F$ (50 years) | $\beta$ | $P_F$ (50 years) |
| Non-isolated $T_1$=0.13sec | 1g | 0.704 | 0.276 | 0.052 | 0.408 | 0.056 | 0.408 | 0.056 |
| | 2g | 1.407 | 0.276 | 0.015 | 0.408 | 0.017 | 0.408 | 0.017 |
| Horizontally isolated $T_1$=2.4sec | 1g | 0.311 | 0.744 | 0.035 | 0.751 | 0.036 | 0.412 | 0.027 |
| | 2g | 0.439 | 0.611 | 0.019 | 0.619 | 0.019 | 0.412 | 0.016 |
| Horizontally-vertically isolated without rocking $T_1$=2.4sec | 1g | 0.419 | 0.405 | 0.017 | 0.452 | 0.018 | 0.447 | 0.018 |
| | 2g | 0.456 | 0.319 | 0.014 | 0.377 | 0.014 | 0.377 | 0.014 |
| Horizontally-vertically isolated with rocking $T_1$=2.4sec | 1g | 0.428 | 0.404 | 0.016 | 0.451 | 0.017 | 0.447 | 0.017 |
| | 2g | 0.486 | 0.302 | 0.012 | 0.362 | 0.012 | 0.362 | 0.012 |

Table 5-38 Summary of results for probability of failure when considering uncertainties for isolated and non-isolated transformer with $W$=420kip, $f_{AI}$=7.7Hz and inclined bushing. When isolated, $D_{Capacity}$=31.3inch and lower bound friction properties. Location: **Wilsonville, OR**. Far-field motions

<table>
<tr><th rowspan="2">System</th><th rowspan="2">Transverse Bushing Acceleration Limit (g)</th><th colspan="3">Fragility Parameters with Spectral Shape Effects</th><th colspan="2">$\beta_{RTR}$ as computed. $\beta_{MDL}$ as defined in Section 4</th><th colspan="2">$\beta_{RTR}$ bound by 0.4. $\beta_{MDL}$ as defined in Section 4</th></tr>
<tr><th>Median $\widehat{Sa}_F(T_1)$ (g)</th><th>$\beta_{RTR}$</th><th>$P_F$ (50 years)</th><th>$\beta$</th><th>$P_F$ (50 years)</th><th>$\beta$</th><th>$P_F$ (50 years)</th></tr>
<tr><td rowspan="2">Non-isolated $T_1$=0.13sec</td><td>1g</td><td>0.705</td><td>0.276</td><td>0.069</td><td>0.408</td><td>0.079</td><td>0.408</td><td>0.079</td></tr>
<tr><td>2g</td><td>1.410</td><td>0.276</td><td>0.014</td><td>0.408</td><td>0.018</td><td>0.408</td><td>0.018</td></tr>
<tr><td rowspan="2">Horizontally isolated $T_1$=2.4sec</td><td>1g</td><td>0.319</td><td>0.744</td><td>0.034</td><td>0.751</td><td>0.034</td><td>0.412</td><td>0.022</td></tr>
<tr><td>2g</td><td>0.449</td><td>0.611</td><td>0.015</td><td>0.619</td><td>0.016</td><td>0.412</td><td>0.011</td></tr>
<tr><td rowspan="2">Horizontally-vertically isolated without rocking $T_1$=2.4sec</td><td>1g</td><td>0.425</td><td>0.405</td><td>0.012</td><td>0.452</td><td>0.013</td><td>0.447</td><td>0.013</td></tr>
<tr><td>2g</td><td>0.461</td><td>0.319</td><td>0.009</td><td>0.377</td><td>0.010</td><td>0.377</td><td>0.010</td></tr>
<tr><td rowspan="2">Horizontally-vertically isolated with rocking $T_1$=2.4sec</td><td>1g</td><td>0.434</td><td>0.404</td><td>0.012</td><td>0.451</td><td>0.013</td><td>0.447</td><td>0.013</td></tr>
<tr><td>2g</td><td>0.492</td><td>0.302</td><td>0.008</td><td>0.362</td><td>0.008</td><td>0.362</td><td>0.008</td></tr>
</table>

Table 5-39 Summary of results for probability of failure when considering uncertainties for isolated and non-isolated transformer with $W$=420kip, $f_{AI}$=7.7Hz and inclined bushing. When isolated, $D_{Capacity}$=31.3inch and lower bound friction properties. Location: **Curry County, OR**. Far-field motions

| System | Transverse Bushing Acceleration Limit (g) | Fragility Parameters with Spectral Shape Effects | | | $\beta_{RTR}$ as computed. $\beta_{MDL}$ as defined in Section 4 | | $\beta_{RTR}$ bound by 0.4. $\beta_{MDL}$ as defined in Section 4 | |
|---|---|---|---|---|---|---|---|---|
| | | Median $\widehat{Sa}_F(T_1)$ (g) | $\beta_{RTR}$ | $P_F$ (50 years) | $\beta$ | $P_F$ (50 years) | $\beta$ | $P_F$ (50 years) |
| Non-isolated $T_1$=0.13sec | 1g | 0.778 | 0.276 | 0.107 | 0.408 | 0.108 | 0.408 | 0.108 |
| | 2g | 1.556 | 0.276 | 0.036 | 0.408 | 0.039 | 0.408 | 0.039 |
| Horizontally isolated $T_1$=2.4sec | 1g | 0.677 | 0.744 | 0.040 | 0.751 | 0.040 | 0.412 | 0.030 |
| | 2g | 0.885 | 0.611 | 0.024 | 0.619 | 0.024 | 0.412 | 0.019 |
| Horizontally-vertically isolated without rocking $T_1$=2.4sec | 1g | 0.642 | 0.405 | 0.033 | 0.452 | 0.034 | 0.447 | 0.034 |
| | 2g | 0.655 | 0.319 | 0.030 | 0.377 | 0.031 | 0.377 | 0.031 |
| Horizontally-vertically isolated with rocking $T_1$=2.4sec | 1g | 0.664 | 0.404 | 0.030 | 0.451 | 0.032 | 0.447 | 0.032 |
| | 2g | 0.689 | 0.302 | 0.027 | 0.362 | 0.028 | 0.362 | 0.028 |

Table 5-40 Summary of results for probability of failure when considering uncertainties for isolated and non-isolated transformer with $W$=420kip, $f_{AI}$=7.7Hz and inclined bushing. When isolated, $D_{Capacity}$=31.3inch and lower bound friction properties. Location: **Troutdale, OR**. Far-field motions

| System | Transverse Bushing Acceleration Limit (g) | Fragility Parameters with Spectral Shape Effects | | | $\beta_{RTR}$ as computed. $\beta_{MDL}$ as defined in Section 4 | | $\beta_{RTR}$ bound by 0.4. $\beta_{MDL}$ as defined in Section 4 | |
|---|---|---|---|---|---|---|---|---|
| | | Median $\widehat{Sa}_F(T_1)$ (g) | $\beta_{RTR}$ | $P_F$ (50 years) | $\beta$ | $P_F$ (50 years) | $\beta$ | $P_F$ (50 years) |
| Non-isolated $T_1$=0.13sec | 1g | 0.702 | 0.276 | 0.061 | 0.408 | 0.071 | 0.408 | 0.071 |
| | 2g | 1.403 | 0.276 | 0.011 | 0.408 | 0.015 | 0.408 | 0.015 |
| Horizontally isolated $T_1$=2.4sec | 1g | 0.310 | 0.744 | 0.033 | 0.751 | 0.033 | 0.412 | 0.020 |
| | 2g | 0.437 | 0.611 | 0.014 | 0.619 | 0.014 | 0.412 | 0.010 |
| Horizontally-vertically isolated without rocking $T_1$=2.4sec | 1g | 0.418 | 0.405 | 0.011 | 0.452 | 0.012 | 0.447 | 0.011 |
| | 2g | 0.454 | 0.319 | 0.008 | 0.377 | 0.008 | 0.377 | 0.008 |
| Horizontally-vertically isolated with rocking $T_1$=2.4sec | 1g | 0.427 | 0.404 | 0.010 | 0.451 | 0.011 | 0.447 | 0.010 |
| | 2g | 0.485 | 0.302 | 0.006 | 0.362 | 0.007 | 0.362 | 0.007 |

Table 5-41 Summary of results for probability of failure when considering uncertainties for isolated and non-isolated transformer with $W$=420kip, $f_{AI}$=4.3Hz and inclined bushing. When isolated, $D_{Capacity}$=31.3inch and lower bound friction properties. Location: **Vancouver, WA**. Far-field motions

| System | Transverse Bushing Acceleration Limit (g) | Fragility Parameters with Spectral Shape Effects | | | $\beta_{RTR}$ as computed. $\beta_{MDL}$ as defined in Section 4 | | $\beta_{RTR}$ bound by 0.4. $\beta_{MDL}$ as defined in Section 4 | |
|---|---|---|---|---|---|---|---|---|
| | | Median $\widehat{Sa}_F(T_1)$ (g) | $\beta_{RTR}$ | $P_F$ (50 years) | $\beta$ | $P_F$ (50 years) | $\beta$ | $P_F$ (50 years) |
| Non-isolated $T_1$=0.24sec | 1g | 1.030 | 0.173 | 0.045 | 0.346 | 0.053 | 0.346 | 0.053 |
| | 2g | 2.061 | 0.173 | 0.006 | 0.346 | 0.009 | 0.346 | 0.009 |
| Horizontally isolated $T_1$=2.4sec | 1g | 0.408 | 0.672 | 0.020 | 0.679 | 0.020 | 0.412 | 0.013 |
| | 2g | 0.470 | 0.607 | 0.014 | 0.615 | 0.014 | 0.412 | 0.009 |
| Horizontally-vertically isolated without rocking $T_1$=2.4sec | 1g | 0.563 | 0.423 | 0.006 | 0.468 | 0.007 | 0.447 | 0.007 |
| | 2g | 0.647 | 0.341 | 0.004 | 0.395 | 0.004 | 0.395 | 0.004 |
| Horizontally-vertically isolated with rocking $T_1$=2.4sec | 1g | 0.370 | 0.746 | 0.027 | 0.772 | 0.028 | 0.447 | 0.017 |
| | 2g | 0.664 | 0.388 | 0.004 | 0.437 | 0.004 | 0.437 | 0.004 |

Table 5-42 Summary of results for probability of failure when considering uncertainties for isolated and non-isolated transformer with $W$=420kip, $f_{AI}$=4.3Hz and inclined bushing. When isolated, $D_{Capacity}$=31.3inch and lower bound friction properties. Location: **Saranap, CA**. Far-field motions

| System | Transverse Bushing Acceleration Limit (g) | Fragility Parameters with Spectral Shape Effects | | | $\beta_{RTR}$ as computed. $\beta_{MDL}$ as defined in Section 4 | | $\beta_{RTR}$ bound by 0.4. $\beta_{MDL}$ as defined in Section 4 | |
|---|---|---|---|---|---|---|---|---|
| | | Median $\widehat{Sa}_F(T_1)$ (g) | $\beta_{RTR}$ | $P_F$ (50 years) | $\beta$ | $P_F$ (50 years) | $\beta$ | $P_F$ (50 years) |
| Non-isolated $T_1$=0.24sec | 1g | 1.105 | 0.173 | 0.153 | 0.346 | 0.192 | 0.346 | 0.192 |
| | 2g | 2.211 | 0.173 | 0.012 | 0.346 | 0.023 | 0.346 | 0.023 |
| Horizontally isolated $T_1$=2.4sec | 1g | 0.920 | 0.672 | 0.024 | 0.679 | 0.025 | 0.412 | 0.008 |
| | 2g | 1.014 | 0.607 | 0.014 | 0.615 | 0.015 | 0.412 | 0.005 |
| Horizontally-vertically isolated without rocking $T_1$=2.4sec | 1g | 0.928 | 0.423 | 0.008 | 0.468 | 0.010 | 0.447 | 0.009 |
| | 2g | 0.973 | 0.341 | 0.004 | 0.395 | 0.006 | 0.395 | 0.006 |
| Horizontally-vertically isolated with rocking $T_1$=2.4sec | 1g | 0.959 | 0.746 | 0.029 | 0.772 | 0.032 | 0.447 | 0.008 |
| | 2g | 1.037 | 0.388 | 0.004 | 0.437 | 0.006 | 0.437 | 0.006 |

Table 5-43 Summary of results for probability of failure when considering uncertainties for isolated and non-isolated transformer with $W$=420kip, $f_{AI}$=4.3Hz and inclined bushing. When isolated, $D_{Capacity}$=31.3inch and lower bound friction properties. Location: **Chehalis, WA**. Far-field motions

| System | Transverse Bushing Acceleration Limit (g) | Fragility Parameters with Spectral Shape Effects | | | $\beta_{RTR}$ as computed. $\beta_{MDL}$ as defined in Section 4 | | $\beta_{RTR}$ bound by 0.4. $\beta_{MDL}$ as defined in Section 4 | |
|---|---|---|---|---|---|---|---|---|
| | | Median $\widehat{Sa}_F(T_1)$ (g) | $\beta_{RTR}$ | $P_F$ (50 years) | $\beta$ | $P_F$ (50 years) | $\beta$ | $P_F$ (50 years) |
| Non-isolated $T_1$=0.24sec | 1g | 1.043 | 0.173 | 0.069 | 0.346 | 0.081 | 0.346 | 0.081 |
| | 2g | 2.087 | 0.173 | 0.011 | 0.346 | 0.016 | 0.346 | 0.016 |
| Horizontally isolated $T_1$=2.4sec | 1g | 0.426 | 0.672 | 0.025 | 0.679 | 0.025 | 0.412 | 0.017 |
| | 2g | 0.489 | 0.607 | 0.017 | 0.615 | 0.018 | 0.412 | 0.013 |
| Horizontally-vertically isolated without rocking $T_1$=2.4sec | 1g | 0.579 | 0.423 | 0.009 | 0.468 | 0.010 | 0.447 | 0.010 |
| | 2g | 0.661 | 0.341 | 0.006 | 0.395 | 0.007 | 0.395 | 0.007 |
| Horizontally-vertically isolated with rocking $T_1$=2.4sec | 1g | 0.389 | 0.746 | 0.032 | 0.772 | 0.034 | 0.447 | 0.021 |
| | 2g | 0.680 | 0.388 | 0.006 | 0.437 | 0.007 | 0.437 | 0.007 |

Table 5-44 Summary of results for probability of failure when considering uncertainties for isolated and non-isolated transformer with $W$=420kip, $f_{AI}$=4.3Hz and inclined bushing. When isolated, $D_{Capacity}$=31.3inch and lower bound friction properties. Location: **Aberdeen, WA**. Far-field motions

| System | Transverse Bushing Acceleration Limit (g) | Fragility Parameters with Spectral Shape Effects | | | $\beta_{RTR}$ as computed. $\beta_{MDL}$ as defined in Section 4 | | $\beta_{RTR}$ bound by 0.4. $\beta_{MDL}$ as defined in Section 4 | |
|---|---|---|---|---|---|---|---|---|
| | | Median $\widehat{Sa}_F(T_1)$ (g) | $\beta_{RTR}$ | $P_F$ (50 years) | $\beta$ | $P_F$ (50 years) | $\beta$ | $P_F$ (50 years) |
| Non-isolated $T_1$=0.24sec | 1g | 1.064 | 0.173 | 0.091 | 0.346 | 0.100 | 0.346 | 0.100 |
| | 2g | 2.130 | 0.173 | 0.026 | 0.346 | 0.030 | 0.346 | 0.030 |
| Horizontally isolated $T_1$=2.4sec | 1g | 0.545 | 0.672 | 0.029 | 0.679 | 0.029 | 0.412 | 0.023 |
| | 2g | 0.618 | 0.607 | 0.023 | 0.615 | 0.023 | 0.412 | 0.020 |
| Horizontally-vertically isolated without rocking $T_1$=2.4sec | 1g | 0.673 | 0.423 | 0.017 | 0.468 | 0.018 | 0.447 | 0.018 |
| | 2g | 0.748 | 0.341 | 0.014 | 0.395 | 0.014 | 0.395 | 0.014 |
| Horizontally-vertically isolated with rocking $T_1$=2.4sec | 1g | 0.519 | 0.746 | 0.033 | 0.772 | 0.033 | 0.447 | 0.026 |
| | 2g | 0.778 | 0.388 | 0.013 | 0.437 | 0.014 | 0.437 | 0.014 |

Table 5-45 Summary of results for probability of failure when considering uncertainties for isolated and non-isolated transformer with $W$=420kip, $f_{AI}$=4.3Hz and inclined bushing. When isolated, $D_{Capacity}$=31.3inch and lower bound friction properties. Location: **Loma Linda, CA**. Far-field motions

| System | Transverse Bushing Acceleration Limit (g) | Fragility Parameters with Spectral Shape Effects | | | $\beta_{RTR}$ as computed. $\beta_{MDL}$ as defined in Section 4 | | $\beta_{RTR}$ bound by 0.4. $\beta_{MDL}$ as defined in Section 4 | |
|---|---|---|---|---|---|---|---|---|
| | | Median $\widehat{Sa}_F(T_1)$ (g) | $\beta_{RTR}$ | $P_F$ (50 years) | $\beta$ | $P_F$ (50 years) | $\beta$ | $P_F$ (50 years) |
| Non-isolated $T_1$=0.24sec | 1g | 1.119 | 0.173 | 0.203 | 0.346 | 0.236 | 0.346 | 0.236 |
| | 2g | 2.241 | 0.173 | 0.029 | 0.346 | 0.043 | 0.346 | 0.043 |
| Horizontally isolated $T_1$=2.4sec | 1g | 0.925 | 0.672 | 0.074 | 0.679 | 0.075 | 0.412 | 0.048 |
| | 2g | 1.019 | 0.607 | 0.055 | 0.615 | 0.056 | 0.412 | 0.039 |
| Horizontally-vertically isolated without rocking $T_1$=2.4sec | 1g | 0.931 | 0.423 | 0.048 | 0.468 | 0.052 | 0.447 | 0.050 |
| | 2g | 0.976 | 0.341 | 0.039 | 0.395 | 0.042 | 0.395 | 0.042 |
| Horizontally-vertically isolated with rocking $T_1$=2.4sec | 1g | 0.965 | 0.746 | 0.078 | 0.772 | 0.081 | 0.447 | 0.047 |
| | 2g | 1.040 | 0.388 | 0.036 | 0.437 | 0.039 | 0.437 | 0.039 |

Table 5-46 Summary of results for probability of failure when considering uncertainties for isolated and non-isolated transformer with $W$=420kip, $f_{AI}$=4.3Hz and inclined bushing. When isolated, $D_{Capacity}$=31.3inch and lower bound friction properties. Location: **Hillsboro, OR**. Far-field motions

| System | Transverse Bushing Acceleration Limit (g) | Fragility Parameters with Spectral Shape Effects | | | $\beta_{RTR}$ as computed. $\beta_{MDL}$ as defined in Section 4 | | $\beta_{RTR}$ bound by 0.4. $\beta_{MDL}$ as defined in Section 4 | |
|---|---|---|---|---|---|---|---|---|
| | | Median $\widehat{Sa}_F(T_1)$ (g) | $\beta_{RTR}$ | $P_F$ (50 years) | $\beta$ | $P_F$ (50 years) | $\beta$ | $P_F$ (50 years) |
| Non-isolated $T_1$=0.24sec | 1g | 1.037 | 0.173 | 0.051 | 0.059 | 0.346 | 0.059 | 0.059 |
| | 2g | 2.074 | 0.173 | 0.009 | 0.012 | 0.346 | 0.012 | 0.012 |
| Horizontally isolated $T_1$=2.4sec | 1g | 0.425 | 0.672 | 0.022 | 0.679 | 0.022 | 0.412 | 0.015 |
| | 2g | 0.488 | 0.607 | 0.016 | 0.615 | 0.016 | 0.412 | 0.011 |
| Horizontally-vertically isolated without rocking $T_1$=2.4sec | 1g | 0.578 | 0.423 | 0.008 | 0.468 | 0.009 | 0.447 | 0.008 |
| | 2g | 0.660 | 0.341 | 0.005 | 0.395 | 0.006 | 0.395 | 0.006 |
| Horizontally-vertically isolated with rocking $T_1$=2.4sec | 1g | 0.388 | 0.746 | 0.028 | 0.772 | 0.029 | 0.447 | 0.019 |
| | 2g | 0.679 | 0.388 | 0.005 | 0.437 | 0.006 | 0.437 | 0.006 |

Table 5-47 Summary of results for probability of failure when considering uncertainties for isolated and non-isolated transformer with $W$=420kip, $f_{AI}$=4.3Hz and inclined bushing. When isolated, $D_{Capacity}$=31.3inch and lower bound friction properties. Location: **Eugene, OR**. Far-field motions.

| System | Transverse Bushing Acceleration Limit (g) | Fragility Parameters with Spectral Shape Effects | | | $\beta_{RTR}$ as computed. $\beta_{MDL}$ as defined in Section 4 | | $\beta_{RTR}$ bound by 0.4. $\beta_{MDL}$ as defined in Section 4 | |
|---|---|---|---|---|---|---|---|---|
| | | Median $\widehat{Sa}_F(T_1)$ (g) | $\beta_{RTR}$ | $P_F$ (50 years) | $\beta$ | $P_F$ (50 years) | $\beta$ | $P_F$ (50 years) |
| Non-isolated $T_1$=0.24sec | 1g | 1.030 | 0.173 | 0.043 | 0.346 | 0.046 | 0.346 | 0.046 |
| | 2g | 2.062 | 0.173 | 0.010 | 0.346 | 0.012 | 0.346 | 0.012 |
| Horizontally isolated $T_1$=2.4sec | 1g | 0.417 | 0.672 | 0.022 | 0.679 | 0.022 | 0.412 | 0.017 |
| | 2g | 0.479 | 0.607 | 0.016 | 0.615 | 0.017 | 0.412 | 0.013 |
| Horizontally-vertically isolated without rocking $T_1$=2.4sec | 1g | 0.571 | 0.423 | 0.010 | 0.468 | 0.010 | 0.447 | 0.010 |
| | 2g | 0.654 | 0.341 | 0.007 | 0.395 | 0.007 | 0.395 | 0.007 |
| Horizontally-vertically isolated with rocking $T_1$=2.4sec | 1g | 0.380 | 0.746 | 0.027 | 0.772 | 0.028 | 0.447 | 0.021 |
| | 2g | 0.672 | 0.388 | 0.007 | 0.437 | 0.007 | 0.437 | 0.007 |

Table 5-48 Summary of results for probability of failure when considering uncertainties for isolated and non-isolated transformer with $W$=420kip, $f_{AI}$=4.3Hz and inclined bushing. When isolated, $D_{Capacity}$=31.3inch and lower bound friction properties. Location: **Wilsonville, OR**. Far-field motions

| System | Transverse Bushing Acceleration Limit (g) | Fragility Parameters with Spectral Shape Effects | | | $\beta_{RTR}$ as computed. $\beta_{MDL}$ as defined in Section 4 | | $\beta_{RTR}$ bound by 0.4. $\beta_{MDL}$ as defined in Section 4 | |
|---|---|---|---|---|---|---|---|---|
| | | Median $\widehat{Sa}_F(T_1)$ (g) | $\beta_{RTR}$ | $P_F$ (50 years) | $\beta$ | $P_F$ (50 years) | $\beta$ | $P_F$ (50 years) |
| Non-isolated $T_1$=0.24sec | 1g | 1.030 | 0.173 | 0.045 | 0.346 | 0.053 | 0.346 | 0.053 |
| | 2g | 2.061 | 0.173 | 0.007 | 0.346 | 0.010 | 0.346 | 0.010 |
| Horizontally isolated $T_1$=2.4sec | 1g | 0.427 | 0.672 | 0.019 | 0.679 | 0.019 | 0.412 | 0.012 |
| | 2g | 0.491 | 0.607 | 0.013 | 0.615 | 0.013 | 0.412 | 0.009 |
| Horizontally-vertically isolated without rocking $T_1$=2.4sec | 1g | 0.580 | 0.423 | 0.006 | 0.468 | 0.007 | 0.447 | 0.007 |
| | 2g | 0.662 | 0.341 | 0.004 | 0.395 | 0.004 | 0.395 | 0.004 |
| Horizontally-vertically isolated with rocking $T_1$=2.4sec | 1g | 0.391 | 0.746 | 0.025 | 0.772 | 0.026 | 0.447 | 0.016 |
| | 2g | 0.681 | 0.388 | 0.004 | 0.437 | 0.004 | 0.437 | 0.004 |

Table 5-49 Summary of results for probability of failure when considering uncertainties for isolated and non-isolated transformer with $W$=420kip, $f_{AI}$=4.3Hz and inclined bushing. When isolated, $D_{Capacity}$=31.3inch and lower bound friction properties. Location: **Curry County, OR**. Far-field motions

| System | Transverse Bushing Acceleration Limit (g) | Fragility Parameters with Spectral Shape Effects | | | $\beta_{RTR}$ as computed. $\beta_{MDL}$ as defined in Section 4 | | $\beta_{RTR}$ bound by 0.4. $\beta_{MDL}$ as defined in Section 4 | |
|---|---|---|---|---|---|---|---|---|
| | | Median $\widehat{Sa}_F(T_1)$ (g) | $\beta_{RTR}$ | $P_F$ (50 years) | $\beta$ | $P_F$ (50 years) | $\beta$ | $P_F$ (50 years) |
| Non-isolated $T_1$=0.24sec | 1g | 1.107 | 0.173 | 0.087 | 0.346 | 0.092 | 0.346 | 0.092 |
| | 2g | 2.215 | 0.173 | 0.027 | 0.346 | 0.031 | 0.346 | 0.031 |
| Horizontally isolated $T_1$=2.4sec | 1g | 0.891 | 0.672 | 0.025 | 0.679 | 0.026 | 0.412 | 0.019 |
| | 2g | 0.984 | 0.607 | 0.020 | 0.615 | 0.020 | 0.412 | 0.016 |
| Horizontally-vertically isolated without rocking $T_1$=2.4sec | 1g | 0.910 | 0.423 | 0.019 | 0.468 | 0.020 | 0.447 | 0.019 |
| | 2g | 0.958 | 0.341 | 0.016 | 0.395 | 0.017 | 0.395 | 0.017 |
| Horizontally-vertically isolated with rocking $T_1$=2.4sec | 1g | 0.924 | 0.746 | 0.026 | 0.772 | 0.027 | 0.447 | 0.019 |
| | 2g | 1.019 | 0.388 | 0.015 | 0.437 | 0.016 | 0.437 | 0.016 |

Table 5-50 Summary of results for probability of failure when considering uncertainties for isolated and non-isolated transformer with $W$=420kip, $f_{AI}$=4.3Hz and inclined bushing. When isolated, $D_{Capacity}$=31.3inch and lower bound friction properties. Location: **Troutdale, OR**. Far-field motions

| System | Transverse Bushing Acceleration Limit (g) | Fragility Parameters with Spectral Shape Effects | | | $\beta_{RTR}$ as computed. $\beta_{MDL}$ as defined in Section 4 | | $\beta_{RTR}$ bound by 0.4. $\beta_{MDL}$ as defined in Section 4 | |
|---|---|---|---|---|---|---|---|---|
| | | Median $\widehat{Sa}_F(T_1)$ (g) | $\beta_{RTR}$ | $P_F$ (50 years) | $\beta$ | $P_F$ (50 years) | $\beta$ | $P_F$ (50 years) |
| Non-isolated $T_1$=0.24sec | 1g | 1.023 | 0.173 | 0.038 | 0.346 | 0.046 | 0.346 | 0.046 |
| | 2g | 2.047 | 0.173 | 0.005 | 0.346 | 0.007 | 0.346 | 0.007 |
| Horizontally isolated $T_1$=2.4sec | 1g | 0.415 | 0.672 | 0.018 | 0.679 | 0.018 | 0.412 | 0.011 |
| | 2g | 0.477 | 0.607 | 0.012 | 0.615 | 0.012 | 0.412 | 0.008 |
| Horizontally-vertically isolated without rocking $T_1$=2.4sec | 1g | 0.569 | 0.423 | 0.005 | 0.468 | 0.006 | 0.447 | 0.006 |
| | 2g | 0.653 | 0.341 | 0.003 | 0.395 | 0.003 | 0.395 | 0.003 |
| Horizontally-vertically isolated with rocking $T_1$=2.4sec | 1g | 0.377 | 0.746 | 0.024 | 0.772 | 0.025 | 0.447 | 0.014 |
| | 2g | 0.670 | 0.388 | 0.003 | 0.437 | 0.004 | 0.437 | 0.004 |

Table 5-51 Summary of results for probability of failure when considering uncertainties for isolated and non-isolated transformer with $W$=420kip, $f_{AI}$=11.3Hz and inclined bushing. When isolated, $D_{Capacity}$=31.3inch and lower bound friction properties. Location: **Vancouver, WA**. Far-field motions

| System | Transverse Bushing Acceleration Limit (g) | Fragility Parameters with Spectral Shape Effects | | | $\beta_{RTR}$ as computed. $\beta_{MDL}$ as defined in Section 4 | | $\beta_{RTR}$ bound by 0.4. $\beta_{MDL}$ as defined in Section 4 | |
|---|---|---|---|---|---|---|---|---|
| | | Median $\widehat{Sa}_F(T_1)$ (g) | $\beta_{RTR}$ | $P_F$ (50 years) | $\beta$ | $P_F$ (50 years) | $\beta$ | $P_F$ (50 years) |
| Non-isolated $T_1$=0.09sec | 1g | 0.955 | 0.303 | 0.024 | 0.426 | 0.030 | 0.426 | 0.030 |
| | 2g | 1.909 | 0.303 | 0.003 | 0.426 | 0.005 | 0.426 | 0.005 |
| Horizontally isolated $T_1$=2.4sec | 1g | 0.350 | 0.714 | 0.028 | 0.721 | 0.028 | 0.412 | 0.018 |
| | 2g | 0.425 | 0.672 | 0.019 | 0.679 | 0.019 | 0.412 | 0.012 |
| Horizontally-vertically isolated without rocking $T_1$=2.4sec | 1g | 0.546 | 0.437 | 0.007 | 0.481 | 0.008 | 0.447 | 0.007 |
| | 2g | 0.572 | 0.415 | 0.006 | 0.461 | 0.007 | 0.447 | 0.006 |
| Horizontally-vertically isolated with rocking $T_1$=2.4sec | 1g | 0.648 | 0.381 | 0.004 | 0.430 | 0.005 | 0.430 | 0.005 |
| | 2g | 0.692 | 0.346 | 0.003 | 0.400 | 0.004 | 0.400 | 0.004 |

Table 5-52 Summary of results for probability of failure when considering uncertainties for isolated and non-isolated transformer with $W$=420kip, $f_{AI}$=11.3Hz and inclined bushing. When isolated, $D_{Capacity}$=31.3inch and lower bound friction properties. Location: **Saranap, CA**. Far-field motions

| System | Transverse Bushing Acceleration Limit (g) | Fragility Parameters with Spectral Shape Effects | | | $\beta_{RTR}$ as computed. $\beta_{MDL}$ as defined in Section 4 | | $\beta_{RTR}$ bound by 0.4. $\beta_{MDL}$ as defined in Section 4 | |
|---|---|---|---|---|---|---|---|---|
| | | Median $\widehat{Sa}_F(T_1)$ (g) | $\beta_{RTR}$ | $P_F$ (50 years) | $\beta$ | $P_F$ (50 years) | $\beta$ | $P_F$ (50 years) |
| Non-isolated $T_1$=0.09sec | 1g | 1.139 | 0.303 | 0.079 | 0.426 | 0.106 | 0.426 | 0.106 |
| | 2g | 2.277 | 0.303 | 0.005 | 0.426 | 0.011 | 0.426 | 0.011 |
| Horizontally isolated $T_1$=2.4sec | 1g | 0.656 | 0.714 | 0.062 | 0.721 | 0.063 | 0.412 | 0.024 |
| | 2g | 0.767 | 0.672 | 0.038 | 0.679 | 0.039 | 0.412 | 0.015 |
| Horizontally-vertically isolated without rocking $T_1$=2.4sec | 1g | 0.771 | 0.437 | 0.016 | 0.481 | 0.019 | 0.447 | 0.016 |
| | 2g | 0.795 | 0.415 | 0.013 | 0.461 | 0.016 | 0.447 | 0.015 |
| Horizontally-vertically isolated with rocking $T_1$=2.4sec | 1g | 0.875 | 0.381 | 0.008 | 0.430 | 0.010 | 0.430 | 0.010 |
| | 2g | 0.914 | 0.346 | 0.006 | 0.400 | 0.008 | 0.400 | 0.008 |

Table 5-53 Summary of results for probability of failure when considering uncertainties for isolated and non-isolated transformer with $W$=420kip, $f_{AI}$=11.3Hz and inclined bushing. When isolated, $D_{Capacity}$=31.3inch and lower bound friction properties. Location: **Chehalis, WA**. Far-field motions

| System | Transverse Bushing Acceleration Limit (g) | Fragility Parameters with Spectral Shape Effects | | | $\beta_{RTR}$ as computed. $\beta_{MDL}$ as defined in Section 4 | | $\beta_{RTR}$ bound by 0.4. $\beta_{MDL}$ as defined in Section 4 | |
|---|---|---|---|---|---|---|---|---|
| | | Median $\widehat{Sa}_F(T_1)$ (g) | $\beta_{RTR}$ | $P_F$ (50 years) | $\beta$ | $P_F$ (50 years) | $\beta$ | $P_F$ (50 years) |
| Non-isolated $T_1$=0.09sec | 1g | 0.959 | 0.303 | 0.048 | 0.426 | 0.058 | 0.426 | 0.058 |
| | 2g | 1.918 | 0.303 | 0.007 | 0.426 | 0.011 | 0.426 | 0.011 |
| Horizontally isolated $T_1$=2.4sec | 1g | 0.367 | 0.714 | 0.034 | 0.721 | 0.034 | 0.412 | 0.022 |
| | 2g | 0.445 | 0.672 | 0.023 | 0.679 | 0.023 | 0.412 | 0.015 |
| Horizontally-vertically isolated without rocking $T_1$=2.4sec | 1g | 0.561 | 0.437 | 0.010 | 0.481 | 0.011 | 0.447 | 0.010 |
| | 2g | 0.587 | 0.415 | 0.009 | 0.461 | 0.009 | 0.447 | 0.009 |
| Horizontally-vertically isolated with rocking $T_1$=2.4sec | 1g | 0.663 | 0.381 | 0.006 | 0.430 | 0.007 | 0.430 | 0.007 |
| | 2g | 0.707 | 0.346 | 0.005 | 0.400 | 0.006 | 0.400 | 0.006 |

Table 5-54 Summary of results for probability of failure when considering uncertainties for isolated and non-isolated transformer with $W$=420kip, $f_{AI}$=11.3Hz and inclined bushing. When isolated, $D_{Capacity}$=31.3inch and lower bound friction properties. Location: **Aberdeen, WA**. Far-field motions

| System | Transverse Bushing Acceleration Limit (g) | Fragility Parameters with Spectral Shape Effects | | | $\beta_{RTR}$ as computed. $\beta_{MDL}$ as defined in Section 4 | | $\beta_{RTR}$ bound by 0.4. $\beta_{MDL}$ as defined in Section 4 | |
|---|---|---|---|---|---|---|---|---|
| | | Median $\widehat{Sa}_F(T_1)$ (g) | $\beta_{RTR}$ | $P_F$ (50 years) | $\beta$ | $P_F$ (50 years) | $\beta$ | $P_F$ (50 years) |
| Non-isolated $T_1$=0.09sec | 1g | 1.025 | 0.303 | 0.060 | 0.426 | 0.068 | 0.426 | 0.068 |
| | 2g | 2.049 | 0.303 | 0.014 | 0.426 | 0.017 | 0.426 | 0.017 |
| Horizontally isolated $T_1$=2.4sec | 1g | 0.487 | 0.714 | 0.034 | 0.721 | 0.034 | 0.412 | 0.027 |
| | 2g | 0.580 | 0.672 | 0.026 | 0.679 | 0.027 | 0.412 | 0.022 |
| Horizontally-vertically isolated without rocking $T_1$=2.4sec | 1g | 0.655 | 0.437 | 0.018 | 0.481 | 0.019 | 0.447 | 0.018 |
| | 2g | 0.681 | 0.415 | 0.017 | 0.461 | 0.018 | 0.447 | 0.017 |
| Horizontally-vertically isolated with rocking $T_1$=2.4sec | 1g | 0.759 | 0.381 | 0.014 | 0.430 | 0.014 | 0.430 | 0.014 |
| | 2g | 0.801 | 0.346 | 0.013 | 0.400 | 0.013 | 0.400 | 0.013 |

Table 5-55 Summary of results for probability of failure when considering uncertainties for isolated and non-isolated transformer with $W$=420kip, $f_{AI}$=11.3Hz and inclined bushing. When isolated, $D_{Capacity}$=31.3inch and lower bound friction properties. Location: **Loma Linda, CA**. Far-field motions

| System | Transverse Bushing Acceleration Limit (g) | Fragility Parameters with Spectral Shape Effects | | | $\beta_{RTR}$ as computed. $\beta_{MDL}$ as defined in Section 4 | | $\beta_{RTR}$ bound by 0.4. $\beta_{MDL}$ as defined in Section 4 | |
|---|---|---|---|---|---|---|---|---|
| | | Median $\widehat{Sa}_F(T_1)$ (g) | $\beta_{RTR}$ | $P_F$ (50 years) | $\beta$ | $P_F$ (50 years) | $\beta$ | $P_F$ (50 years) |
| Non-isolated $T_1$=0.09sec | 1g | 1.135 | 0.303 | 0.114 | 0.426 | 0.140 | 0.426 | 0.140 |
| | 2g | 2.271 | 0.303 | 0.013 | 0.426 | 0.021 | 0.426 | 0.021 |
| Horizontally isolated $T_1$=2.4sec | 1g | 1.183 | 0.714 | 0.051 | 0.721 | 0.052 | 0.412 | 0.028 |
| | 2g | 1.333 | 0.672 | 0.037 | 0.679 | 0.038 | 0.412 | 0.021 |
| Horizontally-vertically isolated without rocking $T_1$=2.4sec | 1g | 1.065 | 0.437 | 0.037 | 0.481 | 0.040 | 0.447 | 0.038 |
| | 2g | 1.083 | 0.415 | 0.034 | 0.461 | 0.037 | 0.447 | 0.036 |
| Horizontally-vertically isolated with rocking $T_1$=2.4sec | 1g | 1.160 | 0.381 | 0.027 | 0.430 | 0.030 | 0.430 | 0.030 |
| | 2g | 1.186 | 0.346 | 0.024 | 0.400 | 0.027 | 0.400 | 0.027 |

Table 5-56 Summary of results for probability of failure when considering uncertainties for isolated and non-isolated transformer with $W$=420kip, $f_{AI}$=11.3Hz and inclined bushing. When isolated, $D_{Capacity}$=31.3inch and lower bound friction properties. Location: **Hillsboro, OR**. Far-field motions

| System | Transverse Bushing Acceleration Limit (g) | Fragility Parameters with Spectral Shape Effects | | | $\beta_{RTR}$ as computed. $\beta_{MDL}$ as defined in Section 4 | | $\beta_{RTR}$ bound by 0.4. $\beta_{MDL}$ as defined in Section 4 | |
|---|---|---|---|---|---|---|---|---|
| | | Median $\widehat{Sa}_F(T_1)$ (g) | $\beta_{RTR}$ | $P_F$ (50 years) | $\beta$ | $P_F$ (50 years) | $\beta$ | $P_F$ (50 years) |
| Non-isolated $T_1$=0.09sec | 1g | 0.967 | 0.303 | 0.028 | 0.426 | 0.034 | 0.426 | 0.034 |
| | 2g | 1.934 | 0.303 | 0.005 | 0.426 | 0.006 | 0.426 | 0.006 |
| Horizontally isolated $T_1$=2.4sec | 1g | 0.365 | 0.714 | 0.030 | 0.721 | 0.030 | 0.412 | 0.020 |
| | 2g | 0.443 | 0.672 | 0.020 | 0.679 | 0.021 | 0.412 | 0.014 |
| Horizontally-vertically isolated without rocking $T_1$=2.4sec | 1g | 0.560 | 0.437 | 0.009 | 0.481 | 0.010 | 0.447 | 0.009 |
| | 2g | 0.586 | 0.415 | 0.008 | 0.461 | 0.008 | 0.447 | 0.008 |
| Horizontally-vertically isolated with rocking $T_1$=2.4sec | 1g | 0.662 | 0.381 | 0.006 | 0.430 | 0.006 | 0.430 | 0.006 |
| | 2g | 0.706 | 0.346 | 0.004 | 0.400 | 0.005 | 0.400 | 0.005 |

Table 5-57 Summary of results for probability of failure when considering uncertainties for isolated and non-isolated transformer with $W$=420kip, $f_{AI}$=11.3Hz and inclined bushing. When isolated, $D_{Capacity}$=31.3inch and lower bound friction properties. Location: **Eugene, OR**. Far-field motions

| System | Transverse Bushing Acceleration Limit (g) | Fragility Parameters with Spectral Shape Effects | | | $\beta_{RTR}$ as computed. $\beta_{MDL}$ as defined in Section 4 | | $\beta_{RTR}$ bound by 0.4. $\beta_{MDL}$ as defined in Section 4 | |
|---|---|---|---|---|---|---|---|---|
| | | Median $\widehat{Sa}_F(T_1)$ (g) | $\beta_{RTR}$ | $P_F$ (50 years) | $\beta$ | $P_F$ (50 years) | $\beta$ | $P_F$ (50 years) |
| Non-isolated $T_1$=0.09sec | 1g | 0.949 | 0.303 | 0.023 | 0.426 | 0.026 | 0.426 | 0.026 |
| | 2g | 1.898 | 0.303 | 0.005 | 0.426 | 0.006 | 0.426 | 0.006 |
| Horizontally isolated $T_1$=2.4sec | 1g | 0.358 | 0.714 | 0.029 | 0.721 | 0.029 | 0.412 | 0.022 |
| | 2g | 0.434 | 0.672 | 0.021 | 0.679 | 0.021 | 0.412 | 0.016 |
| Horizontally-vertically isolated without rocking $T_1$=2.4sec | 1g | 0.553 | 0.437 | 0.011 | 0.481 | 0.011 | 0.447 | 0.011 |
| | 2g | 0.579 | 0.415 | 0.010 | 0.461 | 0.010 | 0.447 | 0.010 |
| Horizontally-vertically isolated with rocking $T_1$=2.4sec | 1g | 0.655 | 0.381 | 0.007 | 0.430 | 0.008 | 0.430 | 0.008 |
| | 2g | 0.699 | 0.346 | 0.006 | 0.400 | 0.006 | 0.400 | 0.006 |

Table 5-58 Summary of results for probability of failure when considering uncertainties for isolated and non-isolated transformer with $W$=420kip, $f_{AI}$=11.3Hz and inclined bushing. When isolated, $D_{Capacity}$=31.3inch and lower bound friction properties. Location: **Wilsonville, OR**. Far-field motions

| System | Transverse Bushing Acceleration Limit (g) | Fragility Parameters with Spectral Shape Effects | | | $\beta_{RTR}$ as computed. $\beta_{MDL}$ as defined in Section 4 | | $\beta_{RTR}$ bound by 0.4. $\beta_{MDL}$ as defined in Section 4 | |
|---|---|---|---|---|---|---|---|---|
| | | Median $\widehat{Sa}_F(T_1)$ (g) | $\beta_{RTR}$ | $P_F$ (50 years) | $\beta$ | $P_F$ (50 years) | $\beta$ | $P_F$ (50 years) |
| Non-isolated $T_1$=0.09sec | 1g | 0.953 | 0.303 | 0.025 | 0.426 | 0.030 | 0.426 | 0.030 |
| | 2g | 1.906 | 0.303 | 0.004 | 0.426 | 0.005 | 0.426 | 0.005 |
| Horizontally isolated $T_1$=2.4sec | 1g | 0.369 | 0.714 | 0.026 | 0.721 | 0.026 | 0.412 | 0.017 |
| | 2g | 0.447 | 0.672 | 0.017 | 0.679 | 0.018 | 0.412 | 0.011 |
| Horizontally-vertically isolated without rocking $T_1$=2.4sec | 1g | 0.562 | 0.437 | 0.007 | 0.481 | 0.008 | 0.447 | 0.007 |
| | 2g | 0.588 | 0.415 | 0.006 | 0.461 | 0.007 | 0.447 | 0.006 |
| Horizontally-vertically isolated with rocking $T_1$=2.4sec | 1g | 0.665 | 0.381 | 0.004 | 0.430 | 0.005 | 0.430 | 0.005 |
| | 2g | 0.708 | 0.346 | 0.003 | 0.400 | 0.004 | 0.400 | 0.004 |

Table 5-59 Summary of results for probability of failure when considering uncertainties for isolated and non-isolated transformer with $W$=420kip, $f_{AI}$=11.3Hz and inclined bushing. When isolated, $D_{Capacity}$=31.3inch and lower bound friction properties. Location: **Curry County, OR**. Far-field motions

| System | Transverse Bushing Acceleration Limit (g) | Fragility Parameters with Spectral Shape Effects | | | $\beta_{RTR}$ as computed. $\beta_{MDL}$ as defined in Section 4 | | $\beta_{RTR}$ bound by 0.4. $\beta_{MDL}$ as defined in Section 4 | |
|---|---|---|---|---|---|---|---|---|
| | | Median $\widehat{Sa}_F(T_1)$ (g) | $\beta_{RTR}$ | $P_F$ (50 years) | $\beta$ | $P_F$ (50 years) | $\beta$ | $P_F$ (50 years) |
| Non-isolated $T_1$=0.09sec | 1g | 1.123 | 0.303 | 0.048 | 0.426 | 0.053 | 0.426 | 0.053 |
| | 2g | 2.247 | 0.303 | 0.012 | 0.426 | 0.015 | 0.426 | 0.015 |
| Horizontally isolated $T_1$=2.4sec | 1g | 0.857 | 0.714 | 0.028 | 0.721 | 0.028 | 0.412 | 0.021 |
| | 2g | 0.986 | 0.672 | 0.022 | 0.679 | 0.022 | 0.412 | 0.016 |
| Horizontally-vertically isolated without rocking $T_1$=2.4sec | 1g | 0.893 | 0.437 | 0.020 | 0.481 | 0.021 | 0.447 | 0.020 |
| | 2g | 0.915 | 0.415 | 0.018 | 0.461 | 0.019 | 0.447 | 0.019 |
| Horizontally-vertically isolated with rocking $T_1$=2.4sec | 1g | 0.995 | 0.381 | 0.015 | 0.430 | 0.016 | 0.430 | 0.016 |
| | 2g | 1.029 | 0.346 | 0.014 | 0.400 | 0.015 | 0.400 | 0.015 |

Table 5-60 Summary of results for probability of failure when considering uncertainties for isolated and non-isolated transformer with $W$=420kip, $f_{AI}$=11.3Hz and inclined bushing. When isolated, $D_{Capacity}$=31.3inch and lower bound friction properties. Location: **Troutdale, OR**. Far-field motions

| System | Transverse Bushing Acceleration Limit (g) | Fragility Parameters with Spectral Shape Effects | | | $\beta_{RTR}$ as computed. $\beta_{MDL}$ as defined in Section 4 | | $\beta_{RTR}$ bound by 0.4. $\beta_{MDL}$ as defined in Section 4 | |
|---|---|---|---|---|---|---|---|---|
| | | Median $\widehat{Sa}_F(T_1)$ (g) | $\beta_{RTR}$ | $P_F$ (50 years) | $\beta$ | $P_F$ (50 years) | $\beta$ | $P_F$ (50 years) |
| Non-isolated $T_1$=0.09sec | 1g | 0.948 | 0.303 | 0.021 | 0.426 | 0.027 | 0.426 | 0.027 |
| | 2g | 1.895 | 0.303 | 0.003 | 0.426 | 0.004 | 0.426 | 0.004 |
| Horizontally isolated $T_1$=2.4sec | 1g | 0.356 | 0.714 | 0.025 | 0.721 | 0.025 | 0.412 | 0.015 |
| | 2g | 0.432 | 0.672 | 0.016 | 0.679 | 0.017 | 0.412 | 0.010 |
| Horizontally-vertically isolated without rocking $T_1$=2.4sec | 1g | 0.551 | 0.437 | 0.006 | 0.481 | 0.007 | 0.447 | 0.006 |
| | 2g | 0.577 | 0.415 | 0.005 | 0.461 | 0.006 | 0.447 | 0.005 |
| Horizontally-vertically isolated with rocking $T_1$=2.4sec | 1g | 0.653 | 0.381 | 0.003 | 0.430 | 0.004 | 0.430 | 0.004 |
| | 2g | 0.697 | 0.346 | 0.003 | 0.400 | 0.003 | 0.400 | 0.003 |

The results presented in Tables 5-1 to 5-60 show that there is no or there is insignificant benefit in isolating the considered transformers in any of the ten sites when the transverse acceleration bushing limit is 2g. There are benefits in isolating the considered transformers when the transverse acceleration bushing limit is 1g. Table 5-61 presents a summary of results for the probability of failure in 50 years at the 10 considered sites in the case of the 1g transverse acceleration bushing limit and for horizontal isolation only. The results are for the case $\beta_{RTR}$≤0.4 (last column in each of Tables 5-1 to 5-60). Note that when the transformers are horizontally-vertically isolated, the calculated probabilities of failure are lower than those of the horizontally isolated transformers. The results in Table 5-61 clearly show the benefits of seismic isolation in the reduction of the probabilities of failure. Figure 5-1 presents the results of Table 5-61 in graphical form where the benefits can be better viewed.

The results in Figure 5-1 show that the probability of failure generally improves when the largest displacement capacity isolator is used. The improvement is partially due to the increased displacement capacity (particularly for the locations of the highest seismic hazard-Loma Linda and Saranac, CA) but primarily is due to the difference in the radius of curvature of the largest displacement capacity isolator. Due to the larger radius of curvature (see Figures 1-1 and 1-2) the stiffness is smaller, which results in a reduction in peak acceleration.

Table 5-61 Probabilities of failure in 50 years for non-isolated and horizontally isolated transformers with transverse bushing acceleration limit of 1g (case of $\beta_{RTR} \leq 0.4$)

| Site | Non-isolated | | | Horizontally isolated $D_{Capacity}$=17.7in | | | Horizontally isolated $D_{Capacity}$=31.3in | | |
|---|---|---|---|---|---|---|---|---|---|
| Bushing Frequency (Hz) | 4.3 | 7.7 | 11.3 | 4.3 | 7.7 | 11.3 | 4.3 | 7.7 | 11.3 |
| Vancouver, WA: **1** | 0.053 | 0.080 | 0.030 | 0.015 | 0.026 | 0.024 | 0.013 | 0.023 | 0.018 |
| Saranap, CA: **2** | 0.192 | 0.307 | 0.106 | 0.020 | 0.033 | 0.022 | 0.008 | 0.019 | 0.024 |
| Loma Linda, CA: **3** | 0.236 | 0.346 | 0.140 | 0.056 | 0.075 | 0.055 | 0.048 | 0.051 | 0.028 |
| Aberdeen, WA: **4** | 0.100 | 0.141 | 0.068 | 0.031 | 0.040 | 0.035 | 0.023 | 0.034 | 0.027 |
| Chehalis, WA: **5** | 0.081 | 0.129 | 0.058 | 0.024 | 0.034 | 0.029 | 0.017 | 0.029 | 0.022 |
| Hillsboro, OR: **6** | 0.059 | 0.085 | 0.034 | 0.022 | 0.031 | 0.026 | 0.015 | 0.026 | 0.020 |
| Eugene, OR: **7** | 0.046 | 0.056 | 0.026 | 0.023 | 0.032 | 0.028 | 0.017 | 0.027 | 0.022 |
| Wilsonville, OR: **8** | 0.053 | 0.079 | 0.030 | 0.018 | 0.027 | 0.022 | 0.012 | 0.022 | 0.017 |
| Curry County, OR: **9** | 0.092 | 0.108 | 0.053 | 0.030 | 0.039 | 0.032 | 0.019 | 0.030 | 0.021 |
| Trousdale, OR: **10** | 0.046 | 0.071 | 0.027 | 0.016 | 0.025 | 0.021 | 0.011 | 0.020 | 0.015 |

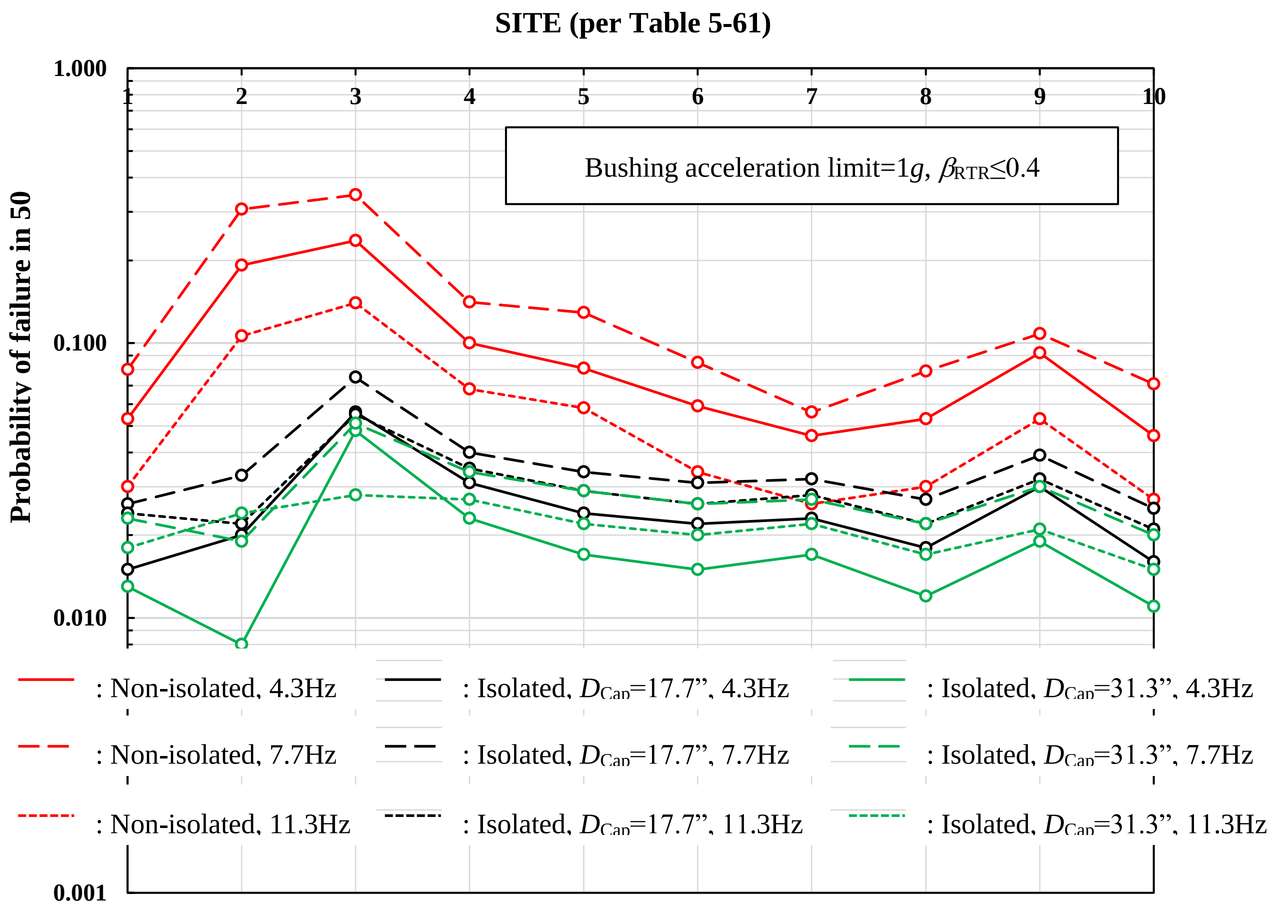


Figure 5-1 Probabilities of failure in 50 years for non-isolated and horizontally isolated transformers with transverse bushing acceleration limit of 1g (case of $\beta_{RTR} \leq 0.4$) for ten sites

# SECTION 6
# RESULTS FOR NEAR-FIELD MOTIONS

Two of the ten considered sites, the Loma Linda and the Saranap, CA sites, qualify for classification as being in the proximity of active faults, with the closest fault being within 1km to 4km. For these locations, the fragility analysis results presented in Sections 2 to 5 need to be re-assessed by conducting the incremental dynamic analysis using motions with near-field characteristics. FEMA (2009) provided a set of such motions consisting of 28 records of bi-directional components (56 individual horizontal components) for use in these cases. Table 6-1 presents a subset of 25 of these records for which the vertical ground motion component was available. In total 50 pairs of horizontal-vertical were available for use in the incremental dynamic analysis.

Figures 6-1 and 6-2 present the 5%-damped acceleration response spectra for the horizontal and vertical ground motions, respectively. The horizontal spectra consist of the 50 spectra of fault normal and fault parallel components, and the vertical spectra consist of the 25 spectra of the vertical components. The average spectra are also shown for each direction. Figure 6-3 presents the ratio of the average vertical spectrum to the average horizontal spectrum of the motions (V/H ratio).

Table 6-1 Near-field ground motions used in dynamic analysis

| Earthquake | | | Recording Station | Site Data | | Values shown are in two horizontal directions, then vertical; units g, in/sec, inch | | |
|---|---|---|---|---|---|---|---|---|
| M | Year | Name | Name | NEHRP Class | Vs_30 (m/sec) | PGA | PGV | PGD |
| Pulse Records Subset | | | | | | | | |
| 6.5 | 1979 | Imperial Valley-06 | El Centro Array #6 | D | 203 | 0.44, 0.40, 1.89 | 44.0, 25.5, 25.0 | 26.2, 9.8, 9.3 |
| 6.5 | 1979 | Imperial Valley-06 | El Centro Array #7 | D | 211 | 0.46, 0.34, 0.58 | 42.8, 17.5, 10.7 | 17.9, 9.4, 3.9 |
| 6.9 | 1980 | Irpinia, Italy-01 | Sturno | B | 1000 | 0.23, 0.31, 0.23 | 16.3, 17.9, 9.5 | 8.7, 9.2, 4.1 |
| 6.9 | 1989 | Loma Prieta | Saratoga - Aloha | C | 371 | 0.36, 0.38, 0.40 | 21.9, 17.0, 11.0 | 11.6, 6.2, 6.8 |
| 6.7 | 1992 | Erzican, Turkey | Erzincan | D | 275 | 0.49, 0.42, 0.23 | 37.4, 17.8, 6.5 | 12.6, 6.5, 4.1 |
| 7 | 1992 | Cape Mendocino | Petrolia | C | 713 | 0.61, 0.63, 0.17 | 32.2, 23.8, 8.0 | 10.0, 10.2, 7.9 |
| 7.3 | 1992 | Landers | Lucerne | C | 685 | 0.71, 0.79, 0.82 | 55.1, 20.8, 16.2 | 95.7, 47.1, 11.7 |
| 6.7 | 1994 | Northridge-01 | Rinaldi Receiving Sta | D | 282 | 0.87, 0.42, 0.96 | 65.7, 24.6, 16.6 | 11.3, 8.4, 1.5 |
| 6.7 | 1994 | Northridge-01 | Sylmar - Olive View | C | 441 | 0.73, 0.60, 0.54 | 48.3, 21.4, 7.3 | 12.5, 4.2, 3.1 |
| 7.5 | 1999 | Kocaeli, Turkey | Izmit | B | 811 | 0.15, 0.22, 0.14 | 8.9, 11.7, 4.9 | 3.9, 6.7, 4.5 |
| 7.6 | 1999 | Chi-Chi, Taiwan | TCU065 | D | 306 | 0.82, 0.59, 0.26 | 50.2, 31.6, 27.3 | 36.7, 23.0, 22.6 |
| 7.6 | 1999 | Chi-Chi, Taiwan | TCU102 | C | 714 | 0.29, 0.17, 0.18 | 41.9, 30.5, 26.9 | 34.6, 21.6, 20.3 |
| 7.1 | 1999 | Duzce, Turkey | Duzce | D | 276 | 0.36, 0.52, 0.35 | 24.5, 31.2, 7.9 | 18.3, 18.9, 8.2 |
| No Pulse Records Subset | | | | | | | | |
| 6.8 | 6.8 | Gazli, USSR | Karakyr | C | 660 | 0.60, 0.71, 1.70 | 25.6, 28.0, 22.2 | 9.5, 9.7, 3.5 |
| 6.5 | 1979 | Imperial Valley-06 | Bonds Corner | D | 223 | 0.76, 0.59, 0.53 | 17.4, 17.2, 4.8 | 6.1, 6.5, 1.3 |
| 6.5 | 1979 | Imperial Valley-06 | Chihuahua | D | 275 | 0.28, 0.27, 0.22 | 12.0, 10.6, 2.0 | 4.2, 3.1, 1.0 |
| 6.8 | 1985 | Nahanni, Canada | Site 1 | C | 660 | 0.85, 1.18, 2.28 | 17.2, 14.4, 16.1 | 6.3, 1.7, 4.0 |
| 6.9 | 1989 | Loma Prieta | BRAN | C | 376 | 0.64, 0.41, 0.51 | 22.0, 15.2, 7.1 | 5.2, 3.6, 1.7 |
| 6.9 | 1989 | Loma Prieta | Corralitos | C | 462 | 0.48, 0.51, 0.46 | 17.9, 16.4, 7.7 | 5.5, 2.8, 5.1 |
| 7 | 1992 | Cape Mendocino | Cape Mendocino | C | 514 | 1.27, 1.43, 0.74 | 22.7, 46.6, 22.9 | 5.4, 15.0, 22.8 |
| 6.7 | 1994 | Northridge-01 | LA - Sepulveda VA | C | 380 | 0.73, 0.71, 0.32 | 24.9, 27.5, 9.8 | 7.4, 5.7, 4.4 |
| 7.5 | 1999 | Kocaeli, Turkey | Yarimca | D | 297 | 0.28, 0.31, 0.24 | 19.0, 28.7, 12.1 | 17.0, 22.1, 11.6 |
| 7.6 | 1999 | Chi-Chi, Taiwan | TCU067 | C | 434 | 0.56, 0.31, 0.24 | 36.1, 18.7, 19.6 | 38.7, 14.4, 13.7 |
| 7.6 | 1999 | Chi-Chi, Taiwan | TCU084 | C | 553 | 1.16, 0.42, 0.32 | 45.3, 17.2, 10.1 | 12.5, 8.2, 5.2 |
| 7.9 | 2002 | Denali, Alaska | TAPS Pump Sta. #10 | C | 553 | 0.33, 0.28, 0.24 | 34.5, 49.7, 20.1 | 35.2, 47.1, 7.8 |

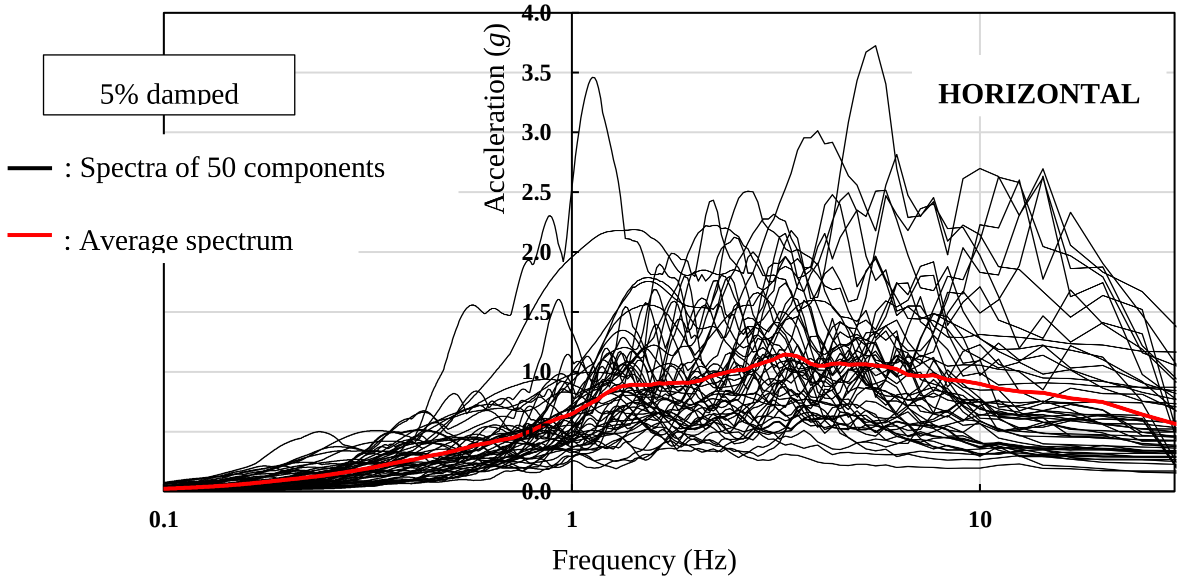


Figure 6-1 Horizontal acceleration response spectra of selected 25 near-field ground motions (total of 50 components)

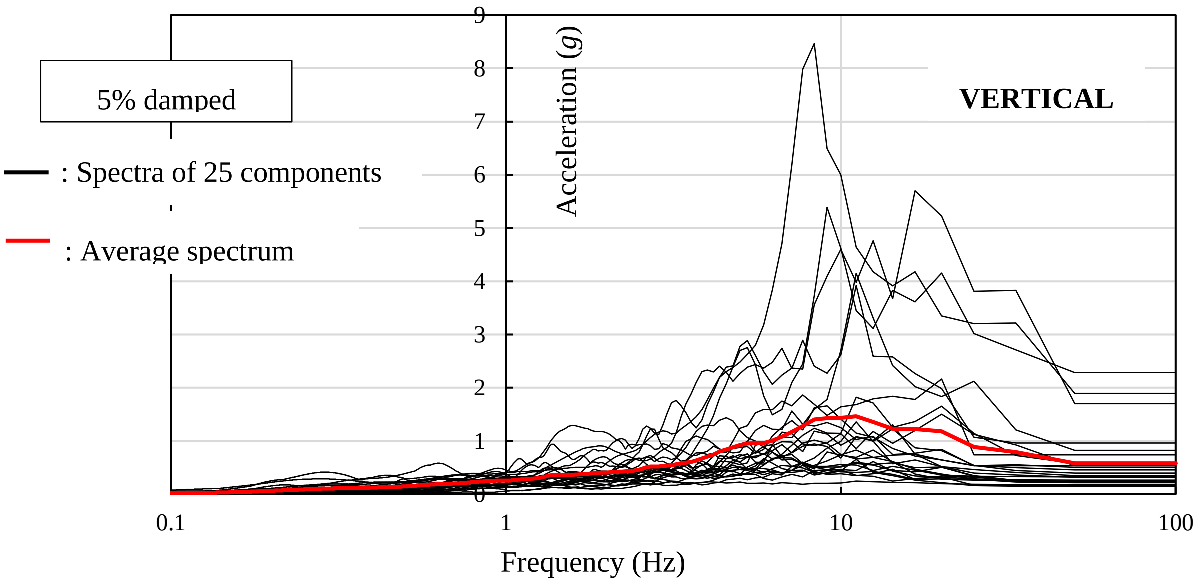


Figure 6-2 Vertical acceleration response spectra of selected 25 near-field ground motions (total of 25 components)

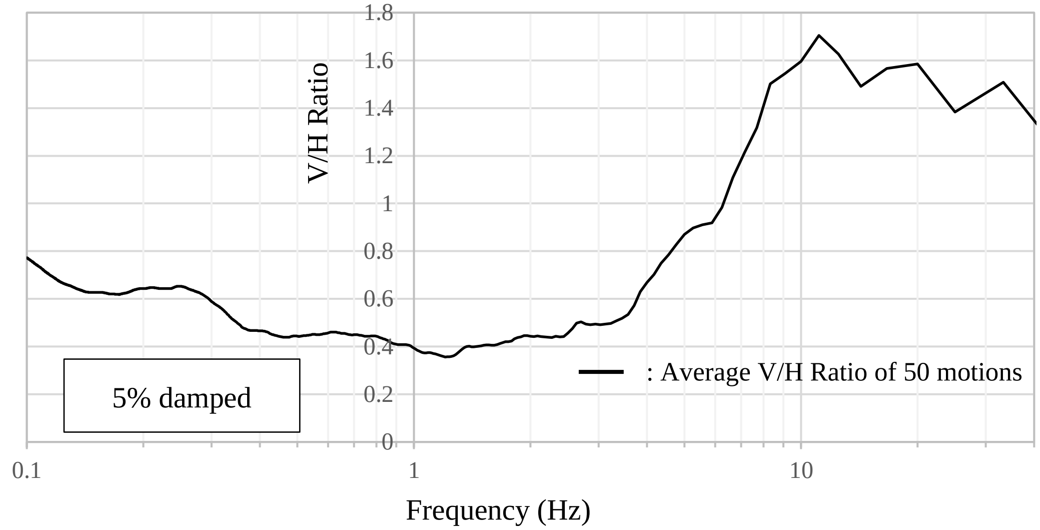


Figure 6-3 Vertical to horizontal average spectral (V/H) ratio of 50 sets of near-field motions

Incremental dynamic analysis was performed using the near-field motions for the three cases of bushing as-installed frequencies (4.3, 7.7 and 11.3Hz) of the 420kip transformer without and with isolators of displacement capacity $D_{Capacity}$=31.3inch. When vertically isolated, the vertical isolation frequency and damping were 2Hz and 0.50, respectively. The isolator friction properties had the lower bound values. The scaling of the motions was based on the use of the spectral acceleration at the fundamental period as the measure of seismic intensity (period equal to 2.4sec for the isolated transformers and equal to the inverse of the as-installed bushing frequency for the non-isolated transformers). The fragility parameters were determined but not adjusted for spectral shape effects based on the procedures of Appendix A. Based on Haselton et al. (2011), the approach of Appendix A is inapplicable to near-field motions with large forward-directivity pulses. Many of the records (see Table 6-1) do contain such pulses. The only way to correctly account for the spectral shape effects is to follow the approach of Lin et al. (2013), which was applied in the study of Kitayama and Constantinou (2019a). However, the approach requires a seismic hazard analysis for each site, construction of conditional spectra for increasing earthquake intensities, and selection and scaling of motions to represent each of these spectra. In the study of Kitayama and Constantinou (2019a), 400 motions were used in the analysis for earthquake intensities representing spectra with 43 years to 10000 return periods. Such study is beyond the scope of this work.

Probabilities of failure in 50 years were calculated based on Equations (2-6) and (2-7) using the same seismic hazard curves used earlier for the results of Section 3. Tables 6-2 to 6-7 present the results where they are compared to those obtained using the far-field motions in Section 3. To be able to better assess the significance of the near-field results, results for the far-field motions without and with the spectral shape effects correction are included in Tables 6-2 to 6-7. As seen in these tables and in the results of Section 3, the correction for spectral shape effects for the far-field motions may result in significant reduction of the probability of failure for isolated transformers at the Saranac and Lima Linda, CA locations, whereas there was increase in the probability of failure for the non-isolated transformers at the same locations.

Table 6-2 Summary of results for probability of failure for isolated and non-isolated transformer with $W$=420kip, $f_{AI}$=4.3Hz and inclined bushing. When isolated, $D_{Capacity}$=31.3inch and lower bound friction properties. Location: **Saranap, CA.** Near-field motions

| System | Transverse Bushing Acceleration Limit (g) | Without Spectral Shape Effects | | | Value reported in Section 3 for Far-field Motions (without spectral shape effects) | Value reported in Section 3 for Far-field Motions (with spectral shape effects) |
|---|---|---|---|---|---|---|
| | | Median $\widehat{Sa}_F(T_1)$ (g) | $\beta_{RTR}$ | $P_F$ (50 years) | $P_F$ (50 years) | $P_F$ (50 years) |
| Non-isolated $T_1$=0.24sec | 1g | 1.029 | 0.157 | 0.181 | 0.182 | 0.153 |
| | 2g | 2.030 | 0.214 | 0.019 | 0.016 | 0.012 |
| Horizontally isolated $T_1$=2.4sec | 1g | 0.497 | 0.696 | 0.103 | 0.109 | 0.024 |
| | 2g | 0.563 | 0.692 | 0.080 | 0.057 | 0.014 |
| Horizontally-vertically isolated without rocking $T_1$=2.4sec | 1g | 0.684 | 0.416 | 0.021 | 0.023 | 0.008 |
| | 2g | 0.710 | 0.308 | 0.012 | 0.014 | 0.004 |
| Horizontally-vertically isolated with rocking $T_1$=2.4sec | 1g | 0.644 | 0.598 | 0.046 | 0.135 | 0.029 |
| | 2g | 0.753 | 0.317 | 0.011 | 0.015 | 0.004 |

Table 6-3 Summary of results for probability of failure for isolated and non-isolated transformer with $W$=420kip, $f_{AI}$=4.3Hz and inclined bushing. When isolated, $D_{Capacity}$=31.3inch and lower bound friction properties. Location: **Loma Linda, CA.** Near-field motions

| System | Transverse Bushing Acceleration Limit (g) | Without Spectral Shape Effects | | | Value reported in Section 3 for Far-field Motions (without spectral shape effects) | Value reported in Section 3 for Far-field Motions (with spectral shape effects) |
|---|---|---|---|---|---|---|
| | | Median $\widehat{Sa}_F(T_1)$ (g) | $\beta_{RTR}$ | $P_F$ (50 years) | $P_F$ (50 years) | $P_F$ (50 years) |
| Non-isolated $T_1$=0.24sec | 1g | 1.029 | 0.157 | 0.234 | 0.234 | 0.203 |
| | 2g | 2.030 | 0.214 | 0.042 | 0.038 | 0.029 |
| Horizontally isolated $T_1$=2.4sec | 1g | 0.497 | 0.696 | 0.193 | 0.201 | 0.074 |
| | 2g | 0.563 | 0.692 | 0.163 | 0.138 | 0.055 |
| Horizontally-vertically isolated without rocking $T_1$=2.4sec | 1g | 0.684 | 0.416 | 0.088 | 0.090 | 0.048 |
| | 2g | 0.710 | 0.308 | 0.073 | 0.074 | 0.039 |
| Horizontally-vertically isolated with rocking $T_1$=2.4sec | 1g | 0.644 | 0.598 | 0.120 | 0.226 | 0.078 |
| | 2g | 0.753 | 0.317 | 0.066 | 0.074 | 0.036 |

Table 6-4 Summary of results for probability of failure for isolated and non-isolated transformer with $W$=420kip, $f_{AI}$=7.7Hz and inclined bushing. When isolated, $D_{Capacity}$=31.3inch and lower bound friction properties. Location: **Saranap, CA.** Near-field motions

| System | Transverse Bushing Acceleration Limit (g) | Without Spectral Shape Effects | | | Value reported in Section 3 for Far-field Motions (without spectral shape effects) | Value reported in Section 3 for Far-field Motions (with spectral shape effects) |
|---|---|---|---|---|---|---|
| | | Median $\widehat{Sa}_F(T_1)$ (g) | $\beta_{RTR}$ | $P_F$ (50 years) | $P_F$ (50 years) | $P_F$ (50 years) |
| Non-isolated $T_1$=0.13sec | 1g | 0.681 | 0.305 | 0.353 | 0.300 | 0.266 |
| | 2g | 1.365 | 0.303 | 0.065 | 0.047 | 0.038 |
| Horizontally isolated $T_1$=2.4sec | 1g | 0.324 | 0.822 | 0.255 | 0.210 | 0.058 |
| | 2g | 0.511 | 0.707 | 0.100 | 0.080 | 0.019 |
| Horizontally-vertically isolated without rocking $T_1$=2.4sec | 1g | 0.483 | 0.357 | 0.050 | 0.064 | 0.024 |
| | 2g | 0.492 | 0.296 | 0.041 | 0.046 | 0.017 |
| Horizontally-vertically isolated with rocking $T_1$=2.4sec | 1g | 0.488 | 0.465 | 0.063 | 0.064 | 0.021 |
| | 2g | 0.503 | 0.282 | 0.037 | 0.035 | 0.013 |

Table 6-5 Summary of results for probability of failure for isolated and non-isolated transformer with $W$=420kip, $f_{AI}$=7.7Hz and inclined bushing. When isolated, $D_{Capacity}$=31.3inch and lower bound friction properties. Location: **Loma Linda, CA.** Near-field motions

| System | Transverse Bushing Acceleration Limit (g) | Without Spectral Shape Effects | | | Value reported in Section 3 for Far-field Motions (without spectral shape effects) | Value reported in Section 3 for Far-field Motions (with spectral shape effects) |
|---|---|---|---|---|---|---|
| | | Median $\widehat{Sa}_F(T_1)$ (g) | $\beta_{RTR}$ | $P_F$ (50 years) | $P_F$ (50 years) | $P_F$ (50 years) |
| Non-isolated $T_1$=0.13sec | 1g | 0.681 | 0.305 | 0.393 | 0.108 | 0.297 |
| | 2g | 1.365 | 0.303 | 0.096 | 0.075 | 0.059 |
| Horizontally isolated $T_1$=2.4sec | 1g | 0.324 | 0.822 | 0.348 | 0.307 | 0.087 |
| | 2g | 0.511 | 0.707 | 0.188 | 0.170 | 0.044 |
| Horizontally-vertically isolated without rocking $T_1$=2.4sec | 1g | 0.483 | 0.357 | 0.150 | 0.167 | 0.073 |
| | 2g | 0.492 | 0.296 | 0.140 | 0.146 | 0.066 |
| Horizontally-vertically isolated with rocking $T_1$=2.4sec | 1g | 0.488 | 0.465 | 0.160 | 0.168 | 0.068 |
| | 2g | 0.503 | 0.282 | 0.134 | 0.127 | 0.060 |

Table 6-6 Summary of results for probability of failure for isolated and non-isolated transformer with $W$=420kip, $f_{AI}$=11.3Hz and inclined bushing. When isolated, $D_{Capacity}$=31.3inch and lower bound friction properties. Location: **Saranap, CA.** Near-field motions

| System | Transverse Bushing Acceleration Limit (g) | Without Spectral Shape Effects | | | Value reported in Section 3 for Far-field Motions (without spectral shape effects) | Value reported in Section 3 for Far-field Motions (with spectral shape effects) |
|---|---|---|---|---|---|---|
| | | Median $\widehat{Sa}_F(T_1)$ (g) | $\beta_{RTR}$ | $P_F$ (50 years) | $P_F$ (50 years) | $P_F$ (50 years) |
| Non-isolated $T_1$=0.09sec | 1g | 0.956 | 0.332 | 0.136 | 0.105 | 0.079 |
| | 2g | 1.910 | 0.337 | 0.014 | 0.008 | 0.005 |
| Horizontally isolated $T_1$=2.4sec | 1g | 0.385 | 0.852 | 0.210 | 0.135 | 0.062 |
| | 2g | 0.515 | 0.713 | 0.100 | 0.071 | 0.038 |
| Horizontally-vertically isolated without rocking $T_1$=2.4sec | 1g | 0.669 | 0.429 | 0.024 | 0.028 | 0.016 |
| | 2g | 0.693 | 0.374 | 0.018 | 0.024 | 0.013 |
| Horizontally-vertically isolated with rocking $T_1$=2.4sec | 1g | 0.734 | 0.406 | 0.016 | 0.015 | 0.008 |
| | 2g | 0.769 | 0.315 | 0.010 | 0.011 | 0.006 |

Table 6-7 Summary of results for probability of failure for isolated and non-isolated transformer with $W$=420kip, $f_{AI}$=11.3Hz and inclined bushing. When isolated, $D_{Capacity}$=31.3inch and lower bound friction properties. Location: **Loma Linda, CA.** Near-field motions

| System | Transverse Bushing Acceleration Limit (g) | Without Spectral Shape Effects | | | Value reported in Section 3 for Far-field Motions (without spectral shape effects) | Value reported in Section 3 for Far-field Motions (with spectral shape effects) |
|---|---|---|---|---|---|---|
| | | Median $\widehat{Sa}_F(T_1)$ (g) | $\beta_{RTR}$ | $P_F$ (50 years) | $P_F$ (50 years) | $P_F$ (50 years) |
| Non-isolated $T_1$=0.09sec | 1g | 0.956 | 0.332 | 0.176 | 0.143 | 0.114 |
| | 2g | 1.910 | 0.337 | 0.027 | 0.019 | 0.013 |
| Horizontally isolated $T_1$=2.4sec | 1g | 0.385 | 0.852 | 0.300 | 0.229 | 0.051 |
| | 2g | 0.515 | 0.713 | 0.187 | 0.152 | 0.037 |
| Horizontally-vertically isolated without rocking $T_1$=2.4sec | 1g | 0.669 | 0.429 | 0.093 | 0.102 | 0.037 |
| | 2g | 0.693 | 0.374 | 0.082 | 0.094 | 0.034 |
| Horizontally-vertically isolated with rocking $T_1$=2.4sec | 1g | 0.734 | 0.406 | 0.076 | 0.075 | 0.027 |
| | 2g | 0.769 | 0.315 | 0.063 | 0.066 | 0.024 |

The results in Tables 6-2 to 6-7 demonstrate relatively small changes, particularly for the isolated transformers, in the probability of failure in 50 years of lifetime obtained for near-field motions by comparison to far-field motions without the correction for the spectral shape effects. This result may appear surprising given the significant differences between the two sets of motions. However, it should be noted that for the isolated transformers, the isolation system allows for small increases in the bushing acceleration as the isolator displacement increases given the fact that the isolators are of large radius of curvature. Also, the isolators considered are of large displacement capacity so that failure of the isolators does not occur in the more demanding near-field motions. That is, the results are valid but limited to the isolator studied (radius of curvature of 61inch for each concave plate and displacement capacity at failure equal to 31.3inch) and cannot be generalized to the other studied isolator of different properties.

Assuming that a correction for the spectral shape effects would produce similar results in the two cases of ground motions, we conclude that consideration of near-field motions did not produce any significant change in the results obtained using the set of far-field motions.

# SECTION 7
# SUMMARY AND CONCLUSIONS

This report presents results on the probability of failure in a lifetime of 50 years of non-isolated and seismically isolated transformers at ten locations in the Western US. The transformer and isolation system models are the same as those used in the earlier studies of Kitayama et al. (2016, 2017). However, this study deviated from the earlier studies of Kitayama et al. (2016, 2017) by (a) scaling the ground motions for use in the incremental dynamic analysis by adjusting the spectral acceleration at the fundamental period (or effective period for isolated transformers) instead of the peak ground acceleration (PGA) in the earlier studies, (b) correcting for the spectral shape effects, which were ignored in the earlier studies, and (c) accounting for uncertainties, which were neglected in earlier studies.

Moreover, the report presents sample results for near-field motions, which however, could not be corrected for spectral shape effects. A comparison of results obtained for near-field and far-field motions, both without correction for spectral shape effects, revealed that for the isolated transformers there is a small difference between the results of the two sets of motions. This was explained by the fact that the considered isolators were of large radius of curvature (so low stiffness) and large displacement capacity so that any increases in isolator displacement demand caused by near-field motions did not cause failure of the isolators or any significant increase in the bushing acceleration. Accordingly, it was concluded that near-field motions do not appreciably change the results obtained by the use of far-field motions, provided that for the two locations considered (Saranap and Loma Linda in California, which are in close proximity to active faults), isolators of the larger displacement capacity and low stiffness are used.

Results obtained for far-field motions show that, in general, scaling of the ground motions based on the spectral acceleration at the fundamental period or the effective period results in significant increases in the probability of failure for the isolated transformers, which are significantly moderated by corrections for the spectral shape effects. By comparison, the changes in the probability of failure of the studied non-isolated transformers were small due to the fact that the fundamental period was very small so that the spectral acceleration at the fundamental period was very close to the PGA which was used in the earlier studies for the scaling.

Based on the new results in this report, combined horizontal-vertical seismic isolation systems offer the lowest probabilities of failure for all cases of transformer and isolation system parameters, and for all considered sites. Horizontal only isolation offers no or offers insignificant advantages over non-isolation when the bushing transverse acceleration limit is 2g. However, horizontal only isolation offers important advantages over non-isolation when the bushing transverse acceleration limit is 1g.

The results of this report, documented in numerous tables, may be used to decide on the benefits offered by a seismic isolation system depending on the location of the transformer and the form and properties of the seismic isolation system. The benefit is assessed on the basis of the probability of failure in 50 years of lifetime. The information may also be used to assess the seismic performance of electric transmission networks under scenarios of component failures.

# SECTION 8
# REFERENCES

Abrahamson NA and Silva WJ. Empirical response spectral attenuation relations for shallow crustal earthquakes, *Seismological Research Letters*, 1997; 68(1), 94-127.

American Society of Civil Engineers (ASCE) (2017). Standard ASCE/SEI 7-16, Minimum design loads for buildings and other structures, Reston, VA.

Baker JW. (2011). Conditional mean spectrum: Tool for ground-motion selection. *Journal of Structural Engineering, ASCE*, 137(3), 332-344.

Haselton, CB and Baker JW. (2006). Ground motion intensity measures for collapse capacity prediction: Choice of optimal spectral period and effect of spectral shape. Eighth National Conference on Earthquake Engineering, pp. 18-22.

Haselton CB, Baker JW, Liel AB and Deierlein GG. (2011). Accounting for ground-motion spectral shape characteristics in structural collapse assessment through an adjustment for epsilon. *Journal of Structural Engineering, ASCE*, 137(3), 332-344.

FEMA. (2009). Quantification of building seismic performance factors. Report *FEMA P695*, Federal Emergency Management Agency, Washington, DC.

Field EH, Jordan TH and Cornell CA. (2003). OpenSHA: A developing community-model-ling environment for seismic hazard analysis. Seismological Research Letters, 74 (4), 406-419.

Kitayama S, Constantinou MC, Lee D. (2016). Procedures and results of assessment of seismic performance of seismically isolated electrical transformers with due consideration for vertical isolation and vertical ground motion effects. Report *MCEER-16-0010*. Multidisciplinary Center for Earthquake Engineering Research, Buffalo, NY.

Kitayama S, Lee D, Constantinou MC and Kempner L. (2017). Probabilistic seismic assessment of seismically isolated electrical transformers considering vertical isolation and vertical ground motion. *Engineering Structures*, 152 (1), pp. 888-900.

Kitayama S and Constantinou MC. (2018a). Seismic Performance assessment of seismically isolated buildings designed by the procedures of ASCE/SEI 7. Report *MCEER-18-0004*, Multidisciplinary Center for Earthquake Engineering Research, Buffalo, NY.

Kitayama S and Constantinou MC. (2018b). Collapse performance of seismically isolated buildings designed by the procedures of ASCE/SEI 7. *Engineering Structures*, 164, pp. 243-258.

Kitayama, S and Constantinou, MC. (2019a). Probabilistic seismic performance assessment of seismically isolated buildings designed by the procedures of ASCE/SEI 7 and other enhanced criteria. *Engineering Structures*, 179, pp. 566-582.

Kitayama, S and Constantinou, MC. (2019b). Effect of displacement restraint on the collapse performance of seismically isolated buildings. *Bulletin of Earthquake Engineering*, https://doi.org/10.1007/s10518-019-00626-z .

Krawinkler H, Zarein F, Medina RA and Ibarra LF. (2006). Decision support for conceptual performance-based design. *Earthquake Engineering and Structural Dynamics*, 35 (1), pp. 115-133.

Lee D and Constantinou MC. (2017). Development and validation of a combined horizontal-vertical seismic isolation system for high-voltage power transformers. Report *MCEER-17-0007*, Multidisciplinary Center for Earthquake Engineering Research, University at Buffalo, Buffalo, NY.

Lee D and Constantinou MC. (2018). Combined horizontal-vertical seismic isolation system for high-voltage power transformers: development, testing and validation. *Bulletin of Earthquake Engineering*, 16, pp. 4273–4296.

Liel B, Haselton CB, Deierlein GG and Baker JW. (2009). Incorporating modeling uncertainties in the assessment of seismic collapse risk of buildings. *Structural Safety*, 31, pp. 197-211.

Lin T, Haselton CB and Baker JW. (2013). Conditional spectrum-based ground motion selection. Part-I: Hazard consistency for risk-based assessments. Earthquake Engineering and Structural Dynamics, 42 (12), pp. 1847-1865.

Masroor A and Mosqueda G. (2015). Assessing the collapse probability of base-isolated buildings considering pounding to moat walls using the FEMA P695 methodology. *Earthquake Spectra*, 31(4), pp. 2069-2086.

NIST. (2011). Selecting and scaling earthquake ground motions for performing response-history analysis, Report *NIST GCR 11-917-15*. Technical Report, prepared by the NEHRP Consultants Joint Venture for the National Institute of Standards and Technology: Gaithersburg, Maryland.

Oikonomou K, Constantinou MC, Reinhorn AM and Kempner Jr. L. (2016). "Seismic Isolation of High Voltage Electrical Power Transformers." Report *MCEER-16-0006*, Multidisciplinary Center for Earthquake Engineering Research, University at Buffalo, Buffalo, NY.

Shinozuka M, Dong X, Chen TC and Jin X. (2007). Seismic performance of electric transmission network under component failures. *Earthquake Engineering and Structural Dynamics*, 36 (2), pp. 227-244.

Shumuta Y. (2007). Practical seismic upgrade of electric transmission network under component failures. *Earthquake Engineering and Structural Dynamics*, 27(2), pp. 209-226.

Vamvatsikos D and Cornell CA. (2002). Incremental dynamic analysis. *Earthquake Engineering and Structural Dynamics*, 31(3), pp. 491–514.

Villaverde R, Pardoen GC and Carnalla S. (2001). Ground motion amplification at flange level of bushings mounted on electric substation transformers. *Earthquake Engineering and Structural Dynamics*, 30(5), pp. 621–32.

**APPENDIX A**
**PROCEDURE FOR CONSIDERATION OF SPECTRAL SHAPE EFFECTS AND RESULTS**

## A.1 Introduction

The construction of fragility curves is based on incremental dynamic analysis (IDA) in which a large sample of actual ground motions is used by increasing their intensity until collapse (or failure by exceeding a certain acceleration level at the bushing) is detected in the analysis model. This approach accounts only for ground-motion intensity in the assessment of collapse or failure. It does not account for the spectral shape of the motions. The shape of the uniform hazard response spectrum for which a design is performed (for example, design of the seismic isolation system for an electrical transformer; one described by a ground-motion hazard of 2% chance of exceedance in 50 years or a return period of 2475 years) can be significantly different than the response spectrum of a real ground motion that is scaled to an equal spectral amplitude at the period of interest.

The following example from FEMA (2009) and Haselton and Baker (2006) demonstrates the issue. Figure A-1 shows the acceleration spectrum of a ground motion recorded in the Loma Prieta earthquake. The Loma Prieta spectrum has a spectral value of 0.9g at 1.0sec period, which has a 2% chance of exceedance in 50 years. The figure also shows the mean expected spectrum predicted by an attenuation prediction model (BJF for Boore, Joyner and Fuma) that is consistent with the event magnitude, distance, and site characteristics associated with this ground motion. Figure A-1 shows that this ground motion has a much different shape than the mean predicted spectrum.

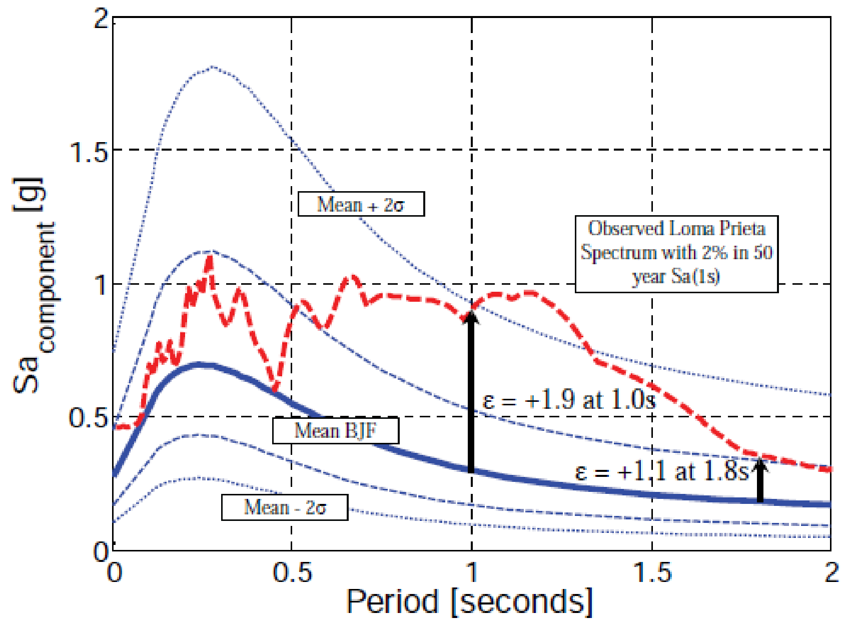


Figure A-1. Comparison of observed and predicted response spectra (from FEMA, 2009 and Haselton and Baker, 2006)

At the1.0sec period, the spectral value of the Loma Prieta record is 1.9 standard deviations above the predicted mean spectral value from the attenuation relationship so this record is said to have an "epsilon" ε=1.9 at the 1.0sec period. "Epsilon" is defined as the number of logarithmic standard deviations between the observed spectral value and the mean spectral acceleration predicted by a ground-motion prediction model. Parameter epsilon is used to characterize the spectral shape.

The approach developed by Haselton et al. (2011) for seismic performance evaluation is based on the use of a general ground-motion set for analysis (the motions in FEMA, 2009) that are selected independently of the ε values for the particular site of the analyzed structure. The results on the failure fragility are then corrected to account for the spectral shape. The correction adjustment is calculated by using values of ε at the considered period (fundamental or effective period $T_1$ in this study) which are computed for the site of the transformer and the considered hazard level (2475 year return period) through the disaggregation of the seismic hazard for the site.

## A.2 Procedure for Correction for Spectral Shape Effects

The procedure involves the following steps:

1. Obtain the target epsilon $\bar{\varepsilon}_0(T_1)$, magnitude $M$, and distance $R$ from de-aggregation of the ground motion hazard (probabilistic seismic hazard analysis) for the specific location of the structure (longitude and latitude), site class (average shear-wave velocity $V_{s30}$=259 m/sec for class D), spectral period and return period. The return period of 2475 years (corresponding to a probability of exceedance of 2% in 50 years) is used because the primary purpose of collapse or failure evaluation is to compute the conditional collapse or failure probability for a 2% in 50 years ground motion. Information was obtained from the USGS website (https://earthquake.usgs.gov/hazards/interactive/ accessed on September 25, 2018) where results of de-aggregation for period of 0.2, 1.0 and 2.0 second were available. Linear interpolation and extrapolation in logarithmic space of the seismic hazard curves (annual frequency of exceedance vs spectral acceleration) was used for other values of period ($T_1$=0.13sec for non-isolated transformer, and $T_1$=2.40sec for isolated transformer).

2. Perform incremental dynamic analysis (IDA) (Vamvatsikos and Cornell, 2002) (for this study the 40 far-field ground motions of FEMA P695) to obtain the collapse capacity in terms of the spectral acceleration at fundamental period $T_1$ at failure for each ground motion, $Sa_{\mathrm{Col},j}(T_1)$ ($j$ is the identification number for the ground motions; $j$ = 1 to 40).

3. Calculate epsilon at $T_1$, $\varepsilon_j(T_1)$ for the $j^{\mathrm{th}}$ ground motion ($j$=1 to 40), defined as the number of standard deviations by which the natural logarithm of $S_{aj}(T_1)$, ln[$S_{aj}(T_1)$], differs from the mean predicted ln[$S_a(T_1)$] for a given magnitude and distance (Baker, 2011):

$$\varepsilon_j(T_1) = \frac{\ln[Sa_j(T_1)] - \mu_{\ln Sa}(M,R,T_1)}{\sigma_{\ln Sa}(T_1)} \quad \text{(A-1)}$$

   In Equation A-1, $\mu_{\ln Sa}(M,R,T_1)$ is the predicted mean of ln[$S_a(T_1)$] at a given magnitude $M$, distance $R$ and period $T_1$, and $\sigma_{\ln Sa}(T_1)$ is the predicted standard deviation of ln[$S_a(T_1)$] at a given $M$, $R$ and $T_1$. Note that $\mu_{\ln Sa}(M,R,T_1)$ and $\sigma_{\ln Sa}(T_1)$ are obtained from any ground motion prediction model (herein the model of Abrahamson and Silva, 1997 was used, which was also used by Haselton et al., 2011). Quantity ln[$S_{aj}(T_1)$] in Equation A-1 is the natural logarithm of the spectral acceleration at $T_1$ of each of 40 original (before scaling) ground motions.

4. Perform a linear regression analysis between $\ln[S_{a\mathrm{Col},j}(T_1)]$ and $\varepsilon_j(T_1)$ and determine parameters $c_0$ and $c_1$ based on the following equation:

$$\ln[S_{a\mathrm{Col}}(T_1)] = c_0 + c_1 \cdot \varepsilon(T_1) \tag{A-2}$$

5. Replace $\varepsilon(T_1)$ with $\bar{\varepsilon}_0(T_1)$ in Equation A-2 and solve to obtain the adjusted mean collapse capacity, $\widehat{Sa}_{\mathrm{Col,adj}}(T_1)$:

$$\widehat{Sa}_{\mathrm{Col,adj}}(T_1)\ (units\ g) = \exp[c_0 + c_1 \cdot \bar{\varepsilon}_0(T_1)] \tag{A-3}$$

The record-to-record dispersion coefficient, $\beta_{\mathrm{RTR}}$, is calculated as the standard deviation of the natural logarithm of $S_{a\mathrm{Col}j}(T_1)$ of the 40 motions without any further adjustment. Note that Haselton et al. (2011) described a procedure for further reduction of the dispersion using the residuals of the regression analysis but the effect was found to be insignificant in this study and was not included in the presented results.

Values of the target epsilon $\bar{\varepsilon}_0(T_1)$, magnitude *M* and distance *R* for return period of 2475 years obtained by de-aggregation of the seismic hazard are presented in Table A-1 at three representative sites out of the ten studied.

Table A-1 Values of $\bar{\varepsilon}_0(T_1)$, *M* and *R* at three representative sites for 2475 years return period earthquake

| Site | Structure | | $\bar{\varepsilon}_0(T_1)$ | *M* | *R* (km) |
|---|---|---|---|---|---|
| Chehalis, WA | Non-isolated | 4.3 Hz | 1.27 | 7.75 | 53.92 |
| | | 7.7 Hz | 1.22 | 7.78 | 53.24 |
| | | 11.3 Hz | 1.19 | 7.82 | 53.01 |
| | Isolated | | 0.72 | 8.78 | 66.48 |
| Loma Linda, CA | Non-isolated | 4.3 Hz | 0.74 | 7.38 | 6.88 |
| | | 7.7 Hz | 0.63 | 7.43 | 6.65 |
| | | 11.3 Hz | 0.58 | 7.48 | 6.43 |
| | Isolated | | 1.10 | 8.01 | 3.61 |
| Troutdale, OR | Non-isolated | 4.3 Hz | 1.11 | 7.03 | 47.74 |
| | | 7.7 Hz | 1.07 | 7.02 | 46.98 |
| | | 11.3 Hz | 1.05 | 7.04 | 47.25 |
| | Isolated | | 0.94 | 8.43 | 100.45 |

The ground motion prediction model of Abrahamson and Silva (1997) was used to construct the median 5%-damped response spectra for the isolated and non-isolated transformers. The spectra are presented in Figures A-2 to A-4 together with the spectra of the 44 ground motions used in the IDA for three of the considered sites. We used program OpenSHA (Field et al., 2003) to construct the spectra based on the Abrahamson and Silva prediction model. The same model also predicted the standard deviation of the 5%-damped response spectrum. It is presented in Figures A-5 to A-7. Isolated and non-isolated transformers have the same standard deviation at each of the three locations.

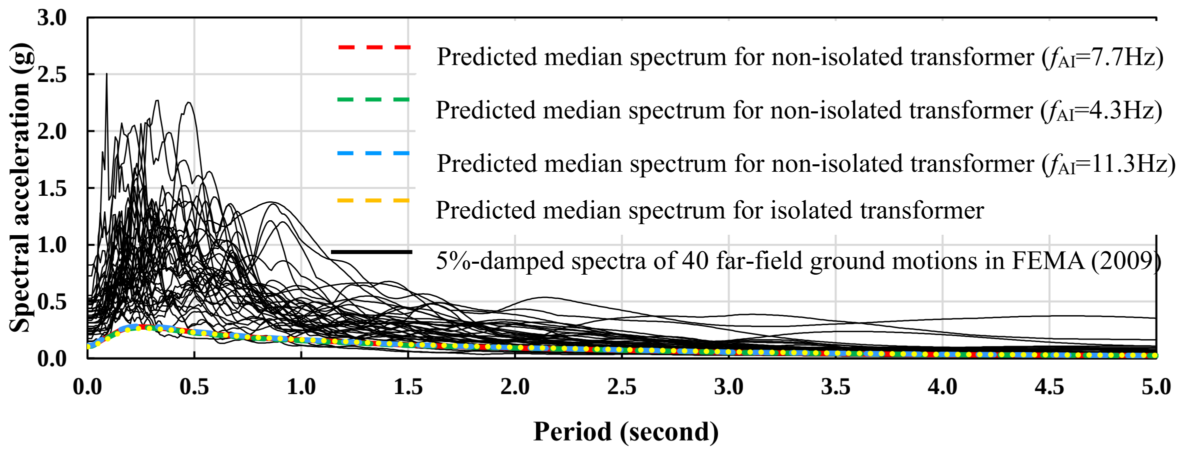


Figure A-2 Response spectra of FEMA far-field motions and predicted median spectra at Chehalis, WA location

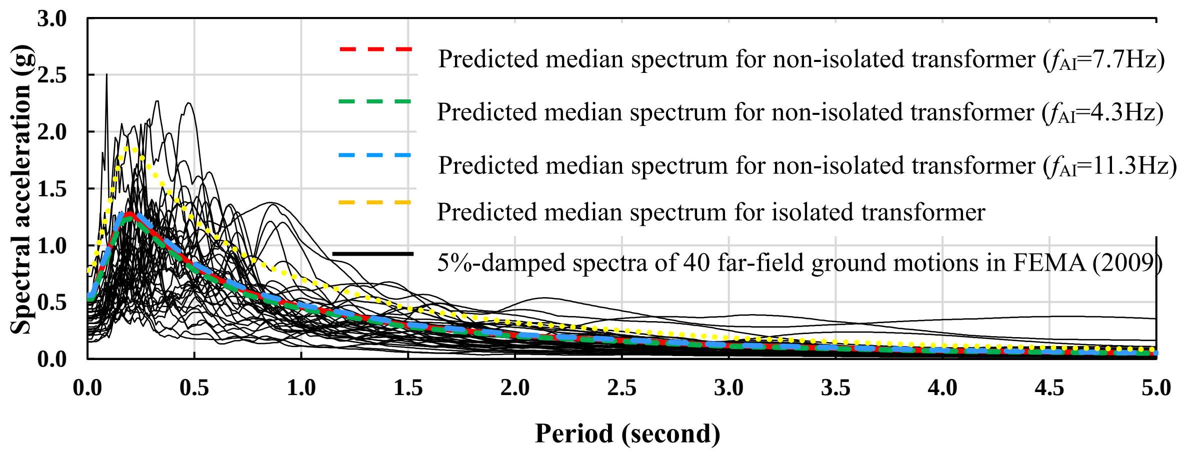


Figure A-3 Response spectra of FEMA far-field motions and predicted median spectra at Loma Linda, CA location

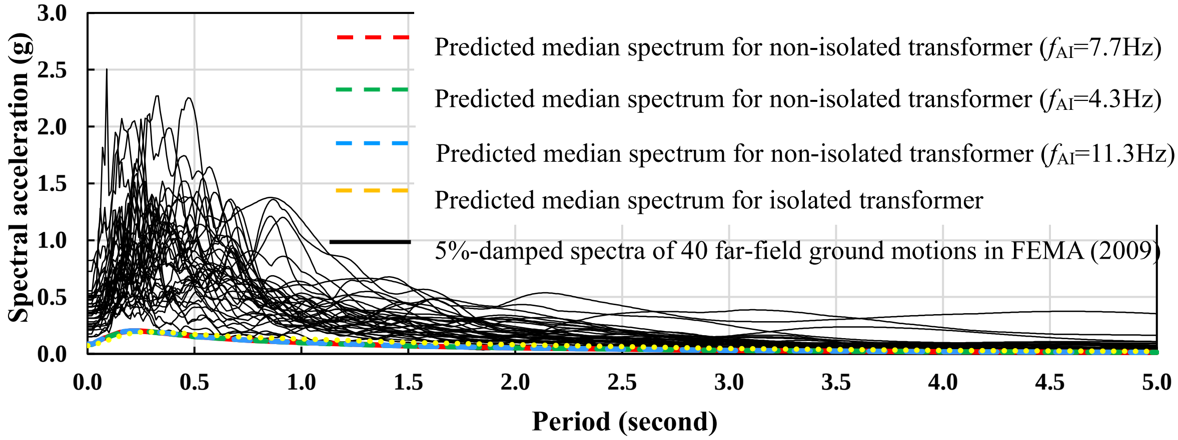


Figure A-4 Response spectra of FEMA far-field motions and predicted median spectra at Troutdale, OR location

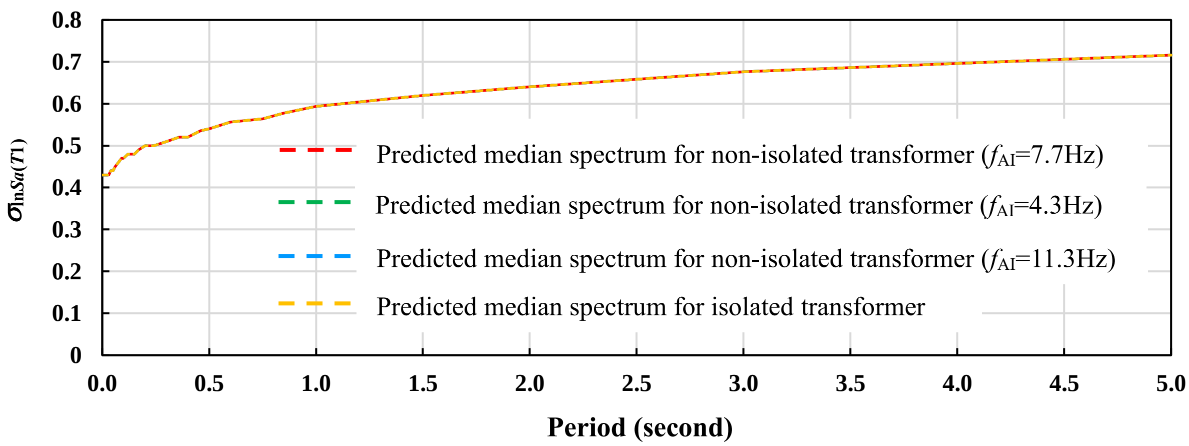


Figure A-5 Standard deviation of natural logarithm of spectral acceleration at Chehalis, WA

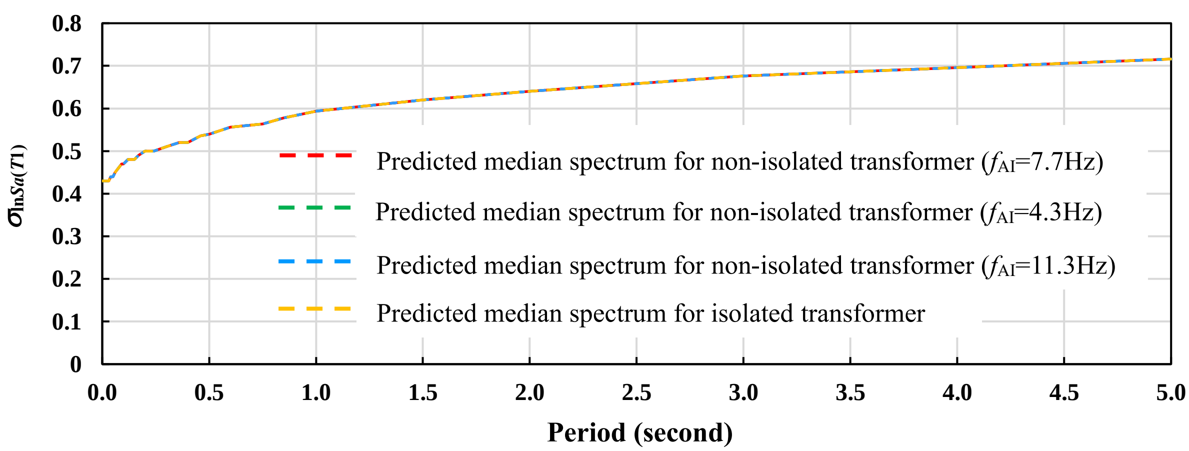


Figure A-6 Standard deviation of natural logarithm of spectral acceleration at Loma Linda, CA

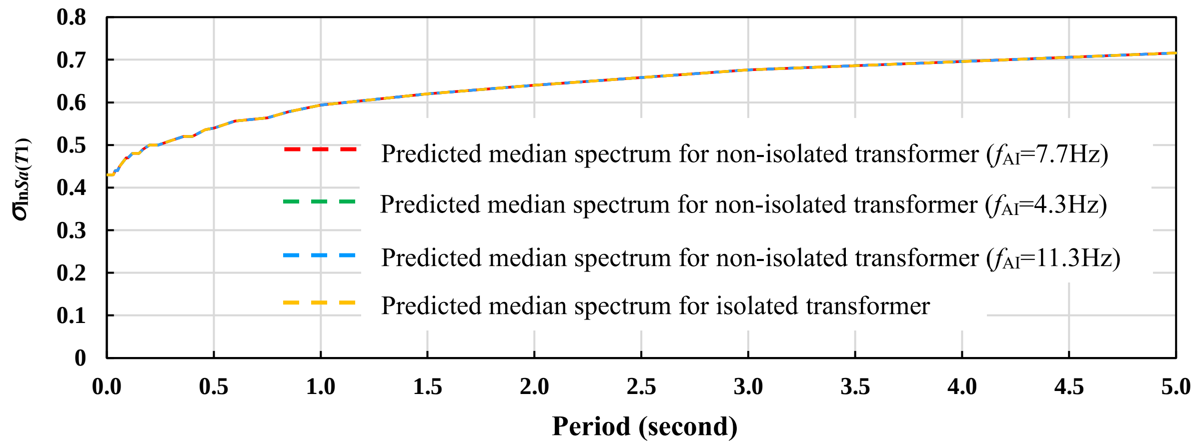


Figure A-7 Standard deviation of natural logarithm of spectral acceleration at Troutdale, OR

The values of $\varepsilon_j(T_1)$ for each of the 40 ground motions ($j$=1 to 40) for the isolated and non-isolated structures were then calculated by use of Equation A-1 and are presented in Figures A-8 to A-10 for the case of the isolated and non-isolated transformers at the three sites. Values of epsilon are higher for the non-isolated transformer.

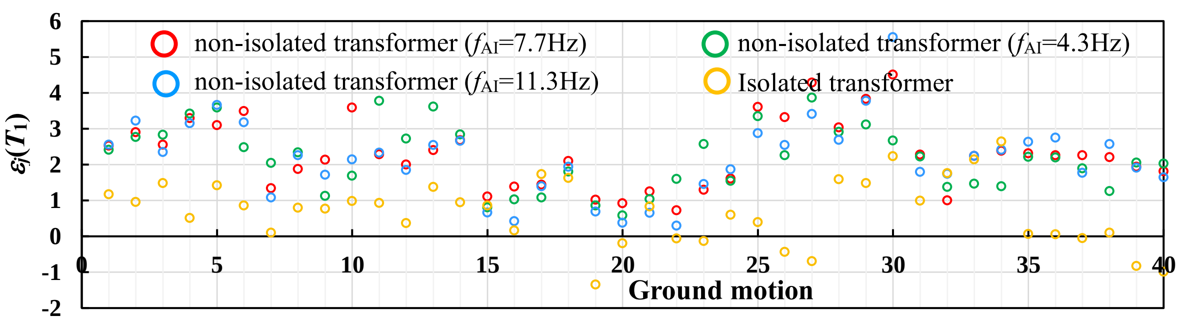


Figure A-8 Calculated values of $\varepsilon_j(T_1)$ for the 40 ground motions used in analysis for Chehalis, WA location

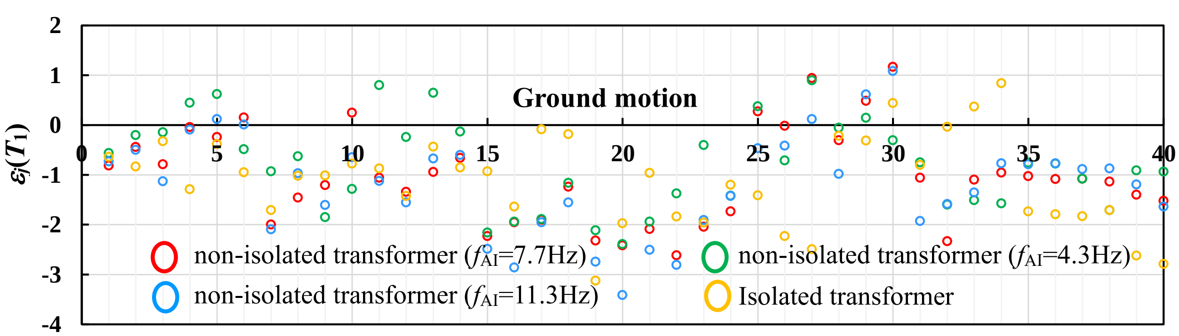


Figure A-9 Calculated values of $\varepsilon_j(T_1)$ for the 40 ground motions used in analysis for Loma Linda, CA location

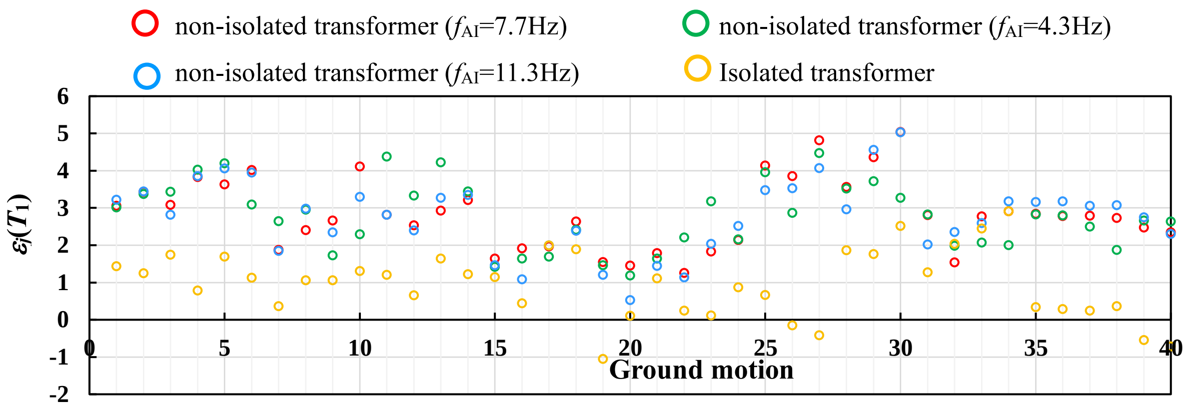


Figure A-10 Calculated values of $\varepsilon_j(T_1)$ for the 40 ground motions used in analysis for Troutdale, OR location

Based on the results of IDA and the information on $\varepsilon_j(T_1)$ in Figures A-8 to A-10, linear regression analysis was performed to establish the relationship between the $\ln[S_{a\mathrm{Col},j}(T_1)]$ and $\varepsilon_j(T_1)$. Figures A-11 to A-46 present the relationship between $\ln[S_{a\mathrm{Col},j}(T_1)]$ and $\varepsilon_j(T_1)$ for the non-isolated transformer and the isolated transformers at the three representative sites. The figures also present the fitted linear regression model of Equation A-2.

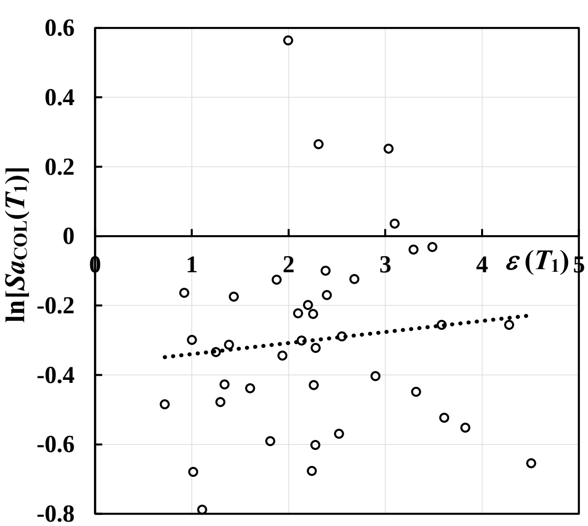


(a) 1$g$ limit ($c_0$=-0.372, $c_1$=0.032)

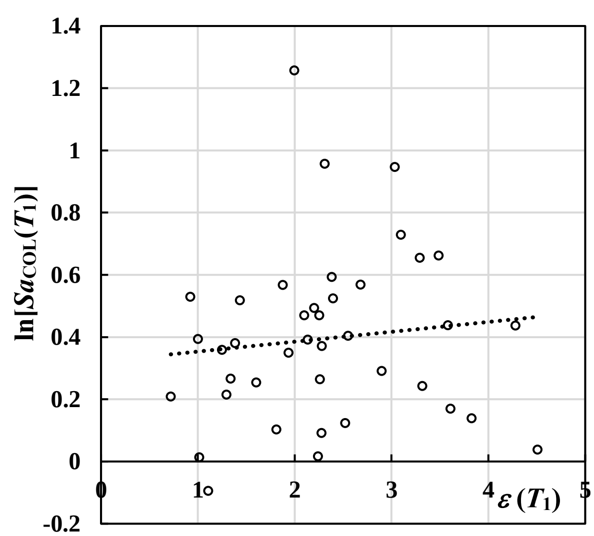


(b) 2$g$ limit ($c_0$=-0.322, $c_1$=0.032)

Figure A-11 Relationship between $\ln[Sa_{\mathrm{Col},j}(T_1)]$ and $\varepsilon_j(T_1)$ of non-isolated transformer with bushing of 7.7Hz as-installed frequency at Chehalis, WA

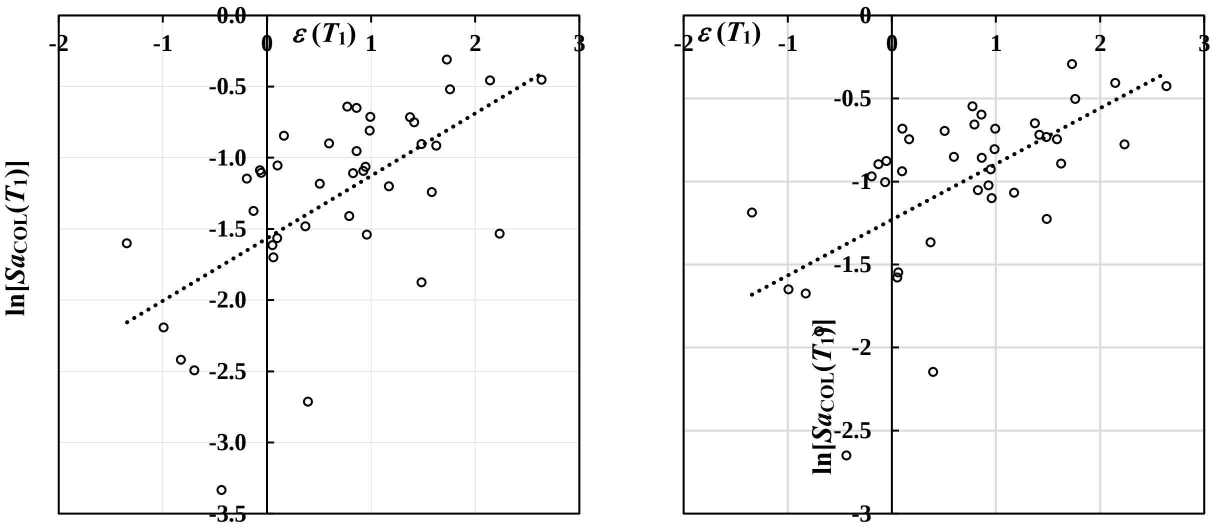


(a) 1$g$ limit ($c_0$=-0.3716, $c_1$=0.0318) (b) 2$g$ limit ($c_0$=-1.230, $c_1$=0.336)

Figure A-12 Relationship between ln[$Sa_{\text{Col},j}(T_1)$] and $\varepsilon_j(T_1)$ of horizontally isolated transformer ($D_{\text{Capacity}}$=17.7inch, lower bound) with as-installed bushing frequency of 7.7Hz at Chehalis, WA

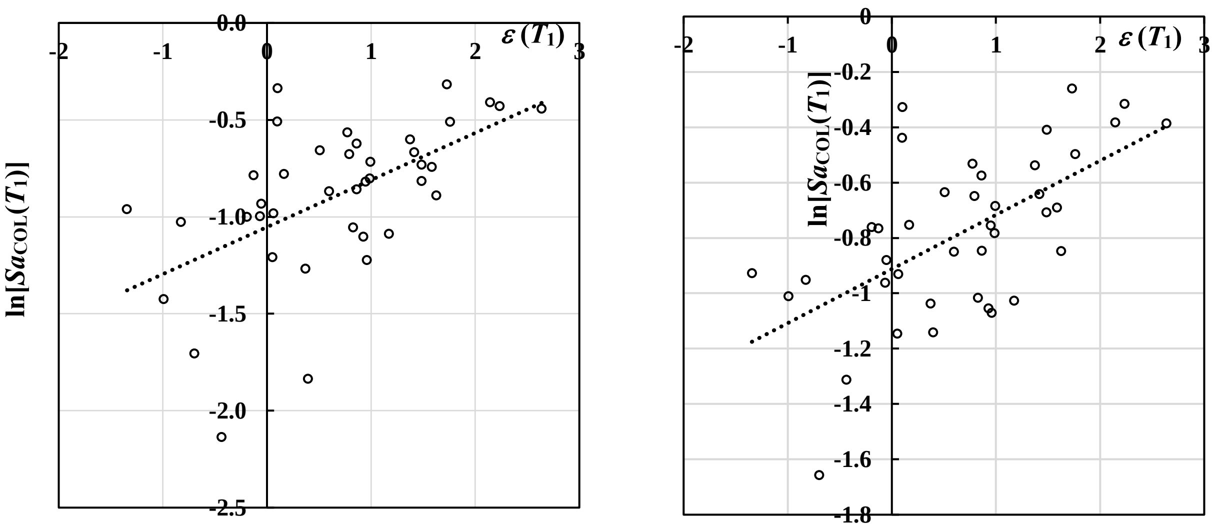


(a) 1$g$ limit ($c_0$=-1.053, $c_1$=0.2427) (b) 2$g$ limit ($c_0$=-0.912, $c_1$=0.196)

Figure A-13 Relationship between ln[$Sa_{\text{Col},j}(T_1)$] and $\varepsilon_j(T_1)$ of horizontally-vertically isolated without rocking transformer ($D_{\text{Capacity}}$=17.7inch, lower bound) with as-installed bushing frequency of 7.7Hz at Chehalis, WA

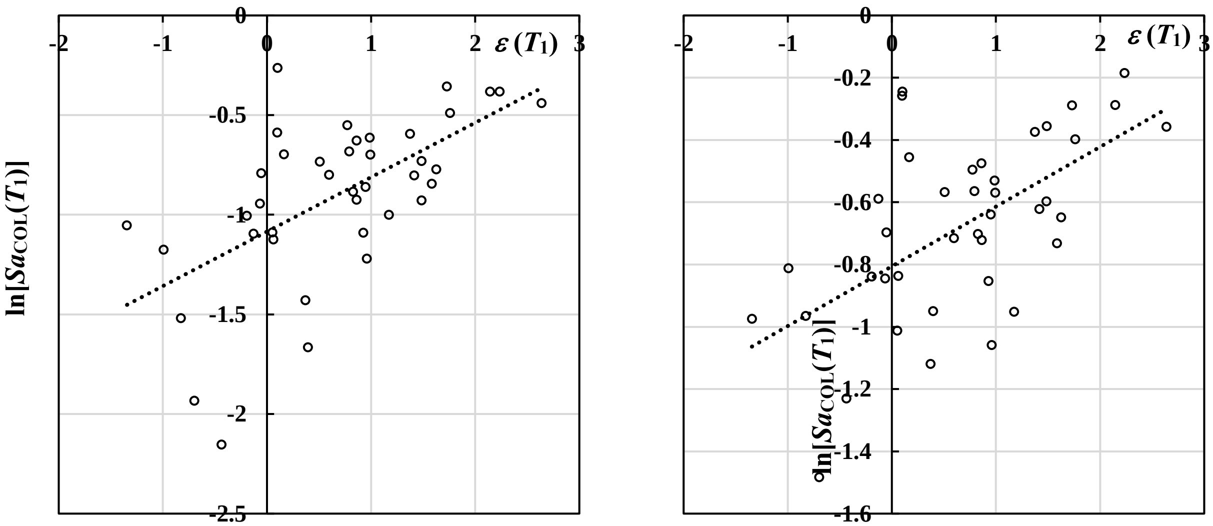


(a) 1*g* limit ($c_0$=-1.085, $c_1$=0.273)

(b) 2*g* limit ($c_0$=-0.806, $c_1$=0.192)

Figure A-14 Relationship between ln[$Sa_{\mathrm{Col},j}(T_1)$] and $\varepsilon_j(T_1)$ of horizontally-vertically isolated with rocking transformer ($D_{\mathrm{Capacity}}$=17.7inch, lower bound) with as-installed bushing frequency of 7.7Hz at Chehalis, WA

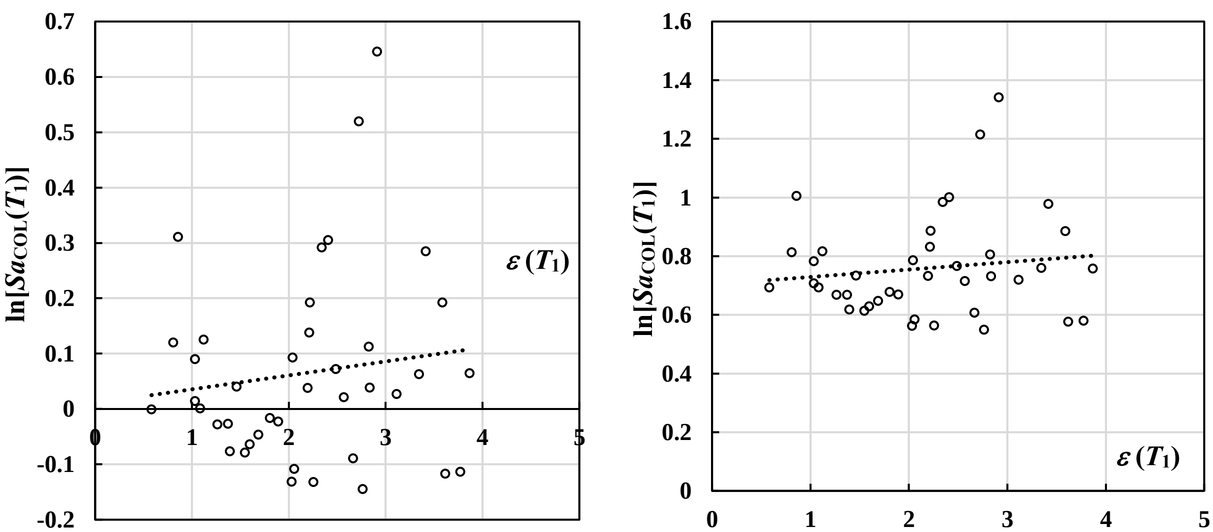


(a) 1*g* limit ($c_0$=-0.010, $c_1$=0.025)

(b) 2*g* limit ($c_0$=0.704, $c_1$=0.025)

Figure A-15 Relationship between ln[$Sa_{\mathrm{Col},j}(T_1)$] and $\varepsilon_j(T_1)$ of non-isolated transformer with bushing of 4.3Hz as-installed frequency at Chehalis, WA

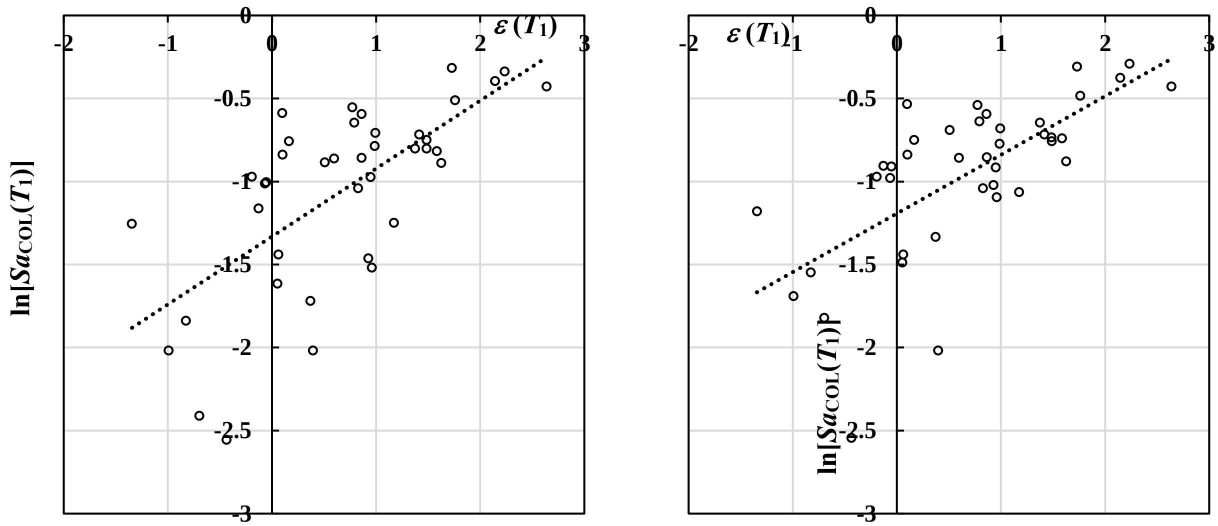


(a) 1$g$ limit ($c_0$=-1.331, $c_1$=0.409)　(b) 2$g$ limit ($c_0$=-1.193, $c_1$=0.353)

Figure A-16 Relationship between ln[$Sa_{\mathrm{Col},j}(T_1)$] and $\varepsilon_j(T_1)$ of horizontally isolated transformer ($D_{\mathrm{Capacity}}$=17.7inch, lower bound) with as-installed bushing frequency of 4.3Hz at Chehalis, WA

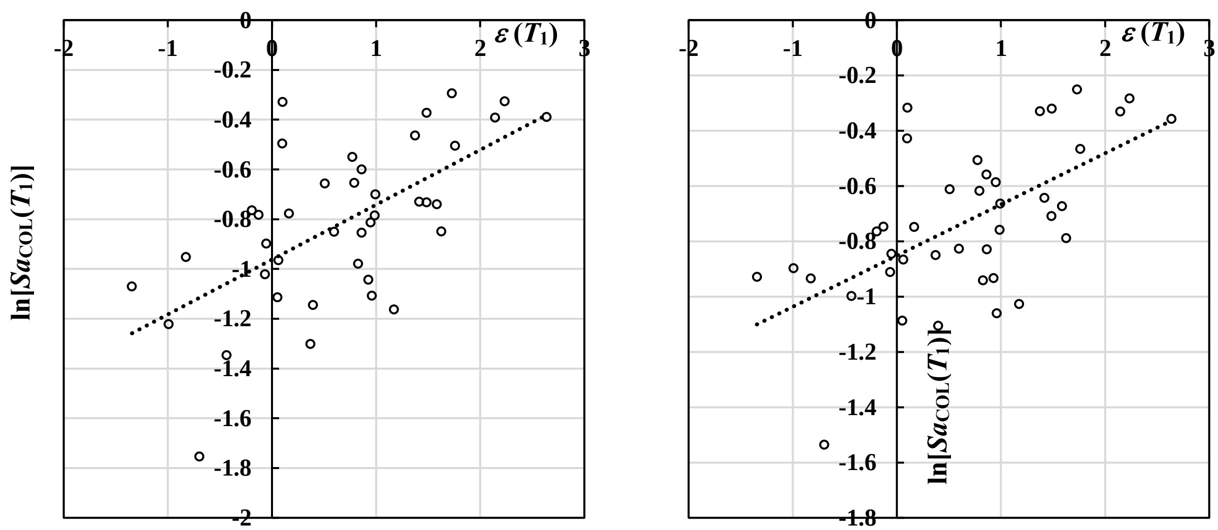


(a) 1$g$ limit ($c_0$=-0.962, $c_1$=0.220)　(b) 2$g$ limit ($c_0$=-0.852, $c_1$=0.185)

Figure A-17 Relationship between ln[$Sa_{\mathrm{Col},j}(T_1)$] and $\varepsilon_j(T_1)$ of horizontally-vertically isolated without rocking transformer ($D_{\mathrm{Capacity}}$=17.7inch, lower bound) with as-installed bushing frequency of 4.3Hz at Chehalis, WA

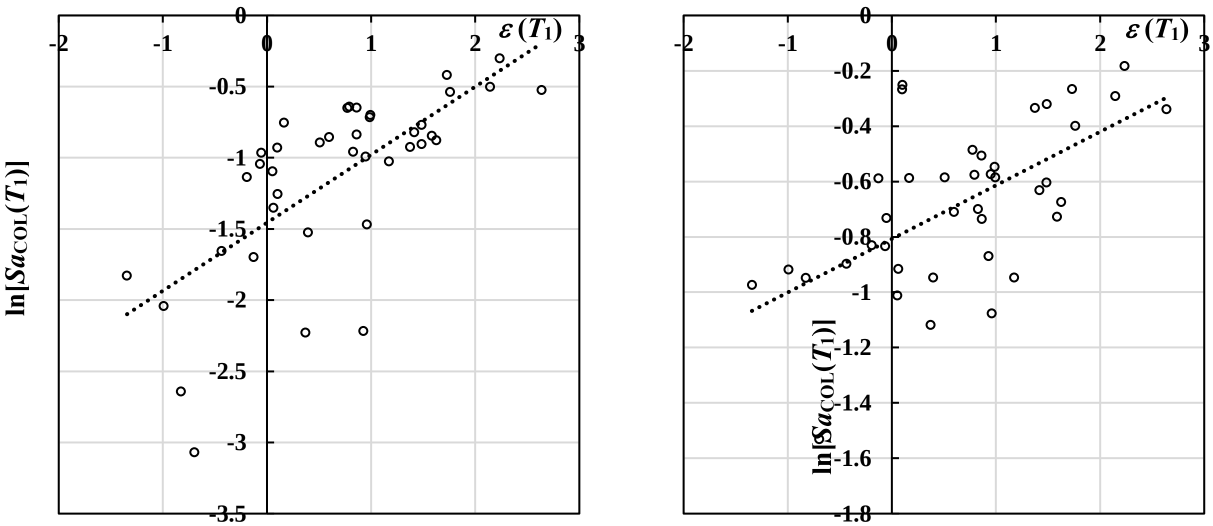


(a) 1*g* limit ($c_0$=-1.457, $c_1$=0.478) (b) 2*g* limit ($c_0$=-0.807, $c_1$=0.194)

Figure A-18 Relationship between ln[$Sa_{\mathrm{Col},j}(T_1)$] and $\varepsilon_j(T_1)$ of horizontally-vertically isolated with rocking transformer ($D_{Capacity}$=17.7inch, lower bound) with as-installed bushing frequency of 4.3Hz at Chehalis, WA

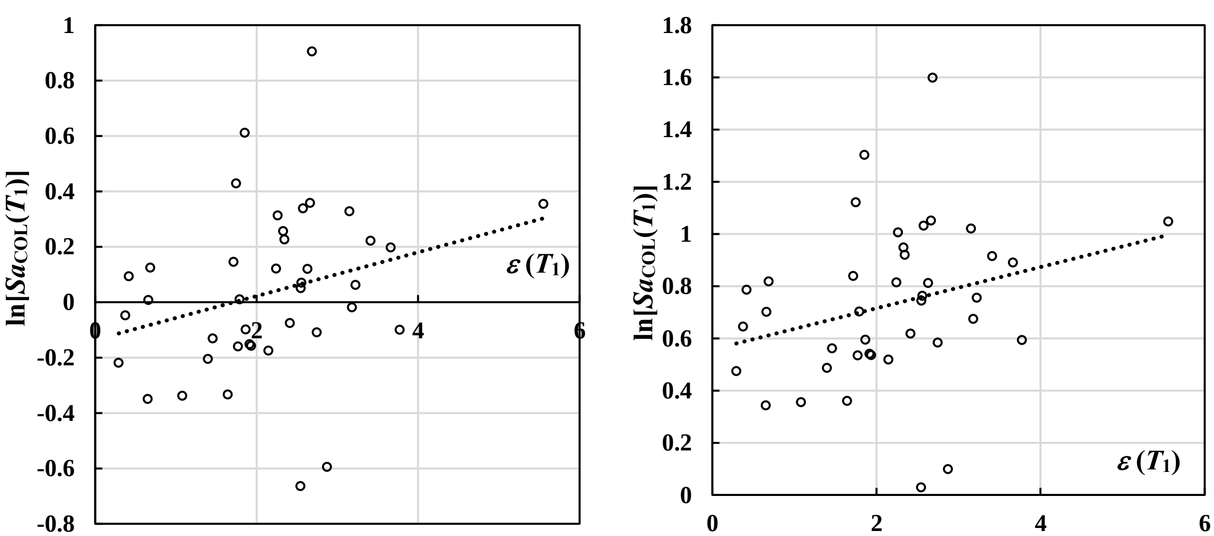


(a) 1*g* limit ($c_0$=-0.136, $c_1$=0.079) (b) 2*g* limit ($c_0$=0.557, $c_1$=0.079)

Figure A-19 Relationship between ln[$Sa_{\mathrm{Col},j}(T_1)$] and $\varepsilon_j(T_1)$ of non-isolated transformer with bushing of 11.3Hz as-installed frequency at Chehalis, WA

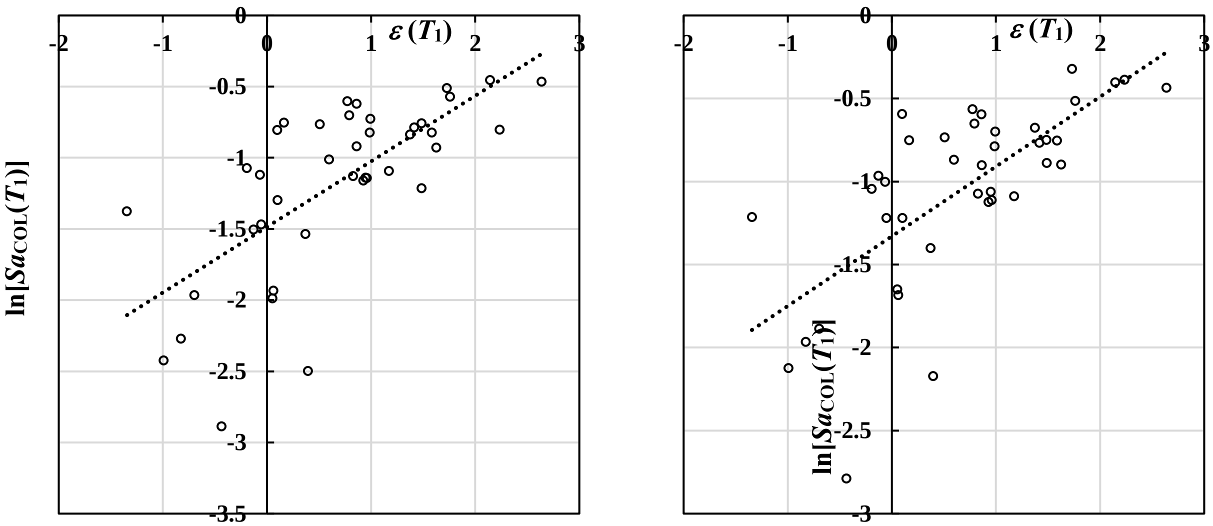


(a) 1$g$ limit ($c_0$=-1.486, $c_1$=0.461) (b) 2$g$ limit ($c_0$=-1.330, $c_1$=0.420)

Figure A-20 Relationship between ln[$Sa_{\mathrm{Col},j}(T_1)$] and $\varepsilon_j(T_1)$ of horizontally isolated transformer ($D_{\mathrm{Capacity}}$=17.7inch, lower bound) with as-installed bushing frequency of 11.3Hz at Chehalis, WA

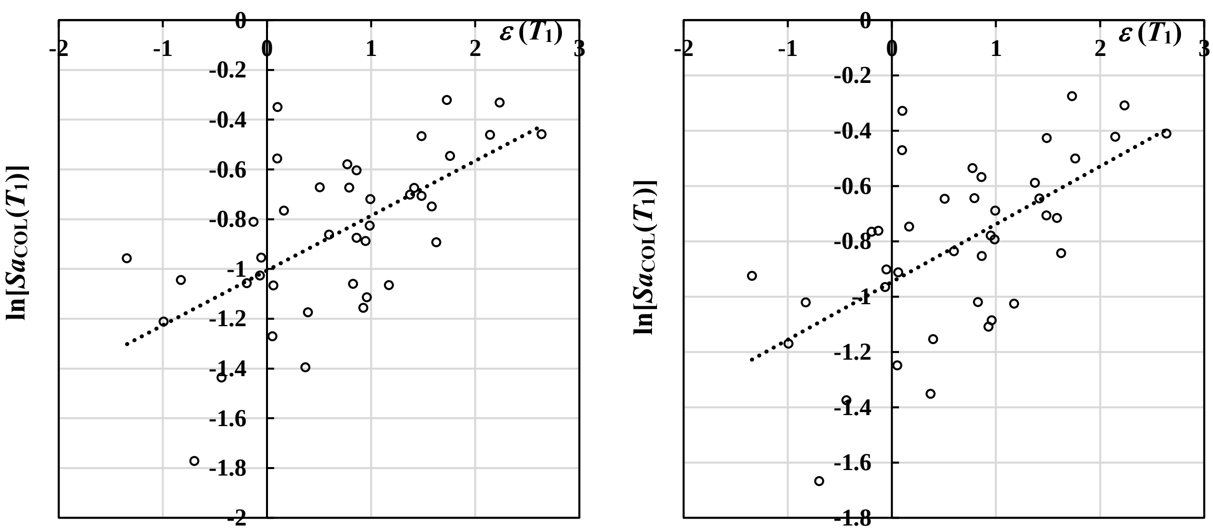


(a) 1$g$ limit ($c_0$=-1.006, $c_1$=0.220) (b) 2$g$ limit ($c_0$=-0.947, $c_1$=0.209)

Figure A-21 Relationship between ln[$Sa_{\mathrm{Col},j}(T_1)$] and $\varepsilon_j(T_1)$ of horizontally-vertically isolated without rocking transformer ($D_{\mathrm{Capacity}}$=17.7inch, lower bound) with as-installed bushing frequency of 11.3Hz at Chehalis, WA

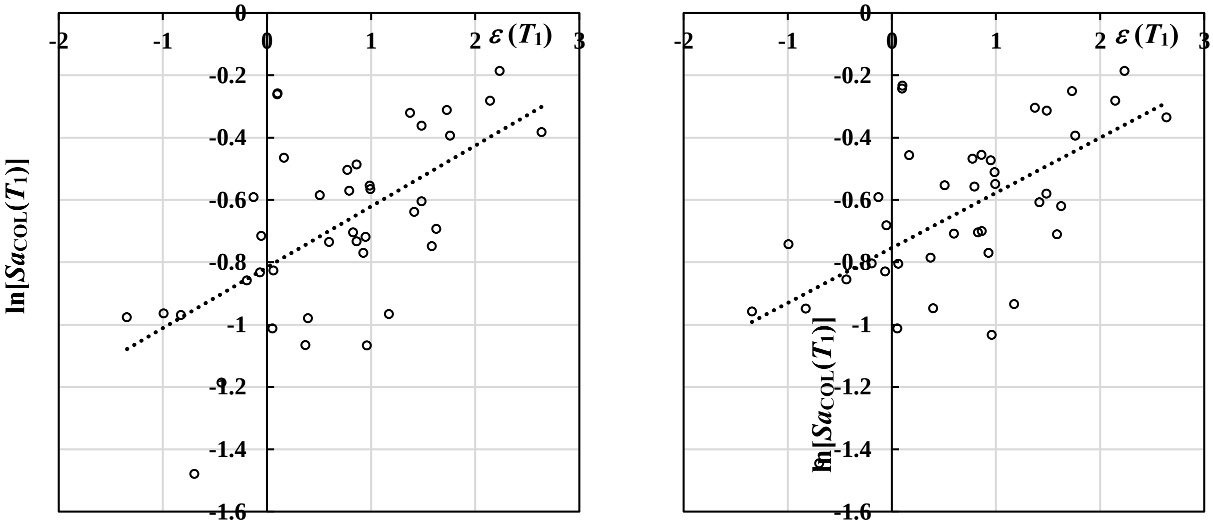


(a) 1$g$ limit ($c_0$=-0.816, $c_1$=0.195) (b) 2$g$ limit ($c_0$=-0.754, $c_1$=0.177)

Figure A-22 Relationship between ln[$Sa_{\mathrm{Col},j}(T_1)$] and $\varepsilon_j(T_1)$ of horizontally-vertically isolated with rocking transformer ($D_{\mathrm{Capacity}}$=17.7inch, lower bound) with as-installed bushing frequency of 11.3Hz at Chehalis, WA

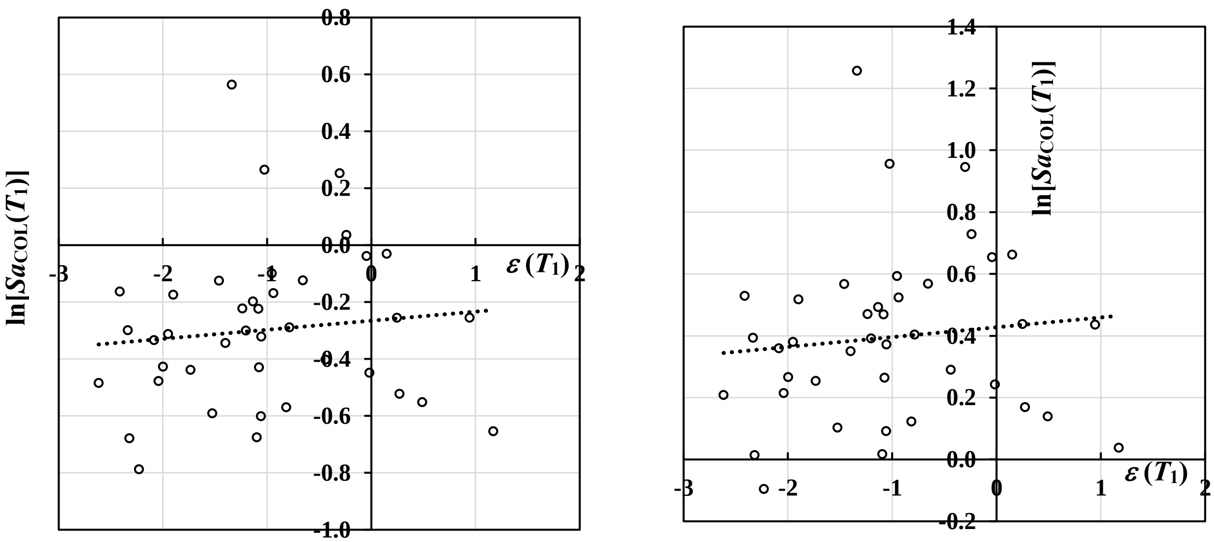


(a) 1$g$ limit ($c_0$=-0.265, $c_1$=0.032) (b) 2$g$ limit ($c_0$=0.428, $c_1$=0.032)

Figure A-23 Relationship between ln[$Sa_{\mathrm{Col},j}(T_1)$] and $\varepsilon_j(T_1)$ of non-isolated transformer with bushing of 7.7Hz as-installed frequency at Loma Linda, CA

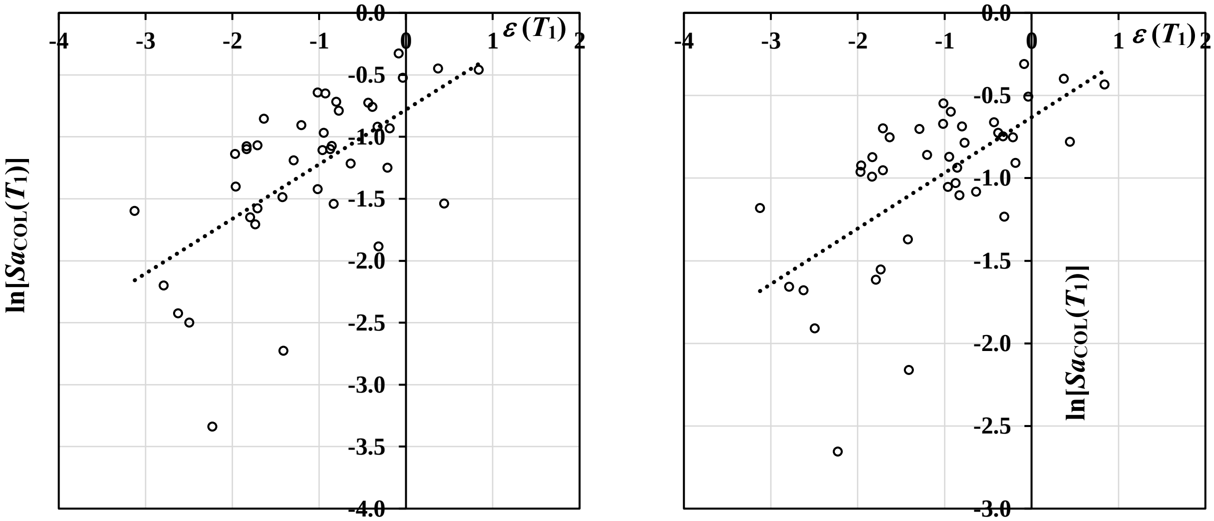


(a) 1*g* limit ($c_0$=-0.781, $c_1$=0.440) (b) 2*g* limit ($c_0$=-0.632, $c_1$=0.337)

Figure A-24 Relationship between $\ln[Sa_{\mathrm{Col},j}(T_1)]$ and $\varepsilon_j(T_1)$ of horizontally isolated transformer ($D_{\mathrm{Capacity}}$=17.7inch, lower bound) with as-installed bushing frequency of 7.7Hz at Loma Linda, CA

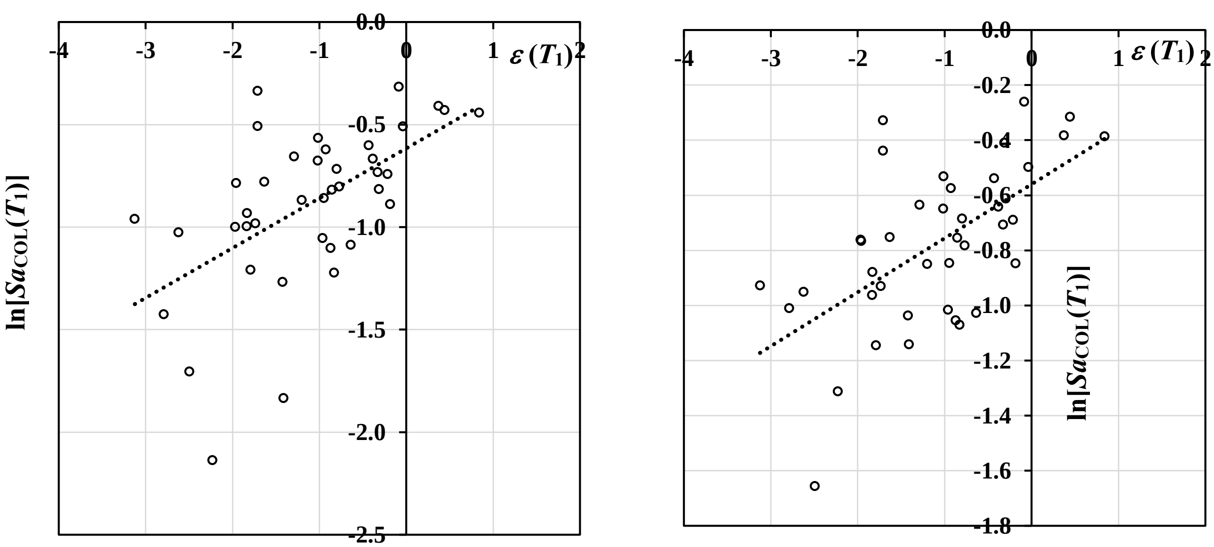


(a) 1*g* limit ($c_0$=-0.616, $c_1$=0.243) (b) 2*g* limit ($c_0$=-0.560, $c_1$=0.196)

Figure A-25 Relationship between $\ln[Sa_{\mathrm{Col},j}(T_1)]$ and $\varepsilon_j(T_1)$ of horizontally-vertically isolated without rocking transformer ($D_{\mathrm{Capacity}}$=17.7inch, lower bound) with as-installed bushing frequency of 7.7Hz at Loma Linda, CA

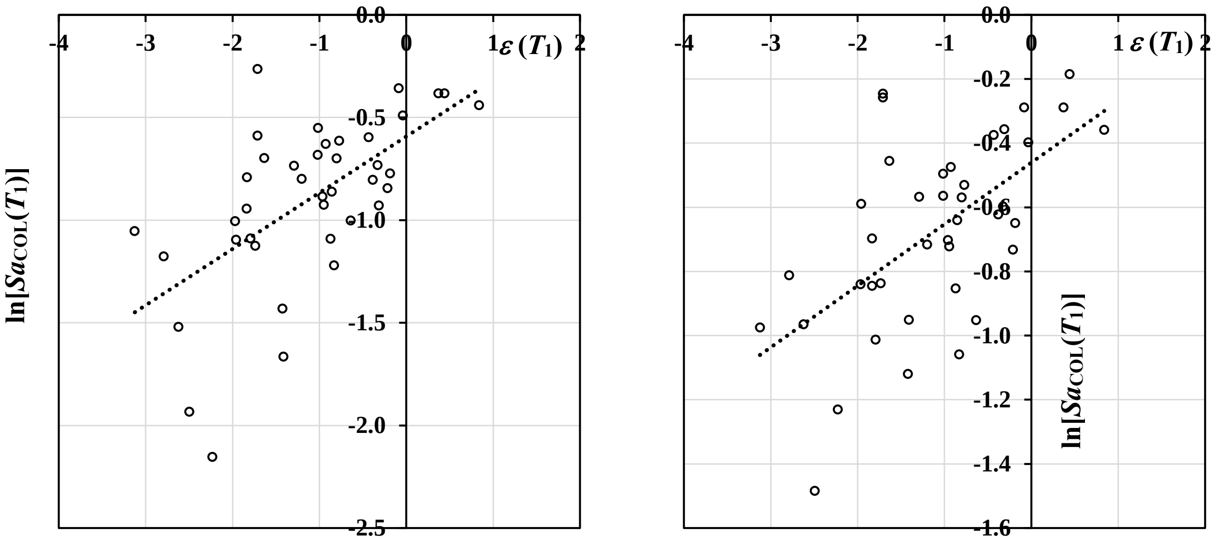


(a) 1$g$ limit ($c_0$=-0.593, $c_1$=0.274) (b) 2$g$ limit ($c_0$=-0.461, $c_1$=0.192)

Figure A-26 Relationship between ln[$Sa_{\mathrm{Col},j}(T_1)$] and $\varepsilon_j(T_1)$ of horizontally-vertically isolated with rocking transformer ($D_{\mathrm{Capacity}}$=17.7inch, lower bound) with as-installed bushing frequency of 7.7Hz at Loma Linda, CA

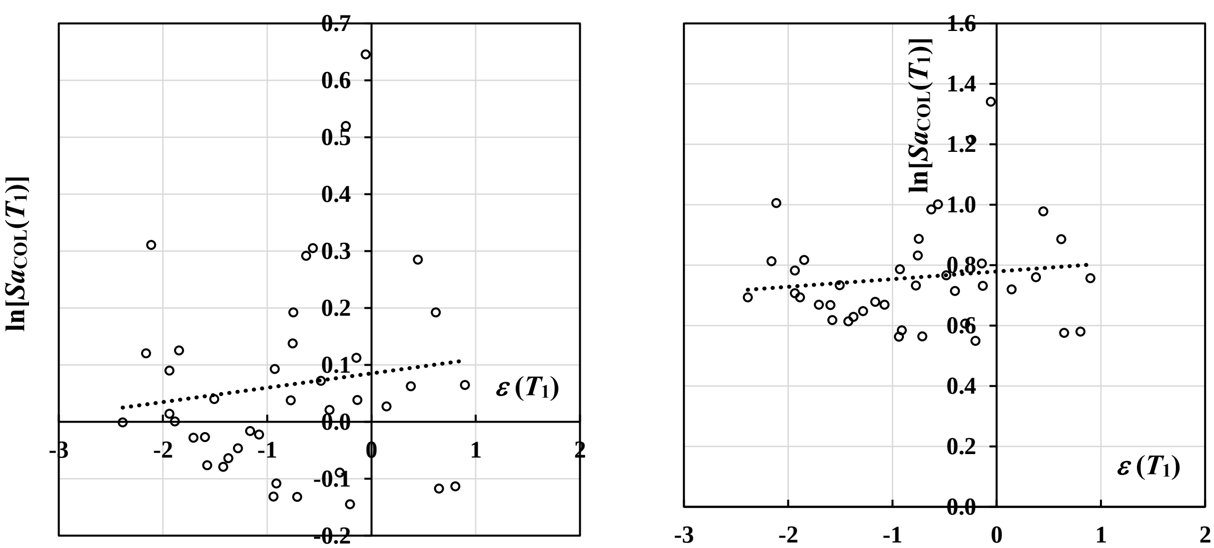


(a) 1$g$ limit ($c_0$=-0.085, $c_1$=0.025) (b) 2$g$ limit ($c_0$=0.779, $c_1$=0.025)

Figure A-27 Relationship between ln[$Sa_{\mathrm{Col},j}(T_1)$] and $\varepsilon_j(T_1)$ of non-isolated transformer with bushing of 4.3Hz as-installed frequency at Loma Linda, CA

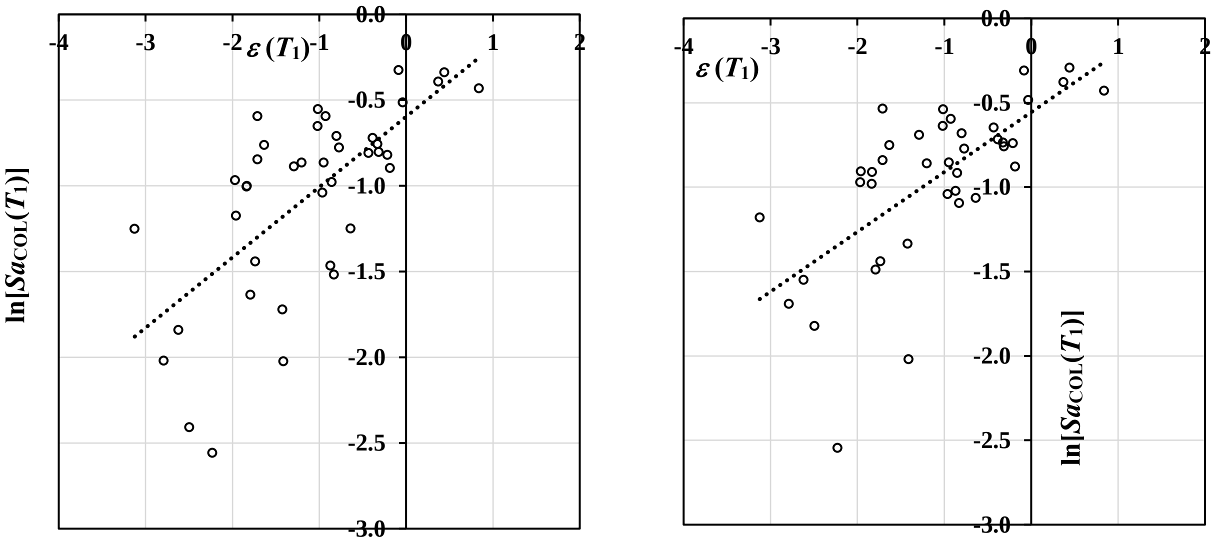


(a) 1$g$ limit ($c_0$=-0.597, $c_1$=0.410) (b) 2$g$ limit ($c_0$=-0.556, $c_1$=0.354)

Figure A-28 Relationship between ln[$Sa_{\mathrm{Col},j}(T_1)$] and $\varepsilon_j(T_1)$ of horizontally isolated transformer ($D_{\mathrm{Capacity}}$=17.7inch, lower bound) with as-installed bushing frequency of 4.3Hz at Loma Linda, CA

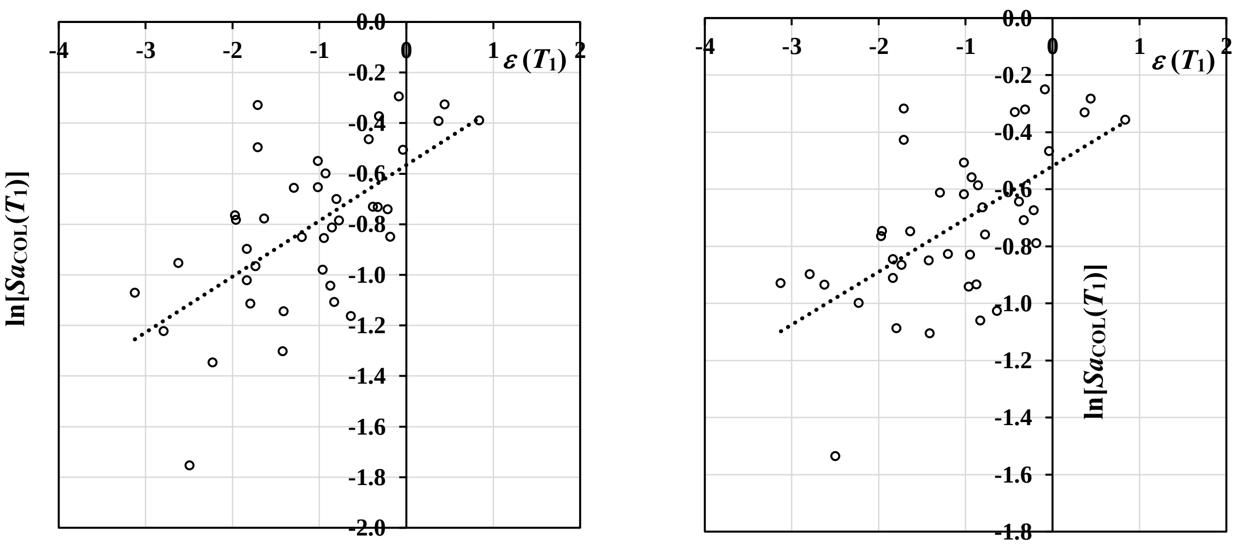


(a) 1$g$ limit ($c_0$=-0.566, $c_1$=0.221) (b) 2$g$ limit ($c_0$=-0.519, $c_1$=0.185)

Figure A-29 Relationship between ln[$Sa_{\mathrm{Col},j}(T_1)$] and $\varepsilon_j(T_1)$ of horizontally-vertically isolated without rocking transformer ($D_{\mathrm{Capacity}}$=17.7inch, lower bound) with as-installed bushing frequency of 4.3Hz at Loma Linda, CA

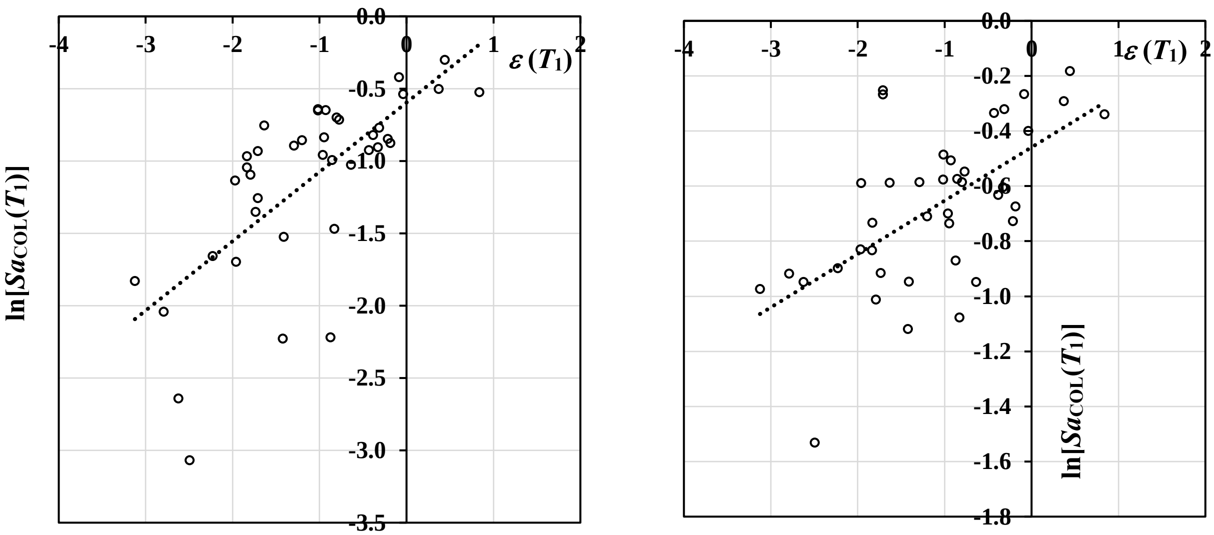


(a) 1$g$ limit ($c_0$=-0.596, $c_1$=0.479) (b) 2$g$ limit ($c_0$=-0.459, $c_1$=0.194)

Figure A-30 Relationship between ln[$Sa_{\mathrm{Col},j}(T_1)$] and $\varepsilon_j(T_1)$ of horizontally-vertically isolated with rocking transformer ($D_{\mathrm{Capacity}}$=17.7inch, lower bound) with as-installed bushing frequency of 4.3Hz at Loma Linda, CA

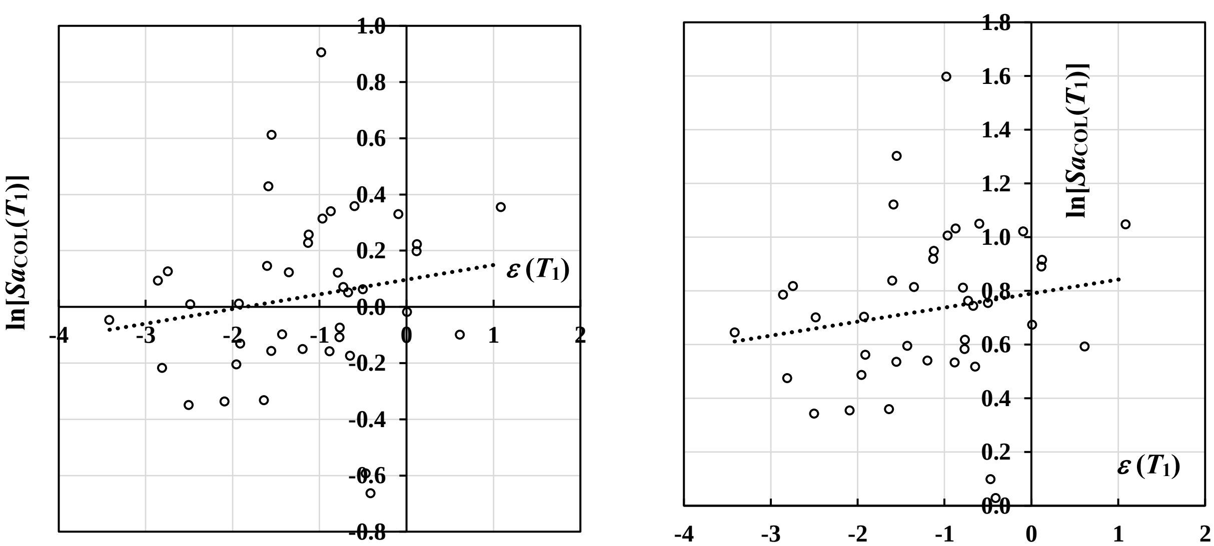


(a) 1$g$ limit ($c_0$=0.097, $c_1$=0.052) (b) 2$g$ limit ($c_0$=0.790, $c_1$=0.052)

Figure A-31 Relationship between ln[$Sa_{\mathrm{Col},j}(T_1)$] and $\varepsilon_j(T_1)$ of non-isolated transformer with bushing of 11.3Hz as-installed frequency at Loma Linda, CA

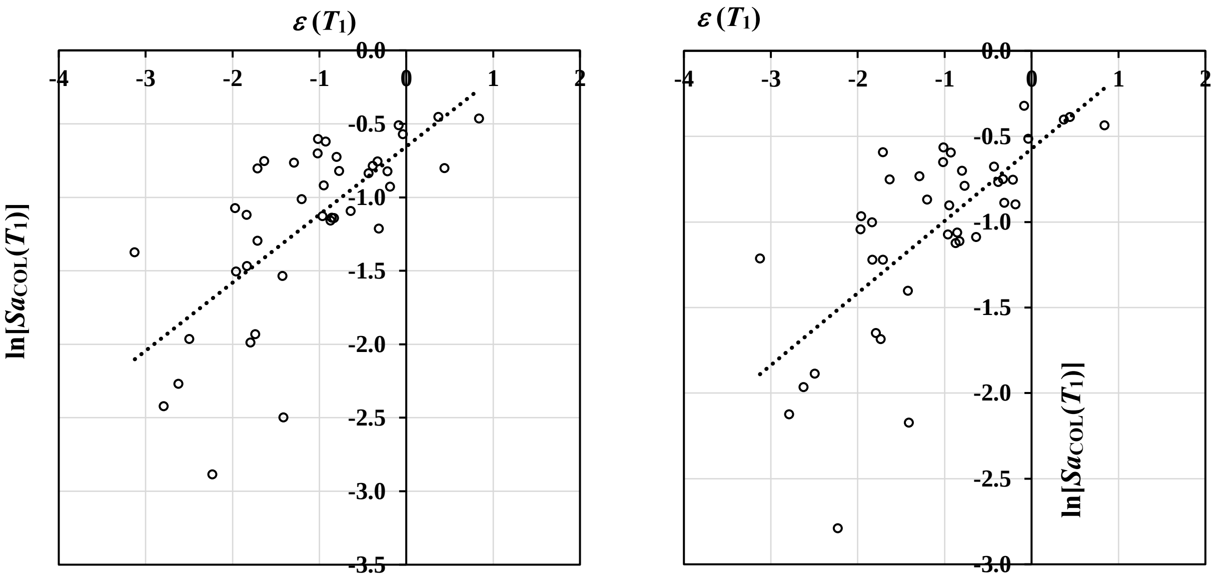


(a) 1$g$ limit ($c_0$=-0.655, $c_1$=0.463)

(b) 2$g$ limit ($c_0$=-0.573, $c_1$=0.422)

Figure A-32 Relationship between ln[$Sa_{\text{Col},j}(T_1)$] and $\varepsilon_j(T_1)$ of horizontally isolated transformer ($D_{\text{Capacity}}$=17.7inch, lower bound) with as-installed bushing frequency of 11.3Hz at Loma Linda, CA

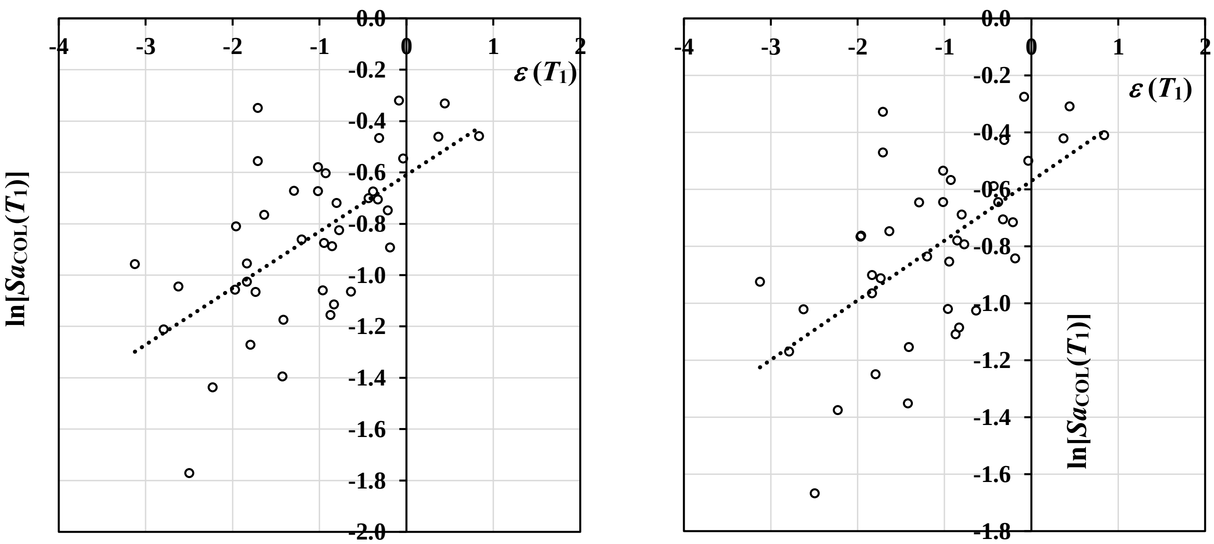


(a) 1$g$ limit ($c_0$=-0.610, $c_1$=0.220)

(b) 2$g$ limit ($c_0$=-0.571, $c_1$=0.209)

Figure A-33 Relationship between ln[$Sa_{\text{Col},j}(T_1)$] and $\varepsilon_j(T_1)$ of horizontally-vertically isolated without rocking transformer ($D_{\text{Capacity}}$=17.7inch, lower bound) with as-installed bushing frequency of 11.3Hz at Loma Linda, CA

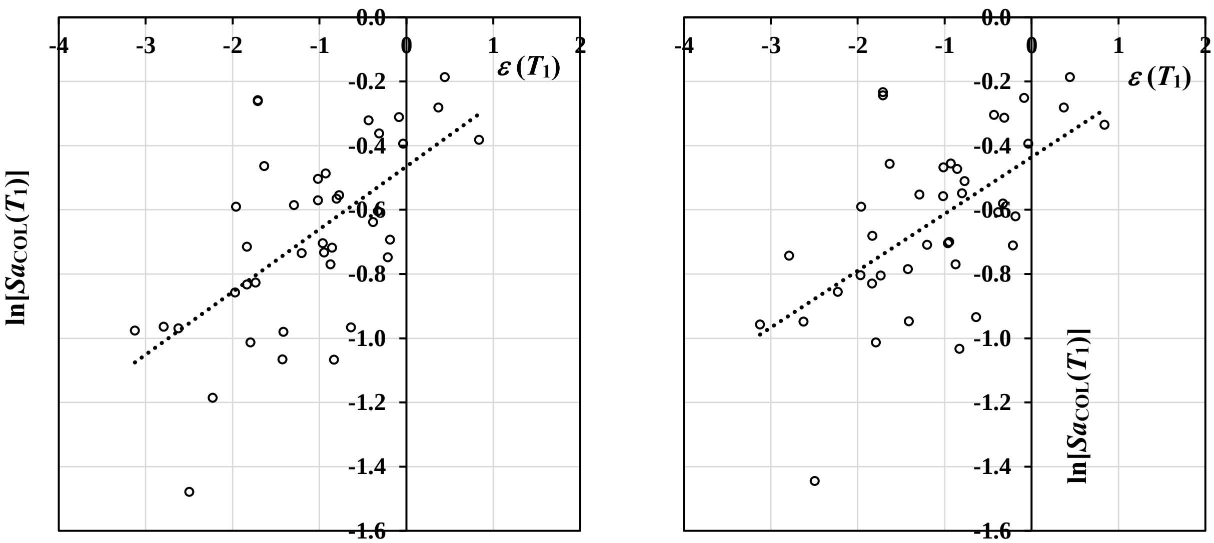


(a) 1$g$ limit ($c_0$=-0.465, $c_1$=0.196)

(b) 2$g$ limit ($c_0$=-0.436, $c_1$=0.177)

Figure A-34 Relationship between ln[$Sa_{\mathrm{Col},j}(T_1)$] and $\varepsilon_j(T_1)$ of horizontally-vertically isolated with rocking transformer ($D_{\mathrm{Capacity}}$=17.7inch, lower bound) with as-installed bushing frequency of 11.3Hz at Loma Linda, CA

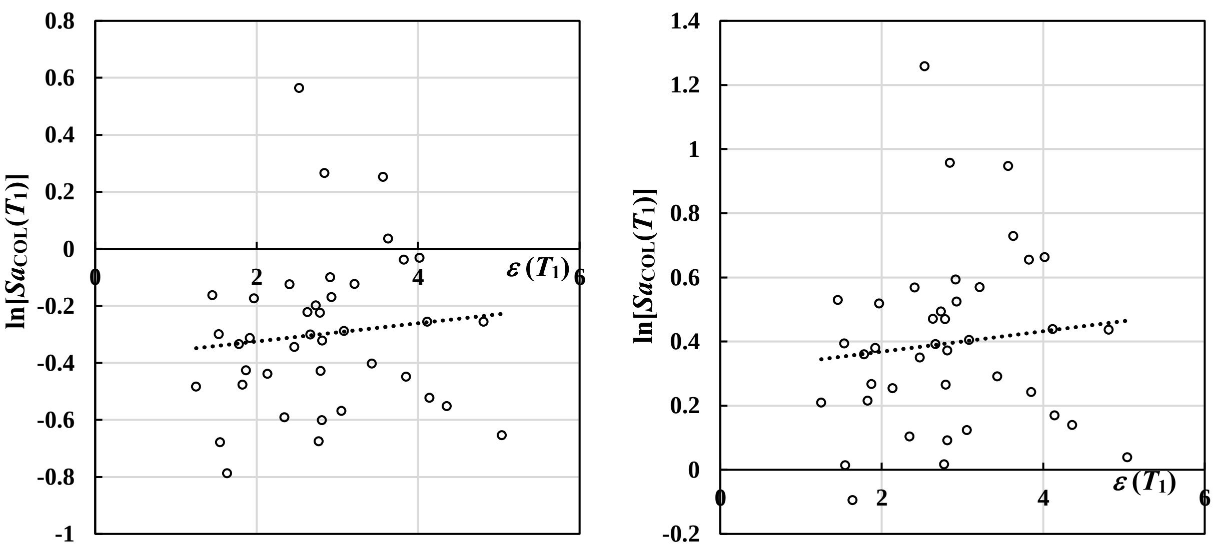


(a) 1$g$ limit ($c_0$=-0.389, $c_1$=0.032)

(b) 2$g$ limit ($c_0$=0.305, $c_1$=0.032)

Figure A-35 Relationship between ln[$Sa_{\mathrm{Col},j}(T_1)$] and $\varepsilon_j(T_1)$ of non-isolated transformer with bushing of 7.7Hz as-installed frequency at Troutdale, OR

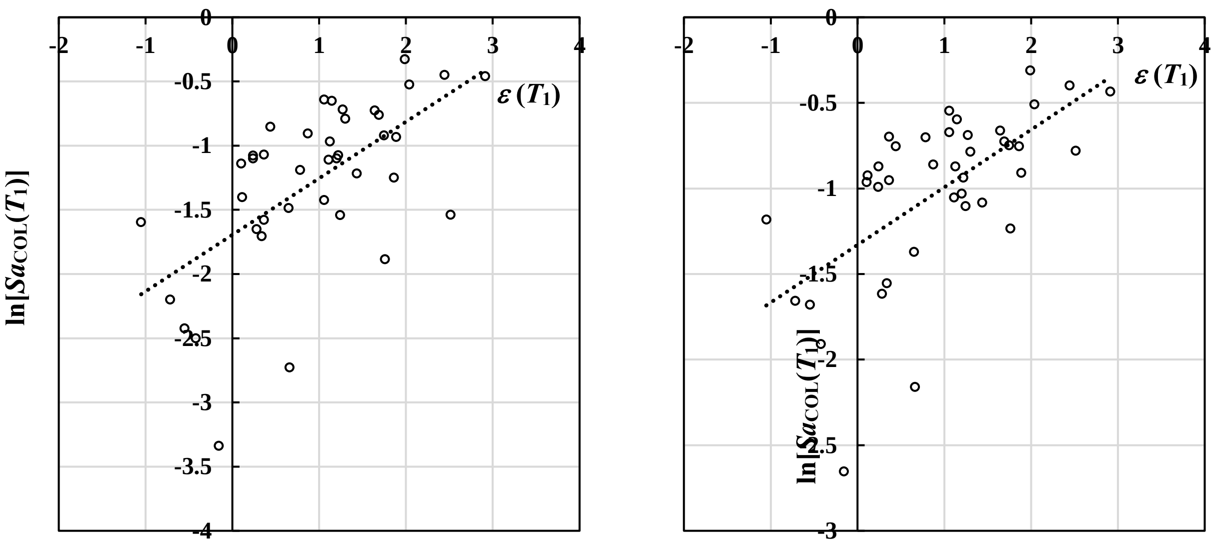


(a) 1$g$ limit ($c_0$=-1.695, $c_1$=0.440) (b) 2$g$ limit ($c_0$=-1.330, $c_1$=0.337)

Figure A-36 Relationship between ln[$Sa_{\mathrm{Col},j}(T_1)$] and $\varepsilon_j(T_1)$ of horizontally isolated transformer ($D_{\mathrm{Capacity}}$=17.7inch, lower bound) with as-installed bushing frequency of 7.7Hz at Troutdale, OR

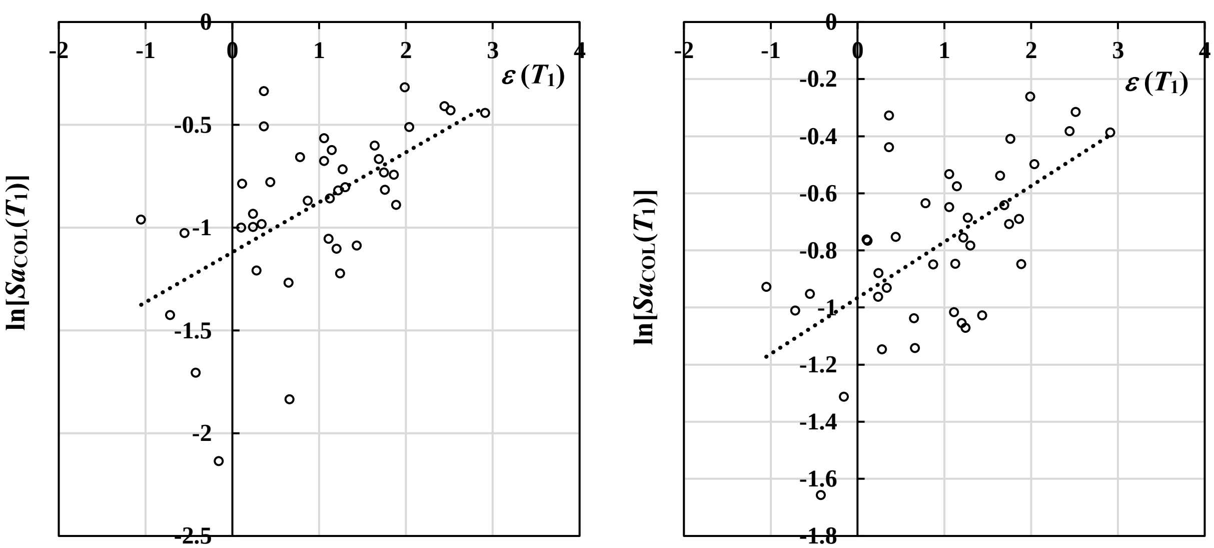


(a) 1$g$ limit ($c_0$=-1.120, $c_1$=0.243) (b) 2$g$ limit ($c_0$=-0.966, $c_1$=0.196)

Figure A-37 Relationship between ln[$Sa_{\mathrm{Col},j}(T_1)$] and $\varepsilon_j(T_1)$ of horizontally-vertically isolated without rocking transformer ($D_{\mathrm{Capacity}}$=17.7inch, lower bound) with as-installed bushing frequency of 7.7Hz at Troutdale, OR

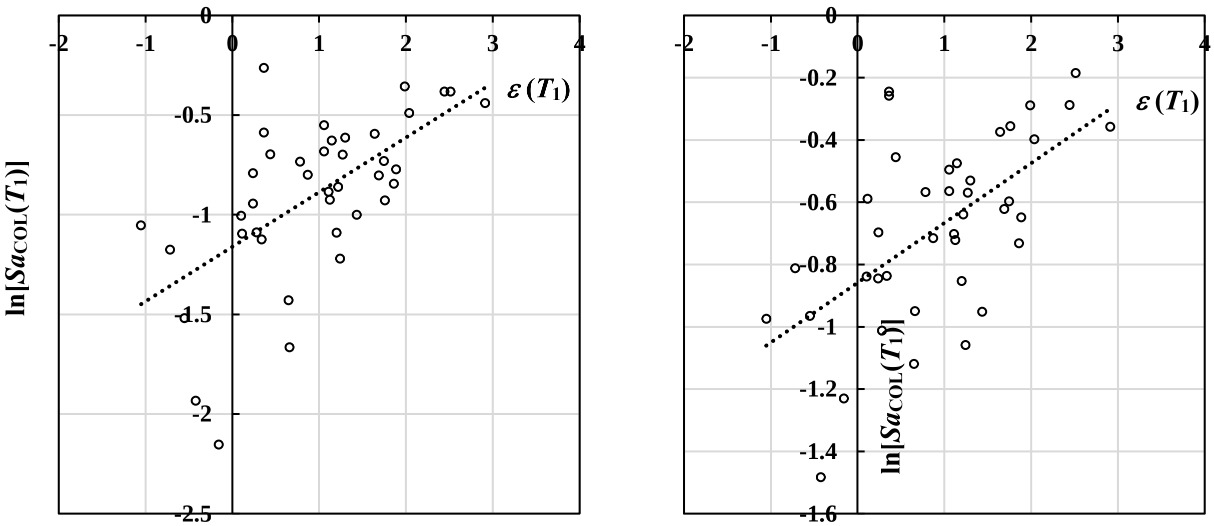


(a) 1$g$ limit ($c_0$=-1.161, $c_1$=0.274)    (b) 2$g$ limit ($c_0$=-0.859, $c_1$=0.192)

Figure A-38 Relationship between ln[$Sa_{\mathrm{Col},j}(T_1)$] and $\varepsilon_j(T_1)$ of horizontally-vertically isolated with rocking transformer ($D_{\mathrm{Capacity}}$=17.7inch, lower bound) with as-installed bushing frequency of 7.7Hz at Troutdale, OR

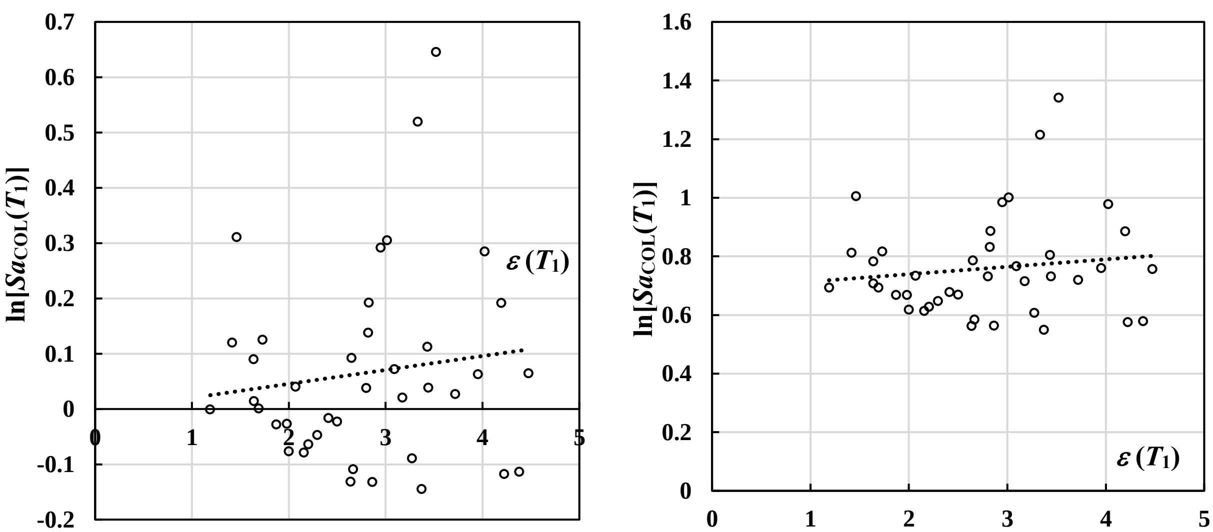


(a) 1$g$ limit ($c_0$=-0.005, $c_1$=0.025)    (b) 2$g$ limit ($c_0$=0.688, $c_1$=0.025)

Figure A-39 Relationship between ln[$Sa_{\mathrm{Col},j}(T_1)$] and $\varepsilon_j(T_1)$ of non-isolated transformer with bushing of 4.3Hz as-installed frequency at Troutdale, OR

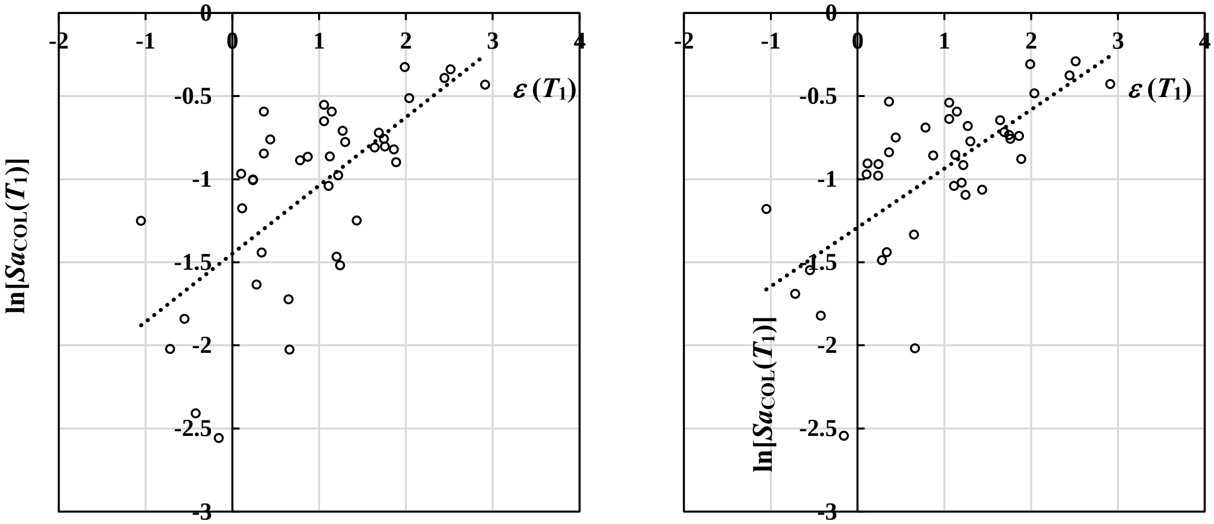


(a) 1$g$ limit ($c_0$=-1.448, $c_1$=0.410) (b) 2$g$ limit ($c_0$=-1.291, $c_1$=0.354)

Figure A-40 Relationship between ln[$Sa_{\mathrm{Col},j}(T_1)$] and $\varepsilon_j(T_1)$ of horizontally isolated transformer (D$_{\mathrm{Capacity}}$=17.7inch, lower bound) with as-installed bushing frequency of 4.3Hz at Troutdale, OR

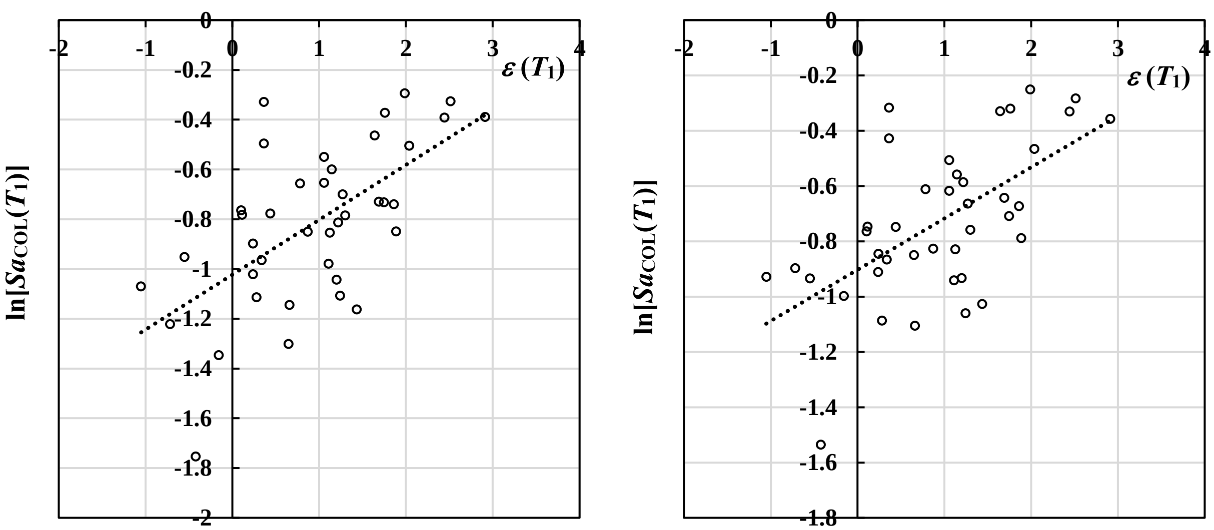


(a) 1$g$ limit ($c_0$=-1.023, $c_1$=0.221) (b) 2$g$ limit ($c_0$=-0.903, $c_1$=0.185)

Figure A-41 Relationship between ln[$Sa_{\mathrm{Col},j}(T_1)$] and $\varepsilon_j(T_1)$ of horizontally-vertically isolated without rocking transformer (D$_{\mathrm{Capacity}}$=17.7inch, lower bound) with as-installed bushing frequency of 4.3Hz at Troutdale, OR

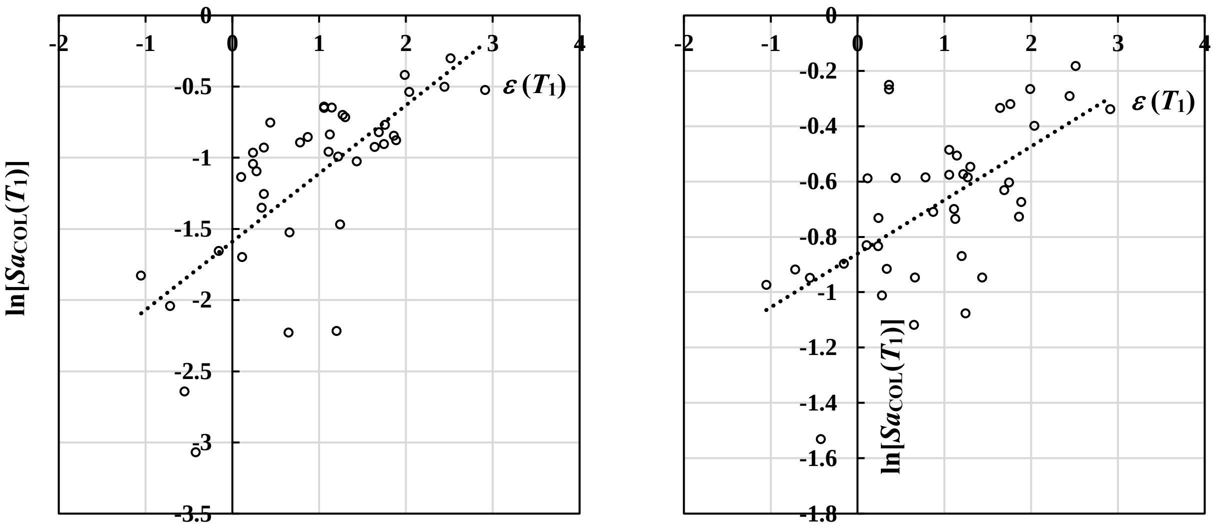


(a) 1$g$ limit ($c_0$=-1.589, $c_1$=0.479) (b) 2$g$ limit ($c_0$=-0.861, $c_1$=0.194)

Figure A-42 Relationship between ln[$Sa_{\mathrm{Col},j}(T_1)$] and $\varepsilon_j(T_1)$ of horizontally-vertically isolated with rocking transformer ($D_{\mathrm{Capacity}}$=17.7inch, lower bound) with as-installed bushing frequency of 4.3Hz at Troutdale, OR

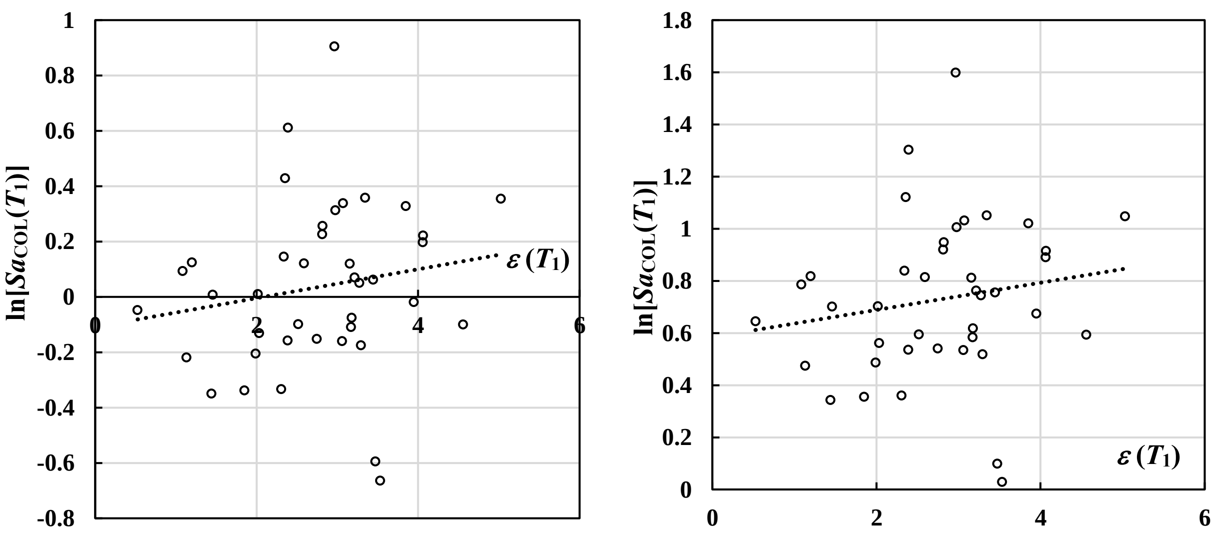


(a) 1$g$ limit ($c_0$=-0.109, $c_1$=0.052) (b) 2$g$ limit ($c_0$=0.584, $c_1$=0.052)

Figure A-43 Relationship between ln[$Sa_{\mathrm{Col},j}(T_1)$] and $\varepsilon_j(T_1)$ of non-isolated transformer with bushing of 11.3Hz as-installed frequency at Troutdale, OR

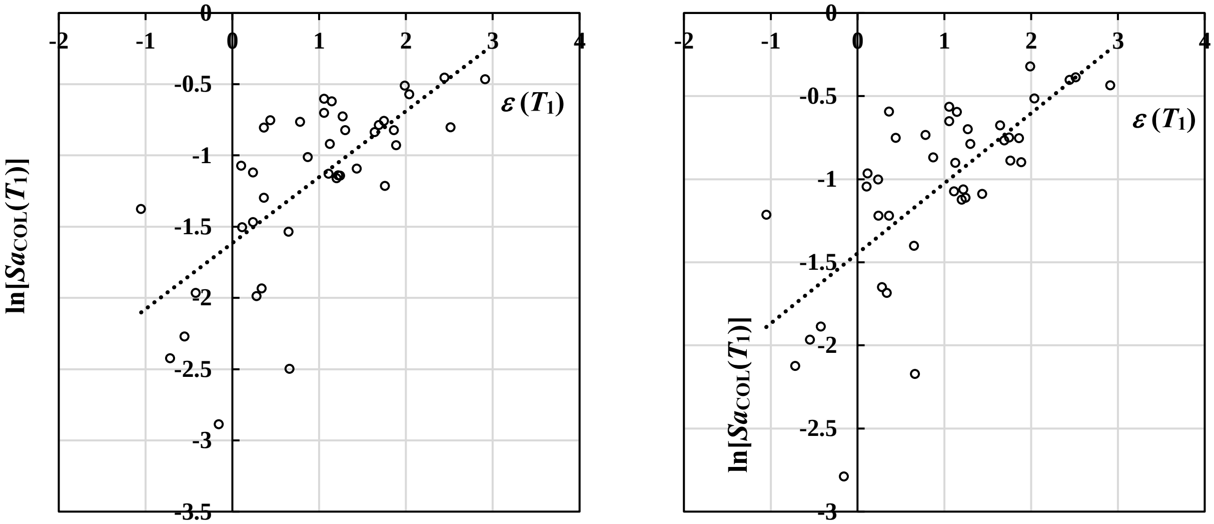


(a) 1*g* limit ($c_0$=-1.615, $c_1$=0.463) (b) 2*g* limit ($c_0$=-1.447, $c_1$=0.422)

Figure A-44 Relationship between ln[$Sa_{\mathrm{Col},j}(T_1)$] and $\varepsilon_j(T_1)$ of horizontally isolated transformer ($\mathrm{D_{Capacity}}$=17.7inch, lower bound) with as-installed bushing frequency of 11.3Hz at Troutdale, OR

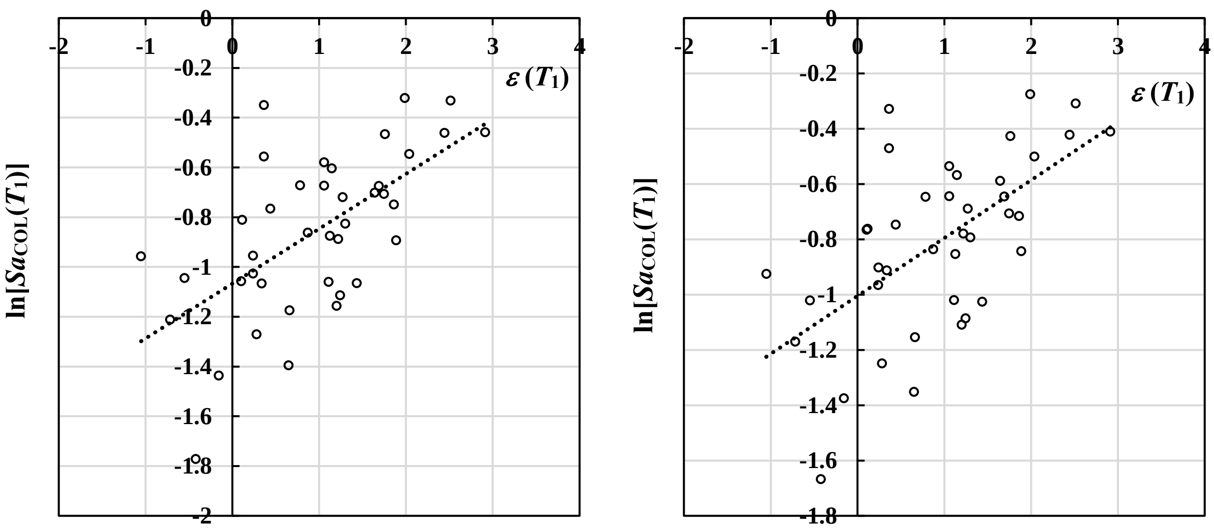


(a) 1*g* limit ($c_0$=-1.067, $c_1$=0.220) (b) 2*g* limit ($c_0$=-1.005, $c_1$=0.209)

Figure A-45 Relationship between ln[$Sa_{\mathrm{Col},j}(T_1)$] and $\varepsilon_j(T_1)$ of horizontally-vertically isolated without rocking transformer ($\mathrm{D_{Capacity}}$=17.7inch, lower bound) with as-installed bushing frequency of 11.3Hz at Troutdale, OR

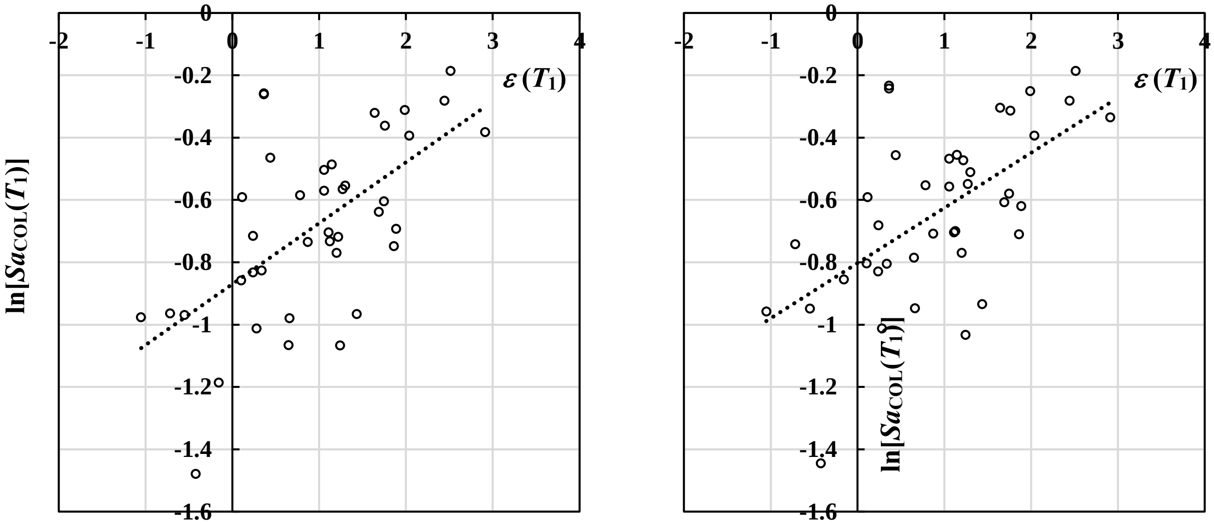


(a) 1$g$ limit ($c_0$=-0.870, $c_1$=0.196) (b) 2$g$ limit ($c_0$=-0.803, $c_1$=0.177)

Figure A-46 Relationship between ln[$Sa_{\mathrm{Col},j}(T_1)$] and $\varepsilon_j(T_1)$ of horizontally-vertically isolated with rocking transformer ($D_{\mathrm{Capacity}}$=17.7inch, lower bound) with as-installed bushing frequency of 11.3Hz at Troutdale, OR

## MCEER Technical Reports

MCEER publishes technical reports on a variety of subjects written by authors funded through MCEER. These reports can be downloaded from the MCEER website at http://www.buffalo.edu/mceer. They can also be requested through NTIS, P.O. Box 1425, Springfield, Virginia 22151. NTIS accession numbers are shown in parenthesis, if available.

NCEER-87-0001 "First-Year Program in Research, Education and Technology Transfer," 3/5/87, (PB88-134275, A04, MF-A01).

NCEER-87-0002 "Experimental Evaluation of Instantaneous Optimal Algorithms for Structural Control," by R.C. Lin, T.T. Soong and A.M. Reinhorn, 4/20/87, (PB88-134341, A04, MF-A01).

NCEER-87-0003 "Experimentation Using the Earthquake Simulation Facilities at University at Buffalo," by A.M. Reinhorn and R.L. Ketter, not available.

NCEER-87-0004 "The System Characteristics and Performance of a Shaking Table," by J.S. Hwang, K.C. Chang and G.C. Lee, 6/1/87, (PB88-134259, A03, MF-A01). This report is available only through NTIS (see address given above).

NCEER-87-0005 "A Finite Element Formulation for Nonlinear Viscoplastic Material Using a Q Model," by O. Gyebi and G. Dasgupta, 11/2/87, (PB88-213764, A08, MF-A01).

NCEER-87-0006 "Symbolic Manipulation Program (SMP) - Algebraic Codes for Two and Three Dimensional Finite Element Formulations," by X. Lee and G. Dasgupta, 11/9/87, (PB88-218522, A05, MF-A01).

NCEER-87-0007 "Instantaneous Optimal Control Laws for Tall Buildings Under Seismic Excitations," by J.N. Yang, A. Akbarpour and P. Ghaemmaghami, 6/10/87, (PB88-134333, A06, MF-A01). This report is only available through NTIS (see address given above).

NCEER-87-0008 "IDARC: Inelastic Damage Analysis of Reinforced Concrete Frame - Shear-Wall Structures," by Y.J. Park, A.M. Reinhorn and S.K. Kunnath, 7/20/87, (PB88-134325, A09, MF-A01). This report is only available through NTIS (see address given above).

NCEER-87-0009 "Liquefaction Potential for New York State: A Preliminary Report on Sites in Manhattan and Buffalo," by M. Budhu, V. Vijayakumar, R.F. Giese and L. Baumgras, 8/31/87, (PB88-163704, A03, MF-A01). This report is available only through NTIS (see address given above).

NCEER-87-0010 "Vertical and Torsional Vibration of Foundations in Inhomogeneous Media," by A.S. Veletsos and K.W. Dotson, 6/1/87, (PB88-134291, A03, MF-A01). This report is only available through NTIS (see address given above).

NCEER-87-0011 "Seismic Probabilistic Risk Assessment and Seismic Margins Studies for Nuclear Power Plants," by Howard H.M. Hwang, 6/15/87, (PB88-134267, A03, MF-A01). This report is only available through NTIS (see address given above).

NCEER-87-0012 "Parametric Studies of Frequency Response of Secondary Systems Under Ground-Acceleration Excitations," by Y. Yong and Y.K. Lin, 6/10/87, (PB88-134309, A03, MF-A01). This report is only available through NTIS (see address given above).

NCEER-87-0013 "Frequency Response of Secondary Systems Under Seismic Excitation," by J.A. HoLung, J. Cai and Y.K. Lin, 7/31/87, (PB88-134317, A05, MF-A01). This report is only available through NTIS (see address given above).

NCEER-87-0014 "Modelling Earthquake Ground Motions in Seismically Active Regions Using Parametric Time Series Methods," by G.W. Ellis and A.S. Cakmak, 8/25/87, (PB88-134283, A08, MF-A01). This report is only available through NTIS (see address given above).

NCEER-87-0015 "Detection and Assessment of Seismic Structural Damage," by E. DiPasquale and A.S. Cakmak, 8/25/87, (PB88-163712, A05, MF-A01). This report is only available through NTIS (see address given above).

NCEER-87-0016 "Pipeline Experiment at Parkfield, California," by J. Isenberg and E. Richardson, 9/15/87, (PB88-163720, A03, MF-A01). This report is available only through NTIS (see address given above).

NCEER-87-0017 "Digital Simulation of Seismic Ground Motion," by M. Shinozuka, G. Deodatis and T. Harada, 8/31/87, (PB88-155197, A04, MF-A01). This report is available only through NTIS (see address given above).

NCEER-87-0018 "Practical Considerations for Structural Control: System Uncertainty, System Time Delay and Truncation of Small Control Forces," J.N. Yang and A. Akbarpour, 8/10/87, (PB88-163738, A08, MF-A01). This report is only available through NTIS (see address given above).

NCEER-87-0019 "Modal Analysis of Nonclassically Damped Structural Systems Using Canonical Transformation," by J.N. Yang, S. Sarkani and F.X. Long, 9/27/87, (PB88-187851, A04, MF-A01).

NCEER-87-0020 "A Nonstationary Solution in Random Vibration Theory," by J.R. Red-Horse and P.D. Spanos, 11/3/87, (PB88-163746, A03, MF-A01).

NCEER-87-0021 "Horizontal Impedances for Radially Inhomogeneous Viscoelastic Soil Layers," by A.S. Veletsos and K.W. Dotson, 10/15/87, (PB88-150859, A04, MF-A01).

NCEER-87-0022 "Seismic Damage Assessment of Reinforced Concrete Members," by Y.S. Chung, C. Meyer and M. Shinozuka, 10/9/87, (PB88-150867, A05, MF-A01). This report is available only through NTIS (see address given above).

NCEER-87-0023 "Active Structural Control in Civil Engineering," by T.T. Soong, 11/11/87, (PB88-187778, A03, MF-A01).

NCEER-87-0024 "Vertical and Torsional Impedances for Radially Inhomogeneous Viscoelastic Soil Layers," by K.W. Dotson and A.S. Veletsos, 12/87, (PB88-187786, A03, MF-A01).

NCEER-87-0025 "Proceedings from the Symposium on Seismic Hazards, Ground Motions, Soil-Liquefaction and Engineering Practice in Eastern North America," October 20-22, 1987, edited by K.H. Jacob, 12/87, (PB88-188115, A23, MF-A01). This report is available only through NTIS (see address given above).

NCEER-87-0026 "Report on the Whittier-Narrows, California, Earthquake of October 1, 1987," by J. Pantelic and A. Reinhorn, 11/87, (PB88-187752, A03, MF-A01). This report is available only through NTIS (see address given above).

NCEER-87-0027 "Design of a Modular Program for Transient Nonlinear Analysis of Large 3-D Building Structures," by S. Srivastav and J.F. Abel, 12/30/87, (PB88-187950, A05, MF-A01). This report is only available through NTIS (see address given above).

NCEER-87-0028 "Second-Year Program in Research, Education and Technology Transfer," 3/8/88, (PB88-219480, A04, MF-A01).

NCEER-88-0001 "Workshop on Seismic Computer Analysis and Design of Buildings With Interactive Graphics," by W. McGuire, J.F. Abel and C.H. Conley, 1/18/88, (PB88-187760, A03, MF-A01). This report is only available through NTIS (see address given above).

NCEER-88-0002 "Optimal Control of Nonlinear Flexible Structures," by J.N. Yang, F.X. Long and D. Wong, 1/22/88, (PB88-213772, A06, MF-A01).

NCEER-88-0003 "Substructuring Techniques in the Time Domain for Primary-Secondary Structural Systems," by G.D. Manolis and G. Juhn, 2/10/88, (PB88-213780, A04, MF-A01).

NCEER-88-0004 "Iterative Seismic Analysis of Primary-Secondary Systems," by A. Singhal, L.D. Lutes and P.D. Spanos, 2/23/88, (PB88-213798, A04, MF-A01).

NCEER-88-0005 "Stochastic Finite Element Expansion for Random Media," by P.D. Spanos and R. Ghanem, 3/14/88, (PB88-213806, A03, MF-A01).

NCEER-88-0006 "Combining Structural Optimization and Structural Control," by F.Y. Cheng and C.P. Pantelides, 1/10/88, (PB88-213814, A05, MF-A01).

NCEER-88-0007 "Seismic Performance Assessment of Code-Designed Structures," by H.H-M. Hwang, J-W. Jaw and H-J. Shau, 3/20/88, (PB88-219423, A04, MF-A01). This report is only available through NTIS (see address given above).

NCEER-88-0008 "Reliability Analysis of Code-Designed Structures Under Natural Hazards," by H.H-M. Hwang, H. Ushiba and M. Shinozuka, 2/29/88, (PB88-229471, A07, MF-A01). This report is only available through NTIS (see address given above).

NCEER-88-0009 "Seismic Fragility Analysis of Shear Wall Structures," by J-W Jaw and H.H-M. Hwang, 4/30/88, (PB89-102867, A04, MF-A01).

NCEER-88-0010 "Base Isolation of a Multi-Story Building Under a Harmonic Ground Motion - A Comparison of Performances of Various Systems," by F-G Fan, G. Ahmadi and I.G. Tadjbakhsh, 5/18/88, (PB89-122238, A06, MF-A01). This report is only available through NTIS (see address given above).

NCEER-88-0011 "Seismic Floor Response Spectra for a Combined System by Green's Functions," by F.M. Lavelle, L.A. Bergman and P.D. Spanos, 5/1/88, (PB89-102875, A03, MF-A01).

NCEER-88-0012 "A New Solution Technique for Randomly Excited Hysteretic Structures," by G.Q. Cai and Y.K. Lin, 5/16/88, (PB89-102883, A03, MF-A01).

NCEER-88-0013 "A Study of Radiation Damping and Soil-Structure Interaction Effects in the Centrifuge," by K. Weissman, supervised by J.H. Prevost, 5/24/88, (PB89-144703, A06, MF-A01).

NCEER-88-0014 "Parameter Identification and Implementation of a Kinematic Plasticity Model for Frictional Soils," by J.H. Prevost and D.V. Griffiths, not available.

NCEER-88-0015 "Two- and Three- Dimensional Dynamic Finite Element Analyses of the Long Valley Dam," by D.V. Griffiths and J.H. Prevost, 6/17/88, (PB89-144711, A04, MF-A01).

NCEER-88-0016 "Damage Assessment of Reinforced Concrete Structures in Eastern United States," by A.M. Reinhorn, M.J. Seidel, S.K. Kunnath and Y.J. Park, 6/15/88, (PB89-122220, A04, MF-A01). This report is only available through NTIS (see address given above).

NCEER-88-0017 "Dynamic Compliance of Vertically Loaded Strip Foundations in Multilayered Viscoelastic Soils," by S. Ahmad and A.S.M. Israil, 6/17/88, (PB89-102891, A04, MF-A01).

NCEER-88-0018 "An Experimental Study of Seismic Structural Response With Added Viscoelastic Dampers," by R.C. Lin, Z. Liang, T.T. Soong and R.H. Zhang, 6/30/88, (PB89-122212, A05, MF-A01). This report is available only through NTIS (see address given above).

NCEER-88-0019 "Experimental Investigation of Primary - Secondary System Interaction," by G.D. Manolis, G. Juhn and A.M. Reinhorn, 5/27/88, (PB89-122204, A04, MF-A01).

NCEER-88-0020 "A Response Spectrum Approach For Analysis of Nonclassically Damped Structures," by J.N. Yang, S. Sarkani and F.X. Long, 4/22/88, (PB89-102909, A04, MF-A01).

NCEER-88-0021 "Seismic Interaction of Structures and Soils: Stochastic Approach," by A.S. Veletsos and A.M. Prasad, 7/21/88, (PB89-122196, A04, MF-A01). This report is only available through NTIS (see address given above).

NCEER-88-0022 "Identification of the Serviceability Limit State and Detection of Seismic Structural Damage," by E. DiPasquale and A.S. Cakmak, 6/15/88, (PB89-122188, A05, MF-A01). This report is available only through NTIS (see address given above).

NCEER-88-0023 "Multi-Hazard Risk Analysis: Case of a Simple Offshore Structure," by B.K. Bhartia and E.H. Vanmarcke, 7/21/88, (PB89-145213, A05, MF-A01).

NCEER-88-0024 "Automated Seismic Design of Reinforced Concrete Buildings," by Y.S. Chung, C. Meyer and M. Shinozuka, 7/5/88, (PB89-122170, A06, MF-A01). This report is available only through NTIS (see address given above).

NCEER-88-0025 "Experimental Study of Active Control of MDOF Structures Under Seismic Excitations," by L.L. Chung, R.C. Lin, T.T. Soong and A.M. Reinhorn, 7/10/88, (PB89-122600, A04, MF-A01).

NCEER-88-0026 "Earthquake Simulation Tests of a Low-Rise Metal Structure," by J.S. Hwang, K.C. Chang, G.C. Lee and R.L. Ketter, 8/1/88, (PB89-102917, A04, MF-A01).

NCEER-88-0027 "Systems Study of Urban Response and Reconstruction Due to Catastrophic Earthquakes," by F. Kozin and H.K. Zhou, 9/22/88, (PB90-162348, A04, MF-A01).

NCEER-88-0028 "Seismic Fragility Analysis of Plane Frame Structures," by H.H-M. Hwang and Y.K. Low, 7/31/88, (PB89-131445, A06, MF-A01).

NCEER-88-0029 "Response Analysis of Stochastic Structures," by A. Kardara, C. Bucher and M. Shinozuka, 9/22/88, (PB89-174429, A04, MF-A01).

NCEER-88-0030 "Nonnormal Accelerations Due to Yielding in a Primary Structure," by D.C.K. Chen and L.D. Lutes, 9/19/88, (PB89-131437, A04, MF-A01).

NCEER-88-0031 "Design Approaches for Soil-Structure Interaction," by A.S. Veletsos, A.M. Prasad and Y. Tang, 12/30/88, (PB89-174437, A03, MF-A01). This report is available only through NTIS (see address given above).

NCEER-88-0032 "A Re-evaluation of Design Spectra for Seismic Damage Control," by C.J. Turkstra and A.G. Tallin, 11/7/88, (PB89-145221, A05, MF-A01).

NCEER-88-0033 "The Behavior and Design of Noncontact Lap Splices Subjected to Repeated Inelastic Tensile Loading," by V.E. Sagan, P. Gergely and R.N. White, 12/8/88, (PB89-163737, A08, MF-A01).

NCEER-88-0034 "Seismic Response of Pile Foundations," by S.M. Mamoon, P.K. Banerjee and S. Ahmad, 11/1/88, (PB89-145239, A04, MF-A01).

NCEER-88-0035 "Modeling of R/C Building Structures With Flexible Floor Diaphragms (IDARC2)," by A.M. Reinhorn, S.K. Kunnath and N. Panahshahi, 9/7/88, (PB89-207153, A07, MF-A01).

NCEER-88-0036 "Solution of the Dam-Reservoir Interaction Problem Using a Combination of FEM, BEM with Particular Integrals, Modal Analysis, and Substructuring," by C-S. Tsai, G.C. Lee and R.L. Ketter, 12/31/88, (PB89-207146, A04, MF-A01).

NCEER-88-0037 "Optimal Placement of Actuators for Structural Control," by F.Y. Cheng and C.P. Pantelides, 8/15/88, (PB89-162846, A05, MF-A01).

NCEER-88-0038 "Teflon Bearings in Aseismic Base Isolation: Experimental Studies and Mathematical Modeling," by A. Mokha, M.C. Constantinou and A.M. Reinhorn, 12/5/88, (PB89-218457, A10, MF-A01). This report is available only through NTIS (see address given above).

NCEER-88-0039 "Seismic Behavior of Flat Slab High-Rise Buildings in the New York City Area," by P. Weidlinger and M. Ettouney, 10/15/88, (PB90-145681, A04, MF-A01).

NCEER-88-0040 "Evaluation of the Earthquake Resistance of Existing Buildings in New York City," by P. Weidlinger and M. Ettouney, 10/15/88, not available.

NCEER-88-0041 "Small-Scale Modeling Techniques for Reinforced Concrete Structures Subjected to Seismic Loads," by W. Kim, A. El-Attar and R.N. White, 11/22/88, (PB89-189625, A05, MF-A01).

NCEER-88-0042 "Modeling Strong Ground Motion from Multiple Event Earthquakes," by G.W. Ellis and A.S. Cakmak, 10/15/88, (PB89-174445, A03, MF-A01).

NCEER-88-0043 "Nonstationary Models of Seismic Ground Acceleration," by M. Grigoriu, S.E. Ruiz and E. Rosenblueth, 7/15/88, (PB89-189617, A04, MF-A01).

NCEER-88-0044 "SARCF User's Guide: Seismic Analysis of Reinforced Concrete Frames," by Y.S. Chung, C. Meyer and M. Shinozuka, 11/9/88, (PB89-174452, A08, MF-A01).

NCEER-88-0045 "First Expert Panel Meeting on Disaster Research and Planning," edited by J. Pantelic and J. Stoyle, 9/15/88, (PB89-174460, A05, MF-A01).

NCEER-88-0046 "Preliminary Studies of the Effect of Degrading Infill Walls on the Nonlinear Seismic Response of Steel Frames," by C.Z. Chrysostomou, P. Gergely and J.F. Abel, 12/19/88, (PB89-208383, A05, MF-A01).

NCEER-88-0047 "Reinforced Concrete Frame Component Testing Facility - Design, Construction, Instrumentation and Operation," by S.P. Pessiki, C. Conley, T. Bond, P. Gergely and R.N. White, 12/16/88, (PB89-174478, A04, MF-A01).

NCEER-89-0001 "Effects of Protective Cushion and Soil Compliancy on the Response of Equipment Within a Seismically Excited Building," by J.A. HoLung, 2/16/89, (PB89-207179, A04, MF-A01).

NCEER-89-0002 "Statistical Evaluation of Response Modification Factors for Reinforced Concrete Structures," by H.H-M. Hwang and J-W. Jaw, 2/17/89, (PB89-207187, A05, MF-A01).

NCEER-89-0003 "Hysteretic Columns Under Random Excitation," by G-Q. Cai and Y.K. Lin, 1/9/89, (PB89-196513, A03, MF-A01).

NCEER-89-0004 "Experimental Study of `Elephant Foot Bulge' Instability of Thin-Walled Metal Tanks," by Z-H. Jia and R.L. Ketter, 2/22/89, (PB89-207195, A03, MF-A01).

NCEER-89-0005 "Experiment on Performance of Buried Pipelines Across San Andreas Fault," by J. Isenberg, E. Richardson and T.D. O'Rourke, 3/10/89, (PB89-218440, A04, MF-A01). This report is available only through NTIS (see address given above).

NCEER-89-0006 "A Knowledge-Based Approach to Structural Design of Earthquake-Resistant Buildings," by M. Subramani, P. Gergely, C.H. Conley, J.F. Abel and A.H. Zaghw, 1/15/89, (PB89-218465, A06, MF-A01).

NCEER-89-0007 "Liquefaction Hazards and Their Effects on Buried Pipelines," by T.D. O'Rourke and P.A. Lane, 2/1/89, (PB89-218481, A09, MF-A01).

NCEER-89-0008 "Fundamentals of System Identification in Structural Dynamics," by H. Imai, C-B. Yun, O. Maruyama and M. Shinozuka, 1/26/89, (PB89-207211, A04, MF-A01).

NCEER-89-0009 "Effects of the 1985 Michoacan Earthquake on Water Systems and Other Buried Lifelines in Mexico," by A.G. Ayala and M.J. O'Rourke, 3/8/89, (PB89-207229, A06, MF-A01).

NCEER-89-R010 "NCEER Bibliography of Earthquake Education Materials," by K.E.K. Ross, Second Revision, 9/1/89, (PB90-125352, A05, MF-A01). This report is replaced by NCEER-92-0018.

NCEER-89-0011 "Inelastic Three-Dimensional Response Analysis of Reinforced Concrete Building Structures (IDARC-3D), Part I - Modeling," by S.K. Kunnath and A.M. Reinhorn, 4/17/89, (PB90-114612, A07, MF-A01). This report is available only through NTIS (see address given above).

NCEER-89-0012 "Recommended Modifications to ATC-14," by C.D. Poland and J.O. Malley, 4/12/89, (PB90-108648, A15, MF-A01).

NCEER-89-0013 "Repair and Strengthening of Beam-to-Column Connections Subjected to Earthquake Loading," by M. Corazao and A.J. Durrani, 2/28/89, (PB90-109885, A06, MF-A01).

NCEER-89-0014 "Program EXKAL2 for Identification of Structural Dynamic Systems," by O. Maruyama, C-B. Yun, M. Hoshiya and M. Shinozuka, 5/19/89, (PB90-109877, A09, MF-A01).

NCEER-89-0015 "Response of Frames With Bolted Semi-Rigid Connections, Part I - Experimental Study and Analytical Predictions," by P.J. DiCorso, A.M. Reinhorn, J.R. Dickerson, J.B. Radziminski and W.L. Harper, 6/1/89, not available.

NCEER-89-0016 "ARMA Monte Carlo Simulation in Probabilistic Structural Analysis," by P.D. Spanos and M.P. Mignolet, 7/10/89, (PB90-109893, A03, MF-A01).

NCEER-89-P017 "Preliminary Proceedings from the Conference on Disaster Preparedness - The Place of Earthquake Education in Our Schools," Edited by K.E.K. Ross, 6/23/89, (PB90-108606, A03, MF-A01).

NCEER-89-0017 "Proceedings from the Conference on Disaster Preparedness - The Place of Earthquake Education in Our Schools," Edited by K.E.K. Ross, 12/31/89, (PB90-207895, A012, MF-A02). This report is available only through NTIS (see address given above).

NCEER-89-0018 "Multidimensional Models of Hysteretic Material Behavior for Vibration Analysis of Shape Memory Energy Absorbing Devices, by E.J. Graesser and F.A. Cozzarelli, 6/7/89, (PB90-164146, A04, MF-A01).

NCEER-89-0019 "Nonlinear Dynamic Analysis of Three-Dimensional Base Isolated Structures (3D-BASIS)," by S. Nagarajaiah, A.M. Reinhorn and M.C. Constantinou, 8/3/89, (PB90-161936, A06, MF-A01). This report has been replaced by NCEER-93-0011.

NCEER-89-0020 "Structural Control Considering Time-Rate of Control Forces and Control Rate Constraints," by F.Y. Cheng and C.P. Pantelides, 8/3/89, (PB90-120445, A04, MF-A01).

NCEER-89-0021 "Subsurface Conditions of Memphis and Shelby County," by K.W. Ng, T-S. Chang and H-H.M. Hwang, 7/26/89, (PB90-120437, A03, MF-A01).

NCEER-89-0022 "Seismic Wave Propagation Effects on Straight Jointed Buried Pipelines," by K. Elhmadi and M.J. O'Rourke, 8/24/89, (PB90-162322, A10, MF-A02).

NCEER-89-0023 "Workshop on Serviceability Analysis of Water Delivery Systems," edited by M. Grigoriu, 3/6/89, (PB90-127424, A03, MF-A01).

NCEER-89-0024 "Shaking Table Study of a 1/5 Scale Steel Frame Composed of Tapered Members," by K.C. Chang, J.S. Hwang and G.C. Lee, 9/18/89, (PB90-160169, A04, MF-A01).

NCEER-89-0025 "DYNA1D: A Computer Program for Nonlinear Seismic Site Response Analysis - Technical Documentation," by Jean H. Prevost, 9/14/89, (PB90-161944, A07, MF-A01). This report is available only through NTIS (see address given above).

NCEER-89-0026 "1:4 Scale Model Studies of Active Tendon Systems and Active Mass Dampers for Aseismic Protection," by A.M. Reinhorn, T.T. Soong, R.C. Lin, Y.P. Yang, Y. Fukao, H. Abe and M. Nakai, 9/15/89, (PB90-173246, A10, MF-A02). This report is available only through NTIS (see address given above).

NCEER-89-0027 "Scattering of Waves by Inclusions in a Nonhomogeneous Elastic Half Space Solved by Boundary Element Methods," by P.K. Hadley, A. Askar and A.S. Cakmak, 6/15/89, (PB90-145699, A07, MF-A01).

NCEER-89-0028 "Statistical Evaluation of Deflection Amplification Factors for Reinforced Concrete Structures," by H.H.M. Hwang, J-W. Jaw and A.L. Ch'ng, 8/31/89, (PB90-164633, A05, MF-A01).

NCEER-89-0029 "Bedrock Accelerations in Memphis Area Due to Large New Madrid Earthquakes," by H.H.M. Hwang, C.H.S. Chen and G. Yu, 11/7/89, (PB90-162330, A04, MF-A01).

NCEER-89-0030 "Seismic Behavior and Response Sensitivity of Secondary Structural Systems," by Y.Q. Chen and T.T. Soong, 10/23/89, (PB90-164658, A08, MF-A01).

NCEER-89-0031 "Random Vibration and Reliability Analysis of Primary-Secondary Structural Systems," by Y. Ibrahim, M. Grigoriu and T.T. Soong, 11/10/89, (PB90-161951, A04, MF-A01).

NCEER-89-0032 "Proceedings from the Second U.S. - Japan Workshop on Liquefaction, Large Ground Deformation and Their Effects on Lifelines, September 26-29, 1989," Edited by T.D. O'Rourke and M. Hamada, 12/1/89, (PB90-209388, A22, MF-A03).

NCEER-89-0033 "Deterministic Model for Seismic Damage Evaluation of Reinforced Concrete Structures," by J.M. Bracci, A.M. Reinhorn, J.B. Mander and S.K. Kunnath, 9/27/89, (PB91-108803, A06, MF-A01).

NCEER-89-0034 "On the Relation Between Local and Global Damage Indices," by E. DiPasquale and A.S. Cakmak, 8/15/89, (PB90-173865, A05, MF-A01).

NCEER-89-0035 "Cyclic Undrained Behavior of Nonplastic and Low Plasticity Silts," by A.J. Walker and H.E. Stewart, 7/26/89, (PB90-183518, A10, MF-A01).

NCEER-89-0036 "Liquefaction Potential of Surficial Deposits in the City of Buffalo, New York," by M. Budhu, R. Giese and L. Baumgrass, 1/17/89, (PB90-208455, A04, MF-A01).

NCEER-89-0037 "A Deterministic Assessment of Effects of Ground Motion Incoherence," by A.S. Veletsos and Y. Tang, 7/15/89, (PB90-164294, A03, MF-A01).

NCEER-89-0038 "Workshop on Ground Motion Parameters for Seismic Hazard Mapping," July 17-18, 1989, edited by R.V. Whitman, 12/1/89, (PB90-173923, A04, MF-A01).

NCEER-89-0039 "Seismic Effects on Elevated Transit Lines of the New York City Transit Authority," by C.J. Costantino, C.A. Miller and E. Heymsfield, 12/26/89, (PB90-207887, A06, MF-A01).

NCEER-89-0040 "Centrifugal Modeling of Dynamic Soil-Structure Interaction," by K. Weissman, Supervised by J.H. Prevost, 5/10/89, (PB90-207879, A07, MF-A01).

NCEER-89-0041 "Linearized Identification of Buildings With Cores for Seismic Vulnerability Assessment," by I-K. Ho and A.E. Aktan, 11/1/89, (PB90-251943, A07, MF-A01).

NCEER-90-0001 "Geotechnical and Lifeline Aspects of the October 17, 1989 Loma Prieta Earthquake in San Francisco," by T.D. O'Rourke, H.E. Stewart, F.T. Blackburn and T.S. Dickerman, 1/90, (PB90-208596, A05, MF-A01).

NCEER-90-0002 "Nonnormal Secondary Response Due to Yielding in a Primary Structure," by D.C.K. Chen and L.D. Lutes, 2/28/90, (PB90-251976, A07, MF-A01).

NCEER-90-0003 "Earthquake Education Materials for Grades K-12," by K.E.K. Ross, 4/16/90, (PB91-251984, A05, MF-A05). This report has been replaced by NCEER-92-0018.

NCEER-90-0004 "Catalog of Strong Motion Stations in Eastern North America," by R.W. Busby, 4/3/90, (PB90-251984, A05, MF-A01).

NCEER-90-0005 "NCEER Strong-Motion Data Base: A User Manual for the GeoBase Release (Version 1.0 for the Sun3)," by P. Friberg and K. Jacob, 3/31/90 (PB90-258062, A04, MF-A01).

NCEER-90-0006 "Seismic Hazard Along a Crude Oil Pipeline in the Event of an 1811-1812 Type New Madrid Earthquake," by H.H.M. Hwang and C-H.S. Chen, 4/16/90, (PB90-258054, A04, MF-A01).

NCEER-90-0007 "Site-Specific Response Spectra for Memphis Sheahan Pumping Station," by H.H.M. Hwang and C.S. Lee, 5/15/90, (PB91-108811, A05, MF-A01).

NCEER-90-0008 "Pilot Study on Seismic Vulnerability of Crude Oil Transmission Systems," by T. Ariman, R. Dobry, M. Grigoriu, F. Kozin, M. O'Rourke, T. O'Rourke and M. Shinozuka, 5/25/90, (PB91-108837, A06, MF-A01).

NCEER-90-0009 "A Program to Generate Site Dependent Time Histories: EQGEN," by G.W. Ellis, M. Srinivasan and A.S. Cakmak, 1/30/90, (PB91-108829, A04, MF-A01).

NCEER-90-0010 "Active Isolation for Seismic Protection of Operating Rooms," by M.E. Talbott, Supervised by M. Shinozuka, 6/8/9, (PB91-110205, A05, MF-A01).

NCEER-90-0011 "Program LINEARID for Identification of Linear Structural Dynamic Systems," by C-B. Yun and M. Shinozuka, 6/25/90, (PB91-110312, A08, MF-A01).

NCEER-90-0012 "Two-Dimensional Two-Phase Elasto-Plastic Seismic Response of Earth Dams," by A.N. Yiagos, Supervised by J.H. Prevost, 6/20/90, (PB91-110197, A13, MF-A02).

NCEER-90-0013 "Secondary Systems in Base-Isolated Structures: Experimental Investigation, Stochastic Response and Stochastic Sensitivity," by G.D. Manolis, G. Juhn, M.C. Constantinou and A.M. Reinhorn, 7/1/90, (PB91-110320, A08, MF-A01).

NCEER-90-0014 "Seismic Behavior of Lightly-Reinforced Concrete Column and Beam-Column Joint Details," by S.P. Pessiki, C.H. Conley, P. Gergely and R.N. White, 8/22/90, (PB91-108795, A11, MF-A02).

NCEER-90-0015 "Two Hybrid Control Systems for Building Structures Under Strong Earthquakes," by J.N. Yang and A. Danielians, 6/29/90, (PB91-125393, A04, MF-A01).

NCEER-90-0016 "Instantaneous Optimal Control with Acceleration and Velocity Feedback," by J.N. Yang and Z. Li, 6/29/90, (PB91-125401, A03, MF-A01).

NCEER-90-0017 "Reconnaissance Report on the Northern Iran Earthquake of June 21, 1990," by M. Mehrain, 10/4/90, (PB91-125377, A03, MF-A01).

NCEER-90-0018 "Evaluation of Liquefaction Potential in Memphis and Shelby County," by T.S. Chang, P.S. Tang, C.S. Lee and H. Hwang, 8/10/90, (PB91-125427, A09, MF-A01).

NCEER-90-0019 "Experimental and Analytical Study of a Combined Sliding Disc Bearing and Helical Steel Spring Isolation System," by M.C. Constantinou, A.S. Mokha and A.M. Reinhorn, 10/4/90, (PB91-125385, A06, MF-A01). This report is available only through NTIS (see address given above).

NCEER-90-0020 "Experimental Study and Analytical Prediction of Earthquake Response of a Sliding Isolation System with a Spherical Surface," by A.S. Mokha, M.C. Constantinou and A.M. Reinhorn, 10/11/90, (PB91-125419, A05, MF-A01).

NCEER-90-0021 "Dynamic Interaction Factors for Floating Pile Groups," by G. Gazetas, K. Fan, A. Kaynia and E. Kausel, 9/10/90, (PB91-170381, A05, MF-A01).

NCEER-90-0022 "Evaluation of Seismic Damage Indices for Reinforced Concrete Structures," by S. Rodriguez-Gomez and A.S. Cakmak, 9/30/90, PB91-171322, A06, MF-A01).

NCEER-90-0023 "Study of Site Response at a Selected Memphis Site," by H. Desai, S. Ahmad, E.S. Gazetas and M.R. Oh, 10/11/90, (PB91-196857, A03, MF-A01).

NCEER-90-0024 "A User's Guide to Strongmo: Version 1.0 of NCEER's Strong-Motion Data Access Tool for PCs and Terminals," by P.A. Friberg and C.A.T. Susch, 11/15/90, (PB91-171272, A03, MF-A01).

NCEER-90-0025 "A Three-Dimensional Analytical Study of Spatial Variability of Seismic Ground Motions," by L-L. Hong and A.H.-S. Ang, 10/30/90, (PB91-170399, A09, MF-A01).

NCEER-90-0026 "MUMOID User's Guide - A Program for the Identification of Modal Parameters," by S. Rodriguez-Gomez and E. DiPasquale, 9/30/90, (PB91-171298, A04, MF-A01).

NCEER-90-0027 "SARCF-II User's Guide - Seismic Analysis of Reinforced Concrete Frames," by S. Rodriguez-Gomez, Y.S. Chung and C. Meyer, 9/30/90, (PB91-171280, A05, MF-A01).

NCEER-90-0028 "Viscous Dampers: Testing, Modeling and Application in Vibration and Seismic Isolation," by N. Makris and M.C. Constantinou, 12/20/90 (PB91-190561, A06, MF-A01).

NCEER-90-0029 "Soil Effects on Earthquake Ground Motions in the Memphis Area," by H. Hwang, C.S. Lee, K.W. Ng and T.S. Chang, 8/2/90, (PB91-190751, A05, MF-A01).

NCEER-91-0001 "Proceedings from the Third Japan-U.S. Workshop on Earthquake Resistant Design of Lifeline Facilities and Countermeasures for Soil Liquefaction, December 17-19, 1990," edited by T.D. O'Rourke and M. Hamada, 2/1/91, (PB91-179259, A99, MF-A04).

NCEER-91-0002 "Physical Space Solutions of Non-Proportionally Damped Systems," by M. Tong, Z. Liang and G.C. Lee, 1/15/91, (PB91-179242, A04, MF-A01).

NCEER-91-0003 "Seismic Response of Single Piles and Pile Groups," by K. Fan and G. Gazetas, 1/10/91, (PB92-174994, A04, MF-A01).

NCEER-91-0004 "Damping of Structures: Part 1 - Theory of Complex Damping," by Z. Liang and G. Lee, 10/10/91, (PB92-197235, A12, MF-A03).

NCEER-91-0005 "3D-BASIS - Nonlinear Dynamic Analysis of Three Dimensional Base Isolated Structures: Part II," by S. Nagarajaiah, A.M. Reinhorn and M.C. Constantinou, 2/28/91, (PB91-190553, A07, MF-A01). This report has been replaced by NCEER-93-0011.

NCEER-91-0006 "A Multidimensional Hysteretic Model for Plasticity Deforming Metals in Energy Absorbing Devices," by E.J. Graesser and F.A. Cozzarelli, 4/9/91, (PB92-108364, A04, MF-A01).

NCEER-91-0007 "A Framework for Customizable Knowledge-Based Expert Systems with an Application to a KBES for Evaluating the Seismic Resistance of Existing Buildings," by E.G. Ibarra-Anaya and S.J. Fenves, 4/9/91, (PB91-210930, A08, MF-A01).

NCEER-91-0008 "Nonlinear Analysis of Steel Frames with Semi-Rigid Connections Using the Capacity Spectrum Method," by G.G. Deierlein, S-H. Hsieh, Y-J. Shen and J.F. Abel, 7/2/91, (PB92-113828, A05, MF-A01).

NCEER-91-0009 "Earthquake Education Materials for Grades K-12," by K.E.K. Ross, 4/30/91, (PB91-212142, A06, MF-A01). This report has been replaced by NCEER-92-0018.

NCEER-91-0010 "Phase Wave Velocities and Displacement Phase Differences in a Harmonically Oscillating Pile," by N. Makris and G. Gazetas, 7/8/91, (PB92-108356, A04, MF-A01).

NCEER-91-0011 "Dynamic Characteristics of a Full-Size Five-Story Steel Structure and a 2/5 Scale Model," by K.C. Chang, G.C. Yao, G.C. Lee, D.S. Hao and Y.C. Yeh," 7/2/91, (PB93-116648, A06, MF-A02).

NCEER-91-0012 "Seismic Response of a 2/5 Scale Steel Structure with Added Viscoelastic Dampers," by K.C. Chang, T.T. Soong, S-T. Oh and M.L. Lai, 5/17/91, (PB92-110816, A05, MF-A01).

NCEER-91-0013 "Earthquake Response of Retaining Walls; Full-Scale Testing and Computational Modeling," by S. Alampalli and A-W.M. Elgamal, 6/20/91, not available.

NCEER-91-0014 "3D-BASIS-M: Nonlinear Dynamic Analysis of Multiple Building Base Isolated Structures," by P.C. Tsopelas, S. Nagarajaiah, M.C. Constantinou and A.M. Reinhorn, 5/28/91, (PB92-113885, A09, MF-A02).

NCEER-91-0015 "Evaluation of SEAOC Design Requirements for Sliding Isolated Structures," by D. Theodossiou and M.C. Constantinou, 6/10/91, (PB92-114602, A11, MF-A03).

NCEER-91-0016 "Closed-Loop Modal Testing of a 27-Story Reinforced Concrete Flat Plate-Core Building," by H.R. Somaprasad, T. Toksoy, H. Yoshiyuki and A.E. Aktan, 7/15/91, (PB92-129980, A07, MF-A02).

NCEER-91-0017 "Shake Table Test of a 1/6 Scale Two-Story Lightly Reinforced Concrete Building," by A.G. El-Attar, R.N. White and P. Gergely, 2/28/91, (PB92-222447, A06, MF-A02).

NCEER-91-0018 "Shake Table Test of a 1/8 Scale Three-Story Lightly Reinforced Concrete Building," by A.G. El-Attar, R.N. White and P. Gergely, 2/28/91, (PB93-116630, A08, MF-A02).

NCEER-91-0019 "Transfer Functions for Rigid Rectangular Foundations," by A.S. Veletsos, A.M. Prasad and W.H. Wu, 7/31/91, not available.

NCEER-91-0020 "Hybrid Control of Seismic-Excited Nonlinear and Inelastic Structural Systems," by J.N. Yang, Z. Li and A. Danielians, 8/1/91, (PB92-143171, A06, MF-A02).

NCEER-91-0021 "The NCEER-91 Earthquake Catalog: Improved Intensity-Based Magnitudes and Recurrence Relations for U.S. Earthquakes East of New Madrid," by L. Seeber and J.G. Armbruster, 8/28/91, (PB92-176742, A06, MF-A02).

NCEER-91-0022 "Proceedings from the Implementation of Earthquake Planning and Education in Schools: The Need for Change - The Roles of the Changemakers," by K.E.K. Ross and F. Winslow, 7/23/91, (PB92-129998, A12, MF-A03).

NCEER-91-0023 "A Study of Reliability-Based Criteria for Seismic Design of Reinforced Concrete Frame Buildings," by H.H.M. Hwang and H-M. Hsu, 8/10/91, (PB92-140235, A09, MF-A02).

NCEER-91-0024 "Experimental Verification of a Number of Structural System Identification Algorithms," by R.G. Ghanem, H. Gavin and M. Shinozuka, 9/18/91, (PB92-176577, A18, MF-A04).

NCEER-91-0025 "Probabilistic Evaluation of Liquefaction Potential," by H.H.M. Hwang and C.S. Lee," 11/25/91, (PB92-143429, A05, MF-A01).

NCEER-91-0026 "Instantaneous Optimal Control for Linear, Nonlinear and Hysteretic Structures - Stable Controllers," by J.N. Yang and Z. Li, 11/15/91, (PB92-163807, A04, MF-A01).

NCEER-91-0027 "Experimental and Theoretical Study of a Sliding Isolation System for Bridges," by M.C. Constantinou, A. Kartoum, A.M. Reinhorn and P. Bradford, 11/15/91, (PB92-176973, A10, MF-A03).

NCEER-92-0001 "Case Studies of Liquefaction and Lifeline Performance During Past Earthquakes, Volume 1: Japanese Case Studies," Edited by M. Hamada and T. O'Rourke, 2/17/92, (PB92-197243, A18, MF-A04).

NCEER-92-0002 "Case Studies of Liquefaction and Lifeline Performance During Past Earthquakes, Volume 2: United States Case Studies," Edited by T. O'Rourke and M. Hamada, 2/17/92, (PB92-197250, A20, MF-A04).

NCEER-92-0003 "Issues in Earthquake Education," Edited by K. Ross, 2/3/92, (PB92-222389, A07, MF-A02).

NCEER-92-0004 "Proceedings from the First U.S. - Japan Workshop on Earthquake Protective Systems for Bridges," Edited by I.G. Buckle, 2/4/92, (PB94-142239, A99, MF-A06).

NCEER-92-0005 "Seismic Ground Motion from a Haskell-Type Source in a Multiple-Layered Half-Space," A.P. Theoharis, G. Deodatis and M. Shinozuka, 1/2/92, not available.

NCEER-92-0006 "Proceedings from the Site Effects Workshop," Edited by R. Whitman, 2/29/92, (PB92-197201, A04, MF-A01).

NCEER-92-0007 "Engineering Evaluation of Permanent Ground Deformations Due to Seismically-Induced Liquefaction," by M.H. Baziar, R. Dobry and A-W.M. Elgamal, 3/24/92, (PB92-222421, A13, MF-A03).

NCEER-92-0008 "A Procedure for the Seismic Evaluation of Buildings in the Central and Eastern United States," by C.D. Poland and J.O. Malley, 4/2/92, (PB92-222439, A20, MF-A04).

NCEER-92-0009 "Experimental and Analytical Study of a Hybrid Isolation System Using Friction Controllable Sliding Bearings," by M.Q. Feng, S. Fujii and M. Shinozuka, 5/15/92, (PB93-150282, A06, MF-A02).

NCEER-92-0010 "Seismic Resistance of Slab-Column Connections in Existing Non-Ductile Flat-Plate Buildings," by A.J. Durrani and Y. Du, 5/18/92, (PB93-116812, A06, MF-A02).

NCEER-92-0011 "The Hysteretic and Dynamic Behavior of Brick Masonry Walls Upgraded by Ferrocement Coatings Under Cyclic Loading and Strong Simulated Ground Motion," by H. Lee and S.P. Prawel, 5/11/92, not available.

NCEER-92-0012 "Study of Wire Rope Systems for Seismic Protection of Equipment in Buildings," by G.F. Demetriades, M.C. Constantinou and A.M. Reinhorn, 5/20/92, (PB93-116655, A08, MF-A02).

NCEER-92-0013 "Shape Memory Structural Dampers: Material Properties, Design and Seismic Testing," by P.R. Witting and F.A. Cozzarelli, 5/26/92, (PB93-116663, A05, MF-A01).

NCEER-92-0014 "Longitudinal Permanent Ground Deformation Effects on Buried Continuous Pipelines," by M.J. O'Rourke, and C. Nordberg, 6/15/92, (PB93-116671, A08, MF-A02).

NCEER-92-0015 "A Simulation Method for Stationary Gaussian Random Functions Based on the Sampling Theorem," by M. Grigoriu and S. Balopoulou, 6/11/92, (PB93-127496, A05, MF-A01).

NCEER-92-0016 "Gravity-Load-Designed Reinforced Concrete Buildings: Seismic Evaluation of Existing Construction and Detailing Strategies for Improved Seismic Resistance," by G.W. Hoffmann, S.K. Kunnath, A.M. Reinhorn and J.B. Mander, 7/15/92, (PB94-142007, A08, MF-A02).

NCEER-92-0017 "Observations on Water System and Pipeline Performance in the Limón Area of Costa Rica Due to the April 22, 1991 Earthquake," by M. O'Rourke and D. Ballantyne, 6/30/92, (PB93-126811, A06, MF-A02).

NCEER-92-0018 "Fourth Edition of Earthquake Education Materials for Grades K-12," Edited by K.E.K. Ross, 8/10/92, (PB93-114023, A07, MF-A02).

NCEER-92-0019 "Proceedings from the Fourth Japan-U.S. Workshop on Earthquake Resistant Design of Lifeline Facilities and Countermeasures for Soil Liquefaction," Edited by M. Hamada and T.D. O'Rourke, 8/12/92, (PB93-163939, A99, MF-E11).

NCEER-92-0020 "Active Bracing System: A Full Scale Implementation of Active Control," by A.M. Reinhorn, T.T. Soong, R.C. Lin, M.A. Riley, Y.P. Wang, S. Aizawa and M. Higashino, 8/14/92, (PB93-127512, A06, MF-A02).

NCEER-92-0021 "Empirical Analysis of Horizontal Ground Displacement Generated by Liquefaction-Induced Lateral Spreads," by S.F. Bartlett and T.L. Youd, 8/17/92, (PB93-188241, A06, MF-A02).

NCEER-92-0022 "IDARC Version 3.0: Inelastic Damage Analysis of Reinforced Concrete Structures," by S.K. Kunnath, A.M. Reinhorn and R.F. Lobo, 8/31/92, (PB93-227502, A07, MF-A02).

NCEER-92-0023 "A Semi-Empirical Analysis of Strong-Motion Peaks in Terms of Seismic Source, Propagation Path and Local Site Conditions, by M. Kamiyama, M.J. O'Rourke and R. Flores-Berrones, 9/9/92, (PB93-150266, A08, MF-A02).

NCEER-92-0024 "Seismic Behavior of Reinforced Concrete Frame Structures with Nonductile Details, Part I: Summary of Experimental Findings of Full Scale Beam-Column Joint Tests," by A. Beres, R.N. White and P. Gergely, 9/30/92, (PB93-227783, A05, MF-A01).

NCEER-92-0025 "Experimental Results of Repaired and Retrofitted Beam-Column Joint Tests in Lightly Reinforced Concrete Frame Buildings," by A. Beres, S. El-Borgi, R.N. White and P. Gergely, 10/29/92, (PB93-227791, A05, MF-A01).

NCEER-92-0026 "A Generalization of Optimal Control Theory: Linear and Nonlinear Structures," by J.N. Yang, Z. Li and S. Vongchavalitkul, 11/2/92, (PB93-188621, A05, MF-A01).

NCEER-92-0027 "Seismic Resistance of Reinforced Concrete Frame Structures Designed Only for Gravity Loads: Part I - Design and Properties of a One-Third Scale Model Structure," by J.M. Bracci, A.M. Reinhorn and J.B. Mander, 12/1/92, (PB94-104502, A08, MF-A02).

NCEER-92-0028 "Seismic Resistance of Reinforced Concrete Frame Structures Designed Only for Gravity Loads: Part II - Experimental Performance of Subassemblages," by L.E. Aycardi, J.B. Mander and A.M. Reinhorn, 12/1/92, (PB94-104510, A08, MF-A02).

NCEER-92-0029 "Seismic Resistance of Reinforced Concrete Frame Structures Designed Only for Gravity Loads: Part III - Experimental Performance and Analytical Study of a Structural Model," by J.M. Bracci, A.M. Reinhorn and J.B. Mander, 12/1/92, (PB93-227528, A09, MF-A01).

NCEER-92-0030 "Evaluation of Seismic Retrofit of Reinforced Concrete Frame Structures: Part I - Experimental Performance of Retrofitted Subassemblages," by D. Choudhuri, J.B. Mander and A.M. Reinhorn, 12/8/92, (PB93-198307, A07, MF-A02).

NCEER-92-0031 "Evaluation of Seismic Retrofit of Reinforced Concrete Frame Structures: Part II - Experimental Performance and Analytical Study of a Retrofitted Structural Model," by J.M. Bracci, A.M. Reinhorn and J.B. Mander, 12/8/92, (PB93-198315, A09, MF-A03).

NCEER-92-0032 "Experimental and Analytical Investigation of Seismic Response of Structures with Supplemental Fluid Viscous Dampers," by M.C. Constantinou and M.D. Symans, 12/21/92, (PB93-191435, A10, MF-A03). This report is available only through NTIS (see address given above).

NCEER-92-0033 "Reconnaissance Report on the Cairo, Egypt Earthquake of October 12, 1992," by M. Khater, 12/23/92, (PB93-188621, A03, MF-A01).

NCEER-92-0034 "Low-Level Dynamic Characteristics of Four Tall Flat-Plate Buildings in New York City," by H. Gavin, S. Yuan, J. Grossman, E. Pekelis and K. Jacob, 12/28/92, (PB93-188217, A07, MF-A02).

NCEER-93-0001 "An Experimental Study on the Seismic Performance of Brick-Infilled Steel Frames With and Without Retrofit," by J.B. Mander, B. Nair, K. Wojtkowski and J. Ma, 1/29/93, (PB93-227510, A07, MF-A02).

NCEER-93-0002 "Social Accounting for Disaster Preparedness and Recovery Planning," by S. Cole, E. Pantoja and V. Razak, 2/22/93, (PB94-142114, A12, MF-A03).

NCEER-93-0003 "Assessment of 1991 NEHRP Provisions for Nonstructural Components and Recommended Revisions," by T.T. Soong, G. Chen, Z. Wu, R-H. Zhang and M. Grigoriu, 3/1/93, (PB93-188639, A06, MF-A02).

NCEER-93-0004 "Evaluation of Static and Response Spectrum Analysis Procedures of SEAOC/UBC for Seismic Isolated Structures," by C.W. Winters and M.C. Constantinou, 3/23/93, (PB93-198299, A10, MF-A03).

NCEER-93-0005 "Earthquakes in the Northeast - Are We Ignoring the Hazard? A Workshop on Earthquake Science and Safety for Educators," edited by K.E.K. Ross, 4/2/93, (PB94-103066, A09, MF-A02).

NCEER-93-0006 "Inelastic Response of Reinforced Concrete Structures with Viscoelastic Braces," by R.F. Lobo, J.M. Bracci, K.L. Shen, A.M. Reinhorn and T.T. Soong, 4/5/93, (PB93-227486, A05, MF-A02).

NCEER-93-0007 "Seismic Testing of Installation Methods for Computers and Data Processing Equipment," by K. Kosar, T.T. Soong, K.L. Shen, J.A. HoLung and Y.K. Lin, 4/12/93, (PB93-198299, A07, MF-A02).

NCEER-93-0008 "Retrofit of Reinforced Concrete Frames Using Added Dampers," by A. Reinhorn, M. Constantinou and C. Li, not available.

NCEER-93-0009 "Seismic Behavior and Design Guidelines for Steel Frame Structures with Added Viscoelastic Dampers," by K.C. Chang, M.L. Lai, T.T. Soong, D.S. Hao and Y.C. Yeh, 5/1/93, (PB94-141959, A07, MF-A02).

NCEER-93-0010 "Seismic Performance of Shear-Critical Reinforced Concrete Bridge Piers," by J.B. Mander, S.M. Waheed, M.T.A. Chaudhary and S.S. Chen, 5/12/93, (PB93-227494, A08, MF-A02).

NCEER-93-0011 "3D-BASIS-TABS: Computer Program for Nonlinear Dynamic Analysis of Three Dimensional Base Isolated Structures," by S. Nagarajaiah, C. Li, A.M. Reinhorn and M.C. Constantinou, 8/2/93, (PB94-141819, A09, MF-A02).

NCEER-93-0012 "Effects of Hydrocarbon Spills from an Oil Pipeline Break on Ground Water," by O.J. Helweg and H.H.M. Hwang, 8/3/93, (PB94-141942, A06, MF-A02).

NCEER-93-0013 "Simplified Procedures for Seismic Design of Nonstructural Components and Assessment of Current Code Provisions," by M.P. Singh, L.E. Suarez, E.E. Matheu and G.O. Maldonado, 8/4/93, (PB94-141827, A09, MF-A02).

NCEER-93-0014 "An Energy Approach to Seismic Analysis and Design of Secondary Systems," by G. Chen and T.T. Soong, 8/6/93, (PB94-142767, A11, MF-A03).

NCEER-93-0015 "Proceedings from School Sites: Becoming Prepared for Earthquakes - Commemorating the Third Anniversary of the Loma Prieta Earthquake," Edited by F.E. Winslow and K.E.K. Ross, 8/16/93, (PB94-154275, A16, MF-A02).

NCEER-93-0016 "Reconnaissance Report of Damage to Historic Monuments in Cairo, Egypt Following the October 12, 1992 Dahshur Earthquake," by D. Sykora, D. Look, G. Croci, E. Karaesmen and E. Karaesmen, 8/19/93, (PB94-142221, A08, MF-A02).

NCEER-93-0017 "The Island of Guam Earthquake of August 8, 1993," by S.W. Swan and S.K. Harris, 9/30/93, (PB94-141843, A04, MF-A01).

NCEER-93-0018 "Engineering Aspects of the October 12, 1992 Egyptian Earthquake," by A.W. Elgamal, M. Amer, K. Adalier and A. Abul-Fadl, 10/7/93, (PB94-141983, A05, MF-A01).

NCEER-93-0019 "Development of an Earthquake Motion Simulator and its Application in Dynamic Centrifuge Testing," by I. Krstelj, Supervised by J.H. Prevost, 10/23/93, (PB94-181773, A-10, MF-A03).

NCEER-93-0020 "NCEER-Taisei Corporation Research Program on Sliding Seismic Isolation Systems for Bridges: Experimental and Analytical Study of a Friction Pendulum System (FPS)," by M.C. Constantinou, P. Tsopelas, Y-S. Kim and S. Okamoto, 11/1/93, (PB94-142775, A08, MF-A02).

NCEER-93-0021 "Finite Element Modeling of Elastomeric Seismic Isolation Bearings," by L.J. Billings, Supervised by R. Shepherd, 11/8/93, not available.

NCEER-93-0022 "Seismic Vulnerability of Equipment in Critical Facilities: Life-Safety and Operational Consequences," by K. Porter, G.S. Johnson, M.M. Zadeh, C. Scawthorn and S. Eder, 11/24/93, (PB94-181765, A16, MF-A03).

NCEER-93-0023 "Hokkaido Nansei-oki, Japan Earthquake of July 12, 1993, by P.I. Yanev and C.R. Scawthorn, 12/23/93, (PB94-181500, A07, MF-A01).

NCEER-94-0001 "An Evaluation of Seismic Serviceability of Water Supply Networks with Application to the San Francisco Auxiliary Water Supply System," by I. Markov, Supervised by M. Grigoriu and T. O'Rourke, 1/21/94, (PB94-204013, A07, MF-A02).

NCEER-94-0002 "NCEER-Taisei Corporation Research Program on Sliding Seismic Isolation Systems for Bridges: Experimental and Analytical Study of Systems Consisting of Sliding Bearings, Rubber Restoring Force Devices and Fluid Dampers," Volumes I and II, by P. Tsopelas, S. Okamoto, M.C. Constantinou, D. Ozaki and S. Fujii, 2/4/94, (PB94-181740, A09, MF-A02 and PB94-181757, A12, MF-A03).

NCEER-94-0003 "A Markov Model for Local and Global Damage Indices in Seismic Analysis," by S. Rahman and M. Grigoriu, 2/18/94, (PB94-206000, A12, MF-A03).

NCEER-94-0004 "Proceedings from the NCEER Workshop on Seismic Response of Masonry Infills," edited by D.P. Abrams, 3/1/94, (PB94-180783, A07, MF-A02).

NCEER-94-0005 "The Northridge, California Earthquake of January 17, 1994: General Reconnaissance Report," edited by J.D. Goltz, 3/11/94, (PB94-193943, A10, MF-A03).

NCEER-94-0006 "Seismic Energy Based Fatigue Damage Analysis of Bridge Columns: Part I - Evaluation of Seismic Capacity," by G.A. Chang and J.B. Mander, 3/14/94, (PB94-219185, A11, MF-A03).

NCEER-94-0007 "Seismic Isolation of Multi-Story Frame Structures Using Spherical Sliding Isolation Systems," by T.M. Al-Hussaini, V.A. Zayas and M.C. Constantinou, 3/17/94, (PB94-193745, A09, MF-A02).

NCEER-94-0008 "The Northridge, California Earthquake of January 17, 1994: Performance of Highway Bridges," edited by I.G. Buckle, 3/24/94, (PB94-193851, A06, MF-A02).

NCEER-94-0009 "Proceedings of the Third U.S.-Japan Workshop on Earthquake Protective Systems for Bridges," edited by I.G. Buckle and I. Friedland, 3/31/94, (PB94-195815, A99, MF-A06).

NCEER-94-0010 "3D-BASIS-ME: Computer Program for Nonlinear Dynamic Analysis of Seismically Isolated Single and Multiple Structures and Liquid Storage Tanks," by P.C. Tsopelas, M.C. Constantinou and A.M. Reinhorn, 4/12/94, (PB94-204922, A09, MF-A02).

NCEER-94-0011 "The Northridge, California Earthquake of January 17, 1994: Performance of Gas Transmission Pipelines," by T.D. O'Rourke and M.C. Palmer, 5/16/94, (PB94-204989, A05, MF-A01).

NCEER-94-0012 "Feasibility Study of Replacement Procedures and Earthquake Performance Related to Gas Transmission Pipelines," by T.D. O'Rourke and M.C. Palmer, 5/25/94, (PB94-206638, A09, MF-A02).

NCEER-94-0013 "Seismic Energy Based Fatigue Damage Analysis of Bridge Columns: Part II - Evaluation of Seismic Demand," by G.A. Chang and J.B. Mander, 6/1/94, (PB95-18106, A08, MF-A02).

NCEER-94-0014 "NCEER-Taisei Corporation Research Program on Sliding Seismic Isolation Systems for Bridges: Experimental and Analytical Study of a System Consisting of Sliding Bearings and Fluid Restoring Force/Damping Devices," by P. Tsopelas and M.C. Constantinou, 6/13/94, (PB94-219144, A10, MF-A03).

NCEER-94-0015 "Generation of Hazard-Consistent Fragility Curves for Seismic Loss Estimation Studies," by H. Hwang and J-R. Huo, 6/14/94, (PB95-181996, A09, MF-A02).

NCEER-94-0016 "Seismic Study of Building Frames with Added Energy-Absorbing Devices," by W.S. Pong, C.S. Tsai and G.C. Lee, 6/20/94, (PB94-219136, A10, A03).

NCEER-94-0017 "Sliding Mode Control for Seismic-Excited Linear and Nonlinear Civil Engineering Structures," by J. Yang, J. Wu, A. Agrawal and Z. Li, 6/21/94, (PB95-138483, A06, MF-A02).

NCEER-94-0018 "3D-BASIS-TABS Version 2.0: Computer Program for Nonlinear Dynamic Analysis of Three Dimensional Base Isolated Structures," by A.M. Reinhorn, S. Nagarajaiah, M.C. Constantinou, P. Tsopelas and R. Li, 6/22/94, (PB95-182176, A08, MF-A02).

NCEER-94-0019 "Proceedings of the International Workshop on Civil Infrastructure Systems: Application of Intelligent Systems and Advanced Materials on Bridge Systems," Edited by G.C. Lee and K.C. Chang, 7/18/94, (PB95-252474, A20, MF-A04).

NCEER-94-0020 "Study of Seismic Isolation Systems for Computer Floors," by V. Lambrou and M.C. Constantinou, 7/19/94, (PB95-138533, A10, MF-A03).

NCEER-94-0021 "Proceedings of the U.S.-Italian Workshop on Guidelines for Seismic Evaluation and Rehabilitation of Unreinforced Masonry Buildings," Edited by D.P. Abrams and G.M. Calvi, 7/20/94, (PB95-138749, A13, MF-A03).

NCEER-94-0022 "NCEER-Taisei Corporation Research Program on Sliding Seismic Isolation Systems for Bridges: Experimental and Analytical Study of a System Consisting of Lubricated PTFE Sliding Bearings and Mild Steel Dampers," by P. Tsopelas and M.C. Constantinou, 7/22/94, (PB95-182184, A08, MF-A02).

NCEER-94-0023 "Development of Reliability-Based Design Criteria for Buildings Under Seismic Load," by Y.K. Wen, H. Hwang and M. Shinozuka, 8/1/94, (PB95-211934, A08, MF-A02).

NCEER-94-0024 "Experimental Verification of Acceleration Feedback Control Strategies for an Active Tendon System," by S.J. Dyke, B.F. Spencer, Jr., P. Quast, M.K. Sain, D.C. Kaspari, Jr. and T.T. Soong, 8/29/94, (PB95-212320, A05, MF-A01).

NCEER-94-0025 "Seismic Retrofitting Manual for Highway Bridges," Edited by I.G. Buckle and I.F. Friedland, published by the Federal Highway Administration (PB95-212676, A15, MF-A03).

NCEER-94-0026 "Proceedings from the Fifth U.S.-Japan Workshop on Earthquake Resistant Design of Lifeline Facilities and Countermeasures Against Soil Liquefaction," Edited by T.D. O'Rourke and M. Hamada, 11/7/94, (PB95-220802, A99, MF-E08).

NCEER-95-0001 "Experimental and Analytical Investigation of Seismic Retrofit of Structures with Supplemental Damping: Part 1 - Fluid Viscous Damping Devices," by A.M. Reinhorn, C. Li and M.C. Constantinou, 1/3/95, (PB95-266599, A09, MF-A02).

NCEER-95-0002 "Experimental and Analytical Study of Low-Cycle Fatigue Behavior of Semi-Rigid Top-And-Seat Angle Connections," by G. Pekcan, J.B. Mander and S.S. Chen, 1/5/95, (PB95-220042, A07, MF-A02).

NCEER-95-0003 "NCEER-ATC Joint Study on Fragility of Buildings," by T. Anagnos, C. Rojahn and A.S. Kiremidjian, 1/20/95, (PB95-220026, A06, MF-A02).

NCEER-95-0004 "Nonlinear Control Algorithms for Peak Response Reduction," by Z. Wu, T.T. Soong, V. Gattulli and R.C. Lin, 2/16/95, (PB95-220349, A05, MF-A01).

NCEER-95-0005 "Pipeline Replacement Feasibility Study: A Methodology for Minimizing Seismic and Corrosion Risks to Underground Natural Gas Pipelines," by R.T. Eguchi, H.A. Seligson and D.G. Honegger, 3/2/95, (PB95-252326, A06, MF-A02).

NCEER-95-0006 "Evaluation of Seismic Performance of an 11-Story Frame Building During the 1994 Northridge Earthquake," by F. Naeim, R. DiSulio, K. Benuska, A. Reinhorn and C. Li, not available.

NCEER-95-0007 "Prioritization of Bridges for Seismic Retrofitting," by N. Basöz and A.S. Kiremidjian, 4/24/95, (PB95-252300, A08, MF-A02).

NCEER-95-0008 "Method for Developing Motion Damage Relationships for Reinforced Concrete Frames," by A. Singhal and A.S. Kiremidjian, 5/11/95, (PB95-266607, A06, MF-A02).

NCEER-95-0009 "Experimental and Analytical Investigation of Seismic Retrofit of Structures with Supplemental Damping: Part II - Friction Devices," by C. Li and A.M. Reinhorn, 7/6/95, (PB96-128087, A11, MF-A03).

NCEER-95-0010 "Experimental Performance and Analytical Study of a Non-Ductile Reinforced Concrete Frame Structure Retrofitted with Elastomeric Spring Dampers," by G. Pekcan, J.B. Mander and S.S. Chen, 7/14/95, (PB96-137161, A08, MF-A02).

NCEER-95-0011 "Development and Experimental Study of Semi-Active Fluid Damping Devices for Seismic Protection of Structures," by M.D. Symans and M.C. Constantinou, 8/3/95, (PB96-136940, A23, MF-A04).

NCEER-95-0012 "Real-Time Structural Parameter Modification (RSPM): Development of Innervated Structures," by Z. Liang, M. Tong and G.C. Lee, 4/11/95, (PB96-137153, A06, MF-A01).

NCEER-95-0013 "Experimental and Analytical Investigation of Seismic Retrofit of Structures with Supplemental Damping: Part III - Viscous Damping Walls," by A.M. Reinhorn and C. Li, 10/1/95, (PB96-176409, A11, MF-A03).

NCEER-95-0014 "Seismic Fragility Analysis of Equipment and Structures in a Memphis Electric Substation," by J-R. Huo and H.H.M. Hwang, 8/10/95, (PB96-128087, A09, MF-A02).

NCEER-95-0015 "The Hanshin-Awaji Earthquake of January 17, 1995: Performance of Lifelines," Edited by M. Shinozuka, 11/3/95, (PB96-176383, A15, MF-A03).

NCEER-95-0016 "Highway Culvert Performance During Earthquakes," by T.L. Youd and C.J. Beckman, available as NCEER-96-0015.

NCEER-95-0017 "The Hanshin-Awaji Earthquake of January 17, 1995: Performance of Highway Bridges," Edited by I.G. Buckle, 12/1/95, not available.

NCEER-95-0018 "Modeling of Masonry Infill Panels for Structural Analysis," by A.M. Reinhorn, A. Madan, R.E. Valles, Y. Reichmann and J.B. Mander, 12/8/95, (PB97-110886, MF-A01, A06).

NCEER-95-0019 "Optimal Polynomial Control for Linear and Nonlinear Structures," by A.K. Agrawal and J.N. Yang, 12/11/95, (PB96-168737, A07, MF-A02).

NCEER-95-0020 "Retrofit of Non-Ductile Reinforced Concrete Frames Using Friction Dampers," by R.S. Rao, P. Gergely and R.N. White, 12/22/95, (PB97-133508, A10, MF-A02).

NCEER-95-0021 "Parametric Results for Seismic Response of Pile-Supported Bridge Bents," by G. Mylonakis, A. Nikolaou and G. Gazetas, 12/22/95, (PB97-100242, A12, MF-A03).

NCEER-95-0022 "Kinematic Bending Moments in Seismically Stressed Piles," by A. Nikolaou, G. Mylonakis and G. Gazetas, 12/23/95, (PB97-113914, MF-A03, A13).

NCEER-96-0001 "Dynamic Response of Unreinforced Masonry Buildings with Flexible Diaphragms," by A.C. Costley and D.P. Abrams," 10/10/96, (PB97-133573, MF-A03, A15).

NCEER-96-0002 "State of the Art Review: Foundations and Retaining Structures," by I. Po Lam, not available.

NCEER-96-0003 "Ductility of Rectangular Reinforced Concrete Bridge Columns with Moderate Confinement," by N. Wehbe, M. Saiidi, D. Sanders and B. Douglas, 11/7/96, (PB97-133557, A06, MF-A02).

NCEER-96-0004 "Proceedings of the Long-Span Bridge Seismic Research Workshop," edited by I.G. Buckle and I.M. Friedland, not available.

NCEER-96-0005 "Establish Representative Pier Types for Comprehensive Study: Eastern United States," by J. Kulicki and Z. Prucz, 5/28/96, (PB98-119217, A07, MF-A02).

NCEER-96-0006 "Establish Representative Pier Types for Comprehensive Study: Western United States," by R. Imbsen, R.A. Schamber and T.A. Osterkamp, 5/28/96, (PB98-118607, A07, MF-A02).

NCEER-96-0007 "Nonlinear Control Techniques for Dynamical Systems with Uncertain Parameters," by R.G. Ghanem and M.I. Bujakov, 5/27/96, (PB97-100259, A17, MF-A03).

NCEER-96-0008 "Seismic Evaluation of a 30-Year Old Non-Ductile Highway Bridge Pier and Its Retrofit," by J.B. Mander, B. Mahmoodzadegan, S. Bhadra and S.S. Chen, 5/31/96, (PB97-110902, MF-A03, A10).

NCEER-96-0009 "Seismic Performance of a Model Reinforced Concrete Bridge Pier Before and After Retrofit," by J.B. Mander, J.H. Kim and C.A. Ligozio, 5/31/96, (PB97-110910, MF-A02, A10).

NCEER-96-0010 "IDARC2D Version 4.0: A Computer Program for the Inelastic Damage Analysis of Buildings," by R.E. Valles, A.M. Reinhorn, S.K. Kunnath, C. Li and A. Madan, 6/3/96, (PB97-100234, A17, MF-A03).

NCEER-96-0011 "Estimation of the Economic Impact of Multiple Lifeline Disruption: Memphis Light, Gas and Water Division Case Study," by S.E. Chang, H.A. Seligson and R.T. Eguchi, 8/16/96, (PB97-133490, A11, MF-A03).

NCEER-96-0012 "Proceedings from the Sixth Japan-U.S. Workshop on Earthquake Resistant Design of Lifeline Facilities and Countermeasures Against Soil Liquefaction, Edited by M. Hamada and T. O'Rourke, 9/11/96, (PB97-133581, A99, MF-A06).

NCEER-96-0013 "Chemical Hazards, Mitigation and Preparedness in Areas of High Seismic Risk: A Methodology for Estimating the Risk of Post-Earthquake Hazardous Materials Release," by H.A. Seligson, R.T. Eguchi, K.J. Tierney and K. Richmond, 11/7/96, (PB97-133565, MF-A02, A08).

NCEER-96-0014 "Response of Steel Bridge Bearings to Reversed Cyclic Loading," by J.B. Mander, D-K. Kim, S.S. Chen and G.J. Premus, 11/13/96, (PB97-140735, A12, MF-A03).

NCEER-96-0015 "Highway Culvert Performance During Past Earthquakes," by T.L. Youd and C.J. Beckman, 11/25/96, (PB97-133532, A06, MF-A01).

NCEER-97-0001 "Evaluation, Prevention and Mitigation of Pounding Effects in Building Structures," by R.E. Valles and A.M. Reinhorn, 2/20/97, (PB97-159552, A14, MF-A03).

NCEER-97-0002 "Seismic Design Criteria for Bridges and Other Highway Structures," by C. Rojahn, R. Mayes, D.G. Anderson, J. Clark, J.H. Hom, R.V. Nutt and M.J. O'Rourke, 4/30/97, (PB97-194658, A06, MF-A03).

NCEER-97-0003 “Proceedings of the U.S.-Italian Workshop on Seismic Evaluation and Retrofit,” Edited by D.P. Abrams and G.M. Calvi, 3/19/97, (PB97-194666, A13, MF-A03).

NCEER-97-0004 "Investigation of Seismic Response of Buildings with Linear and Nonlinear Fluid Viscous Dampers," by A.A. Seleemah and M.C. Constantinou, 5/21/97, (PB98-109002, A15, MF-A03).

NCEER-97-0005 "Proceedings of the Workshop on Earthquake Engineering Frontiers in Transportation Facilities," edited by G.C. Lee and I.M. Friedland, 8/29/97, (PB98-128911, A25, MR-A04).

NCEER-97-0006 "Cumulative Seismic Damage of Reinforced Concrete Bridge Piers," by S.K. Kunnath, A. El-Bahy, A. Taylor and W. Stone, 9/2/97, (PB98-108814, A11, MF-A03).

NCEER-97-0007 "Structural Details to Accommodate Seismic Movements of Highway Bridges and Retaining Walls," by R.A. Imbsen, R.A. Schamber, E. Thorkildsen, A. Kartoum, B.T. Martin, T.N. Rosser and J.M. Kulicki, 9/3/97, (PB98-108996, A09, MF-A02).

NCEER-97-0008 "A Method for Earthquake Motion-Damage Relationships with Application to Reinforced Concrete Frames," by A. Singhal and A.S. Kiremidjian, 9/10/97, (PB98-108988, A13, MF-A03).

NCEER-97-0009 "Seismic Analysis and Design of Bridge Abutments Considering Sliding and Rotation," by K. Fishman and R. Richards, Jr., 9/15/97, (PB98-108897, A06, MF-A02).

NCEER-97-0010 "Proceedings of the FHWA/NCEER Workshop on the National Representation of Seismic Ground Motion for New and Existing Highway Facilities," edited by I.M. Friedland, M.S. Power and R.L. Mayes, 9/22/97, (PB98-128903, A21, MF-A04).

NCEER-97-0011 "Seismic Analysis for Design or Retrofit of Gravity Bridge Abutments," by K.L. Fishman, R. Richards, Jr. and R.C. Divito, 10/2/97, (PB98-128937, A08, MF-A02).

NCEER-97-0012 "Evaluation of Simplified Methods of Analysis for Yielding Structures," by P. Tsopelas, M.C. Constantinou, C.A. Kircher and A.S. Whittaker, 10/31/97, (PB98-128929, A10, MF-A03).

NCEER-97-0013 "Seismic Design of Bridge Columns Based on Control and Repairability of Damage," by C-T. Cheng and J.B. Mander, 12/8/97, (PB98-144249, A11, MF-A03).

NCEER-97-0014 "Seismic Resistance of Bridge Piers Based on Damage Avoidance Design," by J.B. Mander and C-T. Cheng, 12/10/97, (PB98-144223, A09, MF-A02).

NCEER-97-0015 “Seismic Response of Nominally Symmetric Systems with Strength Uncertainty,” by S. Balopoulou and M. Grigoriu, 12/23/97, (PB98-153422, A11, MF-A03).

NCEER-97-0016 “Evaluation of Seismic Retrofit Methods for Reinforced Concrete Bridge Columns,” by T.J. Wipf, F.W. Klaiber and F.M. Russo, 12/28/97, (PB98-144215, A12, MF-A03).

NCEER-97-0017 “Seismic Fragility of Existing Conventional Reinforced Concrete Highway Bridges,” by C.L. Mullen and A.S. Cakmak, 12/30/97, (PB98-153406, A08, MF-A02).

NCEER-97-0018 “Loss Asssessment of Memphis Buildings,” edited by D.P. Abrams and M. Shinozuka, 12/31/97, (PB98-144231, A13, MF-A03).

NCEER-97-0019 “Seismic Evaluation of Frames with Infill Walls Using Quasi-static Experiments,” by K.M. Mosalam, R.N. White and P. Gergely, 12/31/97, (PB98-153455, A07, MF-A02).

NCEER-97-0020 “Seismic Evaluation of Frames with Infill Walls Using Pseudo-dynamic Experiments,” by K.M. Mosalam, R.N. White and P. Gergely, 12/31/97, (PB98-153430, A07, MF-A02).

NCEER-97-0021 “Computational Strategies for Frames with Infill Walls: Discrete and Smeared Crack Analyses and Seismic Fragility,” by K.M. Mosalam, R.N. White and P. Gergely, 12/31/97, (PB98-153414, A10, MF-A02).

NCEER-97-0022 "Proceedings of the NCEER Workshop on Evaluation of Liquefaction Resistance of Soils," edited by T.L. Youd and I.M. Idriss, 12/31/97, (PB98-155617, A15, MF-A03).

MCEER-98-0001 "Extraction of Nonlinear Hysteretic Properties of Seismically Isolated Bridges from Quick-Release Field Tests," by Q. Chen, B.M. Douglas, E.M. Maragakis and I.G. Buckle, 5/26/98, (PB99-118838, A06, MF-A01).

MCEER-98-0002 "Methodologies for Evaluating the Importance of Highway Bridges," by A. Thomas, S. Eshenaur and J. Kulicki, 5/29/98, (PB99-118846, A10, MF-A02).

MCEER-98-0003 "Capacity Design of Bridge Piers and the Analysis of Overstrength," by J.B. Mander, A. Dutta and P. Goel, 6/1/98, (PB99-118853, A09, MF-A02).

MCEER-98-0004 "Evaluation of Bridge Damage Data from the Loma Prieta and Northridge, California Earthquakes," by N. Basoz and A. Kiremidjian, 6/2/98, (PB99-118861, A15, MF-A03).

MCEER-98-0005 "Screening Guide for Rapid Assessment of Liquefaction Hazard at Highway Bridge Sites," by T. L. Youd, 6/16/98, (PB99-118879, A06, not available on microfiche).

MCEER-98-0006 "Structural Steel and Steel/Concrete Interface Details for Bridges," by P. Ritchie, N. Kauhl and J. Kulicki, 7/13/98, (PB99-118945, A06, MF-A01).

MCEER-98-0007 "Capacity Design and Fatigue Analysis of Confined Concrete Columns," by A. Dutta and J.B. Mander, 7/14/98, (PB99-118960, A14, MF-A03).

MCEER-98-0008 "Proceedings of the Workshop on Performance Criteria for Telecommunication Services Under Earthquake Conditions," edited by A.J. Schiff, 7/15/98, (PB99-118952, A08, MF-A02).

MCEER-98-0009 "Fatigue Analysis of Unconfined Concrete Columns," by J.B. Mander, A. Dutta and J.H. Kim, 9/12/98, (PB99-123655, A10, MF-A02).

MCEER-98-0010 "Centrifuge Modeling of Cyclic Lateral Response of Pile-Cap Systems and Seat-Type Abutments in Dry Sands," by A.D. Gadre and R. Dobry, 10/2/98, (PB99-123606, A13, MF-A03).

MCEER-98-0011 "IDARC-BRIDGE: A Computational Platform for Seismic Damage Assessment of Bridge Structures," by A.M. Reinhorn, V. Simeonov, G. Mylonakis and Y. Reichman, 10/2/98, (PB99-162919, A15, MF-A03).

MCEER-98-0012 "Experimental Investigation of the Dynamic Response of Two Bridges Before and After Retrofitting with Elastomeric Bearings," by D.A. Wendichansky, S.S. Chen and J.B. Mander, 10/2/98, (PB99-162927, A15, MF-A03).

MCEER-98-0013 "Design Procedures for Hinge Restrainers and Hinge Sear Width for Multiple-Frame Bridges," by R. Des Roches and G.L. Fenves, 11/3/98, (PB99-140477, A13, MF-A03).

MCEER-98-0014 "Response Modification Factors for Seismically Isolated Bridges," by M.C. Constantinou and J.K. Quarshie, 11/3/98, (PB99-140485, A14, MF-A03).

MCEER-98-0015 "Proceedings of the U.S.-Italy Workshop on Seismic Protective Systems for Bridges," edited by I.M. Friedland and M.C. Constantinou, 11/3/98, (PB2000-101711, A22, MF-A04).

MCEER-98-0016 "Appropriate Seismic Reliability for Critical Equipment Systems: Recommendations Based on Regional Analysis of Financial and Life Loss," by K. Porter, C. Scawthorn, C. Taylor and N. Blais, 11/10/98, (PB99-157265, A08, MF-A02).

MCEER-98-0017 "Proceedings of the U.S. Japan Joint Seminar on Civil Infrastructure Systems Research," edited by M. Shinozuka and A. Rose, 11/12/98, (PB99-156713, A16, MF-A03).

MCEER-98-0018 "Modeling of Pile Footings and Drilled Shafts for Seismic Design," by I. PoLam, M. Kapuskar and D. Chaudhuri, 12/21/98, (PB99-157257, A09, MF-A02).

MCEER-99-0001 "Seismic Evaluation of a Masonry Infilled Reinforced Concrete Frame by Pseudodynamic Testing," by S.G. Buonopane and R.N. White, 2/16/99, (PB99-162851, A09, MF-A02).

MCEER-99-0002 "Response History Analysis of Structures with Seismic Isolation and Energy Dissipation Systems: Verification Examples for Program SAP2000," by J. Scheller and M.C. Constantinou, 2/22/99, (PB99-162869, A08, MF-A02).

MCEER-99-0003 "Experimental Study on the Seismic Design and Retrofit of Bridge Columns Including Axial Load Effects," by A. Dutta, T. Kokorina and J.B. Mander, 2/22/99, (PB99-162877, A09, MF-A02).

MCEER-99-0004 "Experimental Study of Bridge Elastomeric and Other Isolation and Energy Dissipation Systems with Emphasis on Uplift Prevention and High Velocity Near-source Seismic Excitation," by A. Kasalanati and M. C. Constantinou, 2/26/99, (PB99-162885, A12, MF-A03).

MCEER-99-0005 "Truss Modeling of Reinforced Concrete Shear-flexure Behavior," by J.H. Kim and J.B. Mander, 3/8/99, (PB99-163693, A12, MF-A03).

MCEER-99-0006 "Experimental Investigation and Computational Modeling of Seismic Response of a 1:4 Scale Model Steel Structure with a Load Balancing Supplemental Damping System," by G. Pekcan, J.B. Mander and S.S. Chen, 4/2/99, (PB99-162893, A11, MF-A03).

MCEER-99-0007 "Effect of Vertical Ground Motions on the Structural Response of Highway Bridges," by M.R. Button, C.J. Cronin and R.L. Mayes, 4/10/99, (PB2000-101411, A10, MF-A03).

MCEER-99-0008 "Seismic Reliability Assessment of Critical Facilities: A Handbook, Supporting Documentation, and Model Code Provisions," by G.S. Johnson, R.E. Sheppard, M.D. Quilici, S.J. Eder and C.R. Scawthorn, 4/12/99, (PB2000-101701, A18, MF-A04).

MCEER-99-0009 "Impact Assessment of Selected MCEER Highway Project Research on the Seismic Design of Highway Structures," by C. Rojahn, R. Mayes, D.G. Anderson, J.H. Clark, D'Appolonia Engineering, S. Gloyd and R.V. Nutt, 4/14/99, (PB99-162901, A10, MF-A02).

MCEER-99-0010 "Site Factors and Site Categories in Seismic Codes," by R. Dobry, R. Ramos and M.S. Power, 7/19/99, (PB2000-101705, A08, MF-A02).

MCEER-99-0011 "Restrainer Design Procedures for Multi-Span Simply-Supported Bridges," by M.J. Randall, M. Saiidi, E. Maragakis and T. Isakovic, 7/20/99, (PB2000-101702, A10, MF-A02).

MCEER-99-0012 "Property Modification Factors for Seismic Isolation Bearings," by M.C. Constantinou, P. Tsopelas, A. Kasalanati and E. Wolff, 7/20/99, (PB2000-103387, A11, MF-A03).

MCEER-99-0013 "Critical Seismic Issues for Existing Steel Bridges," by P. Ritchie, N. Kauhl and J. Kulicki, 7/20/99, (PB2000-101697, A09, MF-A02).

MCEER-99-0014 "Nonstructural Damage Database," by A. Kao, T.T. Soong and A. Vender, 7/24/99, (PB2000-101407, A06, MF-A01).

MCEER-99-0015 "Guide to Remedial Measures for Liquefaction Mitigation at Existing Highway Bridge Sites," by H.G. Cooke and J. K. Mitchell, 7/26/99, (PB2000-101703, A11, MF-A03).

MCEER-99-0016 "Proceedings of the MCEER Workshop on Ground Motion Methodologies for the Eastern United States," edited by N. Abrahamson and A. Becker, 8/11/99, (PB2000-103385, A07, MF-A02).

MCEER-99-0017 "Quindío, Colombia Earthquake of January 25, 1999: Reconnaissance Report," by A.P. Asfura and P.J. Flores, 10/4/99, (PB2000-106893, A06, MF-A01).

MCEER-99-0018 "Hysteretic Models for Cyclic Behavior of Deteriorating Inelastic Structures," by M.V. Sivaselvan and A.M. Reinhorn, 11/5/99, (PB2000-103386, A08, MF-A02).

MCEER-99-0019 "Proceedings of the 7th U.S.- Japan Workshop on Earthquake Resistant Design of Lifeline Facilities and Countermeasures Against Soil Liquefaction," edited by T.D. O'Rourke, J.P. Bardet and M. Hamada, 11/19/99, (PB2000-103354, A99, MF-A06).

MCEER-99-0020 "Development of Measurement Capability for Micro-Vibration Evaluations with Application to Chip Fabrication Facilities," by G.C. Lee, Z. Liang, J.W. Song, J.D. Shen and W.C. Liu, 12/1/99, (PB2000-105993, A08, MF-A02).

MCEER-99-0021 "Design and Retrofit Methodology for Building Structures with Supplemental Energy Dissipating Systems," by G. Pekcan, J.B. Mander and S.S. Chen, 12/31/99, (PB2000-105994, A11, MF-A03).

MCEER-00-0001 "The Marmara, Turkey Earthquake of August 17, 1999: Reconnaissance Report," edited by C. Scawthorn; with major contributions by M. Bruneau, R. Eguchi, T. Holzer, G. Johnson, J. Mander, J. Mitchell, W. Mitchell, A. Papageorgiou, C. Scaethorn, and G. Webb, 3/23/00, (PB2000-106200, A11, MF-A03).

MCEER-00-0002 "Proceedings of the MCEER Workshop for Seismic Hazard Mitigation of Health Care Facilities," edited by G.C. Lee, M. Ettouney, M. Grigoriu, J. Hauer and J. Nigg, 3/29/00, (PB2000-106892, A08, MF-A02).

MCEER-00-0003 "The Chi-Chi, Taiwan Earthquake of September 21, 1999: Reconnaissance Report," edited by G.C. Lee and C.H. Loh, with major contributions by G.C. Lee, M. Bruneau, I.G. Buckle, S.E. Chang, P.J. Flores, T.D. O'Rourke, M. Shinozuka, T.T. Soong, C-H. Loh, K-C. Chang, Z-J. Chen, J-S. Hwang, M-L. Lin, G-Y. Liu, K-C. Tsai, G.C. Yao and C-L. Yen, 4/30/00, (PB2001-100980, A10, MF-A02).

MCEER-00-0004 "Seismic Retrofit of End-Sway Frames of Steel Deck-Truss Bridges with a Supplemental Tendon System: Experimental and Analytical Investigation," by G. Pekcan, J.B. Mander and S.S. Chen, 7/1/00, (PB2001-100982, A10, MF-A02).

MCEER-00-0005 "Sliding Fragility of Unrestrained Equipment in Critical Facilities," by W.H. Chong and T.T. Soong, 7/5/00, (PB2001-100983, A08, MF-A02).

MCEER-00-0006 "Seismic Response of Reinforced Concrete Bridge Pier Walls in the Weak Direction," by N. Abo-Shadi, M. Saiidi and D. Sanders, 7/17/00, (PB2001-100981, A17, MF-A03).

MCEER-00-0007 "Low-Cycle Fatigue Behavior of Longitudinal Reinforcement in Reinforced Concrete Bridge Columns," by J. Brown and S.K. Kunnath, 7/23/00, (PB2001-104392, A08, MF-A02).

MCEER-00-0008 "Soil Structure Interaction of Bridges for Seismic Analysis," I. PoLam and H. Law, 9/25/00, (PB2001-105397, A08, MF-A02).

MCEER-00-0009 "Proceedings of the First MCEER Workshop on Mitigation of Earthquake Disaster by Advanced Technologies (MEDAT-1), edited by M. Shinozuka, D.J. Inman and T.D. O'Rourke, 11/10/00, (PB2001-105399, A14, MF-A03).

MCEER-00-0010 "Development and Evaluation of Simplified Procedures for Analysis and Design of Buildings with Passive Energy Dissipation Systems, Revision 01," by O.M. Ramirez, M.C. Constantinou, C.A. Kircher, A.S. Whittaker, M.W. Johnson, J.D. Gomez and C. Chrysostomou, 11/16/01, (PB2001-105523, A23, MF-A04).

MCEER-00-0011 "Dynamic Soil-Foundation-Structure Interaction Analyses of Large Caissons," by C-Y. Chang, C-M. Mok, Z-L. Wang, R. Settgast, F. Waggoner, M.A. Ketchum, H.M. Gonnermann and C-C. Chin, 12/30/00, (PB2001-104373, A07, MF-A02).

MCEER-00-0012 "Experimental Evaluation of Seismic Performance of Bridge Restrainers," by A.G. Vlassis, E.M. Maragakis and M. Saiid Saiidi, 12/30/00, (PB2001-104354, A09, MF-A02).

MCEER-00-0013 "Effect of Spatial Variation of Ground Motion on Highway Structures," by M. Shinozuka, V. Saxena and G. Deodatis, 12/31/00, (PB2001-108755, A13, MF-A03).

MCEER-00-0014 "A Risk-Based Methodology for Assessing the Seismic Performance of Highway Systems," by S.D. Werner, C.E. Taylor, J.E. Moore, II, J.S. Walton and S. Cho, 12/31/00, (PB2001-108756, A14, MF-A03).

MCEER-01-0001 "Experimental Investigation of P-Delta Effects to Collapse During Earthquakes," by D. Vian and M. Bruneau, 6/25/01, (PB2002-100534, A17, MF-A03).

MCEER-01-0002 "Proceedings of the Second MCEER Workshop on Mitigation of Earthquake Disaster by Advanced Technologies (MEDAT-2)," edited by M. Bruneau and D.J. Inman, 7/23/01, (PB2002-100434, A16, MF-A03).

MCEER-01-0003 "Sensitivity Analysis of Dynamic Systems Subjected to Seismic Loads," by C. Roth and M. Grigoriu, 9/18/01, (PB2003-100884, A12, MF-A03).

MCEER-01-0004 "Overcoming Obstacles to Implementing Earthquake Hazard Mitigation Policies: Stage 1 Report," by D.J. Alesch and W.J. Petak, 12/17/01, (PB2002-107949, A07, MF-A02).

MCEER-01-0005 "Updating Real-Time Earthquake Loss Estimates: Methods, Problems and Insights," by C.E. Taylor, S.E. Chang and R.T. Eguchi, 12/17/01, (PB2002-107948, A05, MF-A01).

MCEER-01-0006 "Experimental Investigation and Retrofit of Steel Pile Foundations and Pile Bents Under Cyclic Lateral Loadings," by A. Shama, J. Mander, B. Blabac and S. Chen, 12/31/01, (PB2002-107950, A13, MF-A03).

MCEER-02-0001 "Assessment of Performance of Bolu Viaduct in the 1999 Duzce Earthquake in Turkey" by P.C. Roussis, M.C. Constantinou, M. Erdik, E. Durukal and M. Dicleli, 5/8/02, (PB2003-100883, A08, MF-A02).

MCEER-02-0002 "Seismic Behavior of Rail Counterweight Systems of Elevators in Buildings," by M.P. Singh, Rildova and L.E. Suarez, 5/27/02. (PB2003-100882, A11, MF-A03).

MCEER-02-0003 "Development of Analysis and Design Procedures for Spread Footings," by G. Mylonakis, G. Gazetas, S. Nikolaou and A. Chauncey, 10/02/02, (PB2004-101636, A13, MF-A03, CD-A13).

MCEER-02-0004 "Bare-Earth Algorithms for Use with SAR and LIDAR Digital Elevation Models," by C.K. Huyck, R.T. Eguchi and B. Houshmand, 10/16/02, (PB2004-101637, A07, CD-A07).

MCEER-02-0005 "Review of Energy Dissipation of Compression Members in Concentrically Braced Frames," by K.Lee and M. Bruneau, 10/18/02, (PB2004-101638, A10, CD-A10).

MCEER-03-0001 "Experimental Investigation of Light-Gauge Steel Plate Shear Walls for the Seismic Retrofit of Buildings" by J. Berman and M. Bruneau, 5/2/03, (PB2004-101622, A10, MF-A03, CD-A10).

MCEER-03-0002 "Statistical Analysis of Fragility Curves," by M. Shinozuka, M.Q. Feng, H. Kim, T. Uzawa and T. Ueda, 6/16/03, (PB2004-101849, A09, CD-A09).

MCEER-03-0003 "Proceedings of the Eighth U.S.-Japan Workshop on Earthquake Resistant Design f Lifeline Facilities and Countermeasures Against Liquefaction," edited by M. Hamada, J.P. Bardet and T.D. O'Rourke, 6/30/03, (PB2004-104386, A99, CD-A99).

MCEER-03-0004 "Proceedings of the PRC-US Workshop on Seismic Analysis and Design of Special Bridges," edited by L.C. Fan and G.C. Lee, 7/15/03, (PB2004-104387, A14, CD-A14).

MCEER-03-0005 "Urban Disaster Recovery: A Framework and Simulation Model," by S.B. Miles and S.E. Chang, 7/25/03, (PB2004-104388, A07, CD-A07).

MCEER-03-0006 "Behavior of Underground Piping Joints Due to Static and Dynamic Loading," by R.D. Meis, M. Maragakis and R. Siddharthan, 11/17/03, (PB2005-102194, A13, MF-A03, CD-A00).

MCEER-04-0001 "Experimental Study of Seismic Isolation Systems with Emphasis on Secondary System Response and Verification of Accuracy of Dynamic Response History Analysis Methods," by E. Wolff and M. Constantinou, 1/16/04 (PB2005-102195, A99, MF-E08, CD-A00).

MCEER-04-0002 "Tension, Compression and Cyclic Testing of Engineered Cementitious Composite Materials," by K. Kesner and S.L. Billington, 3/1/04, (PB2005-102196, A08, CD-A08).

MCEER-04-0003 "Cyclic Testing of Braces Laterally Restrained by Steel Studs to Enhance Performance During Earthquakes," by O.C. Celik, J.W. Berman and M. Bruneau, 3/16/04, (PB2005-102197, A13, MF-A03, CD-A00).

MCEER-04-0004 "Methodologies for Post Earthquake Building Damage Detection Using SAR and Optical Remote Sensing: Application to the August 17, 1999 Marmara, Turkey Earthquake," by C.K. Huyck, B.J. Adams, S. Cho, R.T. Eguchi, B. Mansouri and B. Houshmand, 6/15/04, (PB2005-104888, A10, CD-A00).

MCEER-04-0005 "Nonlinear Structural Analysis Towards Collapse Simulation: A Dynamical Systems Approach," by M.V. Sivaselvan and A.M. Reinhorn, 6/16/04, (PB2005-104889, A11, MF-A03, CD-A00).

MCEER-04-0006 "Proceedings of the Second PRC-US Workshop on Seismic Analysis and Design of Special Bridges," edited by G.C. Lee and L.C. Fan, 6/25/04, (PB2005-104890, A16, CD-A00).

MCEER-04-0007 "Seismic Vulnerability Evaluation of Axially Loaded Steel Built-up Laced Members," by K. Lee and M. Bruneau, 6/30/04, (PB2005-104891, A16, CD-A00).

MCEER-04-0008 "Evaluation of Accuracy of Simplified Methods of Analysis and Design of Buildings with Damping Systems for Near-Fault and for Soft-Soil Seismic Motions," by E.A. Pavlou and M.C. Constantinou, 8/16/04, (PB2005-104892, A08, MF-A02, CD-A00).

MCEER-04-0009 "Assessment of Geotechnical Issues in Acute Care Facilities in California," by M. Lew, T.D. O'Rourke, R. Dobry and M. Koch, 9/15/04, (PB2005-104893, A08, CD-A00).

MCEER-04-0010 "Scissor-Jack-Damper Energy Dissipation System," by A.N. Sigaher-Boyle and M.C. Constantinou, 12/1/04 (PB2005-108221).

MCEER-04-0011 "Seismic Retrofit of Bridge Steel Truss Piers Using a Controlled Rocking Approach," by M. Pollino and M. Bruneau, 12/20/04 (PB2006-105795).

MCEER-05-0001 "Experimental and Analytical Studies of Structures Seismically Isolated with an Uplift-Restraint Isolation System," by P.C. Roussis and M.C. Constantinou, 1/10/05 (PB2005-108222).

MCEER-05-0002 "A Versatile Experimentation Model for Study of Structures Near Collapse Applied to Seismic Evaluation of Irregular Structures," by D. Kusumastuti, A.M. Reinhorn and A. Rutenberg, 3/31/05 (PB2006-101523).

MCEER-05-0003 "Proceedings of the Third PRC-US Workshop on Seismic Analysis and Design of Special Bridges," edited by L.C. Fan and G.C. Lee, 4/20/05, (PB2006-105796).

MCEER-05-0004 "Approaches for the Seismic Retrofit of Braced Steel Bridge Piers and Proof-of-Concept Testing of an Eccentrically Braced Frame with Tubular Link," by J.W. Berman and M. Bruneau, 4/21/05 (PB2006-101524).

MCEER-05-0005 "Simulation of Strong Ground Motions for Seismic Fragility Evaluation of Nonstructural Components in Hospitals," by A. Wanitkorkul and A. Filiatrault, 5/26/05 (PB2006-500027).

MCEER-05-0006 "Seismic Safety in California Hospitals: Assessing an Attempt to Accelerate the Replacement or Seismic Retrofit of Older Hospital Facilities," by D.J. Alesch, L.A. Arendt and W.J. Petak, 6/6/05 (PB2006-105794).

MCEER-05-0007 "Development of Seismic Strengthening and Retrofit Strategies for Critical Facilities Using Engineered Cementitious Composite Materials," by K. Kesner and S.L. Billington, 8/29/05 (PB2006-111701).

MCEER-05-0008 "Experimental and Analytical Studies of Base Isolation Systems for Seismic Protection of Power Transformers," by N. Murota, M.Q. Feng and G-Y. Liu, 9/30/05 (PB2006-111702).

MCEER-05-0009 "3D-BASIS-ME-MB: Computer Program for Nonlinear Dynamic Analysis of Seismically Isolated Structures," by P.C. Tsopelas, P.C. Roussis, M.C. Constantinou, R. Buchanan and A.M. Reinhorn, 10/3/05 (PB2006-111703).

MCEER-05-0010 "Steel Plate Shear Walls for Seismic Design and Retrofit of Building Structures," by D. Vian and M. Bruneau, 12/15/05 (PB2006-111704).

MCEER-05-0011 "The Performance-Based Design Paradigm," by M.J. Astrella and A. Whittaker, 12/15/05 (PB2006-111705).

MCEER-06-0001 "Seismic Fragility of Suspended Ceiling Systems," H. Badillo-Almaraz, A.S. Whittaker, A.M. Reinhorn and G.P. Cimellaro, 2/4/06 (PB2006-111706).

MCEER-06-0002 "Multi-Dimensional Fragility of Structures," by G.P. Cimellaro, A.M. Reinhorn and M. Bruneau, 3/1/06 (PB2007-106974, A09, MF-A02, CD A00).

MCEER-06-0003 "Built-Up Shear Links as Energy Dissipators for Seismic Protection of Bridges," by P. Dusicka, A.M. Itani and I.G. Buckle, 3/15/06 (PB2006-111708).

MCEER-06-0004 "Analytical Investigation of the Structural Fuse Concept," by R.E. Vargas and M. Bruneau, 3/16/06 (PB2006-111709).

MCEER-06-0005 "Experimental Investigation of the Structural Fuse Concept," by R.E. Vargas and M. Bruneau, 3/17/06 (PB2006-111710).

MCEER-06-0006 "Further Development of Tubular Eccentrically Braced Frame Links for the Seismic Retrofit of Braced Steel Truss Bridge Piers," by J.W. Berman and M. Bruneau, 3/27/06 (PB2007-105147).

MCEER-06-0007 "REDARS Validation Report," by S. Cho, C.K. Huyck, S. Ghosh and R.T. Eguchi, 8/8/06 (PB2007-106983).

MCEER-06-0008 "Review of Current NDE Technologies for Post-Earthquake Assessment of Retrofitted Bridge Columns," by J.W. Song, Z. Liang and G.C. Lee, 8/21/06 (PB2007-106984).

MCEER-06-0009 "Liquefaction Remediation in Silty Soils Using Dynamic Compaction and Stone Columns," by S. Thevanayagam, G.R. Martin, R. Nashed, T. Shenthan, T. Kanagalingam and N. Ecemis, 8/28/06 (PB2007-106985).

MCEER-06-0010 "Conceptual Design and Experimental Investigation of Polymer Matrix Composite Infill Panels for Seismic Retrofitting," by W. Jung, M. Chiewanichakorn and A.J. Aref, 9/21/06 (PB2007-106986).

MCEER-06-0011 "A Study of the Coupled Horizontal-Vertical Behavior of Elastomeric and Lead-Rubber Seismic Isolation Bearings," by G.P. Warn and A.S. Whittaker, 9/22/06 (PB2007-108679).

MCEER-06-0012 "Proceedings of the Fourth PRC-US Workshop on Seismic Analysis and Design of Special Bridges: Advancing Bridge Technologies in Research, Design, Construction and Preservation," Edited by L.C. Fan, G.C. Lee and L. Ziang, 10/12/06 (PB2007-109042).

MCEER-06-0013 "Cyclic Response and Low Cycle Fatigue Characteristics of Plate Steels," by P. Dusicka, A.M. Itani and I.G. Buckle, 11/1/06 06 (PB2007-106987).

MCEER-06-0014 "Proceedings of the Second US-Taiwan Bridge Engineering Workshop," edited by W.P. Yen, J. Shen, J-Y. Chen and M. Wang, 11/15/06 (PB2008-500041).

MCEER-06-0015 "User Manual and Technical Documentation for the REDARS™ Import Wizard," by S. Cho, S. Ghosh, C.K. Huyck and S.D. Werner, 11/30/06 (PB2007-114766).

MCEER-06-0016 "Hazard Mitigation Strategy and Monitoring Technologies for Urban and Infrastructure Public Buildings: Proceedings of the China-US Workshops," edited by X.Y. Zhou, A.L. Zhang, G.C. Lee and M. Tong, 12/12/06 (PB2008-500018).

MCEER-07-0001 "Static and Kinetic Coefficients of Friction for Rigid Blocks," by C. Kafali, S. Fathali, M. Grigoriu and A.S. Whittaker, 3/20/07 (PB2007-114767).

MCEER-07-0002 "Hazard Mitigation Investment Decision Making: Organizational Response to Legislative Mandate," by L.A. Arendt, D.J. Alesch and W.J. Petak, 4/9/07 (PB2007-114768).

MCEER-07-0003 "Seismic Behavior of Bidirectional-Resistant Ductile End Diaphragms with Unbonded Braces in Straight or Skewed Steel Bridges," by O. Celik and M. Bruneau, 4/11/07 (PB2008-105141).

MCEER-07-0004 "Modeling Pile Behavior in Large Pile Groups Under Lateral Loading," by A.M. Dodds and G.R. Martin, 4/16/07(PB2008-105142).

MCEER-07-0005 "Experimental Investigation of Blast Performance of Seismically Resistant Concrete-Filled Steel Tube Bridge Piers," by S. Fujikura, M. Bruneau and D. Lopez-Garcia, 4/20/07 (PB2008-105143).

MCEER-07-0006 "Seismic Analysis of Conventional and Isolated Liquefied Natural Gas Tanks Using Mechanical Analogs," by I.P. Christovasilis and A.S. Whittaker, 5/1/07, not available.

MCEER-07-0007 "Experimental Seismic Performance Evaluation of Isolation/Restraint Systems for Mechanical Equipment – Part 1: Heavy Equipment Study," by S. Fathali and A. Filiatrault, 6/6/07 (PB2008-105144).

MCEER-07-0008 "Seismic Vulnerability of Timber Bridges and Timber Substructures," by A.A. Sharma, J.B. Mander, I.M. Friedland and D.R. Allicock, 6/7/07 (PB2008-105145).

MCEER-07-0009 "Experimental and Analytical Study of the XY-Friction Pendulum (XY-FP) Bearing for Bridge Applications," by C.C. Marin-Artieda, A.S. Whittaker and M.C. Constantinou, 6/7/07 (PB2008-105191).

MCEER-07-0010 "Proceedings of the PRC-US Earthquake Engineering Forum for Young Researchers," Edited by G.C. Lee and X.Z. Qi, 6/8/07 (PB2008-500058).

MCEER-07-0011 "Design Recommendations for Perforated Steel Plate Shear Walls," by R. Purba and M. Bruneau, 6/18/07, (PB2008-105192).

MCEER-07-0012 "Performance of Seismic Isolation Hardware Under Service and Seismic Loading," by M.C. Constantinou, A.S. Whittaker, Y. Kalpakidis, D.M. Fenz and G.P. Warn, 8/27/07, (PB2008-105193).

MCEER-07-0013 "Experimental Evaluation of the Seismic Performance of Hospital Piping Subassemblies," by E.R. Goodwin, E. Maragakis and A.M. Itani, 9/4/07, (PB2008-105194).

MCEER-07-0014 "A Simulation Model of Urban Disaster Recovery and Resilience: Implementation for the 1994 Northridge Earthquake," by S. Miles and S.E. Chang, 9/7/07, (PB2008-106426).

MCEER-07-0015 "Statistical and Mechanistic Fragility Analysis of Concrete Bridges," by M. Shinozuka, S. Banerjee and S-H. Kim, 9/10/07, (PB2008-106427).

MCEER-07-0016 "Three-Dimensional Modeling of Inelastic Buckling in Frame Structures," by M. Schachter and AM. Reinhorn, 9/13/07, (PB2008-108125).

MCEER-07-0017 "Modeling of Seismic Wave Scattering on Pile Groups and Caissons," by I. Po Lam, H. Law and C.T. Yang, 9/17/07 (PB2008-108150).

MCEER-07-0018 "Bridge Foundations: Modeling Large Pile Groups and Caissons for Seismic Design," by I. Po Lam, H. Law and G.R. Martin (Coordinating Author), 12/1/07 (PB2008-111190).

MCEER-07-0019 "Principles and Performance of Roller Seismic Isolation Bearings for Highway Bridges," by G.C. Lee, Y.C. Ou, Z. Liang, T.C. Niu and J. Song, 12/10/07 (PB2009-110466).

MCEER-07-0020 "Centrifuge Modeling of Permeability and Pinning Reinforcement Effects on Pile Response to Lateral Spreading," by L.L Gonzalez-Lagos, T. Abdoun and R. Dobry, 12/10/07 (PB2008-111191).

MCEER-07-0021 "Damage to the Highway System from the Pisco, Perú Earthquake of August 15, 2007," by J.S. O'Connor, L. Mesa and M. Nykamp, 12/10/07, (PB2008-108126).

MCEER-07-0022 "Experimental Seismic Performance Evaluation of Isolation/Restraint Systems for Mechanical Equipment – Part 2: Light Equipment Study," by S. Fathali and A. Filiatrault, 12/13/07 (PB2008-111192).

MCEER-07-0023 "Fragility Considerations in Highway Bridge Design," by M. Shinozuka, S. Banerjee and S.H. Kim, 12/14/07 (PB2008-111193).

MCEER-07-0024 "Performance Estimates for Seismically Isolated Bridges," by G.P. Warn and A.S. Whittaker, 12/30/07 (PB2008-112230).

MCEER-08-0001 "Seismic Performance of Steel Girder Bridge Superstructures with Conventional Cross Frames," by L.P. Carden, A.M. Itani and I.G. Buckle, 1/7/08, (PB2008-112231).

MCEER-08-0002 "Seismic Performance of Steel Girder Bridge Superstructures with Ductile End Cross Frames with Seismic Isolators," by L.P. Carden, A.M. Itani and I.G. Buckle, 1/7/08 (PB2008-112232).

MCEER-08-0003 "Analytical and Experimental Investigation of a Controlled Rocking Approach for Seismic Protection of Bridge Steel Truss Piers," by M. Pollino and M. Bruneau, 1/21/08 (PB2008-112233).

MCEER-08-0004 "Linking Lifeline Infrastructure Performance and Community Disaster Resilience: Models and Multi-Stakeholder Processes," by S.E. Chang, C. Pasion, K. Tatebe and R. Ahmad, 3/3/08 (PB2008-112234).

MCEER-08-0005 "Modal Analysis of Generally Damped Linear Structures Subjected to Seismic Excitations," by J. Song, Y-L. Chu, Z. Liang and G.C. Lee, 3/4/08 (PB2009-102311).

MCEER-08-0006 "System Performance Under Multi-Hazard Environments," by C. Kafali and M. Grigoriu, 3/4/08 (PB2008-112235).

MCEER-08-0007 "Mechanical Behavior of Multi-Spherical Sliding Bearings," by D.M. Fenz and M.C. Constantinou, 3/6/08 (PB2008-112236).

MCEER-08-0008 "Post-Earthquake Restoration of the Los Angeles Water Supply System," by T.H.P. Tabucchi and R.A. Davidson, 3/7/08 (PB2008-112237).

MCEER-08-0009 "Fragility Analysis of Water Supply Systems," by A. Jacobson and M. Grigoriu, 3/10/08 (PB2009-105545).

MCEER-08-0010 "Experimental Investigation of Full-Scale Two-Story Steel Plate Shear Walls with Reduced Beam Section Connections," by B. Qu, M. Bruneau, C-H. Lin and K-C. Tsai, 3/17/08 (PB2009-106368).

MCEER-08-0011 "Seismic Evaluation and Rehabilitation of Critical Components of Electrical Power Systems," S. Ersoy, B. Feizi, A. Ashrafi and M. Ala Saadeghvaziri, 3/17/08 (PB2009-105546).

MCEER-08-0012 "Seismic Behavior and Design of Boundary Frame Members of Steel Plate Shear Walls," by B. Qu and M. Bruneau, 4/26/08 . (PB2009-106744).

MCEER-08-0013 "Development and Appraisal of a Numerical Cyclic Loading Protocol for Quantifying Building System Performance," by A. Filiatrault, A. Wanitkorkul and M. Constantinou, 4/27/08 (PB2009-107906).

MCEER-08-0014 "Structural and Nonstructural Earthquake Design: The Challenge of Integrating Specialty Areas in Designing Complex, Critical Facilities," by W.J. Petak and D.J. Alesch, 4/30/08 (PB2009-107907).

MCEER-08-0015 "Seismic Performance Evaluation of Water Systems," by Y. Wang and T.D. O'Rourke, 5/5/08 (PB2009-107908).

MCEER-08-0016 "Seismic Response Modeling of Water Supply Systems," by P. Shi and T.D. O'Rourke, 5/5/08 (PB2009-107910).

MCEER-08-0017 "Numerical and Experimental Studies of Self-Centering Post-Tensioned Steel Frames," by D. Wang and A. Filiatrault, 5/12/08 (PB2009-110479).

MCEER-08-0018 "Development, Implementation and Verification of Dynamic Analysis Models for Multi-Spherical Sliding Bearings," by D.M. Fenz and M.C. Constantinou, 8/15/08 (PB2009-107911).

MCEER-08-0019 "Performance Assessment of Conventional and Base Isolated Nuclear Power Plants for Earthquake Blast Loadings," by Y.N. Huang, A.S. Whittaker and N. Luco, 10/28/08 (PB2009-107912).

MCEER-08-0020 "Remote Sensing for Resilient Multi-Hazard Disaster Response – Volume I: Introduction to Damage Assessment Methodologies," by B.J. Adams and R.T. Eguchi, 11/17/08 (PB2010-102695).

MCEER-08-0021 "Remote Sensing for Resilient Multi-Hazard Disaster Response – Volume II: Counting the Number of Collapsed Buildings Using an Object-Oriented Analysis: Case Study of the 2003 Bam Earthquake," by L. Gusella, C.K. Huyck and B.J. Adams, 11/17/08 (PB2010-100925).

MCEER-08-0022 "Remote Sensing for Resilient Multi-Hazard Disaster Response – Volume III: Multi-Sensor Image Fusion Techniques for Robust Neighborhood-Scale Urban Damage Assessment," by B.J. Adams and A. McMillan, 11/17/08 (PB2010-100926).

MCEER-08-0023 "Remote Sensing for Resilient Multi-Hazard Disaster Response – Volume IV: A Study of Multi-Temporal and Multi-Resolution SAR Imagery for Post-Katrina Flood Monitoring in New Orleans," by A. McMillan, J.G. Morley, B.J. Adams and S. Chesworth, 11/17/08 (PB2010-100927).

MCEER-08-0024 "Remote Sensing for Resilient Multi-Hazard Disaster Response – Volume V: Integration of Remote Sensing Imagery and VIEWS$^{TM}$ Field Data for Post-Hurricane Charley Building Damage Assessment," by J.A. Womble, K. Mehta and B.J. Adams, 11/17/08 (PB2009-115532).

MCEER-08-0025 "Building Inventory Compilation for Disaster Management: Application of Remote Sensing and Statistical Modeling," by P. Sarabandi, A.S. Kiremidjian, R.T. Eguchi and B. J. Adams, 11/20/08 (PB2009-110484).

MCEER-08-0026 "New Experimental Capabilities and Loading Protocols for Seismic Qualification and Fragility Assessment of Nonstructural Systems," by R. Retamales, G. Mosqueda, A. Filiatrault and A. Reinhorn, 11/24/08 (PB2009-110485).

MCEER-08-0027 "Effects of Heating and Load History on the Behavior of Lead-Rubber Bearings," by I.V. Kalpakidis and M.C. Constantinou, 12/1/08 (PB2009-115533).

MCEER-08-0028 "Experimental and Analytical Investigation of Blast Performance of Seismically Resistant Bridge Piers," by S.Fujikura and M. Bruneau, 12/8/08 (PB2009-115534).

MCEER-08-0029 "Evolutionary Methodology for Aseismic Decision Support," by Y. Hu and G. Dargush, 12/15/08.

MCEER-08-0030 "Development of a Steel Plate Shear Wall Bridge Pier System Conceived from a Multi-Hazard Perspective," by D. Keller and M. Bruneau, 12/19/08 (PB2010-102696).

MCEER-09-0001 "Modal Analysis of Arbitrarily Damped Three-Dimensional Linear Structures Subjected to Seismic Excitations," by Y.L. Chu, J. Song and G.C. Lee, 1/31/09 (PB2010-100922).

MCEER-09-0002 "Air-Blast Effects on Structural Shapes," by G. Ballantyne, A.S. Whittaker, A.J. Aref and G.F. Dargush, 2/2/09 (PB2010-102697).

MCEER-09-0003 "Water Supply Performance During Earthquakes and Extreme Events," by A.L. Bonneau and T.D. O'Rourke, 2/16/09 (PB2010-100923).

MCEER-09-0004 "Generalized Linear (Mixed) Models of Post-Earthquake Ignitions," by R.A. Davidson, 7/20/09 (PB2010-102698).

MCEER-09-0005 "Seismic Testing of a Full-Scale Two-Story Light-Frame Wood Building: NEESWood Benchmark Test," by I.P. Christovasilis, A. Filiatrault and A. Wanitkorkul, 7/22/09 (PB2012-102401).

MCEER-09-0006 "IDARC2D Version 7.0: A Program for the Inelastic Damage Analysis of Structures," by A.M. Reinhorn, H. Roh, M. Sivaselvan, S.K. Kunnath, R.E. Valles, A. Madan, C. Li, R. Lobo and Y.J. Park, 7/28/09 (PB2010-103199).

MCEER-09-0007 "Enhancements to Hospital Resiliency: Improving Emergency Planning for and Response to Hurricanes," by D.B. Hess and L.A. Arendt, 7/30/09 (PB2010-100924).

MCEER-09-0008 "Assessment of Base-Isolated Nuclear Structures for Design and Beyond-Design Basis Earthquake Shaking," by Y.N. Huang, A.S. Whittaker, R.P. Kennedy and R.L. Mayes, 8/20/09 (PB2010-102699).

MCEER-09-0009 "Quantification of Disaster Resilience of Health Care Facilities," by G.P. Cimellaro, C. Fumo, A.M Reinhorn and M. Bruneau, 9/14/09 (PB2010-105384).

MCEER-09-0010 "Performance-Based Assessment and Design of Squat Reinforced Concrete Shear Walls," by C.K. Gulec and A.S. Whittaker, 9/15/09 (PB2010-102700).

MCEER-09-0011 "Proceedings of the Fourth US-Taiwan Bridge Engineering Workshop," edited by W.P. Yen, J.J. Shen, T.M. Lee and R.B. Zheng, 10/27/09 (PB2010-500009).

MCEER-09-0012 "Proceedings of the Special International Workshop on Seismic Connection Details for Segmental Bridge Construction," edited by W. Phillip Yen and George C. Lee, 12/21/09 (PB2012-102402).

MCEER-10-0001 "Direct Displacement Procedure for Performance-Based Seismic Design of Multistory Woodframe Structures," by W. Pang and D. Rosowsky, 4/26/10 (PB2012-102403).

MCEER-10-0002 "Simplified Direct Displacement Design of Six-Story NEESWood Capstone Building and Pre-Test Seismic Performance Assessment," by W. Pang, D. Rosowsky, J. van de Lindt and S. Pei, 5/28/10 (PB2012-102404).

MCEER-10-0003 "Integration of Seismic Protection Systems in Performance-Based Seismic Design of Woodframed Structures," by J.K. Shinde and M.D. Symans, 6/18/10 (PB2012-102405).

MCEER-10-0004 "Modeling and Seismic Evaluation of Nonstructural Components: Testing Frame for Experimental Evaluation of Suspended Ceiling Systems," by A.M. Reinhorn, K.P. Ryu and G. Maddaloni, 6/30/10 (PB2012-102406).

MCEER-10-0005 "Analytical Development and Experimental Validation of a Structural-Fuse Bridge Pier Concept," by S. El-Bahey and M. Bruneau, 10/1/10 (PB2012-102407).

MCEER-10-0006 "A Framework for Defining and Measuring Resilience at the Community Scale: The PEOPLES Resilience Framework," by C.S. Renschler, A.E. Frazier, L.A. Arendt, G.P. Cimellaro, A.M. Reinhorn and M. Bruneau, 10/8/10 (PB2012-102408).

MCEER-10-0007 "Impact of Horizontal Boundary Elements Design on Seismic Behavior of Steel Plate Shear Walls," by R. Purba and M. Bruneau, 11/14/10 (PB2012-102409).

MCEER-10-0008 "Seismic Testing of a Full-Scale Mid-Rise Building: The NEESWood Capstone Test," by S. Pei, J.W. van de Lindt, S.E. Pryor, H. Shimizu, H. Isoda and D.R. Rammer, 12/1/10 (PB2012-102410).

MCEER-10-0009 "Modeling the Effects of Detonations of High Explosives to Inform Blast-Resistant Design," by P. Sherkar, A.S. Whittaker and A.J. Aref, 12/1/10 (PB2012-102411).

MCEER-10-0010 "L'Aquila Earthquake of April 6, 2009 in Italy: Rebuilding a Resilient City to Withstand Multiple Hazards," by G.P. Cimellaro, I.P. Christovasilis, A.M. Reinhorn, A. De Stefano and T. Kirova, 12/29/10.

MCEER-11-0001 "Numerical and Experimental Investigation of the Seismic Response of Light-Frame Wood Structures," by I.P. Christovasilis and A. Filiatrault, 8/8/11 (PB2012-102412).

MCEER-11-0002 "Seismic Design and Analysis of a Precast Segmental Concrete Bridge Model," by M. Anagnostopoulou, A. Filiatrault and A. Aref, 9/15/11.

MCEER-11-0003 'Proceedings of the Workshop on Improving Earthquake Response of Substation Equipment," Edited by A.M. Reinhorn, 9/19/11 (PB2012-102413).

MCEER-11-0004 "LRFD-Based Analysis and Design Procedures for Bridge Bearings and Seismic Isolators," by M.C. Constantinou, I. Kalpakidis, A. Filiatrault and R.A. Ecker Lay, 9/26/11.

MCEER-11-0005 "Experimental Seismic Evaluation, Model Parameterization, and Effects of Cold-Formed Steel-Framed Gypsum Partition Walls on the Seismic Performance of an Essential Facility," by R. Davies, R. Retamales, G. Mosqueda and A. Filiatrault, 10/12/11.

MCEER-11-0006 "Modeling and Seismic Performance Evaluation of High Voltage Transformers and Bushings," by A.M. Reinhorn, K. Oikonomou, H. Roh, A. Schiff and L. Kempner, Jr., 10/3/11.

MCEER-11-0007 "Extreme Load Combinations: A Survey of State Bridge Engineers," by G.C. Lee, Z. Liang, J.J. Shen and J.S. O'Connor, 10/14/11.

MCEER-12-0001 "Simplified Analysis Procedures in Support of Performance Based Seismic Design," by Y.N. Huang and A.S. Whittaker.

MCEER-12-0002 "Seismic Protection of Electrical Transformer Bushing Systems by Stiffening Techniques," by M. Koliou, A. Filiatrault, A.M. Reinhorn and N. Oliveto, 6/1/12.

MCEER-12-0003 "Post-Earthquake Bridge Inspection Guidelines," by J.S. O'Connor and S. Alampalli, 6/8/12.

MCEER-12-0004 "Integrated Design Methodology for Isolated Floor Systems in Single-Degree-of-Freedom Structural Fuse Systems," by S. Cui, M. Bruneau and M.C. Constantinou, 6/13/12.

MCEER-12-0005 "Characterizing the Rotational Components of Earthquake Ground Motion," by D. Basu, A.S. Whittaker and M.C. Constantinou, 6/15/12.

MCEER-12-0006 "Bayesian Fragility for Nonstructural Systems," by C.H. Lee and M.D. Grigoriu, 9/12/12.

MCEER-12-0007 "A Numerical Model for Capturing the In-Plane Seismic Response of Interior Metal Stud Partition Walls," by R.L. Wood and T.C. Hutchinson, 9/12/12.

MCEER-12-0008 "Assessment of Floor Accelerations in Yielding Buildings," by J.D. Wieser, G. Pekcan, A.E. Zaghi, A.M. Itani and E. Maragakis, 10/5/12.

MCEER-13-0001 "Experimental Seismic Study of Pressurized Fire Sprinkler Piping Systems," by Y. Tian, A. Filiatrault and G. Mosqueda, 4/8/13.

MCEER-13-0002 "Enhancing Resource Coordination for Multi-Modal Evacuation Planning," by D.B. Hess, B.W. Conley and C.M. Farrell, 2/8/13.

MCEER-13-0003 "Seismic Response of Base Isolated Buildings Considering Pounding to Moat Walls," by A. Masroor and G. Mosqueda, 2/26/13.

MCEER-13-0004 "Seismic Response Control of Structures Using a Novel Adaptive Passive Negative Stiffness Device," by D.T.R. Pasala, A.A. Sarlis, S. Nagarajaiah, A.M. Reinhorn, M.C. Constantinou and D.P. Taylor, 6/10/13.

MCEER-13-0005 "Negative Stiffness Device for Seismic Protection of Structures," by A.A. Sarlis, D.T.R. Pasala, M.C. Constantinou, A.M. Reinhorn, S. Nagarajaiah and D.P. Taylor, 6/12/13.

MCEER-13-0006 "Emilia Earthquake of May 20, 2012 in Northern Italy: Rebuilding a Resilient Community to Withstand Multiple Hazards," by G.P. Cimellaro, M. Chiriatti, A.M. Reinhorn and L. Tirca, June 30, 2013.

MCEER-13-0007 "Precast Concrete Segmental Components and Systems for Accelerated Bridge Construction in Seismic Regions," by A.J. Aref, G.C. Lee, Y.C. Ou and P. Sideris, with contributions from K.C. Chang, S. Chen, A. Filiatrault and Y. Zhou, June 13, 2013.

MCEER-13-0008 "A Study of U.S. Bridge Failures (1980-2012)," by G.C. Lee, S.B. Mohan, C. Huang and B.N. Fard, June 15, 2013.

MCEER-13-0009 "Development of a Database Framework for Modeling Damaged Bridges," by G.C. Lee, J.C. Qi and C. Huang, June 16, 2013.

MCEER-13-0010 "Model of Triple Friction Pendulum Bearing for General Geometric and Frictional Parameters and for Uplift Conditions," by A.A. Sarlis and M.C. Constantinou, July 1, 2013.

MCEER-13-0011 "Shake Table Testing of Triple Friction Pendulum Isolators under Extreme Conditions," by A.A. Sarlis, M.C. Constantinou and A.M. Reinhorn, July 2, 2013.

MCEER-13-0012 "Theoretical Framework for the Development of MH-LRFD," by G.C. Lee (coordinating author), H.A Capers, Jr., C. Huang, J.M. Kulicki, Z. Liang, T. Murphy, J.J.D. Shen, M. Shinozuka and P.W.H. Yen, July 31, 2013.

MCEER-13-0013 "Seismic Protection of Highway Bridges with Negative Stiffness Devices," by N.K.A. Attary, M.D. Symans, S. Nagarajaiah, A.M. Reinhorn, M.C. Constantinou, A.A. Sarlis, D.T.R. Pasala, and D.P. Taylor, September 3, 2014.

MCEER-14-0001 "Simplified Seismic Collapse Capacity-Based Evaluation and Design of Frame Buildings with and without Supplemental Damping Systems," by M. Hamidia, A. Filiatrault, and A. Aref, May 19, 2014.

MCEER-14-0002 "Comprehensive Analytical Seismic Fragility of Fire Sprinkler Piping Systems," by Siavash Soroushian, Emmanuel "Manos" Maragakis, Arash E. Zaghi, Alicia Echevarria, Yuan Tian and Andre Filiatrault, August 26, 2014.

MCEER-14-0003 "Hybrid Simulation of the Seismic Response of a Steel Moment Frame Building Structure through Collapse," by M. Del Carpio Ramos, G. Mosqueda and D.G. Lignos, October 30, 2014.

MCEER-14-0004 "Blast and Seismic Resistant Concrete-Filled Double Skin Tubes and Modified Steel Jacketed Bridge Columns," by P.P. Fouche and M. Bruneau, June 30, 2015.

MCEER-14-0005 "Seismic Performance of Steel Plate Shear Walls Considering Various Design Approaches," by R. Purba and M. Bruneau, October 31, 2014.

MCEER-14-0006 "Air-Blast Effects on Civil Structures," by Jinwon Shin, Andrew S. Whittaker, Amjad J. Aref and David Cormie, October 30, 2014.

MCEER-14-0007 "Seismic Performance Evaluation of Precast Girders with Field-Cast Ultra High Performance Concrete (UHPC) Connections," by G.C. Lee, C. Huang, J. Song, and J. S. O'Connor, July 31, 2014.

MCEER-14-0008 "Post-Earthquake Fire Resistance of Ductile Concrete-Filled Double-Skin Tube Columns," by Reza Imani, Gilberto Mosqueda and Michel Bruneau, December 1, 2014.

MCEER-14-0009 "Cyclic Inelastic Behavior of Concrete Filled Sandwich Panel Walls Subjected to In-Plane Flexure," by Y. Alzeni and M. Bruneau, December 19, 2014.

MCEER-14-0010 "Analytical and Experimental Investigation of Self-Centering Steel Plate Shear Walls," by D.M. Dowden and M. Bruneau, December 19, 2014.

MCEER-15-0001 "Seismic Analysis of Multi-story Unreinforced Masonry Buildings with Flexible Diaphragms," by J. Aleman, G. Mosqueda and A.S. Whittaker, June 12, 2015.

MCEER-15-0002 "Site Response, Soil-Structure Interaction and Structure-Soil-Structure Interaction for Performance Assessment of Buildings and Nuclear Structures," by C. Bolisetti and A.S. Whittaker, June 15, 2015.

MCEER-15-0003 "Stress Wave Attenuation in Solids for Mitigating Impulsive Loadings," by R. Rafiee-Dehkharghani, A.J. Aref and G. Dargush, August 15, 2015.

MCEER-15-0004 "Computational, Analytical, and Experimental Modeling of Masonry Structures," by K.M. Dolatshahi and A.J. Aref, November 16, 2015.

MCEER-15-0005 "Property Modification Factors for Seismic Isolators: Design Guidance for Buildings," by W.J. McVitty and M.C. Constantinou, June 30, 2015.

MCEER-15-0006 "Seismic Isolation of Nuclear Power Plants using Sliding Bearings," by Manish Kumar, Andrew S. Whittaker and Michael C. Constantinou, December 27, 2015.

MCEER-15-0007 "Quintuple Friction Pendulum Isolator Behavior, Modeling and Validation," by Donghun Lee and Michael C. Constantinou, December 28, 2015.

MCEER-15-0008 "Seismic Isolation of Nuclear Power Plants using Elastomeric Bearings," by Manish Kumar, Andrew S. Whittaker and Michael C. Constantinou, December 29, 2015.

MCEER-16-0001 "Experimental, Numerical and Analytical Studies on the Seismic Response of Steel-Plate Concrete (SC) Composite Shear Walls," by Siamak Epackachi and Andrew S. Whittaker, June 15, 2016.

MCEER-16-0002 "Seismic Demand in Columns of Steel Frames," by Lisa Shrestha and Michel Bruneau, June 17, 2016.

MCEER-16-0003 "Development and Evaluation of Procedures for Analysis and Design of Buildings with Fluidic Self-Centering Systems" by Shoma Kitayama and Michael C. Constantinou, July 21, 2016.

MCEER-16-0004 "Real Time Control of Shake Tables for Nonlinear Hysteretic Systems," by Ki Pung Ryu and Andrei M. Reinhorn, October 22, 2016.

MCEER-16-0006 "Seismic Isolation of High Voltage Electrical Power Transformers," by Kostis Oikonomou, Michael C. Constantinou, Andrei M. Reinhorn and Leon Kemper, Jr., November 2, 2016.

MCEER-16-0007 "Open Space Damping System Theory and Experimental Validation," by Erkan Polat and Michael C. Constantinou, December 13, 2016.

MCEER-16-0008 "Seismic Response of Low Aspect Ratio Reinforced Concrete Walls for Buildings and Safety-Related Nuclear Applications," by Bismarck N. Luna and Andrew S. Whittaker.

MCEER-16-0009 "Buckling Restrained Braces Applications for Superstructure and Substructure Protection in Bridges," by Xiaone Wei and Michel Bruneau, December 28, 2016.

MCEER-16-0010 "Procedures and Results of Assessment of Seismic Performance of Seismically Isolated Electrical Transformers with Due Consideration for Vertical Isolation and Vertical Ground Motion Effects," by Shoma Kitayama, Michael C. Constantinou and Donghun Lee, December 31, 2016.

MCEER-17-0001 "Diagonal Tension Field Inclination Angle in Steel Plate Shear Walls," by Yushan Fu, Fangbo Wang and Michel Bruneau, February 10, 2017.

MCEER-17-0002 "Behavior of Steel Plate Shear Walls Subjected to Long Duration Earthquakes," by Ramla Qureshi and Michel Bruneau, September 1, 2017.

MCEER-17-0003 "Response of Steel-plate Concrete (SC) Wall Piers to Combined In-plane and Out-of-plane Seismic Loadings," by Brian Terranova, Andrew S. Whittaker, Siamak Epackachi and Nebojsa Orbovic, July 17, 2017.

MCEER-17-0004 "Design of Reinforced Concrete Panels for Wind-borne Missile Impact," by Brian Terranova, Andrew S. Whittaker and Len Schwer, July 18, 2017.

MCEER-17-0005 "A Simple Strategy for Dynamic Substructuring and its Application to Soil-Foundation-Structure Interaction," by Aikaterini Stefanaki and Metttupalayam V. Sivaselvan, December 15, 2017.

MCEER-17-0006 "Dynamics of Cable Structures: Modeling and Applications," by Nicholas D. Oliveto and Mettupalayam V. Sivaselvan, December 1, 2017.

MCEER-17-0007 "Development and Validation of a Combined Horizontal-Vertical Seismic Isolation System for High-Voltage-Power Transformers," by Donghun Lee and Michael C. Constantinou, November 3, 2017.

MCEER-18-0001 "Reduction of Seismic Acceleration Parameters for Temporary Bridge Design," by Conor Stucki and Michel Bruneau, March 22, 2018.

MCEER-18-0002 "Seismic Response of Low Aspect Ratio Reinforced Concrete Walls," by Bismarck N. Luna, Jonathan P. Rivera, Siamak Epackachi and Andrew S. Whittaker, April 21, 2018.

MCEER-18-0003 "Seismic Damage Assessment of Low Aspect Ratio Reinforced Concrete Shear Walls," by Jonathan P. Rivera, Bismarck N. Luna and Andrew S. Whittaker, April 16, 2018.

MCEER-18-0004 "Seismic Performance Assessment of Seismically Isolated Buildings Designed by the Procedures of ASCE/SEI 7," by Shoma Kitayama and Michael C. Constantinou, April 14, 2018.

MCEER-19-0001 MCEER-19-0001 "Development and Validation of a Seismic Isolation System for Lightweight Residential Construction," by Huseyin Cisalar and Michael C. Constantinou, March 24, 2019.

MCEER-20-0001 "A Multiscale Study of Reinforced Concrete Shear Walls Subjected to Elevated Temperatures," by Alok Deshpande and Andrew S. Whittaker, June 26, 2020.

MCEER-20-0002 "Further Results on the Assessment of Performance of Seismically Isolated Electrical Transformers," by Shoma Kitayama and Michael C. Constantinou, June 30, 2020.

University at Buffalo
The State University of New York

**MCEER: Earthquake Engineering to Extreme Events**

University at Buffalo, The State University of New York
133A Ketter Hall | Buffalo, NY 14260
*mceer@buffalo.edu; buffalo.edu/mceer*

ISSN 1520-295X